Targeting Arginine Auxotrophy in Colorectal Cancer

Thesis submitted for the degree of Doctor of

Philosophy

at the University of Leicester

by

Constantinos Alexandrou, B.Sc., M.Sc.

Leicester Cancer Research Centre

Department of Genetics and Genome Biology

January 2019

Abstract

Targeting Arginine Auxotrophy in Colorectal Cancer

Constantinos Alexandrou

Arginine is a semi essential amino acid with numerous functions in cellular metabolism. Loss-of-expression of urea cycle enzymes in several malignancies results in arginine auxotrophy and sensitivity to arginine starvation. Lack of expression of the urea cycle enzymes argininosuccinate synthase 1 (ASS1) and ornithine transcarbamylase (OTC) identifies patients bearing urea-cycle defective cancers and therefore likely to benefit from arginine deprivation therapies. PEGylated formulations of the arginine-degrading enzymes arginine deiminase (ADI) and arginase are currently being tested in numerous clinical trials to ascertain the anti-tumour efficacy of pharmacological arginine deprivation.

Here, we report remarkable arginine auxotrophy in colorectal cancer (CRC). We show that CRC cell lines are unable to grow in arginine-free medium and, *in vivo,* dietary withdrawal of arginine decreases the growth of xenograft tumours in mice subcutaneously implanted with ASS1-deficient CRC cells. In addition, CRC cell lines with low or undetectable expression of ASS1 are sensitive to pharmacological arginine depletion mediated by ADI treatment. Notably, ASS1-expressing, ADI-resistant cell lines remain auxotrophic for arginine and are susceptible to arginase activity *in vitro* and *in vivo*. Arginase degrades arginine in urea and ornithine. Cells with fully functional urea cycle can reutilize ornithine through the enzyme OTC. All CRC cell lines analysed show lack of expression of OTC and analysis of tissue microarrays unveils a common lack of OTC expression in CRC patients, suggesting that defective expression of OTC could contribute the observed arginine auxotrophy. Finally, in drug combination studies, we demonstrate that ADI and arginase synergise with the chemotherapeutics 5-Fluorouracil and Oxaliplatin in at least 2 of the cell lines tested.

In summary, we demonstrate that reduced expression of ASS1 and OTC enzymes results in arginine auxotrophy in CRC, a metabolic vulnerability that is amenable to arginine depleting strategies.

Acknowledgements

Table of Contents

List of Tables

List of Figures

List of Abbreviations

18-FDG-PET : 18F-deoxyglucose-positron emission tomography

4E-BP1-3 : Eukaryotic elongation and initiation factor binding proteins 1-3

5-FU : 5-Fluorouracil

ADAM : Arginine Deiminase and Mesothelioma

ADC : Arginine decarboxylase

ADI : Arginine deiminase

AJCC : American committee on cancer

AMBRA1 : Activating molecule in BECN1-regulated autophagy protein 1

AML : Acute myeloid leukemia

APC : Adenomatous polyposis coli

ASL : Argininosuccinate lyase

ASS1: Argininosuccinate synthase 1

ATGs : Autophagy-related genes

Bcl-2 : B-cell lymphoma 2

BCSP : Bowel cancer screening programme

BIM : B-cell lymphoma 2 interacting mediator

BMK-1 : Big MAP kinase 1

BRAF : V-Raf murine sarcoma viral oncogene homolog B

BSA : Bovine serum albumin

BubR1 : Budding uninhibited by Benzimidazoles 1 homolog beta

CAD : Carbamoyl-phosphate synthetase 2, aspartate transcarbamylase, and dihydroorotase

CASTOR1 : Cellular arginine sensor for mTORC1

CGH : Comparative genomic hybridisation

CH_2THF : 5, 10-methylenetetrahydrofolate

CI : Combination index

CIMP : CpG island methylator phenotype

CIN : Chromosomal instability

CK1a : Casein kinase 1 alpha

CMS : Consensus molecular subtypes

CpG : Cytosine preceding guanine

CPS-1 : Carbamoyl synthase 1

CQ : Chloroquine

CRC : Colorectal cancer

CRUK : Cancer research UK

DACH : diaminocyclohexane

DDR : DNA damage response

DEPTOR : DEP domain containing mTOR interacting protein

DMFO : Difluoromethylomithine

DNMT: DNA methyltransferases

dUMP : Deoxyuridine monophosphate

Dvl : Dishevelled

ECL : Enhanced chemiluminescence luminol

EdU : 5-ethynyl-2'- deoxyuridine

EGF : Epidermal growth factor

EGFR : Epidermal growth factor receptor

eIF4E : Eukaryotic initiation factor 4E

EMT : Epithelial mesenchymal transition

ER : Endoplasmic reticulum

Fa-DRI : Fraction affected - dose reduction index

FAP : Familial adenomatous polyposis

FasL : Fas ligand

Fbw7α : F-box and WD40 domain-containing protein 7α

FdUMP : Fluorodeoxyuridine monophosphate

FdUTP : Fluorodeoxyuridine triphosphate

FFPE : Formalin-fixed and paraffin-embedded

FOLFOX : 5-FU with Oxaliplatin and Leucovorin

FOLIFIRI : 5-FU with Oxaliplatin and Irinotecan

FoxO : Forkhead box O

FUTP : Flourouridine triphosphate

GAPs : GTPase activating proteins

GEF : Guanine nucleotide exchange factor

GI : Gastrointestinal track

GLS1 : Glutaminase 1

GLUT1 : Glucose transporter

GRB2 : Growth factor receptor bound protein 2

GSK3-β : Glycogen synthase kinase 3 beta

HCC : Hepatocellular carcinoma

HIF1α : Hypoxia induced factor 1α

hMLH1 : MutL homolog 1

HNPCC : Hereditary non polyposis colorectal cancer

HP : Hyperplastic polyp

HRP : Horseradish peroxidase

ISCs : Intestinal stem cells

JAK : Janus family of tyrosine kinases

JNK : c-Jun N-terminal kinase

KRAS : Kirsten rat sarcoma viral oncogene homolog

LC3A/B : Microtubule-associated protein 1A/1B-light chain 3

LDHA : Lactate dehydrogenase A

LOH : Loss of heterozygosity

LRP : Lipoprotein related protein

MAPK : Mitogen activated protein kinases

mCRC : Metastatic colorectal cancer

MDM2 : Murine double minute 2

mLST8 : Mammalian lethal with Sec13 protein 8

MM : Metastatic melanoma

MMR : Miss match repair

MSI : Microsatellite instable

MTHFD2 : Methylenetetrahydrofolate dehydrogenase 2

mTORC1 : Mammalian target of rapamycin complex 1

NO : Nitric oxide

NOS : Nitric oxide synthase

ODC : Ornithine decarboxylase

OTC : Ornithine transcarbamylase

p70S6K : Ribosomal protein S6 kinase

PARP : Poly ADP-ribose polymerase

PBS : Phosphate buffer saline

PD : Pharmacodynamics

PDK1 : Phosphoinositide dependent kinase 1

PDXs : Patient derived xenografts

PE : Phosphatidylethanolamine

PEG : Polyethylene glycol

PFK : Phosphofructokinase

P-gp : P-glycoprotein

PI3K : Phosphoinositide 3 kinase

PI3KCA : Phosphatidylinositol-4, 5 biphosphate 3 kinase catalytic subunit alpha

PIP_2 : Phosphatidylinositol-4, 5-biphosphate

PIP_3 : Phosphatidylinositol-4, 5-triphosphate

PK : Pharmacokinetics

PRAS40 : Proline-rich Akt substrate of 40kDa

PTEN : Phosphatase and tensin homolog

Rag : Ras-related GTPases

RAPTOR : Regulatory protein associated with mTOR

Rheb : Ras homolog enriched in the brain G protein

RICTOR : Rapamycin insensitive companion of mTOR

RNAseq : RNA sequencing

RTK : Receptor tyrosine kinase

SCLC : Small cell lung carcinoma

SILAC : Stable isotope labelling by amino acids in culture

SOS : son of sevenless

SQSTM1 : Ubiquitin binding protein Sequestosome 1 (p62)

SSA/Ps : Sessile serrated adenomas / polyps

STAT : Signal transducers and activators of transcription

TA cells : Transit amplifying cells

T-ALL : T-cell acute lymphoblastic leukemia

TCF/LEF : T cell factor / lymphoid enhancer factor

TGF-β : Transforming growth factor beta

TMA : Tissue microarray

TNF : Tumour necrosis factor

TNM : Tumour-node-metastasis

TRAIL : TNF related apoptosis-inducing ligand

TS : Thymidylate synthase

TSAs : Traditional adenomas

TSC2 : Tuberous sclerosis complex 2

UICC : Union against cancer

ULKs : UNC-51 like kinases

UPR : Unfolded protein response

USP28 : Ubiquitin-specific protease

WHO : World health organisation

β-TrCP: Beta transducin repeat containing protein5

List of Publications

Constantinos Alexandrou, Saif Sattar Al-Aqbi, Jennifer A. Higgins, William Boyle, Ankur Karmokar, Catherine Andreadi, Jin-Li Luo, David A. Moore, Maria Viskaduraki, Matthew Blades, Graeme I. Murray, Lynne M. Howells, Anne Thomas, Karen Brown, Paul N. Cheng & Alessandro Rufini (2018). Sensitivity of Colorectal Cancer to Arginine Deprivation Therapy is shaped by Differential Expression of Urea Cycle Enzymes. *Scientific Reports*, *8*, 12096.

Chapter 1 – Introduction

1.1 Colorectal Cancer – Statistics

Recent epidemiological studies report that colorectal cancer (CRC) is one of the primary causes of cancer-associated deaths worldwide (Ferlay et al., 2012, Siegel et al., 2017). According to Cancer Research UK (CRUK), CRC is the 4th most common cancer in the UK with more than 40,000 new cases diagnosed every year (Figure 1-1A) (Cancer Research UK, 2013-2015). Encouragingly, CRC mortality rates have shown a progressive decline over the last 50 years (Figure 1-1B), largely due to the introduction of colonoscopy and primary cancer screening programs such as Bowel Cancer Screening Programme (BCSP) (Logan et al., 2012; NHS.UK), improved surgical procedures and patient stratification strategies for more personalised treatment (Welch and Robertson, 2016). Combination treatment approaches with antimetabolites such as fluoropyrimidines and Oxaliplatin have decreased the risk of relapse in patients with advanced stage III who have undergone surgical removal (Figure 1-1C), extending their overall 5-year survival at around 60%. Despite that, almost 30% of the patients treated with these drugs demonstrate relapse which usually leads to death within 2 to 3 years. Promising efforts to improve adjuvant therapy of advance stage III and IV CRCs with targeted immunotherapy have recently demonstrated durable responses but only in a subset of patients deficient in miss match repair genes (dMMR)/ microsatellite instable high (MSI-H) metastatic CRC (mCRC) (Overman et al., 2018). Taken together, there is still urge for better understanding of cancer biology, mechanisms of resistance and the identification of novel biomarkers that could detect patient populations susceptible to alternative treatment strategies for more effective, less cytotoxic regimens.
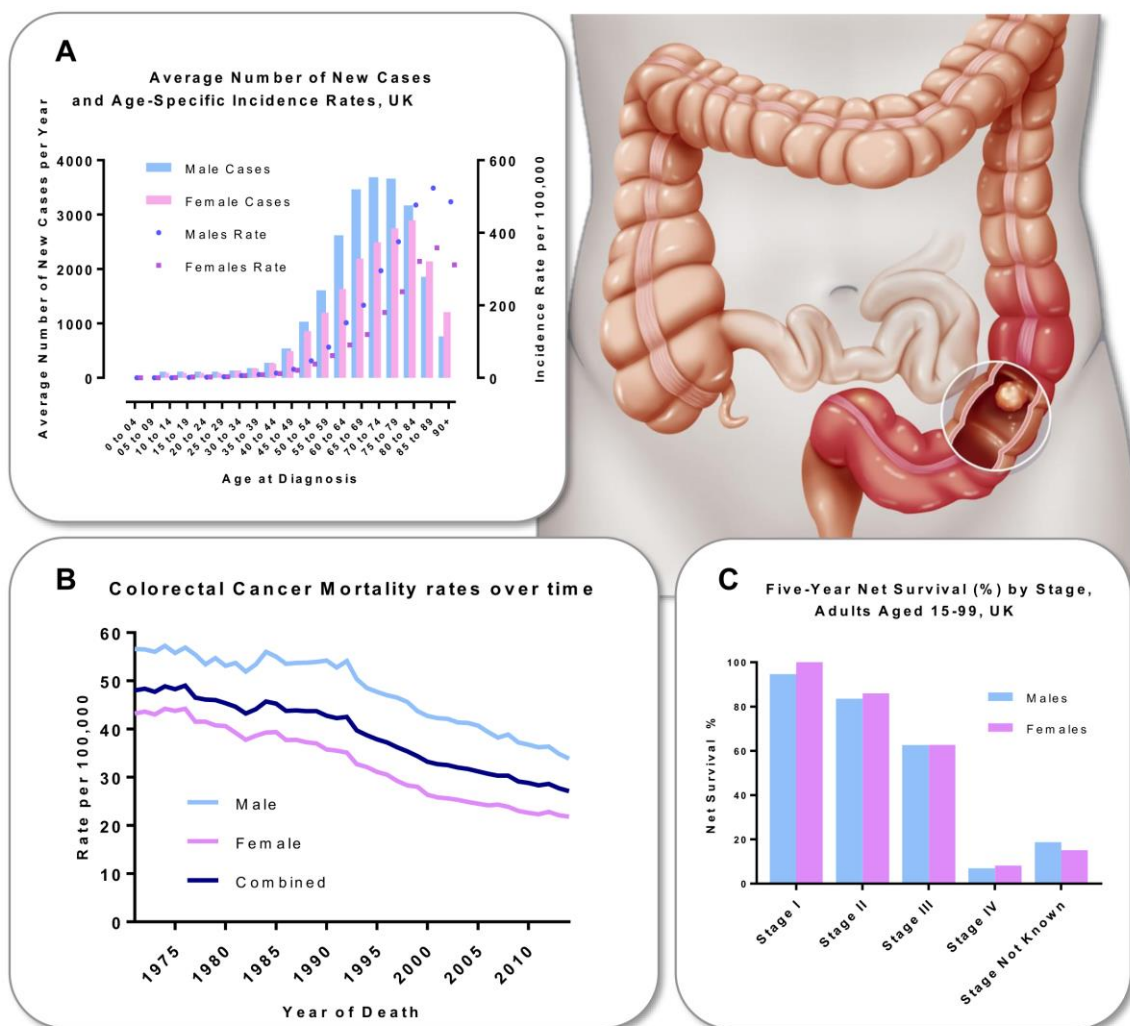
Figure 1-1: CRC statistics, (A) *Average number of new cases occurring in the UK based on age,* ***(B)*** *Mortality rates,* ***(C)*** *% Five-year Net survival distribution of CRC patients among different stages of the disease (Data acquired from Cancer Research UK).*

1.2 Colon Physiology

Colon or large intestine encompasses the lowest part of the gastrointestinal track (GI) from the caecum to the anus. It can be divided into 6 distinct regions, namely caecum, ascending colon, transverse colon, descending colon, sigmoid colon and rectum. Although stomach and small intestine are the two primary segments of the GI where digestion and absorption takes place, colon still has a significant role in those functions (Szmulowicz, 2016). Accordingly, colon is responsible for water and electrolyte absorption, salvage of unabsorbed nutrients

(Rombeau, 2003; Christl and Scheppach, 1997) as well as transport of intestinal contents and expulsion of faeces.

Salvage of unabsorbed nutrients, such as complex carbohydrates and resistant to digest proteins occurs mainly via saccarolytic and proteolytic fermentation. These processes are catalysed by the gut microbiome (bacteria) which is present within the intestinal microenvironment (Nordgaard, 1998). While bacterial digestion of complex carbohydrates takes place in the ascending and proximal transverse colon, the undigested proteins along with mucinous proteins and shedded intestinal epithelial cells, which reach the colon are digested primarily in the distal segment. This compartmentalisation relies primarily on the limited availability of carbohydrates in the distal colon which are the nutrient substrate of choice for most anaerobic bacteria. Fermentation of complex carbohydrates primarily generates short chain fatty acids (such as butyrate, propionate and acetated), whereas bacterial digestion of proteins produces short-chain fatty acids, branched chain amino acids (leucine, isoleucine and valine) amines, ammonia, phenols, indoles and sulphurs. Although toxic constituents like ammonia, phenols, indoles and sulphurs have been associated with ulcerative colitis and colonic carcinogenesis, substances such as butyrate play a pivotal role in colonic function. Reportedly, butyrate is the primary source of energy of the absorptive colonic epithelial cells, covering 70-90% of the energy demands while it acts as an antidiarrheal agent by promoting water, sodium and chloride absorption (Rombeau, 2003; Christl and Scheppach, 1997; Hammer et al., 2008).

Colon's architecture is intended to maximise nutrient and water absorption from food. The epithelial cells, which cover the outer inner layer exposed to the lumen (mucosa), invaginate into the underlying lamina propria (connective tissue) to form the crypts (Semrin et al., 2010; Shen 2009) (Figure 1-2A). The intestinal epithelium represents one of the best known paradigms of self-replenishing tissues in mammals. Due to anoikis – a process of programmed cellular death due to the absence of correct cell/ECM attachment (Frisch and Francis, 1994) – as well as extreme mechanical forces within the lumen that cause the shedding of epithelial cells, human intestinal epithelium renews every 3-5 days (Leblond and Stevens, 1948). Under normal conditions, anoikis restricts proliferation of a rather high proliferative monolayer of cells and prevents reattaching of those in distant locations, acting at the same time as a defence mechanism against mutated cells. This tissue maintenance is sustained by a highly

proliferative, dynamic and multipotent stem cell population located at the base of the crypts. These intestinal stem cells (ISCs) generate the transit amplifying cells (TA cells) which migrate towards the villus area and are the progenitors of differentiated intestinal lineages. After multiple divisions these progenitors stop proliferating and differentiate into enterocytes to satisfy the demand for absorption, goblet cells that secrete mucus to aid the faecal movement via lubrication of the mucosal surface, enteroendocrine cells and tuft cells. Enteroendocrine cells orchestrate normal intestinal function, such as gut motility, control of glucose levels and nutrient absorption),via hormone secretion in response to food stimuli (Gribble and Reimann, 2016), whereas tuft cells may be implicated in the regulation of physiologic response to nutrients, as studies have shown that these cells express chemosensory proteins related to the ones found in taste buds (Bezencon et al., 2007; Hofer et al., 1996; Mace et al., 2007), and orchestrate immune response against parasite infections (Gerbe et al., 2016). Opposite to the migration of cells towards the top of the intestinal crypt, another population of cells namely Paneth cells, descends towards the base of the crypt (Ireland et al., 2005). These highly specialized epithelial cells secrete antimicrobial factors that modulate the host-microbe interactions as well as factors that control the ISCs niche (Clevers and Bevins, 2013) (Figure 1-2C). As reviewed by Clevers and Schepers in 2012, the intestinal crypt homeostasis and its remarkable proliferative rate are principally maintained by the Wnt signalling (Schepers and Clevers, 2012), which explains why genetic aberrations in Wnt pathway are the main driving forces of CRC, as will be discussed below.
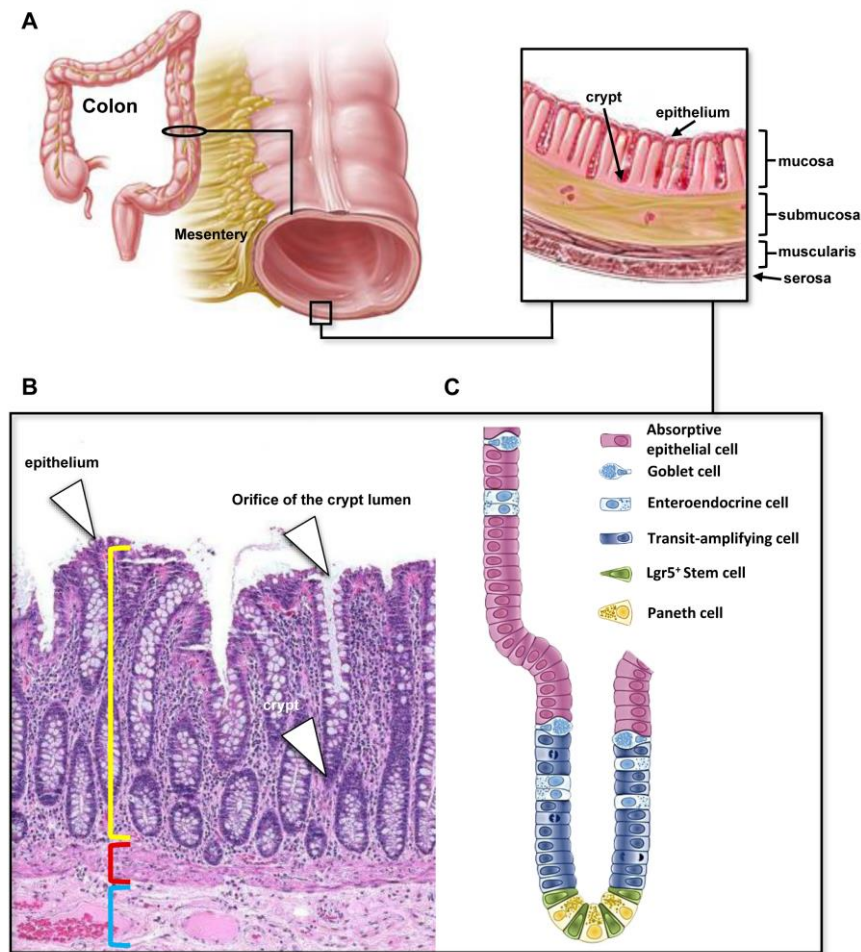
Figure 1-2: Structure of the Intestinal Epithelium (A) *Tissue organisation and crypt structure of normal human colon.* ***(B)*** *Micrograph of a normal human colorectal mucosa. Crypts are in parallel alignment with a significantly increased presence of goblet cells. Mucosa is delimited by yellow brackets, submucosa and muscularis by red and blue respectively* ***(C) Intestinal crypt organisation,*** *the ISCs are situated at the bottom of the crypt (green) along with supportive Paneth cells (yellow). Stem cells are fuelling the transit amplifying compartment with new cells which will eventually move upward and differentiate into functionally specialized intestinal cells. (Adapted from Barker, 2014)*

1.3   Genetic Aetiology of CRC

CRC has often been described as a complex and heterogeneous disease driven mainly by a progressive sequence of genetic and epigenetic changes that, along with lifestyle factors, promote the transformation of normal colonic epithelium to early adenomas and adenocarcinomas (Figure 1-3) (Vogelstein et al., 1988). Epidemiological studies over the past decade suggest that westernised diets high in unsaturated fats, excessive caloric intake, meat consumption, alcohol and decreased physical activity are some of the most prominent lifestyle factors that may promote/contribute to CRC development (Potter, 1999; Slattery, 2000; Huxley et al., 2009). On the other hand, important advances in genome editing and next generation sequencing have identified several genes responsible for CRC predisposition, as well as a broad range of genetic alterations that are present in sporadic CRC cases. In an effort to understand the pathophysiology of CRC and genetic heterogeneity of the disease Vogelstein et al., described a series of driver genetic events in key tumour suppressor genes and oncogenes that accumulate over time and result in tumour initiation and progression in a stepwise fashion (Vogelstein et al., 2018). Among the most frequently genetically altered genes and pathways identified in CRC are the *adenomatous polyposis coli (APC)* and WNT-β-catenin, *KRAS*, *BRAF TP53*, PI3K catalytic subunit-a (*PIK3CA*), SMAD family member 4 (*SMAD4*), Transforming growth factor beta 1 (*TGF-β*) and DNA mismatch – repair pathways (Sjoblom et al., 2006; Cancer Genome Atlas Nework, 2012; Seshagiri et al., 2012). The hierarchical, non-random accumulation of these alterations over different stages of the disease is responsible for CRC initiation and progression (Vogelstein et al., 2013)

1.3.1   The Adenomatous Polyposis Coli (APC) gene and Wnt Signalling in CRC

Adenomatous polyposis coli (*APC*) is a tumour suppressor gene located on chromosome 5q21-q22. It encodes for a 312 kDa protein that counterbalances the Wnt signalling pathway via binding and degradation of the transcription factor β-catenin. *APC* inactivation is one of the earliest events in the development of CRC and its importance is reflected by the high mutational frequency (60-70%) in sporadic cases (Fearon, 2011; Fearon and Vogelstein, 1990) Additionally, 30-40% of sporadic CRCs exhibit loss of heterozygosity (LOH) of chromosome 5q (Powell et al., 1992; White et al., 2012).

Further to its sporadic occurrence, *APC* inactivation can also be inherited via germ line mutations that lead to the Familial Adenomatous Polyposis Syndrome (FAP). FAP patients carry a defective copy of the *APC* that, following LOH of the functional remaining allele, leads to the development of hundreds of benign colonic polyps. Similarly to sporadic tumours, these polyps can progress to adenocarcinomas through the ''conventional'' histopathological stages of hyperplastic polyps to adenomas and eventually adenocarcinomas determined by the progressive accumulation of other mutations (Vogelstein et al., 1988; Thirlwell et al., 2010)

APC which has been characterised as the ''gatekeeper'' of colorectal tumours is involved in several cellular functions that include cell migration, cell to cell adhesion, proliferation, and apoptosis within the intestinal crypt (Polakis, 2007; Aoki and Taketo, 2007; Brocardo and Henderson, 2009). As previously mentioned *APC*'s chief role lies in its ability to negatively regulate the WNT-β catenin signalling pathway which is vital for stem cell homeostasis and transit amplifying cells proliferation within the intestinal crypt compartment (Secreto et al., 2009; Zhang et al., 2009). In ''canonical'' conditions, in the absence of Wnt ligands, APC protein acts as a binding partner with Axin to recruit β-catenin and promote its phosphorylation by casein kinase 1 alpha (CK1a) and glycogen synthase kinase 3 (GSK3-β). This multiprotein complex in known as the β-catenin destruction complex, because phosphorylated β-catenin is targeted for ubiquitination by the β transducin repeat containing (β-TrCP) E3 ubiquitin protein ligase and subsequent degradation by the proteasome (Figure 1-3A). (Aberle et al., 1997; Kitagawa et al., 1999).

In the presence of Wnt ligands, the phosphorylated cytoplasmic tail of low density lipoprotein receptor-related protein (LRP), recruits Axin to the membrane via interactions with Dishevelled (Dvl) subsequently resulting to the inactivation of the destruction complex (Figure 1-3). Accumulation of the newly synthesized and unphosphorylated β-catenin in the cytoplasm results to its translocation to the nucleus. β-catenin in the nucleus interacts with T cell factor/lymphoid enhancer factor (TCF/LEF) family of transcription factors leading to the transcriptional activation of Wnt target genes, such as, c-Myc, epidermal growth factor receptor (EGFR), Cyclin D1 and Lgr5 (Figure 1-3B) (He et al., 1998; Shtutman et al, 1999, McCormick and Tetsu, 1999). Wnt Signalling plays a pivotal role in tissue homeostasis and repair both during development and adulthood via Wnt target genes that regulate

proliferation, differentiation and migration (Schepers and Clevers, 2012). Most importantly, hyper activation of Wnt signalling is thought to be the initiating force for most CRCs as uncontrolled activation of Wnt target genes following loss of APC initiates the pathological transformation of the intestinal epithelium (McCormick and Tetsu, 1999).
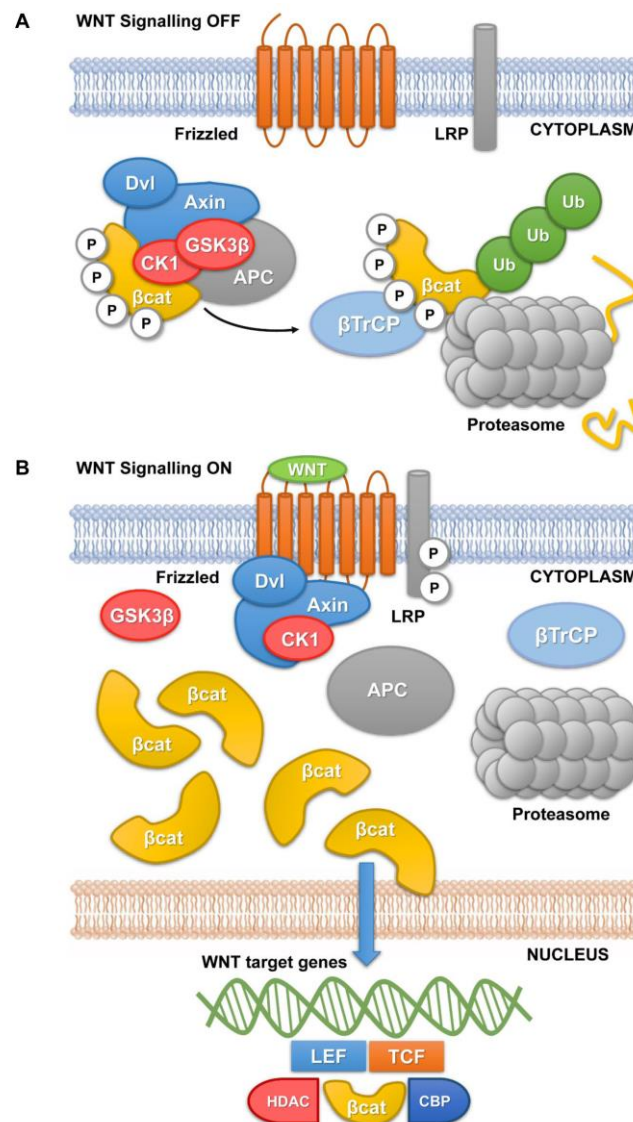
Figure 1-3: Canonical WNT Signalling Pathway. (A) *In the absence of Wnt ligands, Wnt Signaling is OFF due to dissociation of Frizzled receptor and LRP. This dissociation furthers enables AXIN-APC complex to target β-catenin for proteasomal degradation mediated via phosphorylation by GSK3-β and CK1;* **(B)** *Wnt ligands promote recruitment of AXIN-APC complex on the membrane via Dvl and further leading to its inactivation. Accumulation of unphosphorylated β-catenin in the cytoplasm and subsequent translocation in the nucleus initiates Wnt target genes transcription. Adapted from Clevers and Nusse, 2012).*

1.3.2   MAPK Pathway

The mitogen-activated protein kinases (MAPK) signalling pathway plays an important role in cell proliferation, survival, invasion as well as intestinal epithelial differentiation (Taupin and Podoloski, 1999; Dhillon et al., 2007; Garnett and Marais, 2004; Mercer et al., 2005). It is now well established that its deregulation often drives the initiation and progression of CRC (Fang and Richardson, 2005). MAPK Signal transduction is mediated by families of serine/threonine kinases and double specificity threonine/tyrosine kinases (Dhanasekaran et al., 1998). MAPK cascade can be further sub classified in four distinct pathways that involve the extracellular signal regulated kinases (ERK MAPK, Ras/Raf/MEK/ERK), the Big MAP kinase-1 (BMK-1), c-Jun N-terminal kinase (JNK) and p38 (Cossa et al., 2013). Activation of receptor tyrosine kinases (RTKs), such as EGFR, by binding of ligands at the cell membrane, results in a cascade of signal transduction that affects the expression of genes related to cell cycle, metabolism, survival and apoptosis (Fang and Richardson, 2005).

The EGFR signalling is an important pathway in CRC. Its pathological activation via oncogenic mutations or copy number variations of the *EGFR* gene, causes downstream activation of the MAPK cascade, contributing to malignant transformation and cancer progression. Immunohistochemical analysis revealed that in 35-50% of CRC cases, EGFR is overexpressed, and multiple studies have associated increased EGFR expression with worse prognosis (Goldstein and Armin, 2001; Rego et al., 2010; Galizia et al., 2006; Ljuslinder et al., 2011; Resnick et al., 2004; Kario et al., 2005).

Under physiologic conditions, EGFR regulation is controlled via protein tyrosine phosphatases and binding of *de novo* EGFR inhibitors (Anastasi et al., 2003; Kario et al., 2005; Gur et al., 2004; Tarcic et al., 2009; Laederich et al., 2004). Binding of the epidermal growth factor (EGF) to EGFR induces the dimerization of two receptor monomers (homodimerization). This dimerization triggers the auto-phosphorylation of the EGFR intracellular domain in multiple tyrosine residues. As a consequence, these phosphorylated residues recruit adaptor proteins, including son-of-sevenless (SOS) and growth factor receptor bound protein 2 (GRB2) via interactions with the adaptor molecule Shc (Lowenstein et al., 1992; Batzer et al., 1994). This results in the conformational change of SOS, which further recruits the inactive Kirsten rat sarcoma viral oncogene homolog (KRAS). KRAS is a GTP binding protein that oscillate between an active (GTP-bound) and an inactive (GDP bound) state. SOS is a guanine nucleotide

exchange factor (GEF) factor that promotes biding of GTP and activation of KRAS (Hubbard and Miller, 2007; Margolis and Skolnik, 1994). Once active, KRAS recruits V-Raf murine sarcoma viral oncogene homolog B (BRAF) kinase to the cell membrane via direct binding, where it gets activated via dimerization and auto – phosphorylation at Thr599 and Ser602 (Dhillon et al., 2007; Kohler et al., 2016). Subsequently, BRAF kinase promotes a cascade of downstream phosphorylations/activations of kinases MEK1 and MEK2 at Ser218 and Ser222 (Dhillon et al., 2007). Finally, MEK1 and MEK2 phosphorylate ERK kinase (Lu and Xu, 2006) which activates multiple cytoplasmic and nuclear targets involved in cell proliferation and survival (Figure 1-4) (Montagut and Settleman, 2009, Neuziller et al., 2013, Schlessinger et al., 2000, Bernards and Settleman 2004).

Signal transducers and activators of transcription (STAT) proteins can also be activated by the Janus family of tyrosine kinases (JAK) and EGFR via interactions with the phosphorylated cytoplasmic tyrosine residues of the receptor. In response to cytokines and growth factors, STAT proteins promote the activation of genes involved in proliferation, survival, differentiation and apoptosis. Expression of STAT family of transcription factors has also been reported to be upregulated in CRC (Ma et al., 2004, Quesnelle et al., 2007).
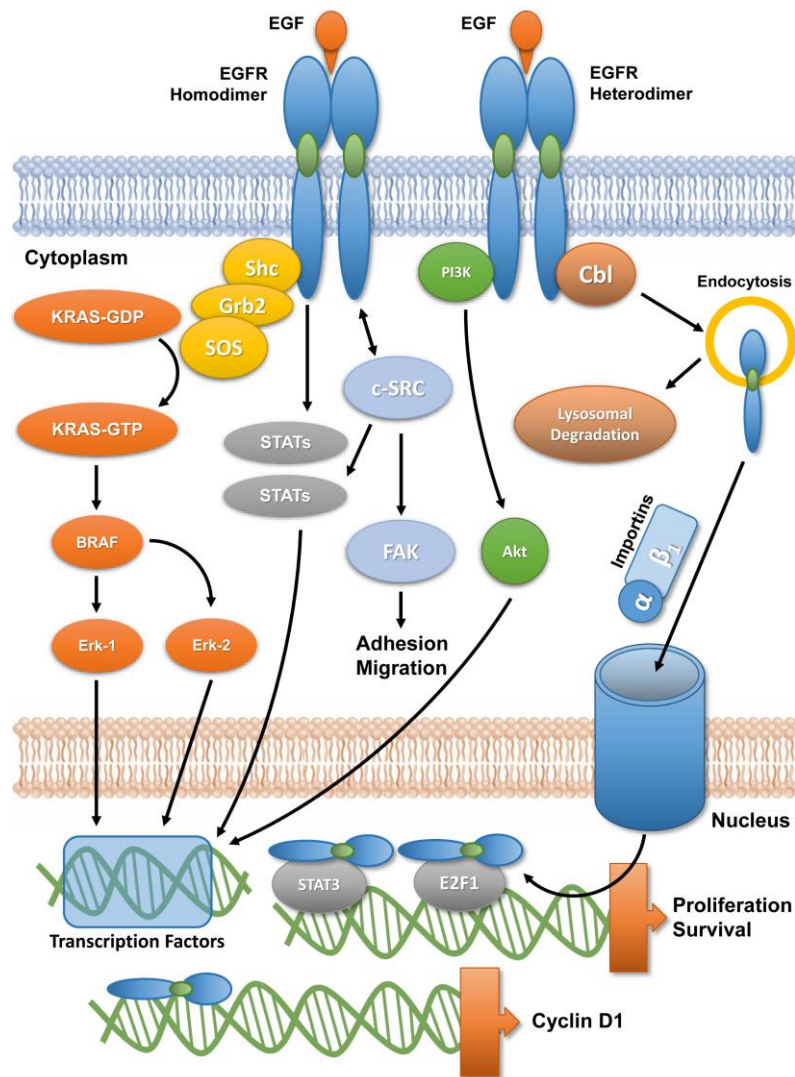
Figure 1-4: EGFR – MAPK Signalling Pathway. *Activation of EGFR by EGF leads to its homodimerisation or heterodimerisation and subsequent autophosphorylation in tyrosine residues in the intracellular portion of the receptor. This results in the recruitment of multiple proteins. STAT transcription factors (grey) bind directly on the receptor unlike RAS/RAF/MEK/ERK (orange) which require the presence of specific adaptor proteins (yellow),(Shc, Grb2 and SOS. Subsequent activation of the RAS/RAF/MEK/ERK signalling results in the transcriptional activation of genes required for cell proliferation and survival. Alternatively EGFR can also act as a transcription factor via endocytosis and importin mediated nuclear translocation (Adapted from Scaltriti and Baselga, 2006).*

1.3.3 Frequently mutated oncogenes and tumour suppressors in CRC

1.3.3.1 KRAS

The Ras family is comprised of three genes *KRAS*, *NRAS* and *HRAS* which encode for small-GTP proteins. These Ras small GTP-binding proteins exhibit high homology in their amino acid sequence and are equally abundantly expressed, however murine genetic studies reveal that only KRAS is critical for normal development (Downward, 2003; Johnson et al., 1997; Malumbres and Barbacid, 2003). As described in section 1.3.2 the membrane bound KRAS gets activated when coupled with GTP and stimulates a variety of effectors/signal transducers, including MAPK and the PI3K/Akt pathway (Malumbres and Barbacid, 2003). The activation and inactivation of KRAS occurs via circles of a GTP bound active and a GDP bound inactive state, respectively. The transition from an inactive to an active state and *vice versa* is regulated via the GTPase-activating proteins (GAPs) and GEFs. Accordingly, as their names imply, GAPs trigger the hydrolysis of GTP bound on KRAS to GDP by KRAS itself, while GEFs facilitated the switch from a KRAS-GDP to a KRAS GTP (Pylayeva et al., 2011; Giehl, 2005; Karnoub and Weinberg, 2008).

With mutational frequencies between 35-45%, KRAS is one of the most commonly mutated oncogenes in CRCs. Codons 12 and 13 are the two predominant hot spots, however mutations can also be found at codons 61, 146 as well as in other residues to a lesser extent. Mutations at codons 12 and 13 decrease the rate of GTP hydrolysis by 3 to 9-fold via disruption of KRAS GTPase activity (Lowy and Willumsen, 2003). The subsequent sustained activation of KRAS results in increased proliferation, alterations in cellular metabolism, suppression of apoptosis and enhanced invasion (Pylayeva et al., 2011; Downward, 1998).

1.3.3.2 BRAF

RAF family of oncogenes encodes for serine/threonine kinases which act downstream the MAPK signalling pathway (Section 1.3.2 and 1.3.3.1) (Garnett et al., 2007; Mercer et al., 2004; Wan et al., 2004). BRAF kinase mediates the signal transduction downstream of KRAS and EGFR signalling. In CRC, BRAF mutations can be found in 10-20% of sporadic cases, 95% of which are positive for the activating mutation $BRAF^{V600E}$. Substitution of valine to glutamate in the kinase region of BRAF results to its constitutive activation which ultimately leads to a

500-fold increased kinase activity in comparison to the wild type. This activation results in the downstream activation of effectors including MEK and the subsequent uncontrolled activation of EGFR signalling in an EGFR independent manner (Scaltriti and Baselga, 2006).

1.3.3.3   PI3KCA

The phosphatidylinositol-4, 5-biphosphate 3-kinase catalytic subunit alpha (*PI3KCA*) gene encodes for one subunit of a heterodimeric lipid kinase, phosphoinositide 3-kinase (PI3K), which acts as the main signalling hub downstream of RTKs, promoting cell growth, proliferation and survival (Fruman and Rommel, 2014). Upon RTK-growth factor stimulation, phosphatidylinositol-4, 5-biphosphate (PIP$_2$) is converted to phosphatidylinositol-4, 5-triphosphate (PIP$_3$) via phosphorylation by PI3K. PIP$_3$ is a pivotal second messenger that recruits AKT and PDK1 to the cytoplasmic membrane, where phosphoinositide-dependent kinase 1 (PDK1) phosphorylates AKT at Threonine 308. With downstream targets that include protein and lipid kinases, E3 ubiquitin ligases, cell cycle regulators, transcription factors, metabolic enzymes, and regulators of G proteins, AKT undoubtedly is a central node in cellular signal transduction. The diversity of AKT downstream targets affects a range of cellular functions that include proliferation, growth, cell survival, metabolism and migration (Manning and Cantley, 2007).

For instance, the initial step towards activation of cellular growth, occurs via activation of the mammalian target of rapamycin complex 1 (mTORC1), which is mediated via phosphorylation and subsequent inactivation of tuberous sclerosis complex 2 (TSC2) by AKT (Inoki et al., 2002; Potter et al., 2002; Manning et al., 2002). Alternatively, AKT phosphorylation by mTORC2/RICTOR at Serine 473 results in its full activation and further signal transduction that activates mTORC1, which regulates translation, protein synthesis and autophagy. Notably, inhibition of mTORC1 initiates a robust negative feedback loop via which growth factor receptor signalling is elevated by increased activation of PI3K, AKT and MAPK pathway (Saxton and Sabatini, 2017; Carracedo et al., 2008).

Back in the late 90s, Cross et al., reported the first identified AKT target, the GSK3 (Cross et al., 1999). GSK3 involvement and regulation by WNT signalling (Section 1.3.1) is not exclusive, as studies have shown that GSK3 can also be regulated independently via growth signals and

the PI3K/AKT cascade. In the presence of exogenous growth signals, AKT phosphorylates both GSK3a and GSK3b at residues (Ser21) and (Ser9), respectively, ultimately leading to their deactivation. Under normal conditions GSK3 exhibits a diverse range of phosphorylations in downstream targets which are further targeted for degradation by specific E3 ubiquitin ligases (Kaidanovich-Bellin and Woodgett, 2011). Among these targets is the transcription factor c-Myc (Sears et al., 2000; Welcker et al., 2004).

PI3K/AKT signalling pathway affects the regulation of Forkhead box O (FoxO) family of transcription factors. FoxO transcription factors are the main regulators of several tumour suppressor genes, including *Fas* ligand *(FasL)* and the pro apoptotic B-cell lymphoma 2 (Bcl-2) interacting mediator of cell death *(BIM)*. Their involvement in pro-survival and cell cycle signal control, renders them important components of CRC pathogenicity. Compelling evidences show that FoxO3a can be deactivated in response to MAPK and PI3K/ AKT signalling pathway. In this regard, FoxO3a targeted phosphorylation by ERK and AKT and subsequent degradation mediated by E3-ubiquitin ligase murine double minute 2 (MDM2), can promotes survival and tumorigenic events (Hu et al., 2004; Yang et al., 2008).

Several mutations in the catalytic subunit of PI3K have been found to increase its activity and subsequent production of the secondary messenger PIP_3 in human malignancies (Carson et al., 2008). Reportedly, two of the most commonly found mutations occurring in cancer are the H1047R and E542K/E545K. More specifically, substitution of Histidine to Arginine at residue 1047 of the kinase domain p110α of PI3K enhances its interaction with the cytoplasmic membrane in a KRAS interaction-independent manner (Burke and Williams, 2015). On the other hand, substitution of Glutamic acid to Lysine at residues 542 and 545 disrupts the interactions between N-SH2 domains of the regulatory subunit p85α, resulting in a constitutively active kinase (Burke et al., 2012; Miled et al., 2007). *PIK3CA* single point mutations are found in 15 to 25 % of sporadic CRCs, whereas double somatic mutations have been reported in 6-9% of CRC patients (Samuels et al., 2004; Wood et al., 2007; Abubaker et al., 2008).

1.3.3.4 PTEN

Another important regulator of the PI3K, with relevance for CRC, is the *Phosphatase and Tensin homolog* (*PTEN*) gene. *PTEN* is a tumour suppressor gene located on chromosome 10. PTEN protein functions both as protein and lipid phosphatase and it is primarily involved in the regulation of PI3K/AKT signalling pathway by antagonising PI3K via dephosphorylation of the secondary messenger PIP_3 to PIP_2 (Chalhoub and Baker, 2009). Ultimately, genetic alteration that inactivates *PTEN* results in enhancement of PI3K/AKT signalling pathway and further increase in cell proliferation, growth and survival (Carracedo and Pandofli, 2008). Of note, loss of PTEN function via hereditary germline mutations leads to Cowden syndrome in which patients exhibit elevated risk for benign gastrointestinal tumours. Beyond germline alterations, PTEN biallelic inactivation can occur through sporadic mutations, promoter hypermethylation and LOH and can be found in approximately 20-30% of sporadic CRCs.

1.3.3.5 TP53

TP53 is one of the most frequently mutated tumour suppressor genes in human cancers and has been extensively characterised as the ''guardian of the genome'' because of its pivotal role in DNA damaged response (Whibley et al., 2009, Campbell et al., 2010). The *p53* gene located on chromosome 17p encodes for a transcription factor that regulates the expression of genes in response to cellular stress, such as DNA damage and hypoxia. P53-regulated genes promote cell cycle arrest, apoptosis and cellular senescence, thereby curbing tumour progression (Kastenhuber and Lowe, 2017). Typically, in response to DNA damage, the DNA damage response (DDR) kinase ATM activates p53 via phosphorylation, which stabilizes p53 protein by inhibiting its proteasomal degradation (Haupt et al., 1997; Honda et al., 1997; Kubbutat et al., 1997). P53 can then activate target genes components of the DNA repair system, which facilitated DNA repair (Williams and Schumacher, 2016), or can induced cell death/senescence. Indeed, one of the most-well known functions of p53 is its ability to mediate proliferative arrest in response to DNA damage via activation of the cyclin dependent kinase inhibitor p21 (Harper et al., 1993; el-Deiry et al., 1993). Alternatively, p53 can also promote cell death via induction of the pro-apoptotic BCL-2 family members which in turn mediate caspase dependent apoptosis (Clarke et al., 1993; Miyashita et al., 1994). Several tumour suppressor genes, including p53, can have one of their alleles inactivated via LOH.

Reportedly, about 70% of CRCs show 17p LOH (Fearon and Vogelstein, 1990; Aoki and Taket, 2007). Additionally, mutations in p53 are present in 40-50% of the sporadic CRC cases (Takayama et al., 2006).

1.3.4   Pathways of Genomic Instability in CRC

1.3.4.1   Chromosomal Instability

Chromosomal Instability (CIN) is the most common type of genomic instability found in CRC (70-85% if CRCs) and it's mainly described by alterations in chromosome numbers and their structure, some of them which may include aneuploidy via loss of the entire chromosome 18, and 17p, in addition to polyploidy in chromosomes 13 and 20 (Muleris et al., 1985; Muleris et al., 1990). CIN, although poorly understood, may be driven by errors during chromosomal segregation and mitotic spindle formation (Grady, 2004; Barber et al., 2008). The molecular mechanisms underlying CIN appear to be complex and highly heterogeneous as they could be driven by alterations in several genes including *Mad2, BubR1* and *Bub3* and *APC* (Alberici and Fodde, 2006). Recent utilisation of comparative genomic hybridisation (CGH) arrays, helped researchers to measure amplifications and deletions in CIN in a high resolution output (Arriba et al., 2017). CIN positive tumours demonstrate up to 70% co-existence with mutations in *APC* gene*,* thus further highlighting the importance of both CIN and APC/ Wnt signalling as driving forces in malignant transformation (Pino and Chung, 2014). As mentioned previously (see section 1.3.3.5), LOH plays a pivotal role in the inactivation of tumour suppressor genes, including p53. Adding to this, downregulation of the budding uninhibited by benzimidazoles 1 homolog beta (BubR1) promoted by TP53 LOH, results in abnormalities during anaphase and chromosomal segregation, which further support the occurrence of CIN phenotype (Zhao et al., 2014).

1.3.4.2   Microsatellite Instability

The study of one the first described inherited cancer syndromes, the Hereditary Non polyposis Colorectal Cancer (HNPCC) syndrome (~3% of CRC cases), by Lynch in 1966 led to the identification of individuals with an autosomal dominant pattern of hereditary CRC (Lynch et al., 1966) without polyposis. These tumours were characterised by increased lymphocytic

infiltration and medullary-growth patterns among other unique histological features (Messerini et al., 1996; Jenkins et al., 2007). Further studies revealed variations between HNPCC and several predisposition genes among different families suggesting that HNPCC was a rather genetically heterogeneous syndrome (Peltomaki et al., 1993; Linblom et al., 1993). Extended genetic analysis of tumour tissues from patients revealed significant length variations of short nucleotide tandem repeats - termed microsatellite DNA sequences - in comparison to normal tissue (Aaltonen et al., 1993). These observations were consistent among all HNPCC patient samples, therefore these cancers were classified as Microsatellite instable (MSI). Accordingly, MSI tumours can be further sub classified into 2 distinct categories: MSI-high and MSI-low. MSI-high tumours were later on linked to mutated Miss Match Repair (MMR) genes (etc., MLH1, MSH2) (Parsons et al., 1993). It has been reported that defects in MMR system can increase the mutation occurrence by 100-fold (Thomas et al., 1996). During the early stages of cancer development, cancer cells heterozygous for MMR mutations are more likely to lose their second allele. Loss of function of DNA repair genes results in the rapid accumulation of mutations in oncogenes and tumour suppressor genes, further accelerating the progression of the disease (Vilar et al., 2010; Fisher and Kolodner, 1995; Rustgi, 2007). Similarly to the HNPCC syndrome, defects in MMR genes are also present in approximately 15% of sporadic tumours (Rustgi, 2007; Thibodeau et al., 1993). The majority of sporadic MSI high tumours exhibit defective MMR system, which is predominantly deregulated due to deactivation of mutL homolog 1 (hMLH1) protein via methylation of its promoter (Nagasaka et al., 2010; Cunninghan et al., 1998).

1.3.4.3 CpG Island Methylator Phenotype

Another common alternative molecular mechanism of gene inactivation among CRC patients is the epigenetic silencing of genes which is mainly driven via abnormal DNA methylation (Toyota et al., 1999). In humans, areas within the promoter region of genes can be rich in cytosine preceding guanine (CpG) dinucleotides. In normal cells, these so-called CpG islands can regulate up to 50% of the human genes expression via methylation or demethylation of cytosine residues (Toyota et al., 1999, Hughes et al., 2012). DNA methyltransferases (DNMT) catalyse the enzymatic transferring of a methyl group to the 5' of a cytosine within the CpG islands producing 5-methylcytosine residues (Lao and Grady, 2011). Hypermethylation of CpG

islands - within the promoter region of genes - results in their transcriptional silencing by interfering with sequence specific binding of transcription factors. CRCs with high methylation frequencies are described as CpG island methylator phenotype (CIMP) high and they all share distinctive molecular and clinicopathological characteristics that may include MSI-high, BRAF mutations, epithelial serration (sessile serrated adenomas) and localisation in proximal colon (Spring et al., 2006).

1.3.5 Modelling the pathways leading to CRC based on genetic alterations and clinicopathological features

Adenomas are defined as confined small lesions that protrude above the surrounding mucosa and to date are considered as precursors of CRC (Brenner et al., 2007). However, only a small percentage of these benign lesions progress to adenocarcinomas. Reportedly, patients bearing adenomas with an average size of 1 cm have 10-15% chances of developing cancer over a significantly prolonged period of time that in some cases extents to over 10 years (Stryker et al., 1987). In this regard, the occurrence of adenomas in individuals at the age of 50 is estimated at 12%, with more than 25% of these treated as cases with high-risk lesions. Notably, in Western countries, the prevalence of adenomas rapidly increases at around 50% after the age of 50 (East et al., 2017).

Morphologically, adenomas can be divided into pedunculated adenomas (with a stalk) and sessile adenomas (without a stalk). Conventional adenomas can be further characterised based on their histology as tubular, tubulovillous and villous adenomas (Shinya and Wolff, 1979). In addition, over the recent years the existence of hyperplastic polyps which are considered as precursor lesions of the serrated pathway (Serrated pathway will be discussed below) has been widely accepted. These polyps are now being identified as serrated polyps, and have been distinguished by World Health Organisation (WHO) in 3 different types: hyperplastic polyps (HP), sessile serrated adenomas/polyps (SSA/Ps) and traditional adenomas (TSAs) (Jass, 2007; Bettington et al., 2013). Most hyperplastic polyps are localised in the distal colon and their diameter does not exceed the 5mm. Morphology of hyperplastic polyps in micrographs is commonly characterised by straight arrangement of the villi/crypts and proliferation zones limited at the lower compartment of the crypt (Torlakovic et al., 2008). SSA/Ps which are often bigger than hyperplastic polyps, localise predominantly in the

proximal colon and account for approximately 15-20% of all major precursor lesions. Crypt organisation in SSA/Ps demonstrates irregularities which are reflected by dilatation of the base of the crypts, branched or dysmature crypts as well as crypts with distinctive L- or inverted T- shapes (East et al., 2017; Torlakovic et al., 2008). Lastly, TSAs, which are mainly found in the distal colon, account for approximately 1% of the serrated polyps. These lesions are described by ectopic crypt formation, in which case the crypts do not invaginate fully in the muscularis mucosa (Bettington et al., 2015)

After almost 3 decades, Fearon's and Vogelstein's simplified model of adenoma – carcinoma sequence (Fearon and Vogelstein, 1990) (Figure 1-5) remains fundamental and evolves as the research's community collective effort adds new findings to further extent our understanding of the complexity of the disease. According to Vogelstein's model, APC driven adenomas develop to carcinomas via the progressive accumulation of mutations in at least seven genes, such as *KRAS, SMAD4, PI3KCA* and *TP53*, (Fearon and Vogelstein, 1990; White, 1998; Polakis, 2000) (Figure 1-5).

Unique histopathological features as well as identification of common genetic aberrations within the distinct premalignant precursors and tumours, gave researchers the possibility to further classify CRCs in 3 distinctive evolutional routes. Accordingly, the traditional pathway, which has been described by Vogelstein as the adenoma-carcinoma sequence, is the most common, with prevalence of approximately 50-70% of CRC cases. Adenocarcinomas, usually located in the distal colon, can rise from tubular, tubulovillous or villous adenomas after the successive accumulation of mutations in *APC, KRAS, PI3KCA, TP53* and CIN. Alternatively, the serrated pathway occurs in approximately 10-20% of the CRCs. As mentioned previously, in the serrated pathway, the transformation of normal mucosa to adenocarcinoma occurs via precursor lesions named ''serrated polyps'', which are identified with BRAF mutations and CIMP-high/MSI-high. This pathway results in tumours localised predominantly in proximal colon and typically feature CIMP, MLH1 deficiency, MSI and relatively good prognosis (Pancione et al., 2012). A third more heterogeneous pathway gives rise to colorectal tumours via partially serrated villous adenomas, SSA/P or TSA, which are characterised by KRAS, BRAF, APC mutations as well as moderate CIMP phenotype, absence or moderate MSI and generally poor prognosis. This pathway is common among 10-30% of all CRCs. Lastly, studies also describe the occurrence of a more infrequent pathway, which involves the de novo ''birth''

of tumours from normal epithelium, without the pre-existence of intermediate precursor lesions (Minamoto et al., 1994; Umetani et al., 2000). These superficial-type of tumours are driven by *APC* and *TP53* mutations and exhibit a significant association with LOH at chromosome 3p. Nonetheless, as reviewed by Yamagishi et al., in 2016, colorectal carcinogenesis as a complex heterogeneous disease may result occasionally by convergence of these pathways and amalgamation of different genotypes (Yamagishi et al., 2016).
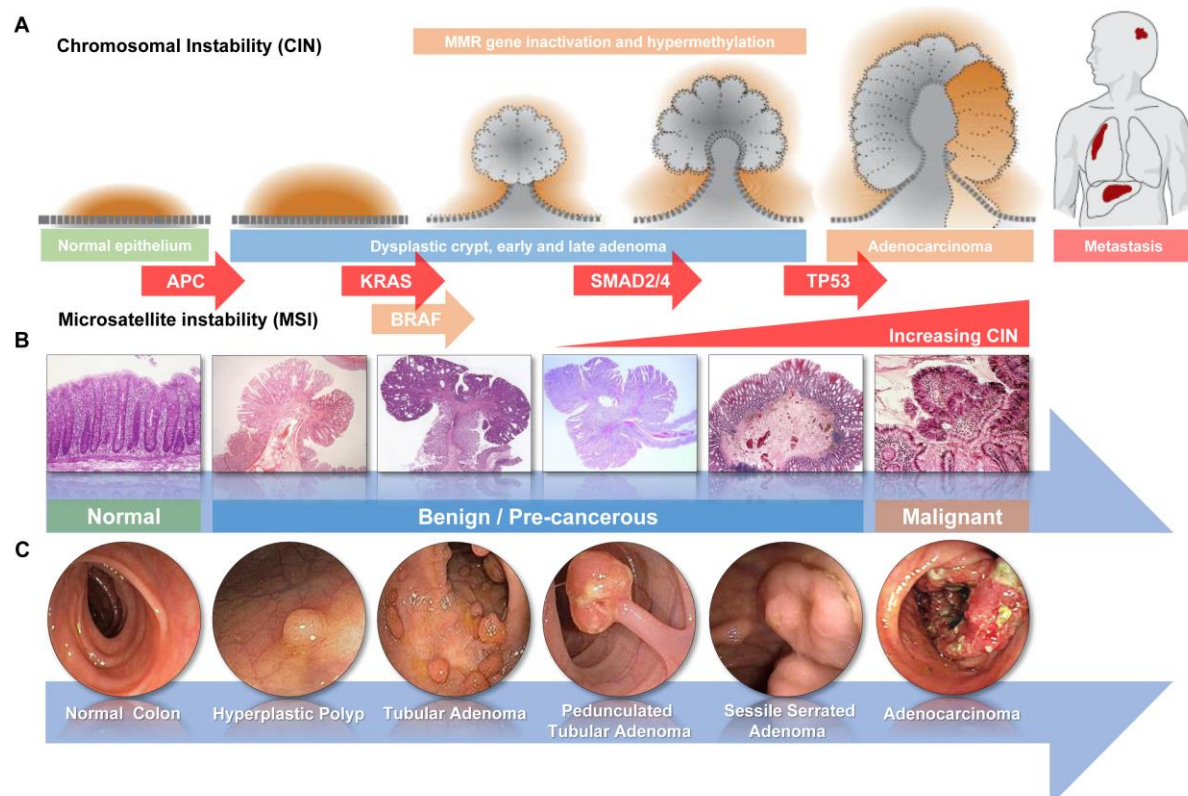
Figure 1-5: Modeling the progression of CRC from normal epithelium to cancer (A) Schematic representation of morphological and genetic changes occuring during the transformation of normal colonic epithelium to adenocarcinoma and metastasis (Diagram adopted from DiPiro et al., 2011). (B) Micrographs of normal colonic epithelium, benign/pre-cancerous lesions and malignant adenocarcinoma (C) Colonoscopy pictures presenting stereomorphological characteristics of normal colon, hypeplastic polyps, tubular and pedunculated tubular adenomas, sessile serrated adenomas and advanced adenocarcinomas (Colonoscopy Images acquired from www.kolumbus.fi)

1.3.6 Molecular Subtypes in CRC – A synopsis

As discussed, CRC is a complex heterogeneous disease driven by the accumulation of multiple genomic alterations that can give rise to tumours with distinct molecular, clinicopathological characteristics, as well as differential drug responses and clinical outcomes (Souglakos et al., 2009). As described previously, CRCs can be initiated by three different molecular pathways that involve CIN, MSI and CIMP. Among others, detection of KRAS and BRAF mutations as well as TNM scoring and MSI status assessment have been implemented in clinical practice to guide the clinical patients management and predict response to adjuvant chemotherapy in CRC. For instance, detection of KRAS/NRAS mutations in CRC patients, has been used as a predictive biomarker to exclude patients from anti-EGFR targeted therapies (Raponi et al., 2008, Souglakos et al., 2009), yet the response rates of KRAS/NRAS wild-type patients to anti-EGFR monotherapy fluctuates somewhere between 20-30% (Rodriguez-Salas et al., 2016). This paradigm highlights the importance of intratumoural and interpatient heterogeneity in CRC as well as the complex interplay between alternated pathways driven by genetic instability. Combinations of these factors, along with hormonal changes, comorbidities and external influences, such as diet may contribute further to differential responses to drug treatments (Rodriguez-Salas et al., 2016), thus further increasing the demand for more robust patients stratification.

Utilising gene expression profiling from large datasets of CRC specimens, several independent research groups managed to identify CRC subtypes. Via an unbiased, hierarchical clustering, these tumours were classified in 4 distinctive molecular subtypes (Consensus Molecular Subtypes, CMS) (Sjoblom et al.,2006; Leary et al., 2008; Vogelstein et al., 2013; De Souza E Melo et al., 2013 (Sadanandam et al., 2014).).

Accordingly, CMS1 (14% of cases) includes patients with a hypermutation, hypermethylation phenotype and high frequency of BRAF^{V600E} mutations, along with a strong immune infiltration of the tumour microenvironment and worse survival after relapse. The CMS2 which accounts for the 37% of tumours, is driven by mutations in *APC, KRAS, TP53*, and *PI3KCA* and follows the conventional adenoma – carcinoma sequence first described by Vogelstein. CMS3 (13% of CRC cases) is identified as the metabolic subtype and is driven by KRAS oncogenic transformation and alterations in metabolic pathways, such as glycolysis and lipid metabolism. Finally, CMS4 which accounts for a substantial 23% of cases, is characterised as

the mesenchymal subtype with a TGF-β signature as well as activation of angiogenesis, stromal infiltration and activation of the epithelial mesenchymal transition (EMT) (Figure 1-6). This subtype has been associated with worse relapse-free and overall survival (Dienstmann et al., 2017).
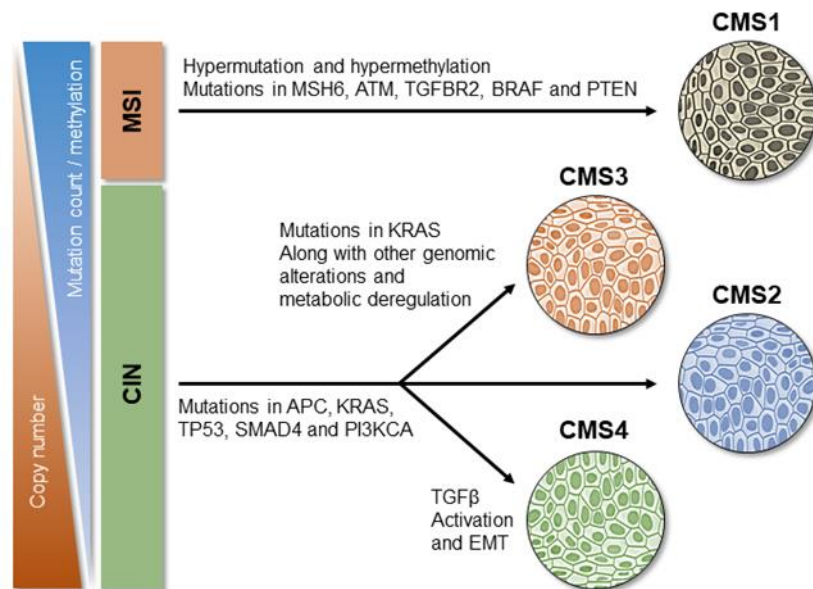
Figure 1-6: CRC transcriptomic subtypes. *Alternative ways of colorectal adenoma–carcinoma sequence with accumulation of genomic and epigenomic aberrations. CMS1 is characterised by a hypermutation, hypermethylation phenotype and augmentation for BRAF^{v600E} mutations, along with a strong immune infiltration of the tumour microenvironment. CMS2 is driven by mutations in APC, KRAS, TP53, and PI3KCA following the conventional adenoma – carcinoma sequence whereas, CMS3 and CMS4 evolve from CMS2 via truncated mutations. CMS3 is identified as the metabolic subtype and is driven by KRAS oncogenic transformation and alterations in metabolic pathways. Finally CMS4 is characterised by activation of TGF-β as well as a strong EMT signature. (Adapted from Dienstmann et al., 2017)*

1.4 Staging of Colorectal Cancer

The staging methodology ''tumour-node-metastasis'' (TNM) has been extensively utilised to classify CRC cases, predict prognostic outcome and support treatment strategies in clinical practice. It was firstly introduced by Denoix (Denoix, 1954) and the American Committee on Cancer (AJCC) and Union against Cancer (UICC) (Zinkin 1983, Jessup et al., 2002), as a staging system that could overcome the limitations and confusion of previously used methods. As a result TNM rapidly replaced the previously used Dukes' staging system (Dukes, 1923, De Vita et al., 2001). Briefly, the Dukes' staging consists of four distinct stages A, B, C and D. Stage A refers to lesions that have not penetrated the colonic and rectal wall and are restrained within the mucosa. Stage B which indicates extrarectal/extracolonic invasion without lymphoid involvement is further divided in B1 and B2, depending on whether the tumours have invaded into the mucosal propria (B1) or have not (B2). Similarly to B, Stage C is sub classified into Stage C1 and C2. C1 defines rectal and colonic tumours that are positive within the lymph nodes but have not invaded through the colorectal wall, and C2 tumours that are positive for lymph node invasion and have also penetrated the colorectum. Finally, Dukes Stage D indicates the presence of metastasis to distant organs (Figure 1-7) (Astler and Coller 1954, Beahrs, 1982, Turnbull, 1975).

The newer and more unified TNM system involves the identification / characterisation of 3 distinct tumour features that are assessed accordingly based on tumour localisation and size (T), involvement of the lymph nodes (N) and presence or absence of metastasis (M) (Table 1-1). Combination of these categories into stage groups describes prognosis and guides treatment strategies for individual patients. Accordingly, Stage I patients are characterised by good prognosis (90% 5-year survival rate) with limited invasion of the colorectal wall and no evidence of nodal involvement and presence of metastasis. Patients with Stage II CRC have an 80% survival rate at 5-year. They are characterised by a more advanced disease where there is evident penetration of the colorectal wall but similarly to Stage I no lymph node invasion nor metastasis are present. Stage III disease describes patients with nodal invasion and a 5-year survival rate reduced to 60% and, finally, Stage IV identifies patients with metastatic disease and the poorest prognosis (~10% 5-year survival rate) (Horton et al., 2005). Sub classifications comparison of the different staging methods is presented in Table 1-1.
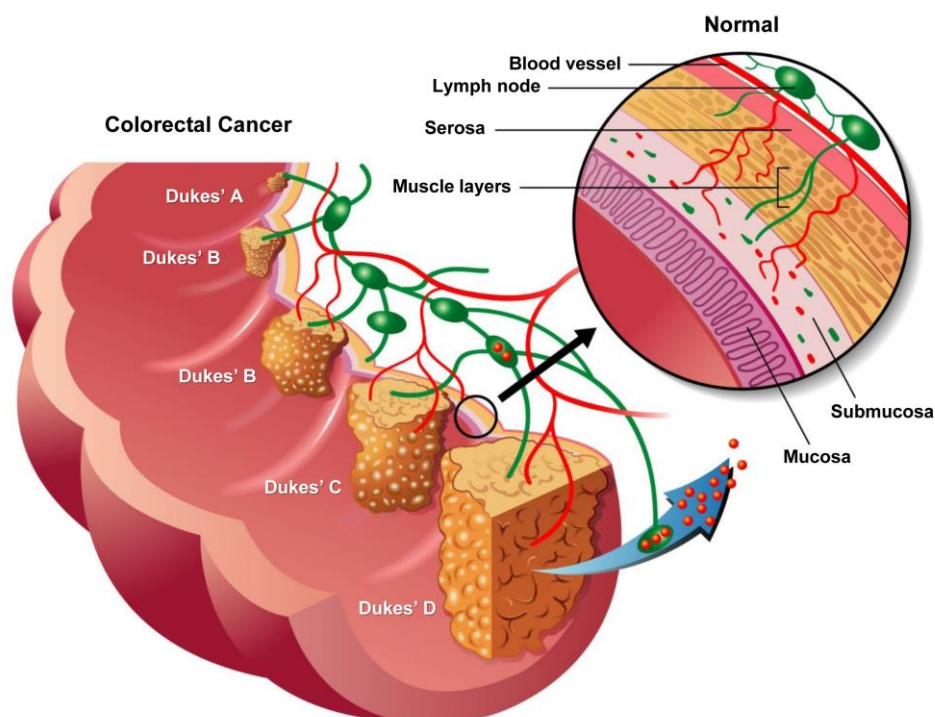
Figure 1-7: CRC staging as defined by Dukes Staging Method. Dukes Stage A: *lesion has infiltrated the mucosa of the intestinal wall and has not spread to the submucosa,* ***Dukes Stage B:*** *Lesion has penetrated the muscle layer and in later stages could also spread though the serosa in nearby tissues,* ***Dukes Stage C:*** *Lesion has expanded through the mucosa and grown into the muscle layers. Lymph node infiltration is also present at this point,* ***Dukes Stage D****: Carcinoma has grown throughout most layers of the intestinal wall, spread into nearby lymph nodes and possibly to distant sides. (Colon Cancer Vector acquired from 123F.com)*

Table 1-1: American Joint Committee on Cancer Stage Groupings for Colorectal Cancer - Comparison between Dukes' and TNM staging systems. Tis: *in situ carcinoma,* ***T1:*** *submucosa,* ***T2:*** *muscularis propria,* ***T3:*** *subserosa,* ***T4:*** *other organs,* ***N0:*** *no node metastasis,* ***N1:*** *1-3 nodes,* ***N2:*** *>4 nodes,* ***M0:*** *no distance metastasis,* ***M1:*** *distant metastasis.* ***MAC:*** *modified Astler-Coller classification based on Dukes' Staging. Adopted by Horton et al., 2005*

Stage	T	N	M	Dukes	MAC
0	Tis	N0	M0	-	-
I	T1	N0	M0	A	A
	T2	N0	M0	A	B1
IIA	T3	N0	M0	B	B2
IIB	T4	N0	M0	B	B3
IIIA	T1-T2	N1	M0	C	C1
IIIB	T3-T4	N1	M0	C	C2/C3
IIIC	Any T	N2	M0	C	C1/C2/C3
IV	Any T	Any N	M1	-	D

1.5   Chemotherapy of CRC

Due to the high intratumoural and interpatient heterogeneity CRC treatment approaches and responses to drugs vary. To date, treatment options depend primarily on CRC staging at diagnosis. Surgery is the first-line treatment for most stage I-III localised cancers. Complete excision of primary colonic tumours can increase the overall 5-year survival to approximately 90% and 70% in stage II and stage III CRC respectively (Siani and Pulica 2014). For advanced staged III and IV CRCs, chemotherapy may precede surgery (neoadjuvant therapy) to reduce tumour volume or follow surgical resection (adjuvant therapy) to minimise the risk of relapse. Alternatively, chemotherapy can also be used as a palliative option to improve the quality of life and prolong survival of terminal CRC patients. The most commonly used chemotherapeutic drugs with relevance to this dissertation are Fluorouracil and Oxaliplatin.

1.5.1   5-Fluorouracil

The fluoropyrimidine 5-Fluoruracil (5-FU) is a uracil analogue that belongs to the widely used family of antimetabolite drugs. Intracellularly, 5-FU can be metabolised in three distinct metabolites, namely, fluorodeoxyuridine monophosphate (FdUMP), fluorodeoxyuridine triphosphate (FdUTP) and flourouridine triphosphate (FUTP). Formation of these metabolites results in subsequent inhibition of thymidylate synthase (TS) and disruption of RNA functions (Longley et al., 2003). TS is a dimeric enzyme that catalyses the conversion of deoxyuridine monophosphate (dUMP) to deoxythimidine monophosphate (dTMP), ultimately providing cells with thymidylate which is essential for DNA replication and repair. The methyl group required for the reductive methylation of dUMP to dTMP by TS is provided by the 5, 10-methylenetetrahydrofolate (CH_2THF) which directly binds on TS. FdUMP blocks the interaction of dUMP with TS via direct binding to the nucleotide-binding site of TS and ternary complex formation with CH_2THF (Sommer and Santi., 1974; Santi et al., 1974). Alternatively, RNA function is heavily disrupted via extensive incorporation of FUTP in the newly synthesised RNA. This results in both inhibition of RNA maturation (Kanamaru et al., 1986; Ghostal and Jacob, 1994) and disruptions in post transcriptional modifications of tRNAs (Santi and Hardy, 1987; Randerath and et al., 1983).

1.5.2 Oxaliplatin

Oxaliplatin {[oxalate (2-)-O, O'] [1R, 2R-cyclo-hexanediamine-N, N'] platinum-(II)} is one of the most commonly used diaminocyclohexane (DACH) platinum based anticancer drugs in the clinic. Similarly to cisplatin and carboplatin, oxaliplatin forms a spectrum of analogous adducts between adjacent GG or GA residues, ultimately leading to disruption of DNA replication and transcription (Todd et al., 2009, Fink et al., 1997).

Bolus administration of 5-FU or Capecitabine orally, in combination with Irinotecan or Oxaliplatin are to date the first options in neoadjuvant and adjuvant chemotherapy of CRC. Clinical trials have shown that combination treatments of 5-FU with Oxaliplatin and Leucovorin (FOLFOX) or Irinotecan (FOLIFIRI) (Van Cutsem et al., 2014) deliver response rates around 40-50% (De Gramont et al., 2000, Douillard et al., 2000). Alternatively, for the treatment of metastatic CRC (mCRC) combinations of monoclonal immunotherapies with bevacizumab (anti-VEGF), cetuximab (anti-EGFR), fluoropyrimidines and Oxaliplatin or Irinotecan have also shown to improve the response of patients (Van Cutsem et al., 2009, Van Cutsem et al., 2011, Bokemeyer et al., 2011, Douillard et al., 2013, Van Cutsem et al., 2015, Bokemeyer et al., 2015, Hurwitz et al., 2004, Saltz t al., 2008).

Despite the encouraging improvements in patient's response rates, these chemotherapeutic drugs often result in normal tissue toxicity which may include lower numbers of neutrophils, neurotoxicity, diarrhoea, stomatitis and necrosis at the site of the intravenous injection (Dranitsaris et al., 2007, Todd et al., 2009, de Gramont et al., 1997, Ocvirk et al., 2010).

1.6 Cancer Metabolism – An Emerging Hallmark of Cancer

CRC remains until now one of the best described paradigms of intratumoural and interpatient heterogeneity (Souglakos et al., 2009). It represents a complex disease with multiple genetic drivers that can give rise to tumours characterised by sustained proliferative signalling, replicative immortality, resistance to cell death, inactivation of tumour suppressor genes, invasion and metastasis (Hanahan and Weinberg 2000). In 2011, Hanahan and Weinberg introduced the concept of metabolic reprogramming as one of the new emerging hallmarks of cancer. The high proliferative status of cancer cells is not solely supported by uncontrolled cell proliferation but often involves modifications in cellular metabolism to support the rapidly proliferative cells with essential nutrients and energy in a rather dynamic and often nutrient derived microenvironment. With regards to this anomalous metabolic rewiring, ''aerobic glycolysis'' was one of the first metabolic alterations observed and described by Warburg in the early 20th century. (Warburg 1930; 1956). Accordingly, highly metabolically active and glucose demanding cancer cells, metabolise large amount of glucose via glycolysis rather than oxidative phosphorylation even in the presence of sufficient oxygen supply. It was then found that glycolysis covers the demand of cancer cells for energy and intermediate macromolecules much faster, but also contributes to achieving redox homeostasis through balancing of NADPH/NADP+ and NADH/NAD+ (Hu et al., 2017). Years later scientists managed to exploit and incorporate this knowledge into clinical practice, as 18F-deoxyglucose-positron emission tomography (18-FDG-PET) became one of the standard imaging methods used to-date in cancer imaging (Cohade et al., 2013). 18-FDG-PET exploits the glucose avidity of cancerous tissue compared to the normal surround tissue. Since then the discovery of several other metabolic alterations in human cancer rendered metabolism one of the most exciting and promising fields in cancer research. Indeed, one of the most successful examples of anticancer therapy is the use of antimetabolites such as methotrexate and the previously described fluoropyrimidines, which primarily target nucleotide metabolism (Van der Heiden, 2011).

1.6.1 Metabolic Reprogramming in Cancer

The substantial development in analytical tools and the fast advancement in cancer genomics and metabolomics over the past decades have substantially reshaped and deepened our understanding of the metabolic rewiring in cancer. The limited availability of nutrients makes the metabolic adaptations a necessity for cancer growth and survival (Van der Heiden et al., 2011, Newsholme et al., 1985, Tatum et al., 2006). Through rewiring of their metabolism, the rapidly dividing cells are able to support their needs for energy (ATP), macromolecules and the maintenance of an appropriate cellular redox status (Cairns et al., 2011). Intriguingly, emerging evidences indicate the close association between metabolic activities and oncogenic signalling pathways (Figure 1-8). As discussed previously (Section 1.3.2, 1.3.3), RAS/MAPK and PI3K/AKT cascades can be triggered in response to external growth factors or mutations (Alberolalla et al., 2003, Ramijaun, 2007, Ahmad et al., 2011; Vara et al., 2004). Activation of PI3K/AKT signalling results in increased glucose intake, which is supported by increase in the expression and enhanced membrane translocation of the glucose transporter (GLUT1), (Lien et al., 2016). Transcriptional regulation of GLUT1 by PI3K occurs via multiple mechanisms which may include, activation of c-Myc (Osthus et al., 2000) or mTORC1 which regulates indirectly hypoxia induced factor 1 α (HIF1α) (Thomas et al., 2006; Wieman et al., 2007; Duvel et al., 2010). PI3K/AKT signalling can alternatively enhance glycolysis via phosphorylation and enzymatic activation of phosphofructokinase (PFK), (Lee et al., 2017). Finally, mTORC1 AKT-driven activation results in increased protein, lipid (Krycer et al., 2010, Yang et al., 2002) and nucleotide biosynthesis (Saxton and Sabatini, 2017).

The oncogenic activities of c-Myc have been described in several types of cancers – and are mostly characterized by the transcriptional activation of multiple genes and microRNA's involved in cellular proliferation (Munoz-Pinedo et al., 2012). Studies over the past decade demonstrated that c-Myc regulates glutaminolysis directly by increasing the glutamine intake and by promoting expression of glutaminase 1 (GLS1), the first enzyme of glutaminolysis (Gao et al., 2004). As mentioned above, c-Myc contributes to the Warburg effect (increased aerobic glycolysis) through the enhanced expression of the glucose transporter GLUT1 and lactate dehydrogenase A (LDHA) (Dang et al., 2009). In summary, these examples outline the ability of oncogenes to induce metabolic reprogramming necessary to sustain the growth of rapidly proliferating cancer cells (Figure 1-8).
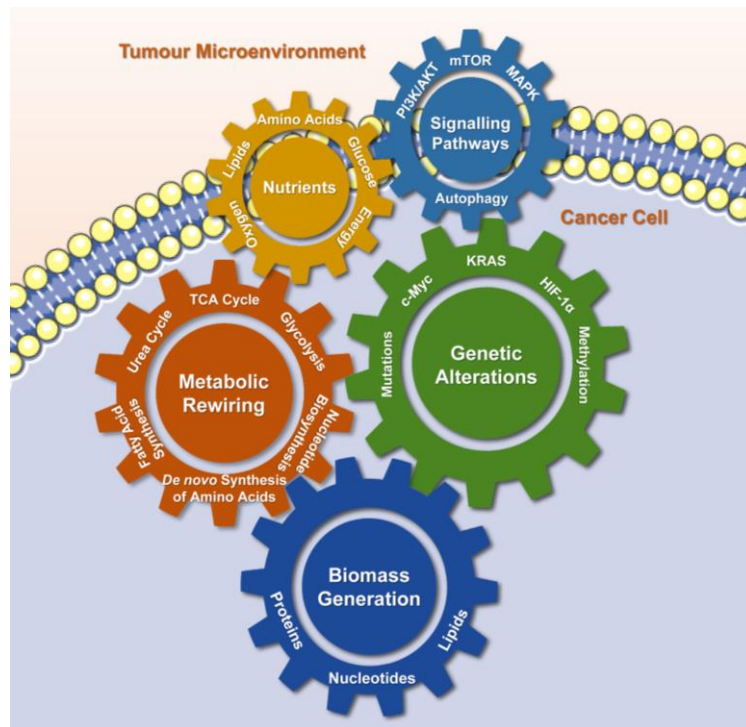
Figure 1-8: Interactions between Metabolic and Genetic Reprogramming in Cancer (Adapted from Sciacovelli et al., 2014)

1.6.2 Arginine Metabolism

Arginine, is generally classified as a non-essential amino acid due to its sufficient endogenous synthesis in adult humans. However, during early developmental stages, or in cases of infection and inflammation or small intestine and kidney dysfunction, insufficient levels of endogenous synthesis may render arginine conditionally essential (Flynn et al., 2002; Barbul, 1986; Abumrad and Barbul, 2004). Arginine is often characterised as one of the most versatile amino acids in mammals. Beyond its role in protein synthesis as a structural component of proteins, it serves as a precursor for the synthesis of several other biomolecules, including polyamines (putrescine, spermidine and spermine), creatine, nitric oxide (NO), urea, proline, glutamate and agmatine (Morris et al., 1998). In adult humans, the *de novo* synthesis of arginine involves the synergistic metabolic functions of both the small intestine and kidney. The spatial and differential expression of the arginine metabolic enzymes results in the intestinal release of citrulline into the blood circulation and its uptake and conversion into arginine by the kidney. More specifically, the epithelial cells of the small intestine utilise glutamine, glutamate and proline to synthesise ornithine which is then converted into

citrulline before being released into the blood circulation. The synthesis of citrulline from ornithine is catalysed by two enzymes, namely, ornithine transcarbamylase (OTC) and carbamoyl synthase 1 (CPS-1) (Figure 1-9). More specifically ornithine, along with carbamoyl phosphate, which is synthesised from bicarbonate and ammonia via the action of CPS-1, are utilised by OTC to synthesize citrulline. Once released in blood circulation, citrulline is absorbed by the tubular cells of the kidney, where in a two-step enzymatic process, argininosuccinate synthase (ASS1) converts citrulline and aspartate into argininosuccinate, whereas argininosuccinate lyase (ASL) converts argininosuccinate into fumarate and arginine (Figure 1-9 and Figure 1-11) (Morris et al., 1998). Alternatively, citrulline can also be utilised by several other cell types for the *de novo* synthesis of arginine. These cell types include macrophages, endothelial cells, adipocytes, myocytes and neurons (Eagle, 1959; Jackson et al., 1986; Morris, 1999). Despite the fact that arginine is classified as a non-essential amino acid, its *de novo* synthesis via the intestinal – renal axis is responsible for only 5-15% (30% in new-borns) of the total arginine, with most of the arginine's need satisfied through nutrition and protein degradation (Morris et al.,1998). (Delage et al., 2010). Under normal conditions arginine metabolism can be compartmentalised according to tissue function. Accordingly, arginine and urea cycle in the liver are used for the elimination of nitrogenous waste, whereas endothelial cells use arginine as an intermediate to generate NO through the citrulline cycle (Husson et al., 2003).
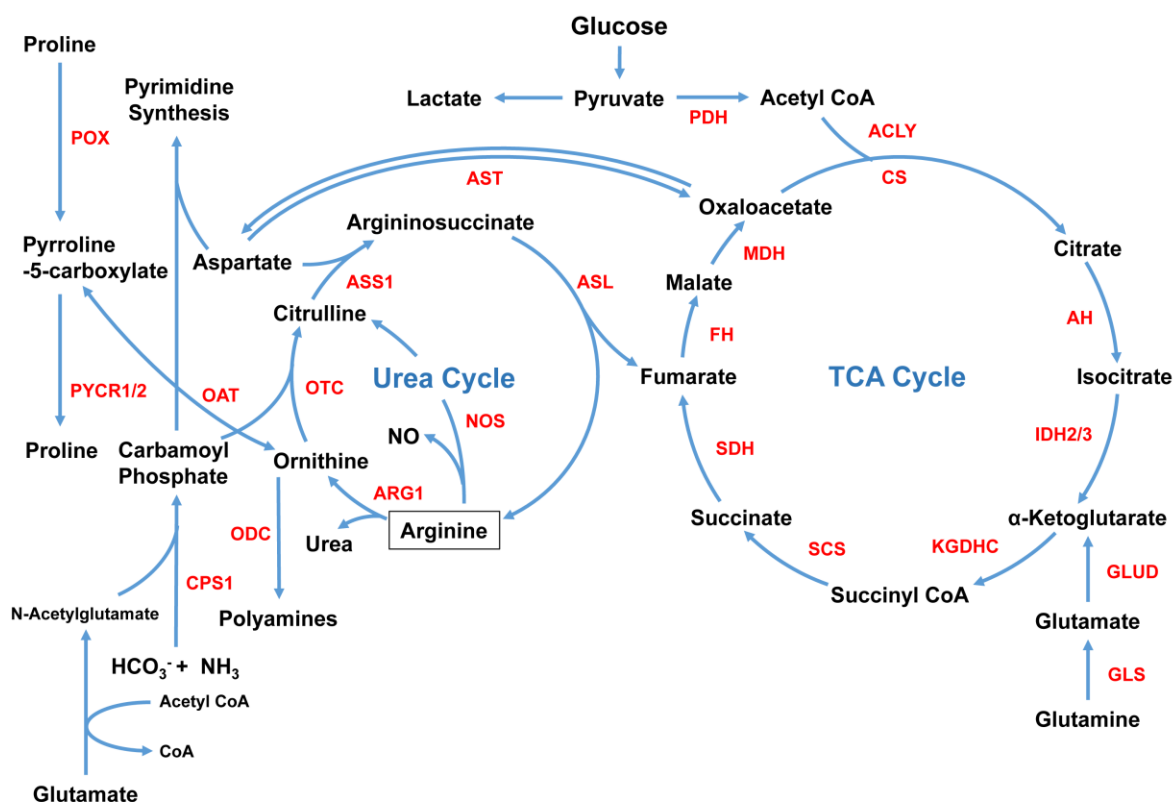
Figure 1-9: Urea and TCA Cycle, *Abbreviations:* ***POX:*** *Proline Oxidase;* ***PYCR1/2:*** *Pyrroline 5 Carboxylate Reductase 1/2;* ***CPS1:*** *Carbamoyl-phosphate synthase 1;* ***ODC:*** *Ornithine Decarboxylase;* ***OAT:*** *Ornithine Aminotransferase;* ***OTC:*** *Ornithine Transcarbamylase;* ***ASS1:*** *Argininosuccinate Synthase 1;* ***ASL:*** *Argininosuccinate Lyase;* ***NOS:*** *Nitric Oxide Synthetase;* ***ARG1:*** *Arginase 1;* ***FH:*** *Fumarase;* ***SDH:*** *Succinate Dehydrogenase;* ***SCS:*** *Succinyl-CoA synthase;* ***KGDHC:*** *α-Ketoglutarate Dehydrogenase;* ***GLUD:*** *Glutamate Dehydrogenase;* ***GLS:*** *Glutaminase;* ***IDH2/3:*** *Isocitrate dehydrogenase;* ***AH:*** *Aconitase;* ***CS:*** *Citrate Synthase;* ***PDH:*** *Pyruvate Dehydrogenase;* ***ACLY:*** *Adenosine Triphosphate Citrate Lyase;* ***MDH:*** *Malate Dehydrogenase (Adopted from Kuo and Feun. 2010).*

1.6.3 Regulation of Growth Proliferation and Survival by Arginine Availability: the crucial role of the mTOR pathway

In humans, the mammalian target of rapamycin (mTOR) signalling responds to nutrient availability, mainly amino acids, and regulates protein synthesis and other metabolic pathways, such as nucleotide and fatty acid synthesis (Saxton and Sabatini, 2017). When nutrients are abundant, mTOR signalling is activated to enhance protein synthesis and anabolism of nucleotides and lipids. mTOR is a serine/threonine kinase, which exists as part of two distinct heteromeric complexes, the mTOR complex 1 (mTORC1), which regulates protein translation and cell proliferation and the mTOR complex 2 (mTORC2), which is primarily responsible for the activation of the PI3K/AKT pathway through direct phosphorylation of Akt (Saxton and Sabatini, 2017). mTORC1 consists of five distinctive protein subunits: the mTOR kinase, the regulatory protein associated with mTOR (RAPTOR) and the mammalian lethal with Sec13 protein 8 (mLST8) (Hara et al., 2003; Kim et al., 2003). The two additional negative regulatory components, are the proline-rich Akt substrate of 40kDa (PRAS40) and DEP domain containing mTOR interacting protein (DEPTOR) (Peterson et al., 2009). mTORC1 activity relies on substrate recruitment mediated by RAPTOR (Nojima et al.,2003) and stabilisation of its kinase activation loop by mLST8 (Yang et al., 2013). On the contrary, mTORC2 contains the rapamycin insensitive companion of mTOR (RICTOR) instead of RAPTOR, along with mTOR, mLST8, DEPTOR (Peterson et al., 2009) as well as Protor1/2 (Woo et al., 2007; Pearce et al., 2007) and mSin1 (Yang et al., 2006; Frias et al., 2006).

Studies have shown that amino acid sensing through the mTORC1 is regulated by both an intra-lysosomal and a cytosolic mechanism. Accordingly, under canonical conditions, sufficient availability of amino acids within the lysosomal matrix stimulates the interaction of the amino acid transporter SLC38A9 with the Rag-Ragulator-v-ATPase complex. This complex further initiates the interaction between Ras-related GTPases (Rag proteins) and the mTORC1, which, in turn, allows the binding between Raptor and mTOR. Rag proteins are heterodimeric GTPases that comprise of RagA, RagB, RagC and Rag D (Sancak et al., 2010; Bar-Peled et al., 2012). Their association with the Ragulator protein at the surface of the lysosomes results in the recruitment of mTOR and subsequent, activation of the mTORC1 on the lysosomal surface which is enabled by the GTP-loaded Ras homolog enriched in the brain G protein (Rheb)

(Figure 1-10) (Jung et al., 2015; Rebsamen et al., 2015; Zoncu et al., 2011; Bar-Peled et al., 2012; Wang et al., 2015).

Alternatively, sensing of leucine and arginine concentrations in the cytosol occurs through a distinct pathway that involves Gap activity toward Rags 1 and 2, GATOR1 and GATOR2 complexes (Bar-Peled et al., 2013). Recent studies have shown that Arginine can activate mTORC1 via direct binding to the cellular arginine sensor for mTORC1 (CASTOR1). Cytosolic arginine promotes the disassociation of CASTOR1 from GATOR2, a known mTOR inhibitor. This relieves mTORC1 from GATOR2 inhibitory activity (Figure 1-10) (Saxton et al., 2016b; Chantranupong et al., 2016) further promoting the activation of mTORC1 by the Rag proteins.

Once assembled and activated the mTORC1 phosphorylates the eukaryotic elongation and initiation factor binding proteins 1-3 (4E-BP1-3) (Brunn et al., 1997; Gingras et al., 1999) and activates the ribosomal protein S6 kinase (p70S6K), which, in turn, then phosphorylates the ribosomal protein S6. Phosphorylation of 4E-BP1 by the active mTORC1 releases the eukaryotic initiation factor 4E (eIF4E) from 4E-BP's inhibitory activity, thus enabling the cap dependent translation of mRNA transcripts involved in growth and cell cycle (Hsieh et al., 2010; Thoreen et al., 2012). Additionally, activation of the ribosomal protein S6 enhances the translation of pyrimidine-rich-5' TOP motifs that promote the production of ribosomal proteins involved in protein synthesis (Peterson and Schreiber, 1998; Dufner and Thomas, 1999).

Recent findings have also characterised mTORC1 as a regulator of nucleotide synthesis. Ben-Sahra et al., in 2016 showed that mTORC1 increases the expression of methylenetetrahydrofolate dehydrogenase 2 (MTHFD2). Accordingly, MTHFD2 is critical for purine synthesis as it provides one-carbon units via the mitochondrial tetrahydrofolate cycle. Additionally, it has been shown the mTORC1 further activates the trifunctional, multi-domain enzyme carbamoyl-phosphate synthetase 2, aspartate transcarbamylase, and dihydroorotase (CAD), which catalysed the first step of the pyrimidine *de novo* synthesis pathway (Ben-Sahra et al., 2013; Robitaille et al., 2013).

mTORC1 does not only promotes growth via protein synthesis but also inhibits the catabolic ''self-eating'' process of autophagy, via inhibition of the UNC-51 like kinases (ULKs) (Dunlop and Tee, 2013).

Autophagy is an evolutionary conserved catabolic process by which proteins and cellular organelles are degraded via engulfment by autophagosomes and fusion with lysosomes in an effort to provide cells with essential energy and macromolecules (Mizushima, 2007; Mizushima et al., 2011). Regulation of this catabolic process is mediated by the expression of autophagy-related genes (ATGs) (Mizushima et al., 2011. As Levy et al., reviewed in 2017, autophagy consists of 5 distinctive steps: ''initiation, nucleation of the autophagosome, expansion and elongation of the autophagosome membrane, closure and fusion with the lysosome, and the degradation of intravesicular products'', followed by recycling of the digested metabolites (Levy et al., 2017). Briefly, under starvation, inactivation of the mTORC1 relieves ULK1 from its inhibitory activity, thus allowing the initiation of autophagy. Activation of autophagy occurs via the ULK1 complex which further activates downstream effectors, including a class III PI3K complex, ATG14 and activating molecule in BECN1-regulated autophagy protein 1 (AMBRA1), ultimately promoting vesicle nucleation and autophagosome formation. Autophagosomal expansion is mediated by ATG5-ATG12 along with ATG16. During this stage LC3A proteins are recruited to the autophagosomal membrane via interactions with phosphatidylethanolamine (PE). The synergistic action of ATG4B and ATG7 conjugates LC3A with PE to produce LC3B which is incorporated into the expanding membrane. Consequently, lysosomal fusion with autophagosomes results in the degradation of their contents, hence supplying cells with macromolecules (Levy et al., 2017).

In response to nutrient stress and amino acid deprivation mTORC1 gets inactivated and this causes opposite effects from the ones previously mentioned, that is extensive induction of autophagy and inhibition of protein translation and nucleotide biosynthesis. (Delage et al., 2012; Syed et al., 2013; Changou et al., 2014).
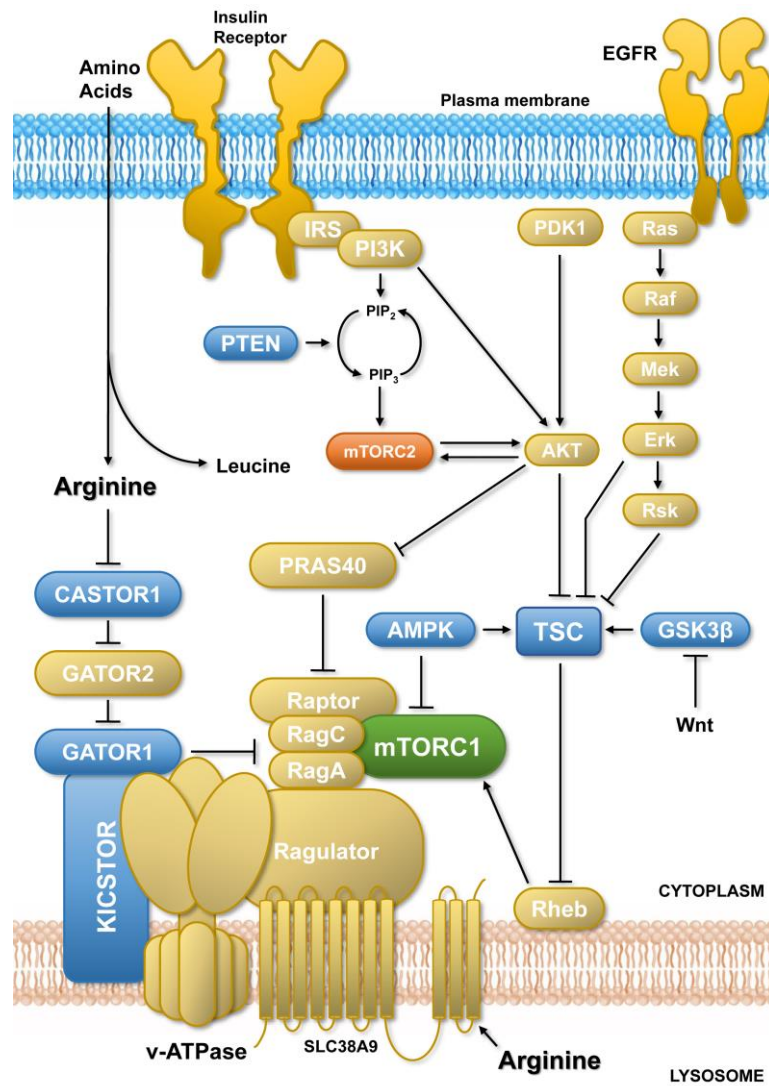
Figure 1-10: mTOR signalling pathway – The amino acid sensing pathway upstream of the mTORC1. (Adapted from Saxton and Sabatini, 2017).

1.6.4 Rewiring of Arginine Metabolism in CRC

Among arginine-derived metabolites, polyamines have been investigated broadly for their implication in CRC development and progression (Gerner and Meyeskens et al., 2004; Gerner, 2010; Basuroy and Gerner, 2006; Vargas et al., 2012). Their involvement in transcriptional control via stabilization and remodelling of chromatin structures (Childs et al., 2003) as well as the translational regulation via promoting phosphorylation changes or unique post translational modifications, such as hypusination of proteins of the translational machinery (Landau et al., 2010) highlight their importance in cell growth and cancer development.

Ornithine decarboxylase (ODC), the first enzyme and the rate limiting step in polyamine synthesis that converts ornithine to putrescine, has been shown to be regulated by the Wnt signalling pathway (Fultz and Gerner 2002). Accordingly, ODC expression is driven by c-Myc, a transcriptional regulator controlled by the Wnt signalling (TC et al., 1998, Bello-Fernandez et al., 1993). In fact, c-Myc upregulation driven by loss of APC in CRC results in increased levels of ODC and polyamine concentrations within the tumours. Reportedly, some polymorphisms of the *ODC* gene, are considered as risk factors for CRC (Martinez et al., 2003). In the FAP mouse model, small intestine exhibits significantly increased concentrations of polyamines and ODC, in comparison to normal mice (Erdman et al., 1999), thus supporting the rationale of targeting polyamine biosynthesis. Accordingly, pharmacological inhibition of ODC using difluoromethylomithine (DMFO) has been investigated as a potential target for the treatment and prevention of CRC (Gerner and Meyeskens et al., 2004; Gerner, 2010; Basuroy and Gerner, 2006; Vargas et al., 2012). Despite restricted antitumor efficacy in late stage tumours (Horn et al., 1987), DMFO has shown promising antigrowth capabilities in early stage adenomas (adenomatous polyps) in both humans (Meyskens et al., 2008) and animal studies (Ignatenko et al., 2011).

Arginine can also be catabolized into NO via the oxidative pathway. The enzyme responsible for this conversion is nitric oxide synthase (NOS) and exists in three distinct isoforms eNOS (endothelial), iNOS (inducible) and nNOS (neuronal). Although NO is well known for its involvement in neurotransmission and vasorelaxation, it is also implicated in several metabolic processes which further affect cell proliferation (Korde et al., 2013). Upregulation of NOS in CRC tumours implies that NO and or its reactive by-products derived from these enzymes play a critical role in colon carcinogenesis via regulation of proliferation and

apoptosis (Zafirellis et al., 2010). Recent evidence from Lu et al., 2013 reveal that there is a significant accumulation of arginine and citrulline in CRC tumours which is also accompanied by a significant increase of the arginine transporter CAT-1. Taken together, the authors report that overexpression of CAT-1, ASS1, ASL and NOS suggest the presence of an accelerated arginine metabolism that channels the exogenous arginine to different biosynthetic routes, therefore implying that CRCs may be arginine dependent (Lu et al., 2013).

Animal studies indicate that arginine and several of its end product molecules (such as polyamines and nitric oxide) are implicated in cancer development. The antigrowth capabilities of arginine withdrawal have been reported in the early 30s when Gilroy observed that supplementation of an arginine free diet in mice could result in decrease in growth of tumour allografts (Gilroy, 1930). Several studies followed since then, demonstrating the anti-proliferative effects of arginine deprivation in HELA cells (Lane et al., 1965) and macrophages (Currie et al., 1978). Similar antigrowth capabilities of arginine withdrawal were reported later by Yerushalmi in 2006 in genetically engineered mice (Yerushalmi et al., 2006), whereas removal of dietary arginine demonstrated inhibition of the development of liver metastases (Yeatman et al., 1991). These findings testify the modulatory effect of arginine in cancer development and progression.

1.6.5   Exploiting Arginine Auxotrophy in Cancer

Auxotrophy is the inability of an organism to synthesise *de novo* a specific organic compound essential for its growth (Agrawal et al., 2012). Several cancer types, including melanoma (Ensor et al., 2002) hepatocellular carcinoma (HCC) (Izzo et al., 2004), lymphoma (Delage et al., 2012) and sarcoma (Bean et al., 2016) have been identified as arginine-auxotroph cancers. Their dependency on external supplementation of arginine is emerging as a primary need for cell growth. ASS1 expression has been identified as one of the key biomarkers of arginine auxotrophy. Its decreased expression due to epigenetic silencing has been well documented in several studies (Lan et al., 2014, Huang et al., 2013) and held responsible for ensuing arginine auxotrophy. However, more recently, other enzymes implicated in arginine metabolism have shown deregulated expression. Accordingly, in a subset of glioblastomas,

ASL deficiency plays a significant role in the tumour dependency on external arginine sources (Philips et al., 2013). In addition, Mussai et al., identify patients with acute myeloid leukemia (AML) deficient for ASS1 and OTC reliant on external arginine supplementation and susceptible to arginine depleting strategies (Mussai et al., 2015). Similarly in HCC, ASS1 positive cell lines that lack OTC expression respond to arginine depletion both *in vitro* and *in vivo* (Cheng et al., 2007).

Association between ASS1 downregulation and clinical aggressiveness in several malignancies exposes ASS1 role as a potential tumour suppressor gene. Reportedly, ASS1 deficiency in oesophageal adenocarcinoma has been associated with lymphatic dissemination (Lagarde et al., 2008), whereas in patients with myxofibrosarcoma (Huang et al., 2013), bladder cancer (Allen et al., 2014) and osteosarcomas (Kobayashi et al., 2010) ASS1 downregulation was correlated with worse survival (Lan et al., 2014). Downregulation of ASS1 could further divert exogenous arginine sources towards alternative biosynthetic pathways. In this regard, melanoma tumours with high expression of iNOS, have been linked with ASS1 deficiency and worse prognosis. It is well established that NO is held responsible for induction of pro survival mechanisms in melanoma, hence external arginine sources could feed NO and pro survival signalling (Ekmekoglou et al., 2006; Su et al., 1981). Adding to this, there are also evidences that ASS1 silenced-tumours acquire advantages in both metastatic proclivity and drug resistance (Delage et al., 2010). For instance, in ovarian cancer, ASS1 deficiency has been linked with resistance to platinum-based drugs and further associated with decreased overall survival as well as relapse-free survival (Nicholson et al., 2009). Similarly, in HCC, ASS1 downregulation has also been correlated with resistance to cisplatin (McAlpine et al., 2014), while Kim and colleagues linked decreased ASS1 and inverse P-glycoprotein (P-gp) expression with Doxorubicin resistance in sarcomas (Kim et al., 2016). Finally, in osteosarcomas, ASS1 reduced expression was associated with pulmonary metastasis in post neoadjuvant chemotherapy and curative resection patient samples (Kobayashi et al., 2010), whilst in myxofibrosarcomas stable re-expression of ASS1 promotes a slower closure phenotype in wound healing experiments as well as reduced invasion of tumour cells in matrigel invasion assays (Huang et a., 2013).

Although the reason for ASS1 silencing is still not fully understood, studies suggest that ASS1 loss in cancers promotes pyrimidine synthesis (Rabinovich at al., 2015). As previously described in section 1.6.2, the physiological role of ASS1 is to catalyse the enzymatic

conversion of citrulline and aspartate into argininosuccinate. As Rabinovich et al., reported, selective downregulation of ASS1 in tumours increases the cytosolic levels of aspartate. Accumulation of aspartate, which serves as a substrate for the CAD enzymatic complex, increases pyrimidine biosynthesis via enhanced substrate availability for the CAD enzymes and by increasing CAD phosphorylation by S6 kinase-mTOR axis (Rabinovich at al., 2015).

Arginine auxotrophy has been exploited as a metabolic vulnerability in several malignancies. Cancer cells deficient in either ASS1, ASL or OTC are susceptible to arginine deprivation strategies and pharmacological agents are currently being tested in both pre-clinical and clinical settings for their antitumor efficacy.

As illustrated by Figure 1-11, arginine depletion could be achieved with the use of several arginine-degrading enzymes, such as arginine decarboxylase (ADC), nitric oxide synthase (NOS), arginine deiminase (ADI) and arginase (Morris, 2004). However limited stability, poor enzymatic activity and reduced Km for arginine in $vivo$ render most of them unsuitable for clinic use. Regardless, two of the most potent enzymes, ADI and arginase, have found their way to clinical settings and have been utilised over the recent years with the purpose of archiving arginine depletion in cancer patients.

1.6.5.1 PEGylated Arginine Deiminase (ADI-PEG20)

The ability of the mycoplasma-derived ADI to degrade arginine to citrulline and ammonia was reported as early as the 1930s (Horn, 1933). In 1963 Kraemer described the anti-growth capabilities of mycoplasma strains in murine lymphoma cell cultures in $vitro$ (Kraemer, 1963; Kraemer, 1964). Several years after, Takaku and colleagues demonstrated that the ADI enzyme purified from $Mycoplasma$ $arginini$ was indeed responsible for Kraemer's initial observation (Takaku et al., 1992). The 43kDa protein has an enzymatic activity of 70%, at pH values 6.0 to 7.5 at 50 °C. Its potency to deplete arginine is dramatically higher compared to bovine liver arginase despite the fact that ADI affinity for arginine (Km value = 0.3mM) is 30 times lower (Miyazaki et al., 1987). To overcome the limitations of decreased half-life (~5hr) and high antigenicity in mammals, scientists formulated a PEGylated version of the enzyme (Ni et al., 2008). In this regard, ADI has been conjugated with polyethylene glycol (PEG) molecules (20kDa), via succinimidyl succinate amide bonds, leading to a compound known as

ADI-PEG20. These PEG molecules are highly water soluble synthetic polymers which contribute to extend the *in vivo* half-life of ADI to 7 days (Holtsberg et al., 2002). Intramuscular administration of ADI-PEG20 (5IU/animal) in mice can effectively catabolise free arginine to almost undetectable levels (Beloussow et al., 2002).

To date, the PEGylated ADI has been tested extensively in multiple malignancies in preclinical models and clinical trials. Among others, the anti-tumour efficacy of ADI-PEG20 has been confirmed in HCC (Ensor et al., 2002), prostate cancer (Kim et al., 2009), small cell lung carcinoma (SCLC) (Kelly et al., 2012), pancreatic cancer (Bowles et al., 2008), lymphoma (Delage et al., 2012), melanoma (Stelter et al., 2013), glioblastoma (Syed et al., 2013), myxofibrosarcomas (Huang et al., 2013) and breast cancer (Qiu et al., 2014). Given the promising anti-tumour efficacy of ADI-PEG20 as a single treatment, scientific interest has also focused on assessing the efficacy of ADI-PEG20 in combination with existing chemotherapeutic agents. In summary, studies report that ADI-PEG20 exhibits synergistic and/or additive effects with 5-FU, PI3K inhibitors, Chloroquine (CQ), Pemetrexed, Cytarabine and tumour necrosis factor (TNF) related apoptosis-inducing ligand (TRAIL) in several malignancies, such as prostate cancer, mesothelioma and more recently breast cancer (Kim et al., 2009; Allen et al., 2014; Tsai et al., 201; You et al., 2013; Qiu et al., 2014; Delage et al., 2012).

In Phase I/II clinical trials, intramuscular administration of ADI-PEG20 at 160IU/m^2 per week in patients with metastatic HCC, extended their overall median survival to at least 400 days, with more than 40% of the patients exhibiting response (Izzo et al., 2004). In a similar setting, groups of advanced HCC patients received either 80 or 160IU/m^2 ADI-PEG20 per week for a total period of 6 months. In summary, results from this study demonstrated increased survival of up to 15.8 months without any significant difference between the two doses (Glazer et al., 2010, Yang et al., 2010). Overall, these studies report that administration of ADI-PEG20 was well tolerated with most common adverse effects being fatigue, allergic reactions on the injection site, followed less commonly by diffuse skin rashes, neutropenia and rarely anaphylactic reactions and serum sickness (Philips et al., 2013). A recent large scale (635 patients) randomised Phase III clinical trial in patients with advanced HCC revealed no overall survival benefit. Lack of response was accompanied by increased immunogenicity (anti-ADI-PEG20 antibodies) in patients treated with ADI-PEG20. This was further correlated with an

approximately 45% decrease in mean blood ADI-PEG20 levels at week 12 (Abou-Alfa et al., 2018).

In patients with metastatic melanoma (MM), weekly administration of 160IU/m^2 resulted in 25% clinical responses with at least one patient exhibiting complete response (Ascierto et al., 2005). However, in a similar setting, another Phase I/II clinical trial reported stable disease as the best response (Ott et al., 2013).

In 2013 Szlosarek et al., conducted the first prospective randomised study in mesothelioma (the Arginine Deiminase and Mesothelioma, ADAM study), in an effort to evaluate the role of ASS1 as a predictive biomarker of response to ADI-PEG20 treatment. In this Phase II trial, administration of ADI-PEG20 improved the progression-free survival compared to the group which was receiving best supportive care only (3.2 vs 2.0 months respectively, p value = 0.03) with an additional 46% of the participants exhibiting partial metabolic response by PET-CT (Szlosarek et al., 2013).

In a follow up study, the efficacy of ADI-PEG20 was evaluated in combination with cisplatin and Pemetrexed in ASS1 deficient thoracic cancers. Results obtained from this small scale Phase I dose escalation trail reveal a response rate of 78% (Beddowes et al., 2017). A Phase II/III in malignant pleural mesothelioma is currently on going. Ongoing clinical trials with ADI-PEG20 are presented in Tables 1-2; 1-3.
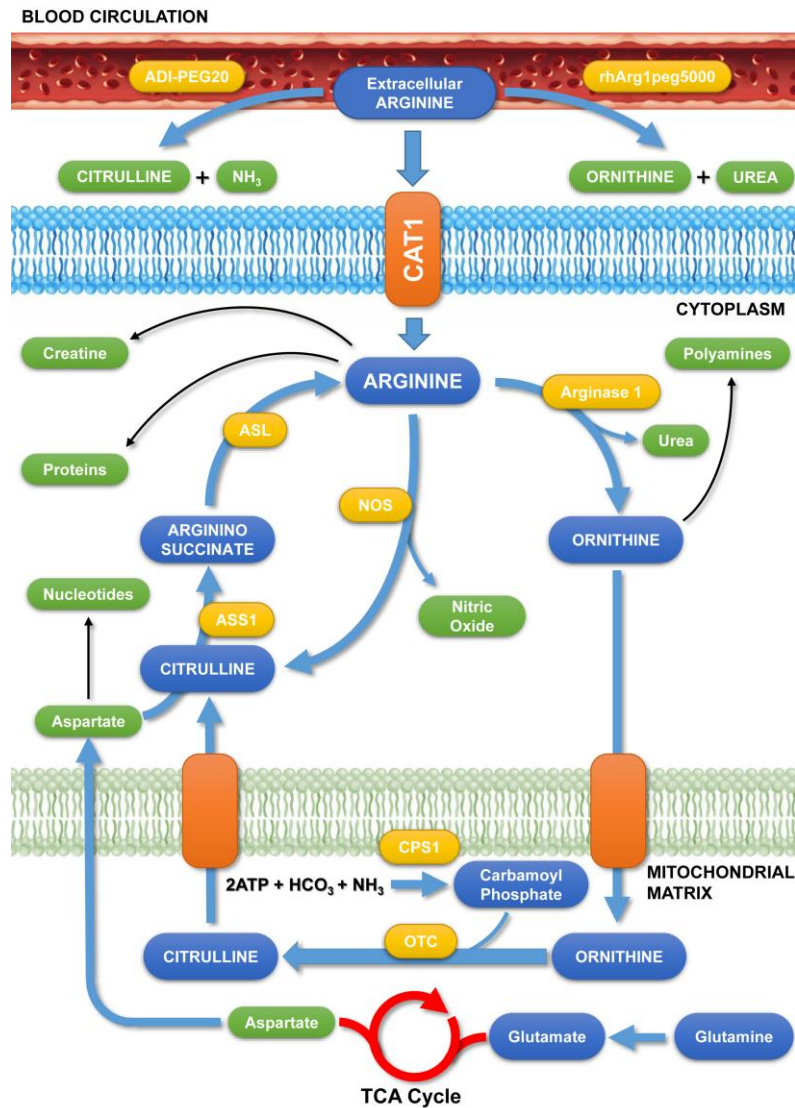
Figure 1-11: Mammalian Metabolism of Arginine – An overview. *Metabolic fate of arginine and arginine intermediate metabolites. Abbreviations: **CAT-1:** cationic amino acid transporter 1 **ASS1:** argininosuccinate synthase 1, **ASL:** argininosuccinate lyase, **OTC:** ornithine transcarbamylase, **CPS1:** carbamoyl phosphate synthase, **NOS:** nitric oxide synthase.*

Table 1-2: Ongoing Clinical Trials for ADI-PEG20 (a), *(Source: www.clinicaltrials.gov)*

	Title	Status	Study Results	Conditions	Interventions	Locations
1	Study ADI-PEG20 Plus Pembrolizumab in Advanced Solid Cancers	Recruiting	No results available	Advanced solid cancers	• Drug: ADI-PEG20 • Drug: Pembrolizumab	Facility National Cheng Kung University, Tainan, Taiwan
2	Phase 1 Study in Subjects With Tumors Requiring Arginine to Assess ADI-PEG20 With Pemetrexed and Cisplatin	Active, not recruiting	No Results Available	Pleural Mesothelioma Malignant, Advanced Peritoneal, Mesothelioma Malignant Advanced, Non-squamous Non-small Cell Lung Carcinoma Stage IIIB/IV (NSCLC), Metastatic Uveal Melanoma, Hepatocellular Carcinoma (HCC), Glioma, Sarcomatoid Cancers	• Drug: ADI-PEG20	Mayo Clinic Rochester, Rochester, Minnesota, United States; Centre for Experimental Cancer Medicine (CECM), London, England, United Kingdom; Cambridge Hospital, Cambridge, United Kingdom; Guys Hospital, London, United Kingdom
3	ADI-PEG20 in Combination With Gemcitabine and Docetaxel for the Treatment of Soft Tissue Sarcoma	Recruiting	No Results Available	Soft Tissue Sarcoma	• Drug: ADI-PEG20 • Drug: Gemcitabine • Drug: Docetaxel	Sarcoma Oncology Centre, Santa Monica, California, United States; Washington University School of Medicine, Saint Louis, Missouri, United States
4	Phase 1B Trial With ADI-PEG20 Plus Nab-Paclitaxel and Gemcitabine in Subjects With Pancreatic Cancer	Active, not recruiting	No Results Available	Advanced Pancreatic Cancer	• Drug: ADI-PEG20	Memorial Sloan-Kettering Cancer Centre, New York, New York, United States
5	Phase 1-2 Study ADI-PEG20 Plus FOLFOX in Subjects With Advanced Gastrointestinal Malignancies Focusing on Hepatocellular Carcinoma	Recruiting	No Results Available	Advanced Gastrointestinal (GI) Malignancies, Hepatocellular Carcinoma, Gastric Cancer Colorectal Cancer	• Drug: ADI-PEG20	Memorial Sloan-Kettering Cancer Centre, New York, New York, United States; Chang Gung Medical Foundation - Kaohsiung, Kaohsiung, Taiwan; National Cheng Kung University Hospital, Tainan, Taiwan; Mackay Memorial Hospital, Taipei, Taiwan; Taipei Veterans General Hospital, Taipei, Taiwan; Tri-Service General Hospital, Taipei, Taiwan; Chang Gung Medical Foundation - Linkou, Taoyuan, Taiwan

Table 1-3: Ongoing Clinical Trials for ADI-PEG20 (b), *(Source: www.clinicaltrials.gov)*

	Title	Status	Study Results	Conditions	Interventions	Locations
6	Phase 1 Trial of ADI-PEG20 Plus Docetaxel in Solid Tumors With Emphasis on Prostate Cancer and Non-Small Cell Lung Cancer	Active, not recruiting	No Results Available	Solid Tumors Prostate Cancer	• Drug: ADI-PEG20	University of California at Davis, Sacramento, California, United States
7	Phase 1 Study of ADI-PEG20 Plus Low Dose Cytarabine in Older Patients With AML	Recruiting	No Results Available	Acute Myeloid Leukemia	• Drug: ADI-PEG20 • Drug: Cytarabine	Kaohsiung Medical University Chung-Ho; Memorial Hospital, Kaohsiung, Taiwan National Cheng Kung University Hospital, Tainan, Taiwan; Chang Gung Memorial Hospital - Linkou, Taoyuan, Taiwan
8	Phase 2/3 Study in Subjects With MPM w/Low ASS1 Expression to Assess ADI-PEG20 With Pemetrexed and Cisplatin	Recruiting	No Results Available	Mesothelioma	• ADI-PEG 20 plus Pemetrexed and Cisplatin • Placebo plus Pemetrexed Cisplatin	Mayo Clinic, Phoenix, Arizona, United States; UCLA Haematology & Oncology - Santa Monica, Los Angeles, California, United States; University of California San Francisco Helen Diller Comprehensive Cancer Centre, San Francisco, California, United States; H. Lee Moffitt Cancer Centre & Research Institute, Tampa, Florida, United States; University of Chicago, Chicago, Illinois, United States; University of Maryland, Marlene & Stewart Greenebaum Comprehensive Cancer Centre, Baltimore, Maryland, United States; Henry Ford Hospital, Detroit, Michigan, United States •Mayo Clinic, Rochester, Minnesota, United States; Memorial Sloan Kettering Cancer Centre, New York, New York, United States; MD Anderson Cancer Centre, Houston, Texas, United States
9	Study in Patients With Tumours Requiring Arginine to Assess ADI-PEG20 With Atezolizumab, Pemetrexed and Carboplatin	Not yet recruiting	No Results Available	Carcinoma, Non-Small-Cell Lung	• Drug: Atezolizumab • Drug: Pemetrexed • Drug: Carboplatin • Drug: ADI-PEG20	-

1.6.5.2   PEGylated Recombinant Human Arginase 1 (rhArg1peg5000)

The manganese –containing enzyme Arginase catalyses the conversion of free arginine into ornithine and urea, therefore can be potentially utilised to target OTC, ASS1 and ASL deficient tumours. Reports of arginase anti-tumour efficacy go back in the 60s when murine and calf derived arginase enzymes were found to inhibit DNA synthesis in 3T3 fibroblasts (Holley et al., 1967) and decrease tumour growth in rats (Bach and Swaine, 1965). Despite the limited enzymatic effectiveness in human plasma due to higher optimal pH values (pH 9.6), recent modifications have managed to increase both the bioavailability and *Km* of the enzyme. Accordingly, PEGylation process has increased the bioavailability of the enzyme from few minutes to 3 days, while *Km* has also been improved from 6mM to 2.9mM. These features, along with lack of immunogenicity and effectiveness in ASS1 positive, ASS1 negative and ADI-PEG20 refractory tumours (Dillon et al., 2002; Tsui et al., 2009), render rhArg1peg5000 (PEG BCT-100) a noteworthy therapeutic agent alternative to ADI-PEG20 (Dillon et al., 2002).

Preclinical studies showed, that rhArg1peg5000 can effectively decrease circulating arginine to negligible levels within 24 hr. Results were also accompanied by a directly proportional 7-fold increase in ornithine concentration. Moreover, these studies revealed a significant anti-tumour effect of rhArg1peg5000 in Hep3B and T-cell acute lymphoblastic leukemia (T-ALL) cell xenografts, both as a single treatment and in combination with 5-FU and Cytarabine (Hernandez et al., 2010; Cheng et al., 2007).

Concerns about rhArg1peg5000 related toxicity had been issued by Mauldin et al. According to their dose-escalation study, intraperitoneal administration of the highest 10mg/kg biweekly dose of arginase resulted in ''uniform lethality, tremendous weight loss, and bone marrow necrosis'' in experimental mice. This phenotype was rescued by supplementation of citrulline, which extended the survival of mice significantly (Mauldin et al., 2012). Nevertheless, in accordance with previous studies, rhArg1peg5000 anti-tumour efficacy has been confirmed both *in vitro* and *in vivo*, in several malignancies, including HCC, prostate cancer, leukemia and metastatic melanoma (Hsueh et al., 2012; Lam et al., 2011) with no evidence of life-threatening toxicity.

In the clinical setting, a recent trial assessed the safety, pharmacokinetics (PK)/ pharmacodynamics (PD) parameters and efficacy of rhArg1peg5000 in patients with

advanced HCC (Yau et al., 2015). rhArg1peg5000 was administered intravenously, at weekly doses of 1600 U/kg. Overall drug treatment, unlike preclinical mouse models described by Mauldin and colleagues, was well tolerated with no major adverse effects. Reportedly, 15% of the patients exhibited liver dysfunction, while 3 other percentiles of patients (10% each) suffered from abdominal pain, abdominal distention and tumour pain. However, none of these adverse effects were directly correlated with the treatment (Yau et al., 2015). As depicted by Table 1-4, to date there are 3 ongoing clinical trials in melanoma, prostate cancer, AML, ALL and paediatric solid tumours that are designed to test further the efficacy of rhArg1peg5000 as monotherapy, and evaluate potential adverse effects (*www.clinicaltrials.gov*).

Table 1-4: Ongoing Clinical Trials for rhArg1peg5000 (PEG-BCT-100), (Source: www.clinicaltrials.gov)

	Title	Status	Study Results	Conditions	Interventions	Locations
1	Recombinant Human Arginase 1 (rhArg1) in Patients With Advanced Arginine Auxotrophic Solid Tumors	Recruiting	No results available	• Melanoma • Prostate Adenocarcinoma	PEG-BCT-100	California Cancer Associates for Research and Excellence, cCARE, San Diego, California, United States; John Wayne Cancer Institute, Santa Monica, California, United States
2	Efficacy and Safety Study of Recombinant Human Arginase 1 in Patients With Relapsed or Refractory Acute Myeloid Leukemia	Active, not recruiting	No results available	• Acute Myeloid Leukemia	PEG-BCT-100	The University of Hong Kong, Queen Mary Hospital, Hong Kong
3	A Study Evaluating the Safety and Activity of PEGylated Recombinant Human Arginase (BCT-100) (PARC)	Not yet recruiting	No results available	• Paediatric Solid Tumor • Paediatric AML • Paediatric ALL	PEG- BCT-100	-

1.6.5.3 Mechanisms of Resistance to Arginine Depleting Strategies

Arginine depleting strategies, including pharmacological and dietary depletion, induce a cellular adaptive responses which support cancer cells to overcome arginine starvation. Re-expression of ASS1, induction of autophagy and production of ADI-PEG20 neutralising antibodies are among the main mechanisms of resistances to arginine deprivation.

As previously mentioned, ASS1 is silenced via methylation of its promoter in human tumours and demethylation of the ASS1 promoter is a common mechanism leading to re-expression of the enzyme and acquired resistance in arginine-starved cancers (Delage et al., 2012; Szlosarek et al., 2013). Alternatively, studies in melanoma and breast cancer cell lines treated with ADI-PEG20 or cultured in arginine-free medium, revealed that ASS1 gene is regulated by two transcriptional factors, namely c-Myc and hypoxia induced factor 1 alpha (HIF-1α). c-Myc and HIF-1α bind on the regulatory E-box sequence (5'-CACGTG) upstream of the *ASS1* gene transcriptional starting site, thus promoting, in the case of c-Myc, or suppressing, in the case of HIF-1a, the expression of ASS1 (Tsai et al., 2009; Hann and Eisernman 1984).

In the presence of ADI-PEG20, VHL-mediated proteasomal degradation of HIF1α relieves E-box regions from HIF-1α inhibitory activity and it allows c-Myc to bind to the E-box sequences leading to increased *ASS1* transcription (Tsai et al., 2012). It has also been proposed that in ADI-PEG20-treated cells, c-Myc is stabilized via inhibition of the ubiquitin-mediated protein degradation apparatus, hence resulting in increased expression of ASS1 (Tsai et al., 2012). There is in fact evidence that ADI-PEG20 enhances the formation of the ubiquitin-specific protease 28 (USP28), which removes ubiquitin molecules attached on c-Myc via the subunit of the E3 ubiquitin ligase complex, F-box and WD40 domain-containing protein 7α (Fbw7α). USP28 counteracts the action of Fbw7a and inhibits proteasomal degradation of c-Myc. This stabilisation of c-Myc is regulated by a complex interplay between signalling pathways that involves the phosphorylation of c-Myc itself by ERK and GSK-3β. Reportedly, c-Myc ubiquitin targeted proteasomal degradation is promoted by the kinase GSK-3β, in which case phosphorylation of c-Myc at threonine residue 58 (T58) results in its recognition by the Fbw7a. Alternatively, phosphorylation of c-Myc at serine 62 (S62), mediated by ERK, prevents c-Myc ubiquitination and subsequent degradation. Furthermore, it's been also shown that PI3K/AKT promotes the stabilisation of c-Myc via inactivation of GSK-3β (Stephen et al., 2014). As discussed previously (Section 1.6.3), mTOR signalling regulates autophagy in response to

energy and amino acid availability. Upon arginine starvation mTORC1 inactivation promotes induction of autophagy to supply the arginine deprived cells with amino acids derived from intracellular organelles breakdown. Induction of autophagy has been described in several cancers, including lymphomas (Delage et al., 2012), glioblastoma (Syed et al., 2013), melanoma (Manca et al., 2012; Wang et al., 2013), and prostate cancer (Kim at al., 2009), as a contributor to cancer resistance to arginine deprivation.

Finally, the mycoplasma derived ADI-PEG20 has shown evidences of immunogenicity in humans in phase II clinical trials. Accordingly, HCC patients were found positive for anti-ADI antibodies after 50 days of exposure to the drug, in which time the levels of arginine in plasma were back to baseline levels. These data suggest that anti-ADI antibodies contributes to ADI-PEG20 resistance (Glazer et al., 2010; Abou-Alfa et al., 2018).

1.7 Hypothesis and Thesis Aims

Tumours deficient in urea cycle enzymes have been targeted extensively with arginine depleting agents ADI-PEG20 (Polaris Pharmaceuticals Inc.), and rhArg1peg5000 (BCT International) over the last decade. Here we make an effort to study whether CRC is dependent on external arginine supplementation. This effort stems from multiple observations: (a) previous studies suggests that most CRCs exhibit high expression of ASS1 (Rho et al., 2008, Dillon et al., 2004), however CRC is a heterogeneous disease (Guinney et al., 2015) and therefore arginine auxotrophy might be exposed in a subset of cancer patients; (b) normal colon tissue is not endowed with the ability to complete arginine biosynthesis and this might extend to CRCs; (c) arginine auxotrophy can manifest independently of ASS1 status (Bobak et al., 2013). Hence, we hypothesise that subsets of CRC may be arginine auxotrophic in an ASS1-independent fashion and that CRC patients could benefit from arginine depleting strategies. In this regard, this PhD study was structured to carry out the following aims:

- To investigate whether CRC cell lines are arginine auxotrophic when grown in arginine-free medium.
- To perform in *vivo* xenograft studies where tumour growth of mice fed with arginine-free diet will be monitored.
- To determine the expression levels of urea cycle enzymes in CRC cell lines and Patient Sample Tissue Microarrays with a focus on expression profile of ASS1 and OTC. Accordingly, to assess ADI-PEG20 and rhArg1peg5000 anti-proliferative efficacy in CRC cell lines.
- To assess the efficacy of these arginine depleting agents *in vivo* in xenograft studies.
- To identify candidate mechanisms of resistance against ADI-PEG20 and rhArg1peg5000 treatment.
- And finally to evaluate whether arginine depleting agents in combination with existing chemotherapeutic drugs could have a synergistic effect *in vitro.*

Chapter 2 - Materials and Methods

2.1 Materials, Reagents and Buffers

Table 2-1: Reagents, materials used and suppliers

Reagents – Materials	Supplier
1X Click-iT® Saponin-based Permeabilization and Wash Reagent	Invitrogen™
5-ethynyl-2´-deoxyuridine (EdU)	Invitrogen™
5-Fluorouracil (5-FU)	Sigma-Aldrich Ltd. UK
ADI-PEG20	Polaris Pharmaceuticals
Ammonium Persulphate (10%)	Sigma-Aldrich Ltd. UK
Arginine Free Diet (57M7)	TestDiet® USA
Arginine Free Medium based on DMEM/F12 Formulation	Home-made
Bicinchoninic acid (BCA) assay	Thermo Scientific™
Bovine Serum Albumin (BSA)	Sigma-Aldrich Ltd. UK
Chloroquine (CQ)	Sigma-Aldrich Ltd. UK
Click-iT™ EdU buffer additive	Invitrogen™
Click-iT™ fixative	Invitrogen™
CL-Xposure Film	Thermo Scientific
Complete Lysis-M Buffer	Roche, Germany
Copper protectant	Invitrogen™
Coulter® Isoton® II diluent	(Beckman Coulter, UK)
DAB chromogen	Leica Biosystems Ltd
Dimethyl sulfoxide (DMSO)	Sigma-Aldrich Ltd. UK
DMEM/F12 medium (1:1) (1X)	Gibco®, Life Sciences™
Dulbecco's Modified Eagle Medium (DMEM) – high glucose (4500mg/L)	Sigma-Aldrich Ltd. UK
EDTA (Ethylenediaminetetraacetic acid)	Sigma-Aldrich Ltd. UK
Enhanced Chemiluminescence Luminol (ECL)	Geneflow Ltd, UK
Etoposide	Sigma-Aldrich Ltd. UK
Fetal calf serum (FCS)	Invitrogen Ltd, UK
FxCycle™ Violet stain	Invitrogen™
Glutamax	Invitrogen Ltd, UK
Haematoxylin	Leica Biosystems Ltd
Hank's Balanced Salt Solution (HBSS – 10X)	ThermoFisher Scientific
HEPES 1M (Buffer Solution)	ThermoFisher Scientific
Human Recombinant Arginase 1 (non-PEGylated)	BioLegend, Inc
HyClone™ Dialysed Fetal Bovine Serum	GE Healthcare, UK
HyClone™ Vitamin Solution (100X)	GE Healthcare, UK
Lipofectamine® RNAiMAX	Invitrogen, UK
Loading Buffer (2x Laemmli)	Sigma-Aldrich Ltd. UK
Matrigel	BD Biosciences, Oxford, UK
McCoy's 5A (1X)	Gibco®, Life Sciences™
Methanol	Fischer Scientific, UK
Minimum Essential Medium Eagle (MEM)	Gibco®, Life Sciences™
Normal Control Diet(5CC7)	TestDiet® USA
Novolink™ DAB Substrate Buffer (Polymer)	Leica Biosystems Ltd
Novolink™ Polymer	Leica Biosystems Ltd
Novolink™ Polymer Detection System	Leica Biosystems Ltd
ON-TARGETplus ASS1 siRNA	Dharmacon, Inc.
ON-TARGETplus Non-targeting siRNA pool	Dharmacon, Inc.
Opti-MEM® reduced serum medium	Invitrogen, UK
Oxaliplatin	Sigma-Aldrich Ltd. UK
PageRuler™	Thermo Scientific
Penicillin - Streptomycin (Pen Strep)	Gibco®, Life Sciences™
Peroxidase Block	Leica Biosystems Ltd
Phosphate Buffered Saline (PBS, pH 7.2) tablets	Oxoid, UK
PhosSTOP phosphatase inhibitor cocktail tablets	Roche, Germany
Post Primary Block	Leica Biosystems Ltd
Protease Inhibitor cocktail tablet	Roche, Germany
Protein Block	Leica Biosystems Ltd
Protogel® 30% (w/v) Acrylamide: 0.8% (w/v) Bisacrylamide Stock Solution (37.5:1 ratio)	Geneflow Ltd, UK
Protogel® Resolving Buffer (4X) 1.5M Tris-HCl, 0.4% SDS, pH 8.8)	Geneflow Ltd, UK
Protogel® Stacking Buffer (0.5M Tris-HCl, 0.4% SDS pH 6.8)	Geneflow Ltd, UK
Recombinant Mycoplasma Arginine Deiminase (non-PEGylated)	Peprotech, Inc
RediJect D-Luciferin Ultra Bioluminescent Substrate	PerkinElmer, Inc
rhArg1peg5000 (PEG-BCT-100)	Bio-Cancer Treatment International, Ltd
Running Buffer - Tris Glycine SDS PAGE Buffer (10x) – 0.25M Tris base, 1.92M glycine, and 1% (w/v) SDS	Geneflow Ltd, UK
Semi-skimmed milk powder	Marvel, UK
Sodium Bicarbonate (NaHCO₃)	Sigma-Aldrich, Ltd. UK
Syringes/needles	BD Biosciences, UK
TEMED (N, N, N', N'-tetramethylethane-1,2-diamine)	Sigma-Aldrich Ltd. UK
Tris-HCl	Sigma-Aldrich Ltd. UK
Trypsin/EDTA	Gibco®, Life Sciences™
Tween® 20	Sigma-Aldrich, Ltd. UK
UltraPure™ DEPC treated water	Thermo Scientific, UK

2.2   Cell lines

*Table 2-2: Cell Lines – Genetic Profiling – Media Requirements, **L:** Allelic Loss, **NL:** No Allelic Loss, **mt:** Mutant, **wt:** Wild Type, **MSI:** Microsatellite Instability, **MSS:** Microsatellite Stable*

Cell Lines	Tissue of Origin	Stage	MSI Status	APC	KRAS	BRAF	P53	Media Requirements
HCT 116	Colorectal Carcinoma	Dukes D	MSI	NL	G13D	wt	wt	McCoy's 5A (1X) + GlutaMAX™ +10% FCS
HCT 116-luc2	Colorectal Carcinoma	Dukes D	MSI	NL	G13D	wt	wt	McCoy's 5A (1X) + GlutaMAX™ +10% FCS
SW 480	Colorectal Adenocarcinoma	Dukes B	MSS	L - mt	wt	G12V	R273H;P309S	Dulbecco's Modified Eagle's Medium - DMEM (4500mg glucose/L) +10%FCS
RKO	Colonic Carcinoma	-	MSI	-	wt	V600E	wt	Minimum Essential Medium Eagle (MEM) +1% Glutamax +10% FCS
HT 29	Colorectal Adenocarcinoma	Dukes C	MSS	NL - mt	wt	V600E	R273H	Dulbecco's Modified Eagle's Medium – DMEM (4500mg glucose/L) +1% Glutamax +10%FCS

2.3   Methods

2.3.1   Maintenance and Passaging of Adherent Cells

All cell lines were resuscitated from a departmental liquid nitrogen bank and let to grow in a humidified incubator at 37 °C supplemented with 5% CO_2. At 70-80% confluency, cells were passaged using a typical tissue culture protocol. Following, two times wash with phosphate buffer saline (PBS) cells were detached using 2X pre-warmed trypsin (5min). After trypsin inactivation a single-cell suspension in fresh warmed media was transferred to a 15mL falcon tube (Corning CentriStar®) and centrifuged at 1500rpm for 5 minutes. The cell pellet was then resuspended in fresh warmed medium. Using a Z2 Coulter Particle Count and Size Analyser (Beckman Coulter, UK), cells were counted and reseeded at a desired seeding density (Cell Culture Flask, CELLSTAR® growth area: 175 cm^2).

Table 2-3: DMEM/F12 Formulation – Amino Acids

Amino Acids	Molecular Weight	Concentration (mg/L)	mM
Glycine	75	18.75	0.25
L-Alanine	89	4.45	0.0499
L-Arginine hydrochloride	211	147.5	0.699
L-Asparagine-H_2O	150	7.5	0.05
L-Aspartic acid	133	6.65	0.05
L-Cysteine hydrochloride-H2O	176	17.56	0.099
L-Cystine 2HCL	313	31.29	0.099
L-Glutamic Acid	147	7.35	0.05
L-Glutamine	146	365	2.5
L-Histidine hydrochloride-H2O	210	31.48	0.149
L-Isoleucine	131	54.47	0.415
L-Leucine	131	59.05	0.450
L-Lysine hydrochloride	183	91.25	0.498
L-Methionine	149	17.24	0.115
L-Phenylalanine	165	35.48	0.215
L-Proline	115	17.25	0.15
L-Serine	105	26.25	0.25
L-Threonine	119	53.45	0.449
L-Tryptophan	204	9.02	0.044
L-Tyrosine disodium salt dehydrate	261	55.79	0.213
L-Valine	117	52.58	0.4517

Table 2-4: DMEM/F12 Formulation – Cell Culture Reagents

Components	Molecular Weight	Concentration	mM
Sodium Bicarbonate (NaHCO₃)	84	2438 (mg/L)	29.02
MEM Vitamin Solution (100X)	-	0.1% (v/v)	-
HEPES 1M (Buffer Solution)	-	0.1% (v/v)	-
Penicillin - Streptomycin (Pen Strep)	-	0.1% (v/v)	-
Hank's Balanced Salt Solution (HBSS – 10X)	-	10% (v/v)	-

2.3.2 Preparation of Whole Cell Lysates

Prior to harvesting and cell lysis treated plates were placed directly on ice to maintain the phosphorylated state of their proteins. Old media was removed prior washing with ice cold phosphate buffer saline (PBS) twice. After a 10-minute incubation on ice with c*O*mplete Lysis M buffer cells were scraped vigorously from petri dishes and transferred in prechilled Eppendorf tubes. Following 1 hr incubation on ice cell lysates were centrifuged at 14000rpm for 5 minutes at 4 °C. The supernatant was transferred and stored in new prechilled Eppendorf tubes and stored at -20 °C until further use.

2.3.3 Protein Quantification – Thermo Scientific™ Pierce™ BCA Assay

The protein quantification of whole cell lysates was based on a colorimetric assay and Bovine Serum Albumin (BSA) standards. The absorbance (595nm) of BSA (y-axis) was plotted against known concentrations of BSA (x-axis) to obtain a linear regression. The protein concentration of unknown protein samples was calculated using their reading absorbance and the equation provided by the standard curve (y=ax+b, where ''a'' is the slope, ''y'' is the reading absorbance of unknown sample and ''x'' the concentration of the unknown sample).

2.3.4 SDS – Page Electrophoresis

2.3.4.1 Gel Preparation

Unless otherwise stated, for all proteins (except Total 4E-BP1 / Phospho 4E-BP1 and LC3A/B, 15% gel), a 10% resolving gel was casted. A gel casting apparatus (Bio-Rad, mini gel apparatus) was set up prior the preparation of a 10% Resolving Gel. A 5% Stacking gel was then prepared (Table 2.5) and a 10 or 15 well comb was inserted into the stacking gel. Gels were let to set before they were wrapped in wet blue roll paper, cling membrane and stored at 4 °C until use.

Table 2-5: Reagents for 5% stacking, and 10% and 15% resolving gels

Reagents	5% Stacking Gel (10 mL)	10% Resolving Gel (20 mL)	15% Resolving Gel (20 mL)
Distilled / deionized water	5.7 mL	8.1 mL	5.4 mL
ProtoGel® Stacking Buffer (0.5M Tris-HCl, 0.4% SDS, pH 6.8)	2.5 mL	-	-
ProtoGel® Resolving Buffer (4X) (1.5M Tris-HCl, 0.4% SDS, pH 8.8)	-	5 mL	5 mL
ProtoGel® 30% (w/v) Acrylamide: 0.8% (w/v) Bis-Acrylamide Stock Solution (37:5:1)	1.7 mL	6.7 mL	9.4 mL
10% Ammonium Persulfate	100 μL	200 μL	200 μL
TEMED (N,N,N',N' – tetra methyl-ethylenediamine)	15 μL	15 μL	15 μL

2.3.4.2 Sample Preparation

Whole cell lysates were let to thaw on ice. Appropriate volumes of protein lysate were diluted in water and equivalent volumes of sample loading buffer (2x Laemmli, Sigma, UK) to provide samples of equal concentration (30μg for 10 well gels or 15μg for 15 well gels). Samples were then placed at a heat block for 5 minutes at 100 °C. Denaturation of proteins was followed by a quick vortex and pulse spin. The samples were kept on ice until loading.

2.3.4.3 Running and Transferring

Protein samples were run at 40mA for 90 minutes (or alternatively to the point where the lowest band of PageRuler™ ladder was at the end of the gel). Following the SDS-PAGE electrophoresis, proteins were transferred to a nitrocellulose membrane. Transfer

"sandwiches" were prepared using the following alignment: **Black cassette – sponge – Whatman™ filter paper – gel - nitrocellulose – Whatman™ filter paper – sponge – clear cassette**. Subsequently, cassettes were placed into a blotter assembly in tank filled with transfer buffer. Proteins were transferred at 100 Volts for 1 hr at room temperature.

2.3.4.4   Detection of Proteins

Following transfer of proteins, membrane blots were blocked with 5% milk for 2 hr at room temperature. Blots were then washed for 5 minutes to remove any excess of blocking solution. Primary antibody solution was added according to Table 2-6 and membranes were incubated overnight at 4°C. The following day, blots were washed with PBST for 10, 5 and 5 minutes respectively and incubated with the horseradish peroxidase (HRP)-conjugated secondary antibodies, diluted in 3% milk, for 1 hr at room temperature. Prior to detection, membranes were washed twice with PBST, once for 10 and 5 minutes respectively.

An Enhanced Chemiluminescence Luminol (ECL) reagent was prepared by mixing two reagents, A and B in 1:1 ratio right before use. After a 2-minute incubation, membranes were drained off from any excess ECL solution, wrapped in plastic film and placed in a Hypercassette™ (Amersham, UK). The membrane was exposed to Thermo Scientific CL-XPosure Film for 15 seconds to 5 minutes and developed using an automated developer (AGFA Curix 60, Germany). Alternatively, high resolution images were captured using the GeneGnome XRQ system (Syngene, UK). The protein band intensity was measured using densitometry performed with ImageJ (ImageJ 1.49u) software. Proteins presented as double bands were selected and quantified as a whole. The relative expression levels of the proteins were normalized against actin.

Table 2-6: Working dilutions of primary and secondary antibodies used.

Primary Antibody	Manufacturer	Working Dilution	Secondary Antibody	Manufacturer	Working Dilution
4E-BP1 Antibody Rabbit mAb	Cell Signaling Technology	1:1000	Anti-Rabbit	Santa Cruz Biotechnology, INC	1:10000
Actin (C-11) Goat mAb	Santa Cruz Biotechnology, INC	1:5000	Anti-Goat	Santa Cruz Biotechnology, INC	1:10000
Anti-CPS1 antibody Mouse Antibody	Abcam plc.	1:1000	Anti-Mouse	Santa Cruz Biotechnology, INC	1:10000
Anti-Ki67 antibody Rabbit mAb	Abcam plc.	1:1000	Anti-Rabbit	Leica Biosystems Ltd	N/A
Anti-Ornithine Carbamoyltransferase antibody	Abcam plc.	1:1000	Anti-Mouse	Santa Cruz Biotechnology, INC	1:10000
Argininosuccinate Lyase (ASL)	Santa Cruz Biotechnology, INC	1:1000	Anti-Mouse	Santa Cruz Biotechnology, INC	1:10000
Argininosuccinate Synthase (ASS1) Mouse mAb	Polaris Pharmaceuticals, INC	1:1000	Anti-Mouse	Santa Cruz Biotechnology, INC	1:10000
c-Myc (D84C12) Rabbit mAb	Cell Signaling Technology	1:1000	Anti-Rabbit	Santa Cruz Biotechnology, INC	1:10000
Cyclin D1 (92G2) Rabbit mAb	Cell Signaling Technology	1:1000	Anti-Rabbit	Santa Cruz Biotechnology, INC	1:10000
Cyclin D3 (DCS22) Mouse mAb	Cell Signaling Technology	1:1000	Anti-Mouse	Santa Cruz Biotechnology, INC	1:10000
LC3A/B (D3U4C) XP® Rabbit mAb	Cell Signaling Technology	1:1000	Anti-Rabbit	Santa Cruz Biotechnology, INC	1:10000
LC3B (D11) XP® Rabbit mAb	Cell Signaling Technology	1:1000	Anti-Rabbit	Leica Biosystems Ltd	N/A
PARP (46D11) Rabbit mAb	Cell Signaling Technology	1:1000	Anti-Rabbit	Santa Cruz Biotechnology, INC	1:10000
Phospho-4E-BP1 (Thr37/46) (236B4) Rabbit mAb	Cell Signaling Technology	1:1000	Anti-Rabbit	Santa Cruz Biotechnology, INC	1:10000
Phospho-S6 Ribosomal Protein (Ser235/236) (D57.2.2E) XP® Rabbit mAb	Cell Signaling Technology	1:1000	Anti-Rabbit	Santa Cruz Biotechnology, INC	1:10000
S6 Ribosomal Protein (5G10) Rabbit mAb	Cell Signaling Technology	1:1000	Anti-Rabbit	Santa Cruz Biotechnology, INC	1:10000

2.3.5 Cell Proliferation Assay

The day prior to treatment, cells were plated in 24 well plates at a density of 4000 cells per well and let to adhere overnight. Cells in exponential growth were changed to home-made arginine free medium (see components in Table 2-3 and 2-4) or control medium or DMEM/F12 (1:1) + 10% Dialyzed Fetal Bovine Serum (FBS) containing various concentrations of drugs. Vehicle controls were included. After 6 days quadruplicate samples were assessed for cell growth by cell counting utilizing the Z2 Coulter Particle Count and Size Analyser. Prior to counting cells were detached in a routine-typical tissue culture fashion. Old media was discarded, and cells were washed with PBS before trypsinised with 2X Trypsin-EDTA. Trypsin was neutralized with fresh media and 1mL single cell suspension was transferred into coulter cups with 9mL of Coulter® Isoton® II diluent. Cells were counted between 8-20 μm.

2.3.5.1 Drug Combination Studies and Evaluation of Synergy

Single treatment IC_{50} values obtained from corresponding dose-response curves were used for the design of the combination experiments. In a 6x6 checkerboard layout; drug concentrations were crossed combined at an equipotency ratio $[(IC_{50})_1/(IC_{50})_2]$ to ensure that the observed effects were achieved by equal contribution of both drugs. Similarly, to previous cell proliferation assays, cells were counted after 6 days of treatment and data obtained from diagonal constant ratio combinations were analysed and evaluated for synergism, additivity or antagonism using the CompuSyn Software (CompuSyn Inc.) according to the Chou and Talalay method (Chou, 2006).

2.3.6 Click-iT® EdU Alexa Fluor® 488 Flow Cytometry Assay

10^6 cells were seeded in large flasks 24 hours before treatment. Cells in exponential growth were changed to arginine free media or medium containing catabolizing agents 24 and 72 hr prior to FACS analysis respectively. The final day; cells were pulsed with 10μM 5–ethyl-2'–deoxyuridine (EdU) for 1 hr at 37 °C, 5% CO2. Cells were harvested according to routine tissue culture protocols and washed with 1% BSA in PBS. After fixation and permeabilization, cells were incubated 15 minutes at room temperature, protected from light. Click-iT® Reaction Cocktail were added to cells according to manufacturer's instructions and mixed well. Samples were further incubated at room temperature for 30 minutes protected from light. A total DNA staining was achieved by adding 1 μL FxCycle™ Violet stain (Life Technologies, UK) in samples containing 1 mL cell suspension. After mixing thoroughly, samples were incubated

for 30 minutes on ice, protected from light. Samples were analysed for total DNA staining in Aria Analyser (BD FACSARIA™ II), using 405nm excitation. Emission was collected in a 450/50 band-pass. For the detection of EdU with Alexa Fluor® 488 azide, we used a 488nm excitation with a green emission filter (530/30 nm). Samples of untreated cells, stained and unstained with EdU or FxCycle™, were also included.

2.3.7   ON-TARGETplus siRNA, ASS1 "knock-down"

6cm dishes were plated with approximately 75.000 cells and let to grow at 30-40% confluency. Prior to transfection, 5nmol vials of ON-TARGETplus ASS1 siRNA were reconstituted using 250µL of UltraPure™ DEPC treated water, aliquoted into 10µL aliquots (20pmol/µL) and stored at -20 °C until use. Similar procedure was followed for the ON-TARGETplus Non-targeting siRNA pool. The day of transfection, siRNA aliquots were let to thaw on ice. The growth media of cells was replaced by 3.5 mL fresh warm growth medium. In two Eppendorf tubes, mixtures of 250µL Opti-MEM® reduced serum medium + 5µL Lipofectamine® RNAiMAX and 250µL Opti-MEM®-reduced serum medium + 5µL (100pmol) siRNA were prepared respectively. The two solutions were mixed well and incubated at room temperature for 5 minutes. 500µL of the previous transfection mix were added to the cells and dishes were incubated overnight at 37 °C, 5% CO_2. Followed by 24 hours transfection, cells were exposed to 750ng / mL of ADI-PEG20 for 48 hours. Controls of untreated and untrasfected cells were also included. At the end of the experiment cells were harvested according to previously mentioned tissue culture protocols, counted and whole cell lysates where prepared for western blot analysis.

2.3.8   Immunohistochemistry

Formalin-fixed and paraffin-embedded (FFPE) tissue sections (4µm) were prepared using standard protocols. Following deparaffinization, rehydrated sections were boiled for 20 minutes in antigen retrieval buffer (1X Tris-EDTA, pH 9 or Citrate buffer pH 6).

2.3.8.1   Novolink™ Polymer Detection System

The immunostaining was performed using the Leica Novolink™ Polymer Detection System (Leica Biosystems, Newcastle, UK). Endogenous peroxidase activity was neutralised using peroxidase block for 5 minutes. Sections were then blocked in protein block buffer for 30 minutes and incubated in primary antibodies for 2 hr at room temperature. Peroxidase chromogenic reaction was then developed with DAB working solution according to

manufacturer's instructions. Slides were counterstained with haematoxylin and mounded with DPX mounting media. Pictures were taken using the Hamamatsu NanoZoomer-XR Digital slide scanner. Immunostaining was evaluated with Aperio ImageScope software from Leica and the semi quantitative approach of H-score using the following formula: [1x (% weak positive cells) + 2x (% positive cells) + 3x (% strong positive cells)].

2.3.8.2 Tissue Microarray Study (TMA)

Accordingly, TMA slides with 650 CRC case samples were constructed and provided by the Grampian Biorepository (www.biorepository.nhsgrampian.org). All tissue samples had come from patients who underwent surgery for primary CRC from 1994 to 2009 at Aberdeen Royal Infirmary (Aberdeen, UK). Excluded from this study were all the patients who had received neoadjuvant chemotherapy or radiotherapy to the date of death from any cause. All alive patients at the time of the censoring (March 2012) were also excluded from this study. The median survival was 103 months (95% CI=86-120 months), the mean survival was 115 months (95% CI=108-123 months) and the median follow up time calculated by the 'reverse Kaplan-Meier' method, was 88 months (95% CI=79-97 months). Clinicopathological features of the patients are presented in table ii in appendices. No written permission was required from patients for the use of FFPE samples. This TMA cohort was approved by the Grampian Biorepository Scientific access group committee (TR000054).

TMA slides were processed according to standard immunohistochemical protocols described in section 2.3.8.1. Expression levels of ASS1 and OTC were assessed blindfolded by WB using PathXL (Clinical Pathology platform) and the semi quantitative approach of H-Score. Results were further validated against automated classification of expression levels using Aperio ImageScope (Leica) and analysed for agreement using the Cohen's Kappa coefficient.

2.4 Animal Studies

All animal work was carried out under the PPL# 60/4370 in accordance with the Animals (Scientific Procedures) Act of 1986.

2.4.1 Preparation, injection and monitoring of tumour xenografts

Prior to xenografting, HCT 116-luc2, RKO and SW 480 cells were harvested at 70-80% confluency and resuspended to a final volume of 100μl Matrigel (BD Biosciences): Serum Free medium [1:1] per mouse.

8-week-old, nude Balb/c mice were purchased from Charles River Laboratories, UK. Mice were exposed to 12h light/dark cycles and kept in ventilated cages in groups of 4, under pathogen free conditions. Mice were injected subcutaneously with 100µL of 10^6 million cells on their right flank. Following a week of inoculation, mice with established tumours were randomized in groups of 8 (n=8) and treated accordingly with ADI-PEG20 5IU/animal once a week or rhArg1peg5000 5mg/animal twice a week or vehicle control (PBS). Balb/c mice baring HCT 116-luc2 tumours were immediately administrated the Arginine free diet or control diet (5CC7) right after the initial cell injections. Body weight and tumour size were closely inspected and measured twice a week. Further to digital calliper measurements, mice bearing HCT 116 luc2 tumours were monitored via the IVIS Spectrum Preclinical Imaging System (PerkinElmer®) once a week. Prior to *in vivo* imaging mice were administered subcutaneously with 150 mg/kg Xenolight RediJect D-Luciferin (PerkinElmer®), anesthetised and imaged with IVIS Spectrum Preclinical Imaging System (PerkinElmer®) 10 minutes post injection (Procedures described were performed by Justina Janus). When tumours reached the 17mm diameter animals were culled for assessment under terminal anaesthesia (5-3% Isoflurane). Blood was collected by cardiac puncture. Tumours were excised, weighted and considerable portions were fixed in formalin for immunohistochemistry. Smaller pieces were snap-freezed in liquid nitrogen and stored in -80ºC for protein and DNA/RNA extraction.

2.5 Statistical Analysis

The error bars represent the ±Standard Error of the Mean (±SEM). Statistical significance between two groups was determined by two-tailed unpaired Student's t-test, whereas multiple One-Way Anova analysis was conducted to compare controls against multiple drug concentrations (Prism version 7.0, GraphPad Software, Inc.). The animal xenograft studies were assessed for statistical significance using the mixed linear regression model in Stata software by Dr Maria Viskadouraki (StataCorp LP, College Station, TX, USA). Statistical analysis of TMA cohort patient data including the Mann-Whitney U test, Wilcoxon signed rank test, chi-squared test, and Cox multi-variate analysis (variables entered as categorical variables) was performed using IBM SPSS version 24 for Windows 7™ (IBM, UK).''

Chapter 3 – Results

3.1 Investigating the effects of Arginine Withdrawal *in vitro*

Preliminary data from previous work in our lab had shown evidences of decreased growth of CRC cell lines exposed to arginine free medium. Based on these observations we were led to further examine the effects of arginine withdrawal in CRC and investigate whether dietary or pharmacological depletion of arginine could potentially be used as targeted therapeutic strategy for CRC patients.

3.1.1 Investigating the effects of L-Arginine withdrawal on cell growth

In order to confirm and expand previous observations, and assess whether L-Arginine external supplementation was essential for the growth of CRC cell lines, we monitored the growth by cell counting over a 7 day period. All 4 cell lines tested, namely HCT 116, RKO, SW 480 and HT 29 showed a remarkable dependency in external arginine supplementation. Essentially, cells failed to grow in the absence of L-Arginine and its metabolites ornithine and citrulline over the entire period of the experiment, suggesting arginine auxotrophy (Figure 3-1).
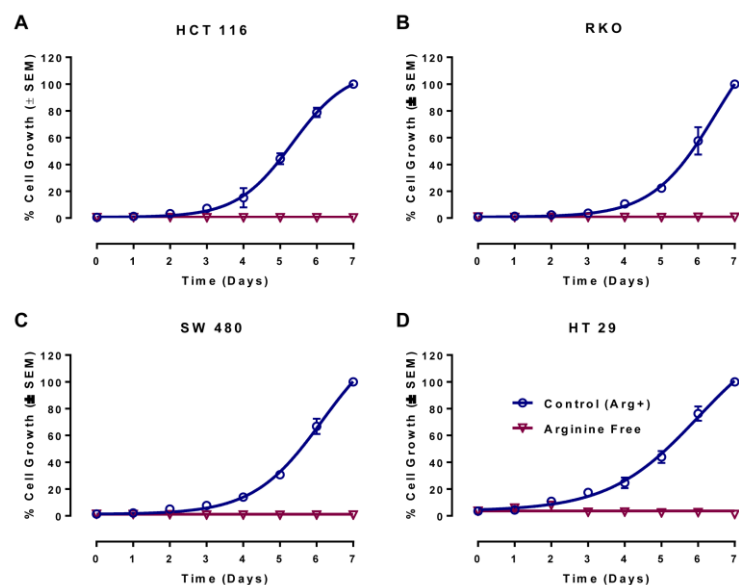
***Figure 3-1: Removal of L-Arginine from Culture Media Inhibits the Cell Proliferation in Colon Cancer Cell Lines.** Growth kinetics of human colon cancer cell lines with or without L-Arginine in Culture media. **(A)** HCT 116, **(B)** SW 480, **(C)** RKO, **(D)** HT 29 cells were seeded in 24well plates and let to adhere overnight in normal growth media. Cells in exponential growth were changed to control and arginine free medium at day 1. The number of cells was counted over a 7-day period. The percentage (%) of Cell Growth was calculated relative to the cell numbers in corresponding H_2O-treated cells (Control), which were chosen as 100% of growth at the end of the experiment. The results were obtained from three independent experiments. The error bars represent the ± Standard Error of the Mean (±SEM, n=3).*

3.1.2 Investigating the effects of L-Arginine withdrawal on cell cycle

The antiproliferative and antigrowth effects of arginine starvation were further investigated by direct measurement of DNA synthesis utilizing the Click-iT® EdU Flow Cytometry assay. Similarly to BrdU, 5-ethynyl-2'- deoxyuridine (EdU) is a thymidine analogue, which is incorporated into DNA during active DNA synthesis. The detection of EdU incorporation is based on a copper catalysed covalent reaction between an azide and an alkyne. Accordingly, an azide coupled to Alexa Fluor® 488 is able to detect the alkyne found in the ethynyl moiety of EdU. Consistent with previous growth kinetics, results obtained from 3 independent experiments demonstrated a significant decrease in EdU incorporation in all 4 cell lines examined tested after 24 hr exposure to arginine free conditions (Figure 3-2). Accordingly, EdU incorporation was almost completely abolished in HCT 116, RKO and SW 480, whereas in HT 29 the decrease reached the 80% in comparison to control.

To further understand the mechanism(s) underlying proliferative arrest and inhibition of DNA synthesis induced by the withdrawal of arginine from culture media, we examined the expression of the proliferation marker Cyclin D1 via western blotting. The antiproliferative effects of arginine withdrawal are also reflected by the decreased levels of Cyclin D1. In time course experiments, cell lysates from arginine fed (+) and arginine starved (-) cells were collected sequentially at 4 different time points over a 24 hr period of time. The results obtained from the western blot analysis demonstrate a significant decrease of Cyclin D1 expression after 6, 10 and 24 hr in most cells cultured in arginine free media (Figure 3-2B). Accordingly, in HCT 166, RKO 144 and SW 480 the relative expression levels of Cyclin D1 decrease consistently after 6, 10 and 24 hr upon arginine withdrawal, whereas in HT 29 cells the expression of Cyclin D1 decreases significantly after 2 and 6 hr and recovers to normal levels after 10 and 24 hr respectively. The recovery of Cyclin D1 expression in HT 29 is supported by the marginal but detectable EdU incorporation in arginine-free samples in the corresponding Click-iT® EdU Flow Cytometry assays (Figure 3-2).
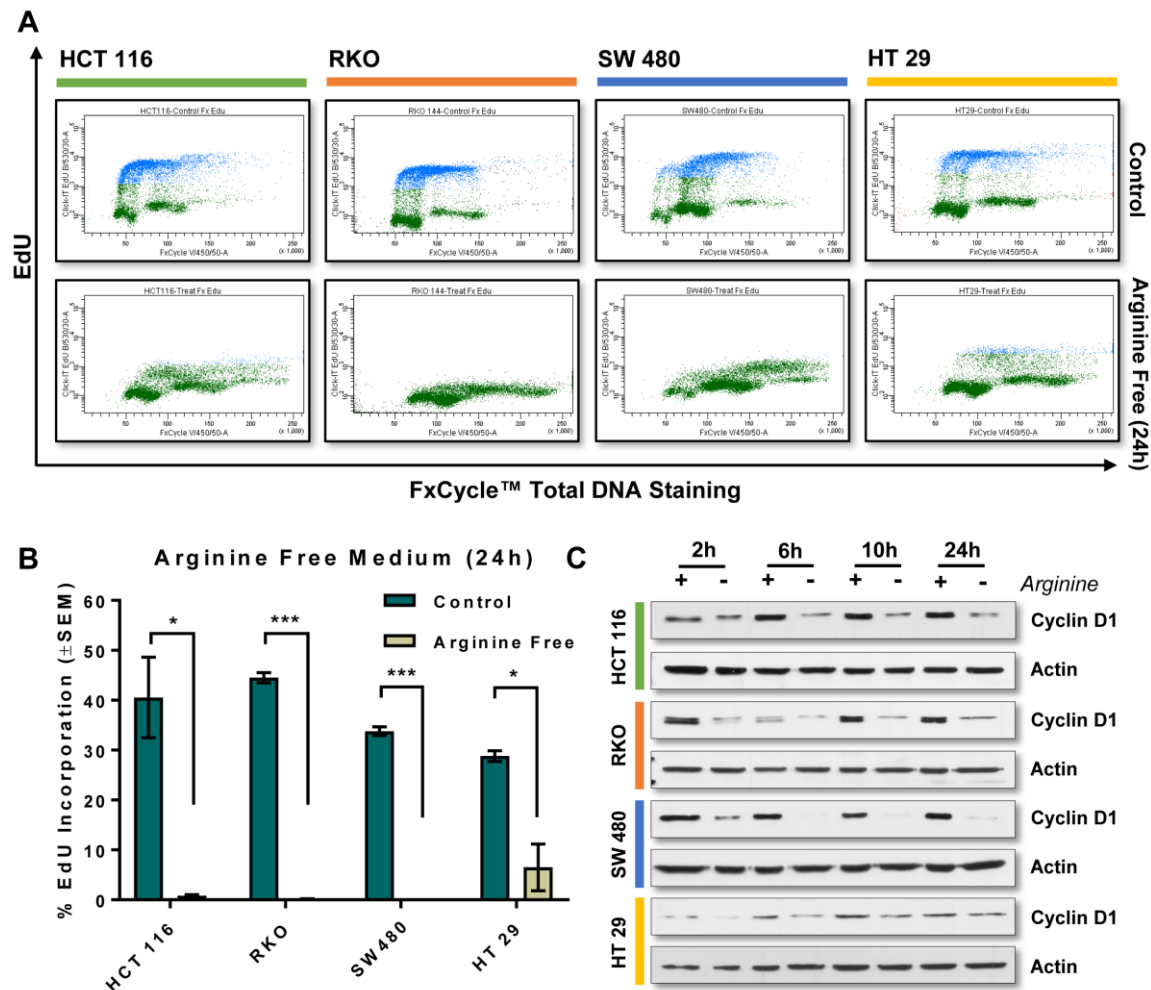
Figure 3-2: *Withdrawal of Arginine from Culture Media decreases the DNA Synthesis and Expression of Cyclin D1 in Colon Cancer Cell Lines. (A)* *Dual parameter plot of Click-iT® EdU® Alexa Fluor® 488 and FxCycle™, EdU and FxCycle™ Violet Fluorescence were detected and measured using 488nm excitation / 530/30 bandpass filter and 405nm excitation / 450/40 bandpass filter respectively. Dual positive cells in blue signify the cells in the S-phase, whereas from left to right, cells in green indicate cells in G_0/G_1 and G_2M respectively. (B)* *% Click-iT® EdU incorporation of colon cancer cell lines at 1 hr post EdU with or without L-Arginine in culture media for 24 hr. (C)* *Western blots of Cyclin D1. Whole cell lysates from Arg+ and Arg free treated cells were collected over a time course of 24 hours. Actin was used as loading control. The results were obtained from three independent experiments. The error bars represent the ± Standard Error of the Mean (±SEM, n=3) (*p<0.05, **p<0.01, ***p<0.001, ****p<0.0001, two-tailed Student's t-test).*

3.1.3   Investigating the effects of L-Arginine withdrawal on mTOR pathway

To investigate whether the observed reduction if proliferation was concomitant with inhibition of the amino acid and energy-sensing mTOR pathway, we further analysed the expression and phosphorylation levels of downstream targets of the mTOR pathway via western blotting.

Activation of p70S6 kinase (p70S6K) by mTORC1 and subsequent phosphorylation of the S6 Ribosomal protein (RS6), induced by growth factors and mitogens, results in increased translation of mRNA transcripts containing an oligopyrimidine track in their 5' untranslated regions (Peterson and Schreiber,1998).

Accordingly, these 5' untranslated regions are present in mRNA transcripts that encode elongation factors and ribosomal proteins essential for mRNA translation, as well as proteins involved in cell cycle progression (Jefferies et al., 1997). Similarly to previously described time course experiments, we demonstrate that the ratio of phosphorylated S6 Ribosomal protein / total S6 ribosomal protein is noticeably decreased in 3 out of 4 cell lines examined. In HCT 116 phosphorylated levels of RS6 were decreased after 6, 10 and 24 hr upon arginine withdrawal, whereas in SW 480 and HT 29 levels were decreased in earlier time points but recovered at 24 hr (Figure 3-3C, D and F).

We further investigated the phosphorylation levels of 4E-BP1. The extracellular concentration of nutrients, such as glucose and amino acids is tightly associated with the cap-dependent translation. These factors can stimulate the cap-dependent translation regulated by mTOR and its downstream targets 4E-BP1. Dissociation of 4E-BP1 from eIF4E and therefore promotion of assembly of the eIF4F complex is triggered by inactivation of 4E-BP1 via phosphorylation by mTORC1 (Saxton and Sabatini, 2017). Western blots presented in Figure 3-3A reveal a more prominent decrease in phospho 4E-BP1 in HCT 116 after 10 and 24 hr . Similar reduction was also observed in RKO and SW 480. The least affected cell line HT 29 exhibits a reduction after 2 and 6 hr, which is followed by a full recovery of the phosphorylation levels after 10 hr (Figure 3-3D).
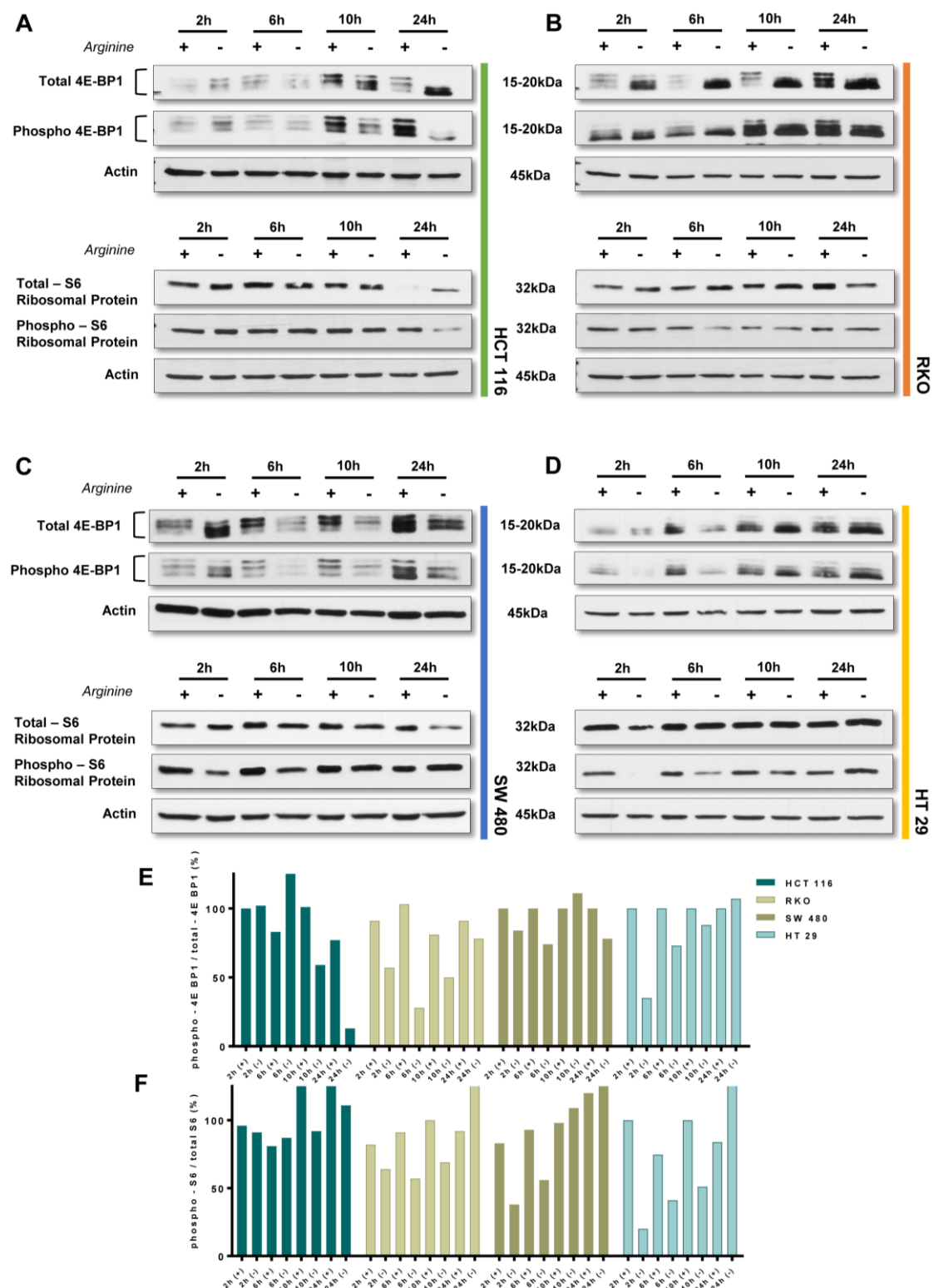
Figure 3-3: Withdrawal of L-Arginine from Culture Media decreases the phosphorylation of 4E-BP1 and S6 Ribosomal Protein. (A, B) *Western blots of Total and Phospho S6 Ribosomal Protein (S240/244).* **(C, D)** *Western blots of Total and Phospho 4E-BP1 (Thr37/46). Whole cell lysates from +Arg and −Arg treated cells were collected over a time course of 24 hr.* **(E, F)** *Phospho / Total Ratio % of 4E-BP1 and S6 as obtained by ImageJ densitometry and normalisation against actin.*

3.2 Investigating the effect of Arginine Withdrawal *in vivo*

3.2.1 Investigating the effect of dietary deprivation of L-Arginine on the growth of HCT 116-luc2 in BALB/c mice

Driven by the remarkable antiproliferative effect of arginine withdrawal *in vitro*, we made an effort to investigate whether dietary withdrawal of arginine could also affect the growth of colon cancer cells *in vivo*. In a pilot *in vivo* xenograft experiment, HCT 116-luc2 cells were subcutaneously injected in immunocompromised nude mice. Animals were subsequently randomized in two groups, one fed the control diet (5CC7) and one fed the arginine free diet (57M7). The growth of tumour xenografts was monitored closely for approximately 30 days. Direct measurements with a digital calliper demonstrated a statistically significant decrease in tumour volume *(p value = 0.03)* in animals fed with arginine free diet (Figure 3-4A). These findings are also supported by a statistically significant difference in tumour weight (Figure 3-4C). The animal welfare was monitored closely by measuring the animal body weight at least once a week. Despite the statistically significant difference (*p value = 0.0005)* in the overall animal body weight between the two diet groups throughout the experiment (Figure 3.4D), we demonstrate via the final normalized body weight at the end of the experiment the difference in animal body weight stemmed from different tumour burden (Figure 3-4E).
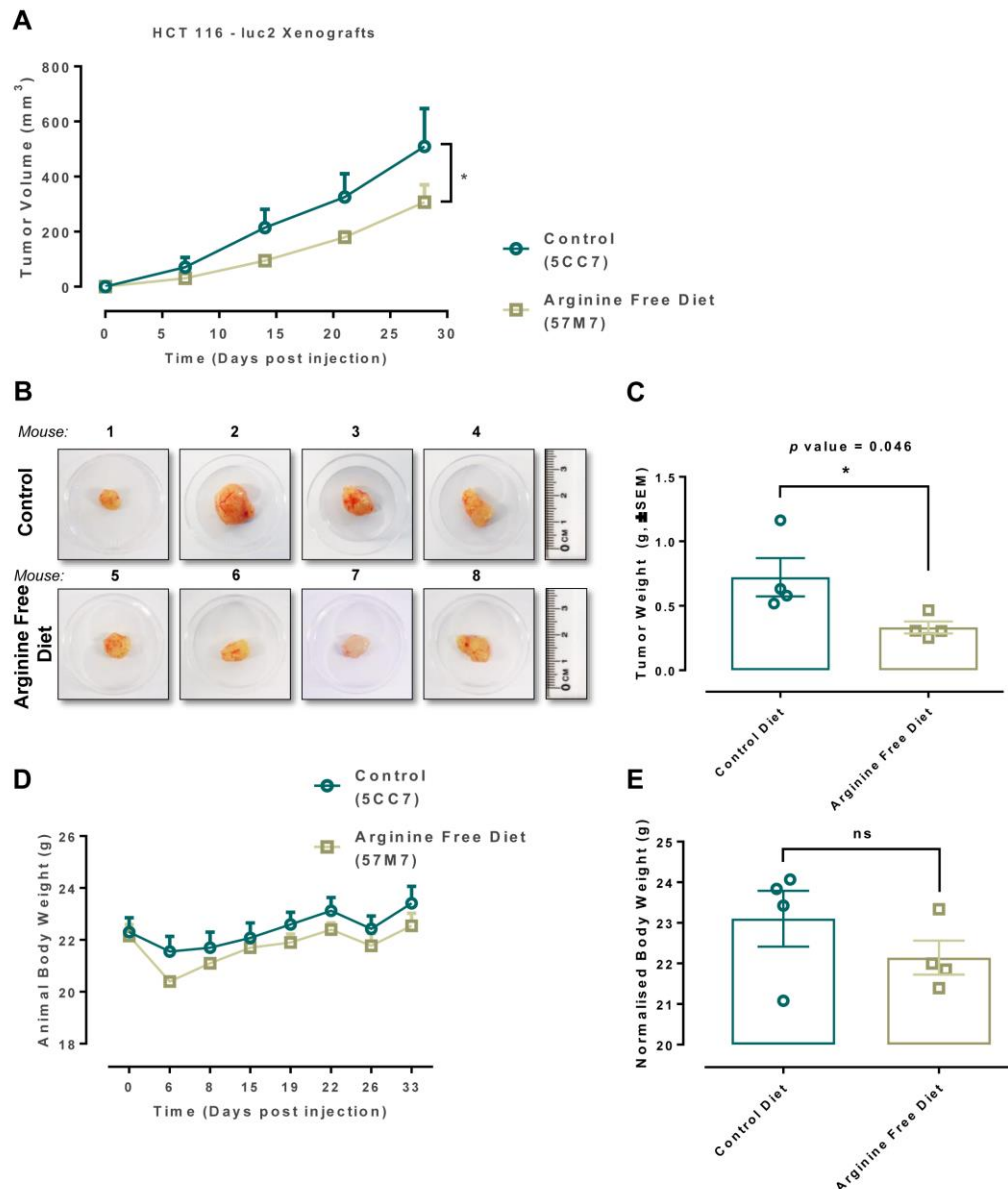
Figure 3-4: Dietary Withdrawal of L-Arginine Decreases the Growth of HCT 116-luc2 Xenografts in nude BALB/c. *Nude immunocompromised mice (n=8) were injected subcutaneously with HCT 116-luc2 and groups of mice (n=4) were fed the normal 5CC7 diet or L-Arginine free diet (57M7). Tumour volume was calculated by direct calliper measurement once per week.* ***(A)*** *Growth curves of tumour xenografts in BALB/c mice fed with control or arginine free diet (n=4 per group, P value=0.03 by mixed linear regression analysis). Data points represents Mean (±SEM)* ***(B)*** *Representative excised tumour xenografts at the of the experiment* ***(C)*** *Tumour weight of excised tumour xenografts (n=4 per group, P value=0.046, by Student's t-test)* ***(D)*** *Body weight of BALB/c mice on control diet or arginine free diet alone (n=4 per group, no significant difference)* ***(E)*** *Normalized body weight of BALB/c mice at the end of the experiment (n=4 per group, ns=no significance, Student's t-test)). The error bars represent the ± Standard Error of the Mean (±SEM). Animal body weight measurements between the two groups were analysed by one-way ANOVA, statistical significance was determined using the Bonferroni-Dunn method, with alpha = 0.05. Statistical significance of differences in tumour weight and normalized final animal weight was assessed by two-tailed Student's t-test (*p<0.05, n=4 per group).*

3.2.2 Monitoring the growth of HCT 116-luc2 xenografts using the IVIS® Spectrum Preclinical Imaging System

The xenograft tumour growth was also monitored twice per week, via bioluminescence using the IVIS® Spectrum Preclinical System. HCT 116-luc2 cells, stably transfected with a luciferase plasmid were used as a bioluminescence source to record the xenograft tumour growth. Sequential images of anesthetized mice (3% Isoflurane), injected with D-Luciferin subcutaneously (150mg/kg) were taken. The tumour area was isolated using specialized software (LivingImage4.5) and the total flux (photons per minute) was plotted against time to reflect the overall growth of the tumour xenografts over time. Due to the use of bioluminescence in this imaging method we were able to detect only living cells capable to metabolize the D-Luciferin.

As shown in the representative images acquired from two individual mice in Figure 3-5A, the overall tumour area and emission signal were lower at all-time points in mice fed with arginine-free diet. However, analysis of total flux (photons per second) against time reveals no significant differences between the two groups (Figure 3-5B). The reason for this lack of significance is unknown, but it is possible that the reduction of the total flux in mice at late time points reflects ensuing necrosis within the tumours.

Finally, immunohistochemical analysis of tumour xenograft sections for Ki67 reveals no significant differences in overall proliferation rates between mice fed with arginine free diet in comparison to the control, while both groups were tested positive for a ASS1 (Figure 3-6).
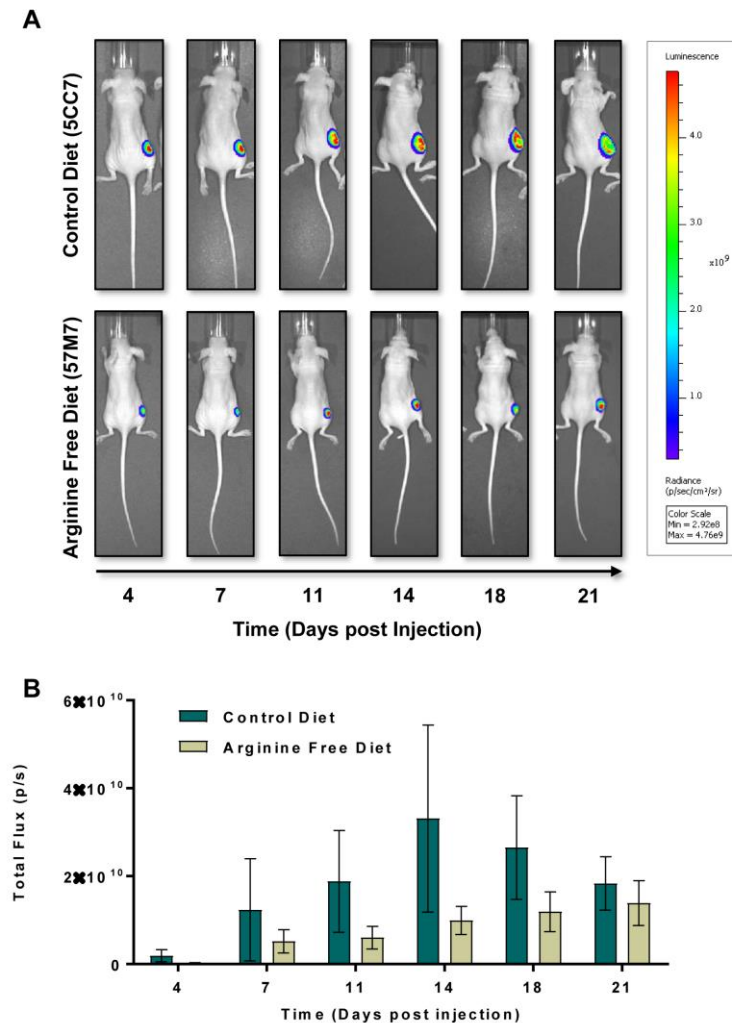
Figure 3-5: Bioluminescent in-vivo Imaging of HCT 116-luc2 Xenograft tumours using the IVIS® Spectrum Preclinical Imaging System. *HCT 116-luc2 tumour xenografts were imaged twice per week. Prior to imaging, mice were injected subcutaneously with RediJect D-Luciferin (150mg/kg), anaesthetized (3% Isoflurane) and placed in imaging chamber. Sequential images were taken every 2 minutes.* **(A)** *Representative sequential images from individual mice fed with Control (5CC7) and Arginine Free Diet (57M7) over time.* **(B)** *Total Flux (photons per second) variation over time. The tumour area was selected and the bioluminescence emission quantified using the LivingImage4.5 software. The error bars represent the ± Standard Error of the Mean (±SEM), n=4 per group. Statistical significance of difference in total flux between the two groups was determined by one-way ANOVA, statistical significance was determined using the Bonferroni-Dunn method, with alpha = 0.05.*
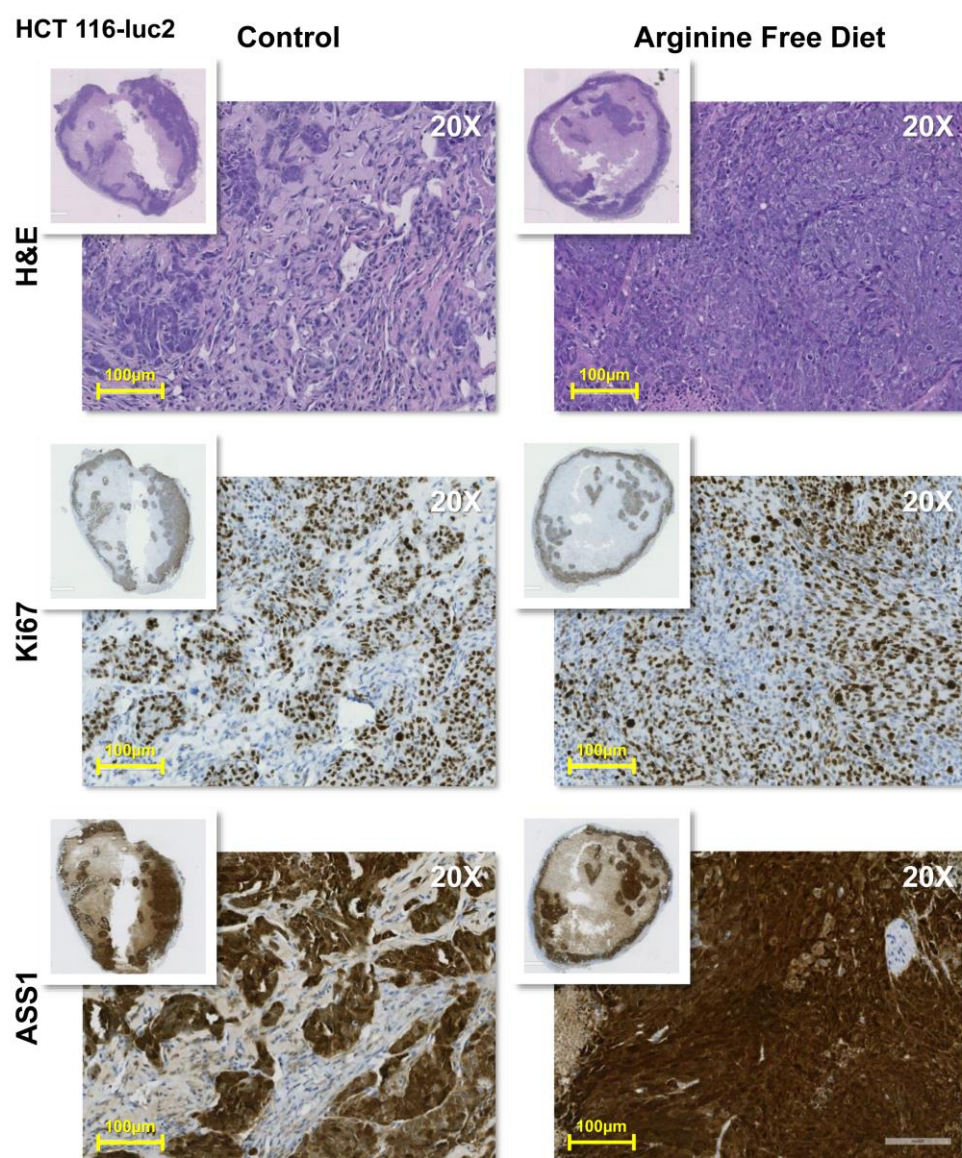
Figure 3-6: Immunohistochemical analysis of HCT 116 – luc2 tumour xenografts, Control vs Arginine Free Diet.
Immunohistochemical staining of xenograft tissue sections with Haematoxylin and Eosin, Ki67 and ASS1 staining.

3.2.3 Summary

In summary, this first part of the study has identified that CRC cell lines can potentially be arginine dependent if external arginine supplementation and arginine precursor's citrulline and ornithine are not provided. All cell lines tested failed to grow in the absence of arginine in the medium. The antigrowth effect of arginine deprivation in vitro was also mirrored by an arrest in total DNA synthesis, as assessed using EdU incorporation assays. Moreover, cell cycle marker Cyclin D1 was also significantly decreased upon 24 hr of arginine withdrawal. In agreement with similar studies (Feun et al., 2008; Savaraj et al., 2010; Chantranupong et al., 2016), our *in vitro* data suggest that arginine withdrawal can also decrease mTOR activity and translation as reflected by decreased phosphorylation levels of its downstream targets 4E-BP1 and ribosomal protein S6.

Finally, dietary removal of arginine *in vivo* led to a significant decrease in tumour volume and weight, as well as reduced photon emission signal measured by IVIS®. Conversely, these data were not accompanied by a significant reduction in proliferation and Ki67 marker, indicating that systemic or tumoural adaptation to arginine free diet was able to sustain similar proliferation levels in both groups. Adding to this, a trend towards decreased photon emission signal in the control group suggests the presence of necrosis within the tumour tissue possibly due poor vascularisation that led to limited availability of oxygen and nutrients. Hence, this might have also affected the proliferation rates of the control, thus further altering the difference between control vs arginine free diet tumours.

Plasma arginine and ornithine levels from published work in mice infused with arginine-free diet reveal a significant decrease in total flux, however citrulline, proline and glutamine remain unvaried. According to Marini et al., the plasma concentration of arginine in mice fed with arginine versus mice fed with arginine free diet was 119±10 µmol/L and 72±5 µmol/L respectively. Their study also revealed that plasma ornithine exhibits a significant reduction of approximately 50%. In conclusion Marini et al, report that plasma arginine, ornithine as well as dietary glutamine and proline (to a lesser extent), were all contributing to *de novo* synthesis of citrulline during arginine starvation (Marini et al., 2010). In line with these findings, our results indicate that arginine free diet can limit the growth rate of HCT 116 xenografts, however plasma arginine and citrulline levels are sufficient to support the growth

of established ASS1 positive tumours in prolonged exposure to arginine free diet in which citrulline may be utilised for further intratumoural and systemic *de novo* synthesis of arginine.

3.3 Investigating the effects of arginine catabolising enzymes *in vitro*

3.3.1 Investigating the effect of arginine catabolising enzymes on cell proliferation

Prompt by the promising *in vitro* data obtained from arginine-free experiments, our next task was to investigate whether arginine catabolising enzymes could potentially be used to target CRC. In a series of cell proliferation assays, arginine sensitive cell lines from previous experiments were exposed to various concentrations of commercially-available arginine catabolising enzymes, Arginine Deiminase (ADI, Peprotech) (Figure 3-7) and Human Recombinant Arginase 1 (BioLegend®) (Figure 3-8).
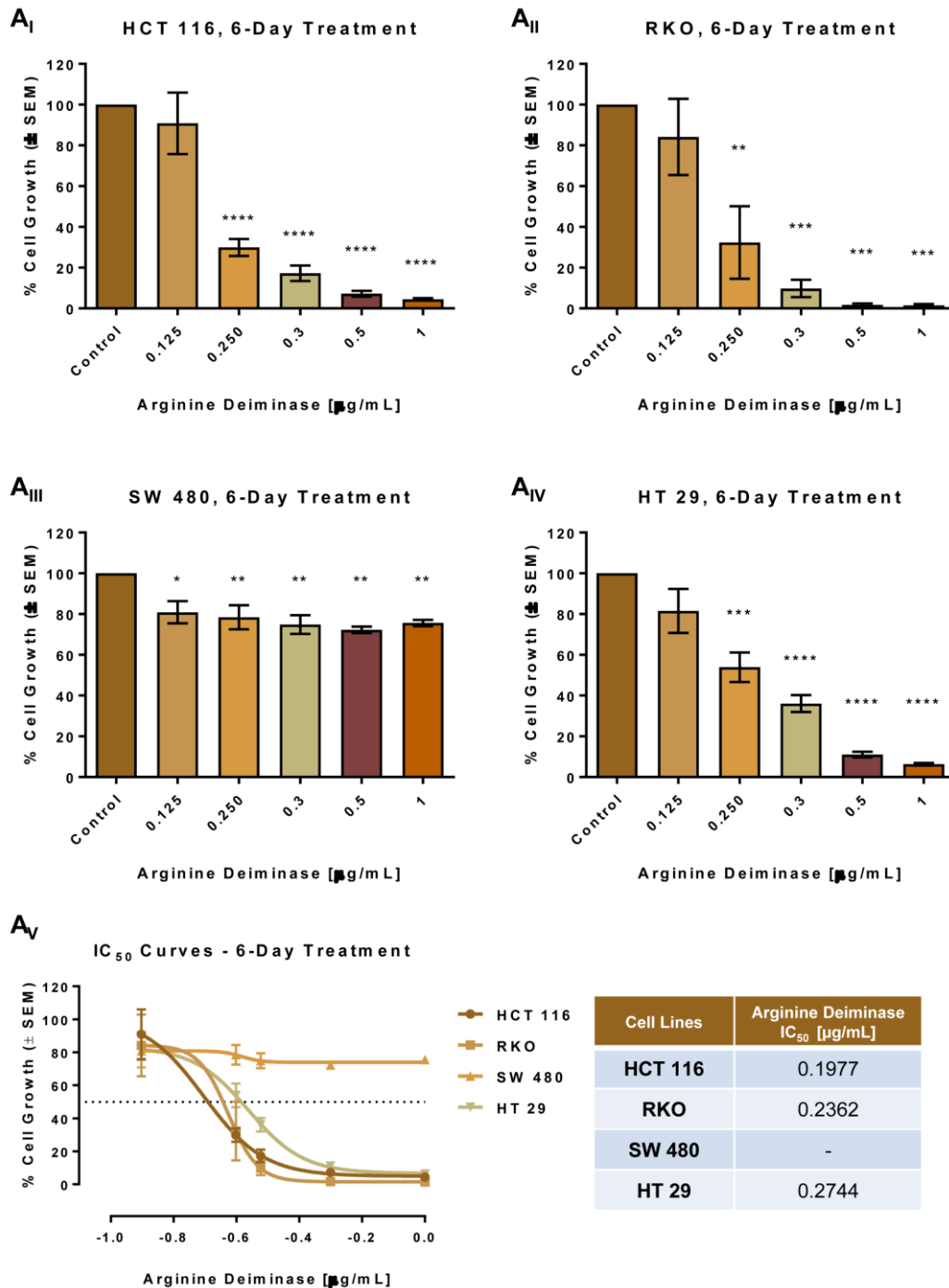
Figure 3-7: Enzymatic Depletion of L-Arginine from Culture Media with Arginine Deiminase (ADI) Inhibits Growth of Colon Cancer Cell Lines. *Colon cancer cell lines **(A$_I$)** HCT 116, **(A$_{II}$)** RKO, **(A$_{III}$)** SW 480, **(A$_{IV}$)** HT 29, were cultured in DMEM/F12 medium containing various concentrations of Arginine Deiminase (ADI). Quadruplicate samples were assessed for cell growth by cell counting. The percentage (%) of Cell Growth from ADI treated cells was calculated relative to the cell numbers in corresponding PBS-treated (Control) cells, which was chosen as 100%. **(A$_V$)** Dose – Response Nonlinear Regression Curves. IC$_{50}$ values were obtained from a nonlinear regression analysis of concentration of the drug vs. response curves utilizing GraphPad Prism. The results were obtained from three independent experiments. The error bars represent the ± Standard Error of the Mean (±SEM) from 3 independent replicates (*p<0.05, **p<0.01, ***p<0.001, ****p<0.0001, two-tailed Student's t-test).*
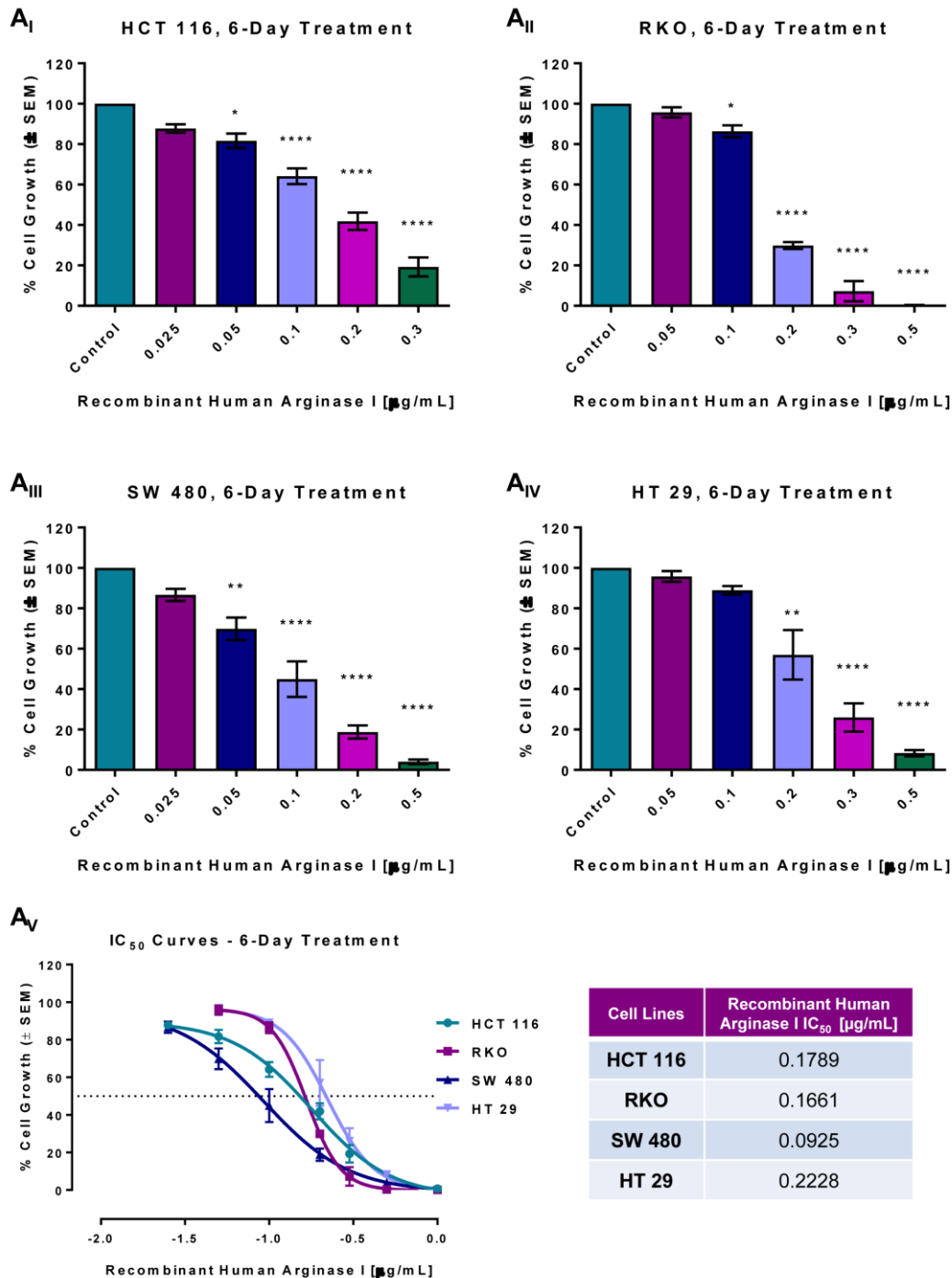
Figure 3-8: Enzymatic Depletion of L-Arginine from Culture Media with Recombinant Human Arginase I Inhibits Growth of Colon Cancer Cell Lines. *Colon cancer cell lines **(A$_I$)** HCT 116, **(A$_{II}$)** RKO, **(A$_{III}$)** SW 480, **(A$_{IV}$)** HT 29, were cultured in DMEM/F12 medium containing various concentrations of Recombinant Human Arginase I. Quadruplicate samples were assessed for cell growth after a 6-Day Period of treatment by cell counting. The percentage (%) of Cell Growth from Recombinant Human Arginase I treated cells was calculated relative to the cell numbers in corresponding PBS-treated (Control) cells, which was chosen as 100%. **(A$_v$)** Dose – Response Nonlinear Regression Curves. IC$_{50}$ values were obtained from a nonlinear regression analysis of concentration of the drug vs. response curves utilizing GraphPad Prism. The results were obtained from three independent experiments. The error bars represent the ± Standard Error of the Mean (±SEM) from 3 independent replicates (*p<0.05, **p<0.01, ***p<0.001, ****p<0.0001, two-tailed Student's t-test).*
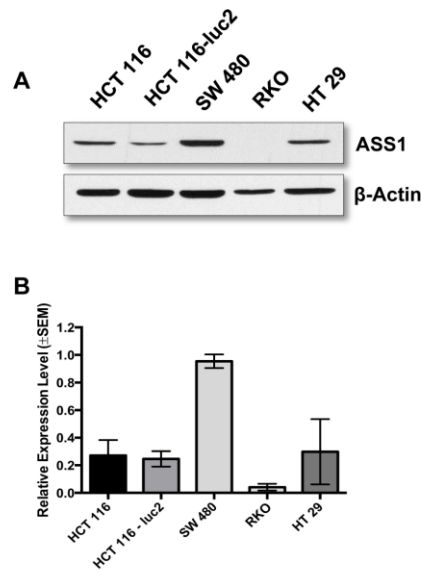
Figure 3-9: Protein Expression Levels of ASS1 in colorectal cancer cell lines. (A) *ASS1 protein expression levels were determined by Western blot analysis (representative results).* ***(B)*** *Relative Expression Levels of ASS1 normalized against actin loading control. The error bars represent the ± Standard Error of the Mean (±SEM) (n= 3 independent experiments).*

As shown in Figure 3-7, 3 out of 4 colorectal cancer cell lines were sensitive to ADI treatment with statistically significant and robust reduction in cell growth starting from 0.025 µM/mL of drug concentration. Interestingly, despite the marginal decrease in cell growth, SW 480 cells were substantially resistant to ADI treatment (Figure 3-7A$_{III}$). The % growth of SW 480 cells was never below 70% of the of control cells.

Conversely, all cell lines exposed to recombinant human arginase 1 exhibited a significant response at enzyme concentrations as low as 0.05µM/mL. Indicatively, IC$_{50}$ values fluctuated from 0.09 – 0.22 µM/mL, with the ADI-resistant SW 480 cell line exhibiting the highest sensitivity (Figure 3-8A$_{III}$).

The mycoplasma derived enzyme, arginine deiminase (ADI) catalyses the conversion of arginine intro citrulline and ammonia. Cells can regenerate arginine from citrulline in two steps via the urea cycle. ASS1 catalyses the conversion of citrulline into argininosuccinate, whereas ASL further converts argininosuccinate to arginine. Therefore, the ability of cells to *de novo* synthesize arginine from citrulline depends on the expression and activity of both ASS1 and ASL (Feun et al., 2011). Western blot assessment of ASS1 expression in ADI-sensitive (HCT 116, RKO, and HT 29) and resistant (SW 480) cell lines showed significant differences. The relative expression levels of ASS1 were significantly lower in the ADI-sensitive cell lines (Figure 3-9).

3.4 Tissue Microarray Study

3.4.1 Investigating the expression levels of ASS1 and OTC in CRC patients

The promising anti-growth effects observed following arginine withdrawal and depletion, led us to investigate the expression levels of ASS1 and OTC in CRC patients.

As previously mentioned in Section 1.6.5, PEGylated forms of the mycoplasma derived arginine deiminase and recombinant human arginase are currently being tested in clinical trials in ASS1 and OTC deficient tumours, respectively. Hence, analysis of expression of arginine metabolism enzymes can potentially identify individuals susceptible to arginine depleting strategies.

Preliminary online dataset analysis on Oncomine® (ThermoFisher®, UK) confirms the robust ASS1 upregulation in colorectal cancer (Figure 5-1C, Appendices). On the contrary, mRNA levels of OTC are significantly lower in the cancer tissue compared to normal tissue control (Figure 5-1A and B). To validate the bioinformatics data, we assessed the expression levels of ASS1 and OTC using a TMA containing more than 600 cases of CRC.

The results presented in Figure 3-10A$_I$, confirm the robust expression of ASS1 protein, with more than 45% of all CRC cases being characterised as strong positive and 33.76% positive. Interestingly, we observed a subset of CRC patients with low or undetectable ASS1 levels (15.69% and ~3% respectively). OTC expression profiling in TMAs is in agreement with results obtained from online dataset analysis, identifying more than 90% of all cases as weak positive (73.65%) or negative (24.49%) with regard to OTC protein levels (Figure 3-10A$_{II}$ and Figure 3-11).
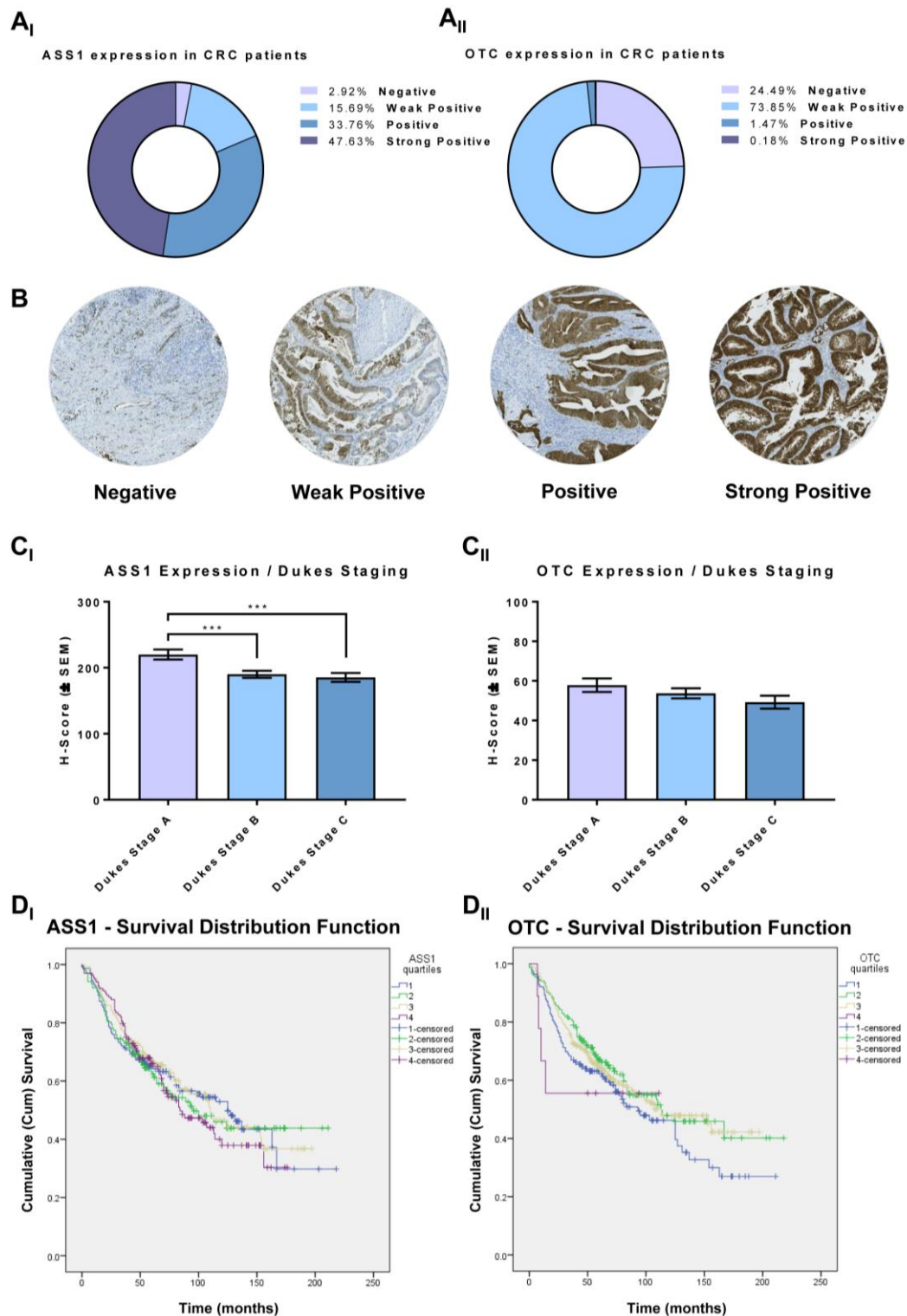
Figure 3-10: Tissue Microarray Study – Expression levels of related to arginine metabolism enzymes, ASS1 and OTC in CRC Patients. (A$_I$)** Distribution of ASS1 and **(A$_{II}$)** Negative, Weak Positive, Positive and Strong Positive in CRC **(B)** Representative micrographs from ASS1 IHC staining at 40x magnification **(C$_I$, C$_{II}$)** H-Score distribution of ASS1 and OTC staining in Dukes Stages respectively (The error bars represent the ± Standard Error of the Mean (±SEM); (p<0.001, two-tailed Student's t-test), **(D$_I$, D$_{II}$)** Kaplan-Meier plot – Survival Distribution of 650 CRC patients stratified by ASS1 and OTC expression (1st quartile: negative/blue, 2nd quartile: weak positive/green 3rd quartile: positive/yellow, 4th quartile: strong positive/purple. Survival curves were analysed for statistically significant difference via the Chi-Square test.*

ASS1 expression differed significantly between Dukes stages (Figure 3-10C$_I$), however there was no relation between ASS1 expression level and patients' survival (Figure 3.10D$_I$) Similarly to ASS1, OTC showed a significant trend towards lower levels in later stages of the disease, without any significant effect on survival (Figure 3-10D$_{II}$ and Figure 3-12A$_{II}$, B$_{II}$).
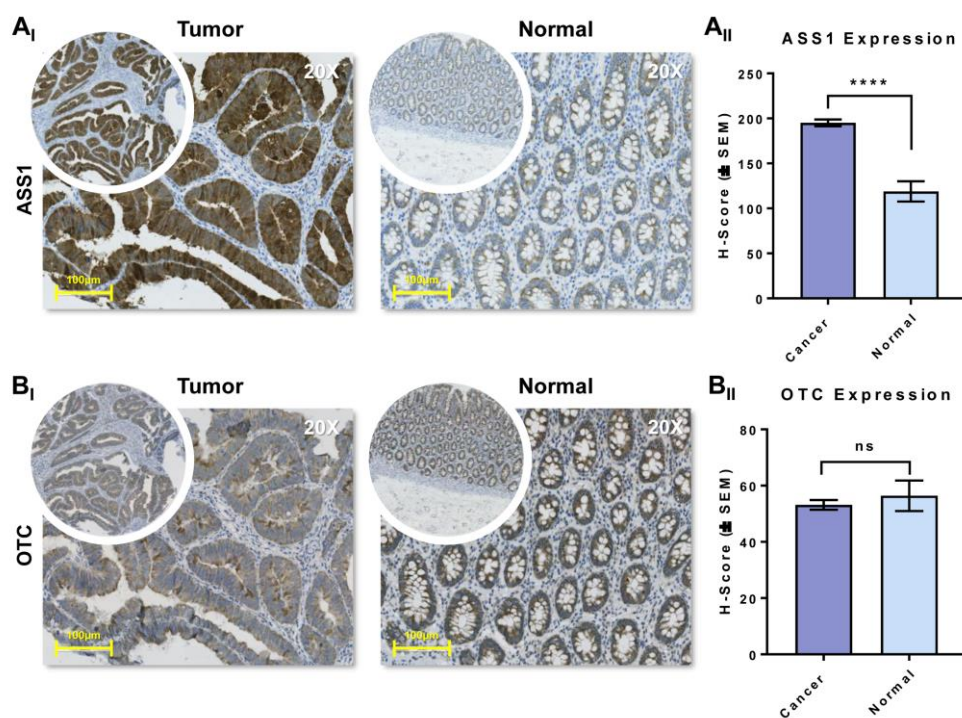
Figure 3-11: Comparison of immunohistochemical staining between Normal vs colorectal cancer tissue sections stained for ASS1 and OTC antibodies. (A$_I$, B$_I$) *Representative cores of Normal vs CRC cases stained with for ASS1 and OTC.* ***(A$_{II}$, B$_{II}$)*** *Expression distribution of ASS1 and OTC in Normal vs CRC cases. Pictures in circles represent the overall staining and tissue differentiation within individual cores whereas square pictures represent areas within the cores at 20x magnification. The error bars represent the ± Standard Error of the Mean (±SEM), (****p<0.0001, two-tailed Student's t-test).*
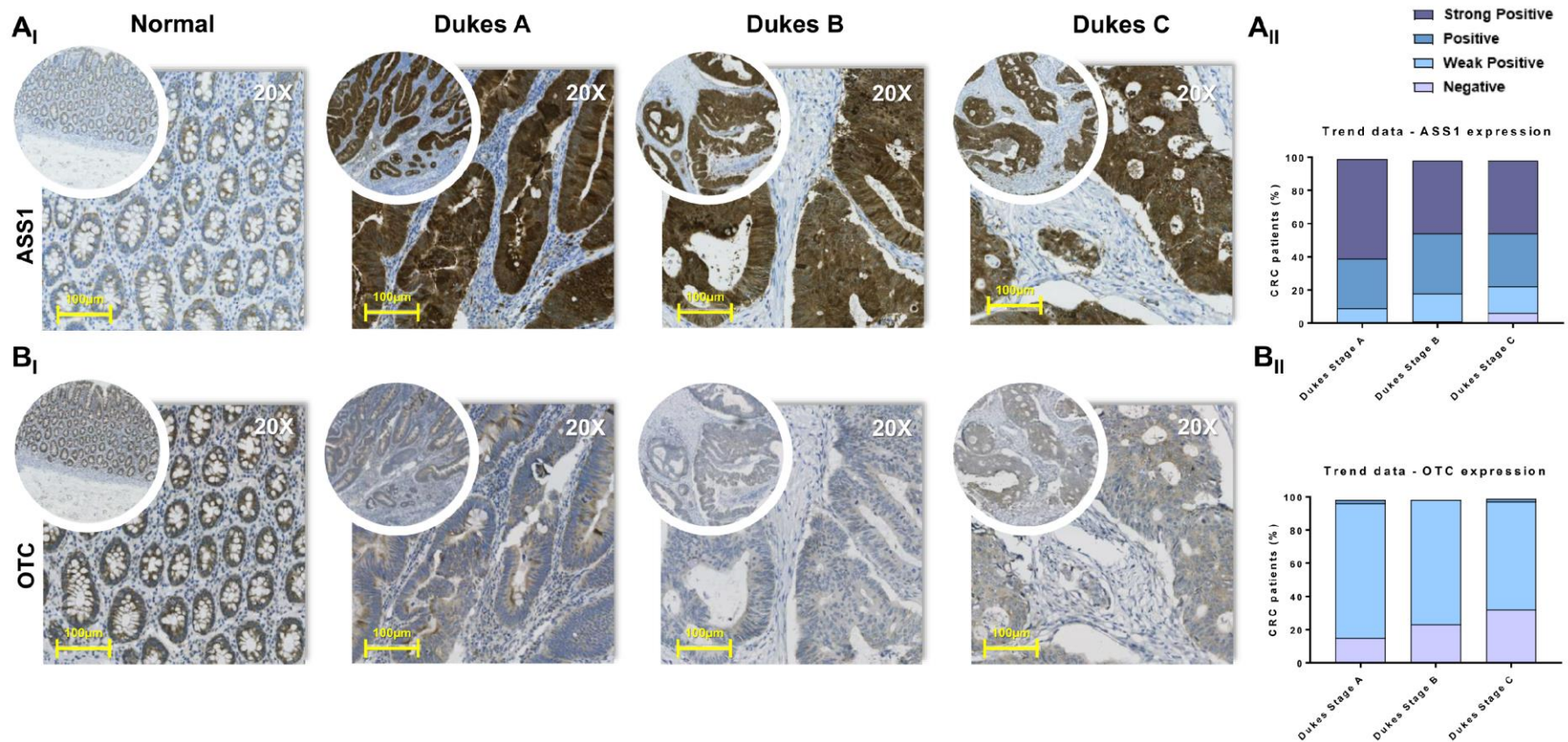
Figure 3-12: Comparison of immunohistochemical staining of colorectal cancer tissue sections for ASS1 and OTC antibodies in relation to Dukes' staging. (A_I, B_I) *Representative cores of CRC patients of ASS1 and OTC in progressive stages of the disease, Dukes A, B and C. (A_{II}, B_{II}) % distribution - trend of ASS1 and OTC expression in CRC in correlation to Dukes' staging. Pictures in circles represent the overall staining and tissue differentiation within individual cores whereas square pictures represent areas within the cores at 20x magnification*

3.4.2 Summary

Despite the lack of any link between ASS1 / OTC expression and patients' survival we managed to identify a small fraction of CRC cases where patients were characterised as negative or ASS1 deficient. To that extent, OTC down-regulation in the vast majority of the cases, along with the previously mentioned subset of ASS1 negative specimens, renders CRC patients potentially susceptible to ADI-PEG20 and rhArg1peg5000 treatment.

3.5 Investigating the effects of arginine catabolizing agents *in vitro*

Prompted by the robust response of CRC cell lines to arginine catabolizing enzymes (Section 3.3) and the altered expression of urea cycle enzyme, we investigated the effects of pharmacological depletion of arginine utilizing the PEGylated forms of arginine deiminase, ADI-PEG20 (Polaris Pharmaceuticals, San Diego) and recombinant human arginase 1 (rhArg1peg5000, BCT International Ltd).

3.5.1 Investigating the effect of ADI-PEG20 on cell growth

CRC cell lines were exposed to a range of concentrations of ADI-PEG20 over a 6-day treatment period. As expected 3 out of 4 cell lines (HCT 116, RKO and HT 29) were sensitive to ADI treatment with statistically significant and robust reduction in % cell growth with IC_{50} values ranging from 0.034 to 0.036 μg/mL (Figure 3-13A$_V$). SW 480 remained resistant to arginine deiminase treatment with a growth reduction never greater than 20% in comparison to the control (Figure 3-13A$_{III}$).
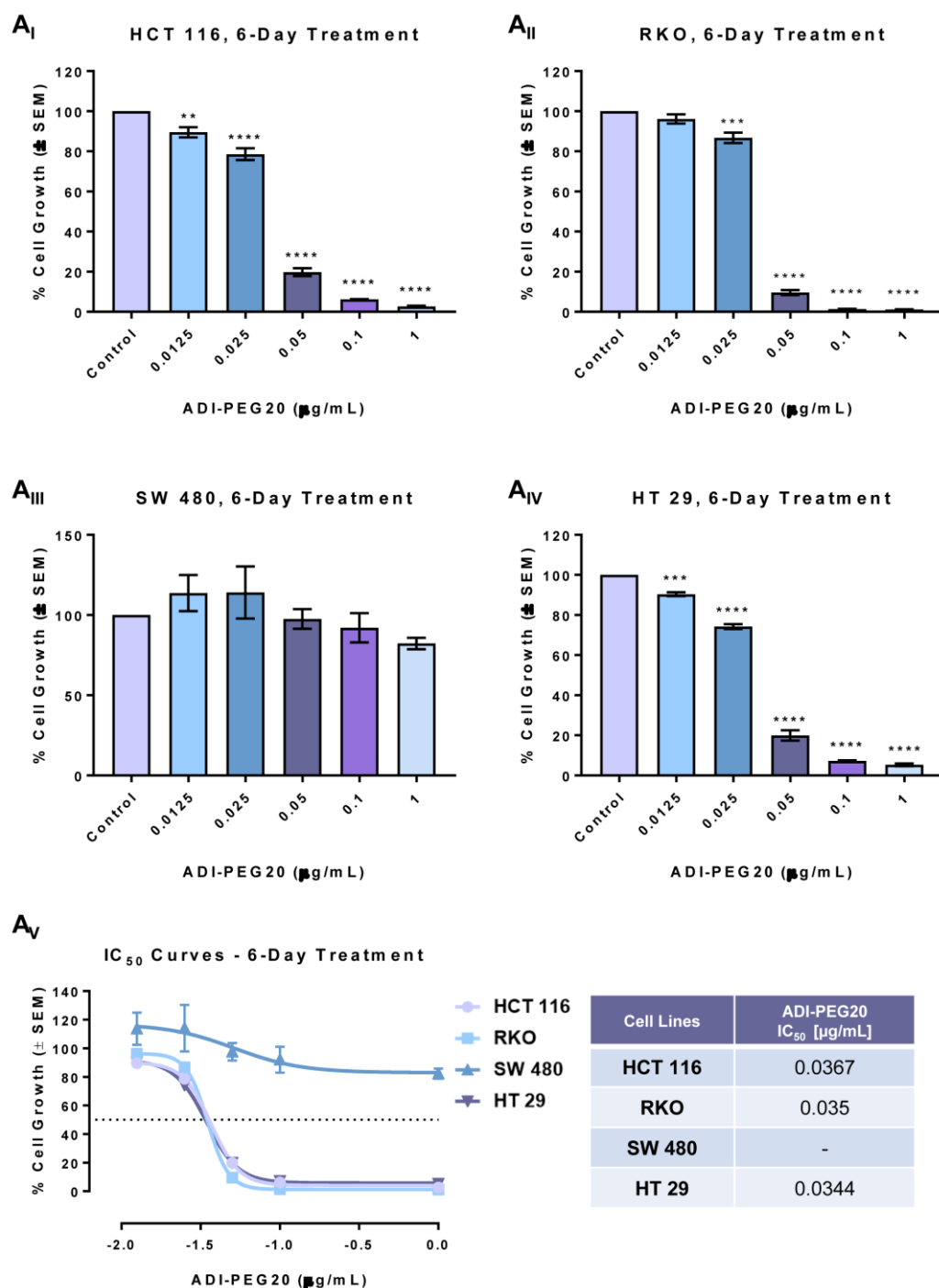
Figure 3-13: Pharmacological Depletion of L-Arginine from Culture Media with ADI-PEG20 Inhibits Growth of Colon Cancer Cell Lines. *Colon cancer cell lines (AI) HCT 116, (AII) RKO, (AIII) SW 480, (AIV) HT 29, were cultured in DMEM/F12 medium containing the indicated concentrations of ADI-PEG20. Quadruplicate samples were assessed for cell growth after a 6-Day Period of treatment by cell counting. The percentage (%) of Cell Growth from ADI-PEG20 treated cells was calculated relative to the cell numbers in corresponding PBS-treated (Control) cells, which was chosen as 100 (Av) Dose – Response Nonlinear Regression Curves. IC50 values were obtained from a nonlinear regression analysis of concentration of the drug vs. response curves utilizing GraphPad Prism. The results were obtained from three independent experiments. The error bars represent the ± Standard Error of the Mean (±SEM). (*p<0.05, **p<0.01, ***p<0.001, ****p<0.0001, two-tailed Student's t-test).*

3.5.2 Investigating the effect of ADI-PEG20 on cell cycle

The anti-proliferative effects of ADI-PEG20 were further investigated by direct measurement of DNA synthesis utilizing the Click-iT® EdU Flow Cytometry assay. CRC cells lines were exposed to 0.5 μg/mL ADI-PEG20 for a 72 hr period of time. Prior to analysis cells were pulsed for 1 hr with EdU and analysed for EdU incorporation using FACS.

Cytofluorimetric data revealed partial reduction of EdU incorporation after 72 hr drug exposure in ASS1 deficient cell lines RKO and HT 29. The reduction in EdU incorporation in RKO was never greater than 40%. HT 29 exhibited a far less but still significant reduction at around 25% percent in comparison to the control. As expected the ASS1-positive, SW 480 did not show any significant decrease in DNA synthesis. Interestingly, in contrast to their response to drug treatment, HCT 116 revealed a paradoxical increase in active DNA synthesis upon 72 hr of exposure to the drug suggesting that ASS1 expression even at lower levels is sufficient to rescue the cell cycle arrest (Figure 3-14B).

Results from EdU incorporation assay were also reflected by data obtained from time course experiments where the expression of Cyclin D1 and Cyclin D3 was gradually recovered to normal levels after 24, 48 and 72 hr of exposure to ADI-PEG20 (Figure 3-14C, D$_{I, II}$)

Ensuing resistance to ADI-PEG20 treatment has been reported and attributed to re-expression of ASS1 enzyme. (Shen et al., 2003, Manca et al., 2011, Tsai et al., 2012). The ability of ASS1 to regenerate *de novo* arginine from citrulline via a two-step process renders cancer cells capable to tolerate arginine depletion with ADI.
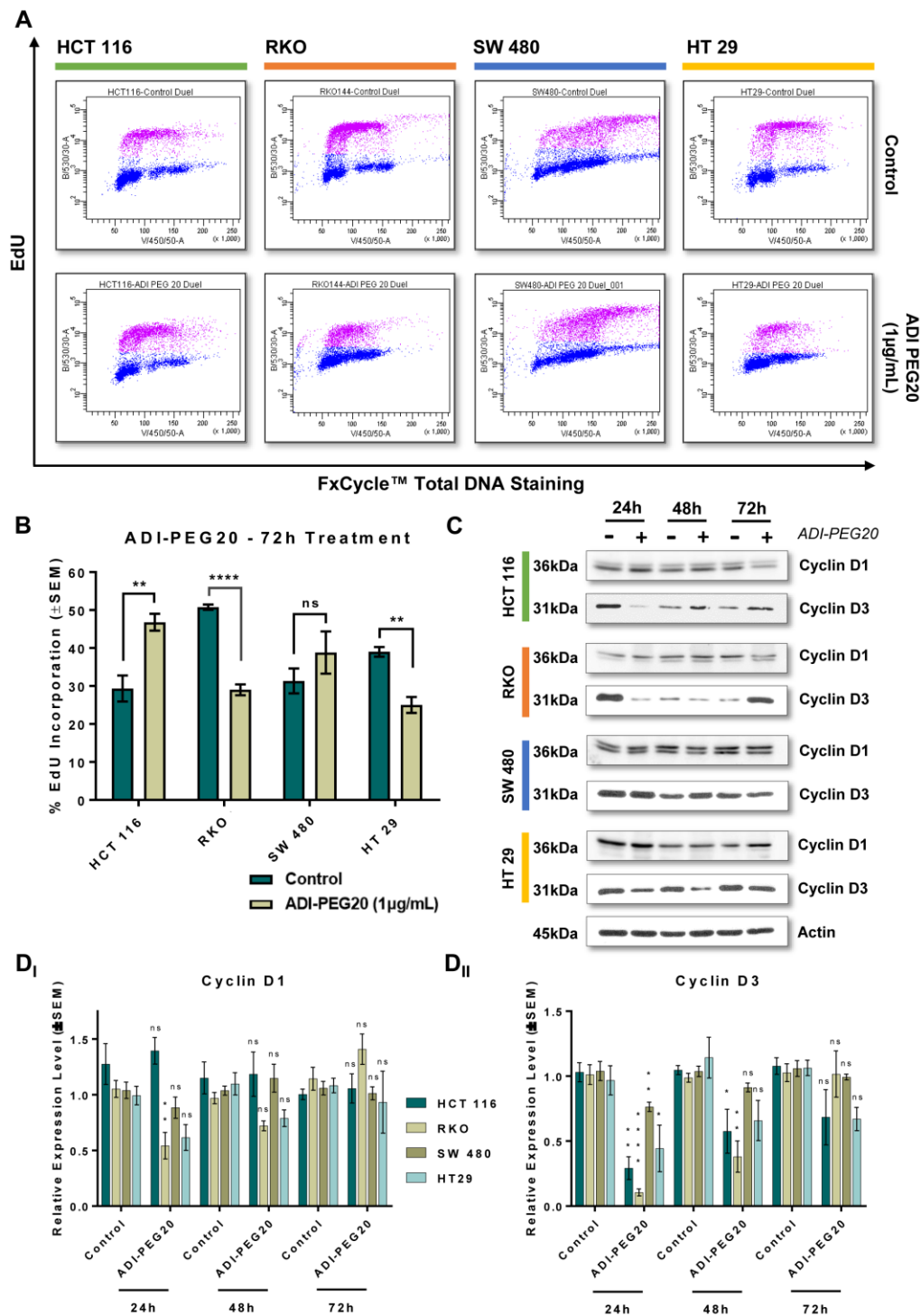
Figure 3-14: ADI-PEG20 impairs cell proliferation by decreasing Cyclin D1 / Cyclin D3 levels and active DNA synthesis. (A) *Dual parameter plot of Click-iT® EdU® Alexa Fluor® 488 and FxCycle™, EdU and FxCycle™ Violet Fluorescence were detected and measured using 488nm excitation / 530/30 bandpass filter and 405nm excitation / 450/40 bandpass filter respectively. Dual positive cells in purple signify the cells in the S-phase, whereas from left to right, cells in blue indicate cells in G_0/G_1 and G_2M respectively **(B)** % Click-iT® EdU incorporation of colon cancer cell lines with or without ADI-PEG20 in culture media for 72 hr. **(C)** Western blots of Cyclin D1 and Cyclin D3. Whole cell lysates from Control and ADI-PEG20 treated cells were collected after 72 hr. Actin was used as loading control (indicative results - all actin controls are presented in the manuscript at the end of this thesis, **(D$_I$, D$_{II}$)** Relative Expression Levels of Cyclin D1 and Cyclin D3 compared to their respective controls. The error bars represent the ± Standard Error of the Mean (±SEM) (*p<0.05, **p<0.01, ***p<0.001, ****p<0.0001, two-tailed Student's t-test).*

Here, we showed that after their initial response to ADI-PEG20, ASS1- deficient CRC cell lines manage to re-express ASS1 upon 72 hr exposure to the drug. More specifically, RKO and HT 29 cells increased their ASS1 expression almost by 80 and 60% respectively (Figure 3-15). In agreement with Tsai et al., re-expression of ASS1 was correlated with high levels of c-Myc which was stabilised upon 48 and 72 hr suggesting transcriptional regulation of ASS1 gene by c-Myc in 2 out of 4 cell lines tested (Figure 3-15A, C) (Tsai et al., 2012).

The ASS1 positive cell line SW 480, exhibited relatively similar levels of ASS1 expression throughout the course of the experiment while HCT 116 levels of ASS1 were also increased. Interestingly, increased ASS1 expression in HCT 116 was not only observed in the treatment group but also in the controls, suggesting that, limited availability of arginine in exhausted media, or changes in cell confluency can   stimulate re-expression of ASS1 in highly proliferative, metabolically demanding cells.

HCT 116 did not show any correlation between ASS1 expression and c-Myc stabilization, suggesting the existence of alternative ways of ASS1 regulation in CRC.
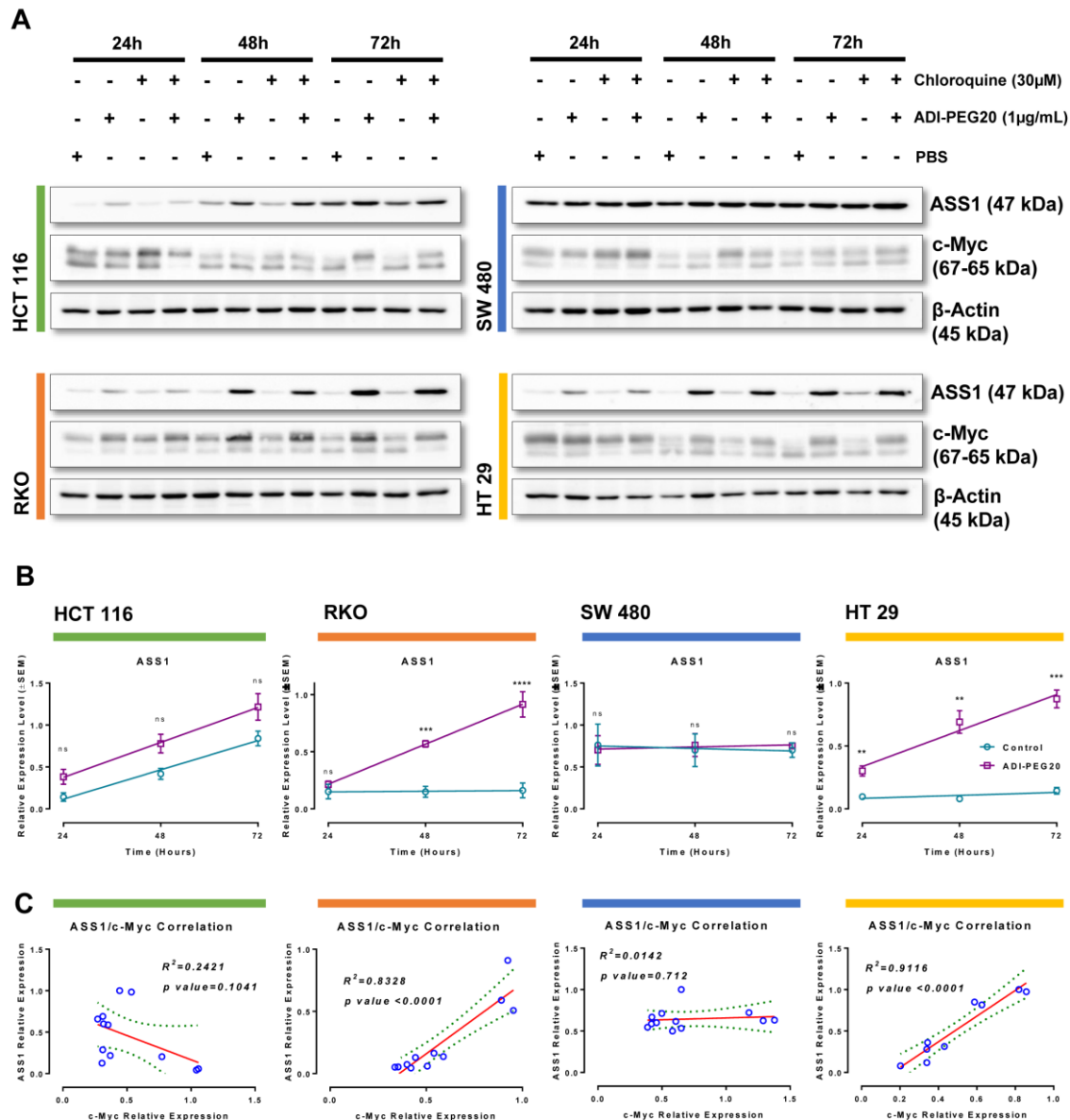
Figure 3-15: Re expression of ASS1 is associated with stabilisation of c-Myc in RKO and HT 29 cell lines treated with ADI-PEG20. (A) *Time course Western blot analysis of ASS1 and c-Myc in response to ADI-PEG20, at 24, 48 and 72 hr accordingly,* **(B)** *Relative Expression levels of ASS1 in response to ADI-PEG20 (Control vs Treatment),* **(C)** *Linear correlation between ASS1 and c-Myc expression in CRC cell lines treated with ADI-PEG20. The error bars represent the ± Standard Error of the Mean (±SEM, n=3) (*p<0.05, **p<0.01, ***p<0.001, ****p<0.0001, two-tailed Student's t-test).*

3.5.3   Investigating the effects of ASS1 in the ADI-PEG20 resistant cell line, SW 480

To confirm that ASS1 is a key biomarker of sensitivity to ADI and ADI-PEG20 treatment, we silenced ASS1 expression in the ADI resistant cell line SW 480 using siRNA technology. Transient knockdown of ASS1 decreased cell proliferation in response to ADI-PEG20 treatment by almost 50% in comparison to the scramble control (Figure 3-16C) Western blot analysis confirmed the successful knockdown of ASS1 (Figure 3-16A). Accordingly, reduction in cell growth in ASS1-knockdown, ADI-PEG20-treated cells was accompanied by a significant reduction in Cyclin D1 levels (Figure 3-16B).
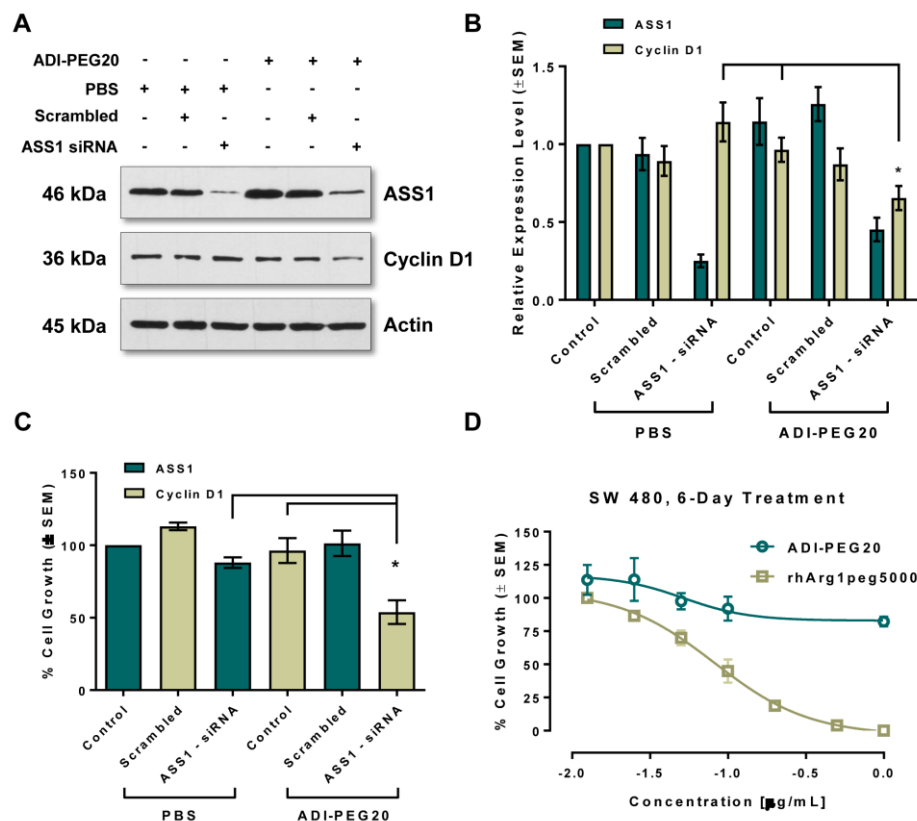
Figure 3-16: Knockdown of ASS1 expression decreases cell proliferation and Cyclin D1 levels in cells treated with ADI-PEG20. *SW 480 colorectal adenocarcinoma cells were left untrasfected or transfected with ASS1 siRNA or scramble control. After 24hr cells were exposed to ADI-PEG20 or PBS vehicle control for 48hr. **(A)** Western blot analysis of ASS1 and Cyclin D1 in SW 480 cells and SW 480 transfected as indicated (representative result of triplicate experiments). **(B)** Relative expression levels of ASS1 and Cyclin D1 normalized against Actin. **(C)** % Cell Growth of SW 480 Control and SW 480 – ASS1 siRNA transfected cells (72h post transfection). **(D)** Dose – Response Curves of SW 480 cells exposed to ranges of concentrations of ADI-PEG20 and rhArg1peg5000 over a 6-Day treatment. The results were obtained from three independent experiments. The error bars represent the ± Standard Error of the Mean (±SEM) (*p<0.05, two-tailed Student's t-test).*

3.5.4 Investigating epigenetic silencing as a way of ASS1 regulation
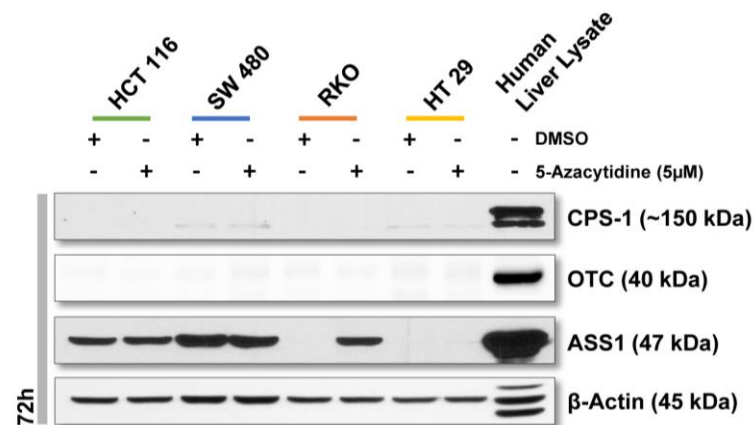
Figure 3-17: Investigating regulation of transcription of arginine-metabolism related enzymes. *Western blot analysis of OTC, CPS1, and ASS1 after 72 hours treatment with 5-Azacytidine (5µM). The results were obtained from three independent experiments (representative results).*

Several reports (Delage et al., 2012; Lan et al., 2013) have identified that regulation of ASS1 gene expression can be controlled epigenetically via methylation of CpG dinucleotides in its promoter regions. RKO and HT 29 are CIMP positive (Ahmed et al., 2013) therefore, we tested whether urea cycle enzymes ASS1 and OTC are regulated through methylation. Lysates from cells exposed to the DNA methyltransferase inhibitor, 5-Azacytidine, were examined via western blotting. Results presented in Figure 3-17 suggest that only in RKO cells ASS1 suppression is methylation dependent. Interestingly, none of the cell lines tested were positive for OTC expression suggesting that OTC gene expression is not regulated via promoter methylation (Figure 3-17). These results are in line with previous observations reported in Section 3.4, where we showed that OTC expression is robustly low in CRC.

3.5.5 Investigating the effect of rhArg1peg5000 on cell growth

Similarly to the non-PEGylated enzyme (Section 3.3.1), rhArg1peg5000 exhibited a remarkable anti-proliferative efficacy in all 4 cell lines tested. After a 6-day period of treatment, HCT 116, RKO and SW 480 and HT 29 responded to drug concentrations as low as 0.050 µg/mL. All cell lines exhibited an extremely significant decrease in growth at higher doses of 0.100-0.500 µg/mL. The IC_{50} of rhArg1peg5000 fluctuated from 0.047 to 0.09 µg/mL (see Table in Figure 3-18). Most importantly, the ADI-PEG20 refractory cell line SW 480 became auxotrophic for arginine indicating the opportunity of alternative targeting of ASS1 positive tumours (Figure 3-18).
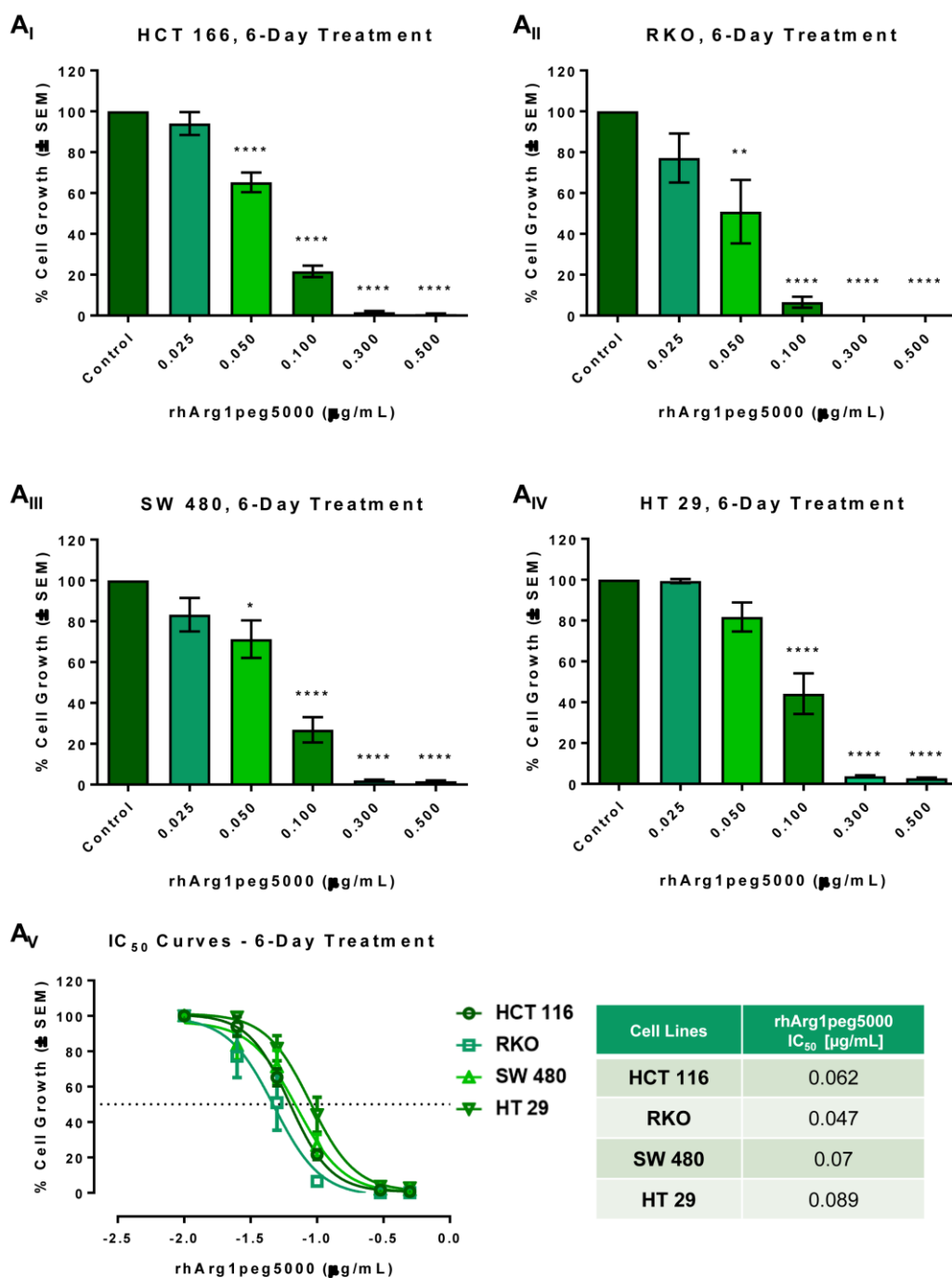
Figure 3-18: Pharmacological Depletion of L-Arginine from Culture Media with PEGylated Recombinant Human Arginase I (rhArg1peg5000) Inhibits Growth of Colon Cancer Cell Lines. *Colon cancer cell lines (**A$_I$**) HCT 116, (**A$_{II}$**) RKO, (**A$_{III}$**) SW 480, (**A$_{IV}$**) HT 29, were cultured in DMEM/F12 medium containing various concentrations of Recombinant Human Arginase I. Quadruplicate samples were assessed for cell growth after a 6-Day Period of treatment by cell counting. The percentage (%) of Cell Growth from rhArg1peg5000 treated cells was calculated relative to the cell numbers in corresponding PBS-treated (Control) cells, which was chosen as 100%. (**A$_v$**) Dose – Response Nonlinear Regression Curves. IC$_{50}$ values (the half maximal concentration of a drug that results in 50% of cell growth compared with the PBS-treated control) were obtained from a nonlinear regression analysis of concentration of the drug vs. response curves utilizing GraphPad Prism. The results were obtained from three independent experiments. The error bars represent the ± Standard Error of the Mean (±SEM) (*p<0.05, **p<0.01, ***p<0.001, ****p<0.0001, two-tailed Student's t-test).*

3.5.6 Investigating the effect of rhArg1peg5000 on cell cycle

To further investigate the antiproliferative capabilities of rhArg1peg5000, we assessed the active DNA synthesis utilizing the EdU incorporation assay. Similarly to arginine free media experiments (Figure 3-19), we found that depletion of arginine using 0.5 µg/mL rhArg1peg5000 led to a significant proliferative arrest in all cell lines tested (Figure 3-19B), with dramatic reduction in % EdU incorporation in RKO, SW 480, and HT 29, upon 72 hr treatment. HCT 116 also exhibited a significant decrease in EdU incorporation, though to a lesser extent.

In agreement with these findings, rhArg1peg5000 treatment decreased expression of proliferation markers, Cyclins D1 and D3 (Figure 3-19C, D_I, D_{II}). All cell lines displayed a sharp decrease in Cyclin D3 with a mild recovery occurring at 72 hr in SW 480 and HT 29. A less prominent, yet significant, decrease in Cyclin D1 expression was observed in RKO and SW 480. Despite the dramatic reduction in Cyclin D3 at all time-points, HCT 116 analysis reveals only a small reduction in Cyclin D1 at 48 hr, in line with results obtained from EdU incorporation assay. The cell lines' response to rhArg1peg5000 was independent of ASS1 expression, signifying the potential use of arginase as an alternative approach for arginine depleting strategies. This notion is strongly supported by Western blot analysis that reveals no compensatory expression of OTC in any of the cell lines (Figure 3-20).
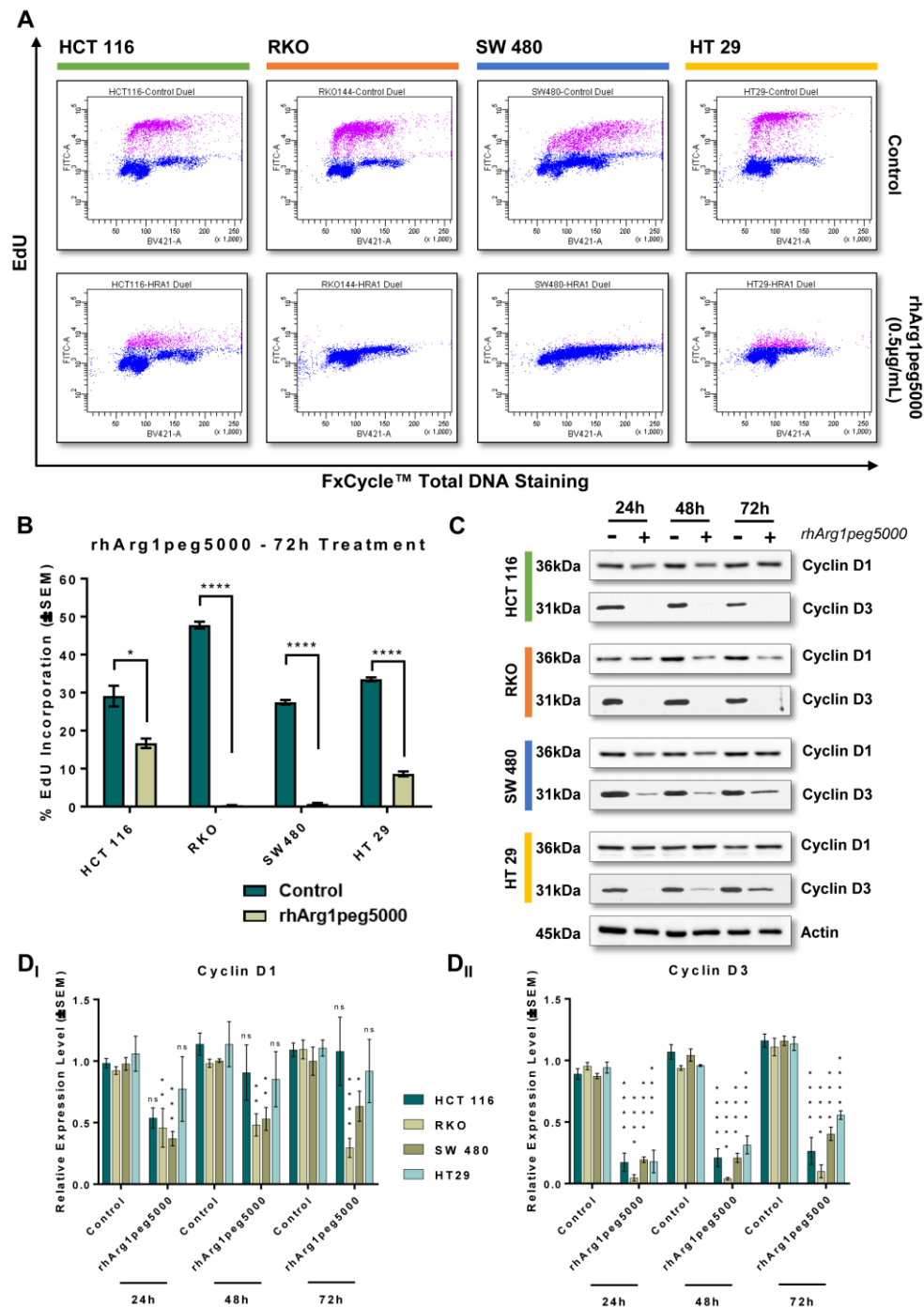
***Figure 3-19: rhArg1peg5000 impairs cell proliferation by decreasing Cyclin D1 / Cyclin D3 levels and active DNA synthesis (A)** Dual parameter plot of Click-iT® EdU® Alexa Fluor® 488 and FxCycle™, EdU and FxCycle™ Violet Fluorescence were detected and measured using 488nm excitation / 530/30 bandpass filter and 405nm excitation / 450/40 bandpass filter respectively. Dual positive cells in purple signify the cells in the S-phase, whereas from left to right, cells in blue indicate cells in G_0/G_1 and G_2/M respectively **(B)** % Click-iT® EdU incorporation of colon cancer cell lines with or without rhArg1peg5000 in culture media for 72 hr. **(C)** Western blots of Cyclin D1 and Cyclin D3. Whole cell lysates from Control and rhArg1peg5000 treated cells were collected after 72 hr. Actin was used as loading control (indicative results - all actin controls are presented in the manuscript at the end of this thesis. **(D_I, D_{II})** Relative Expression Levels of Cyclin D1 and Cyclin D3 compared to their respective controls. The error bars represent the ± Standard Error of the Mean (±SEM) (*p<0.05, **p<0.01, ***p<0.001, ****p<0.0001, two-tailed Student's t-test).*
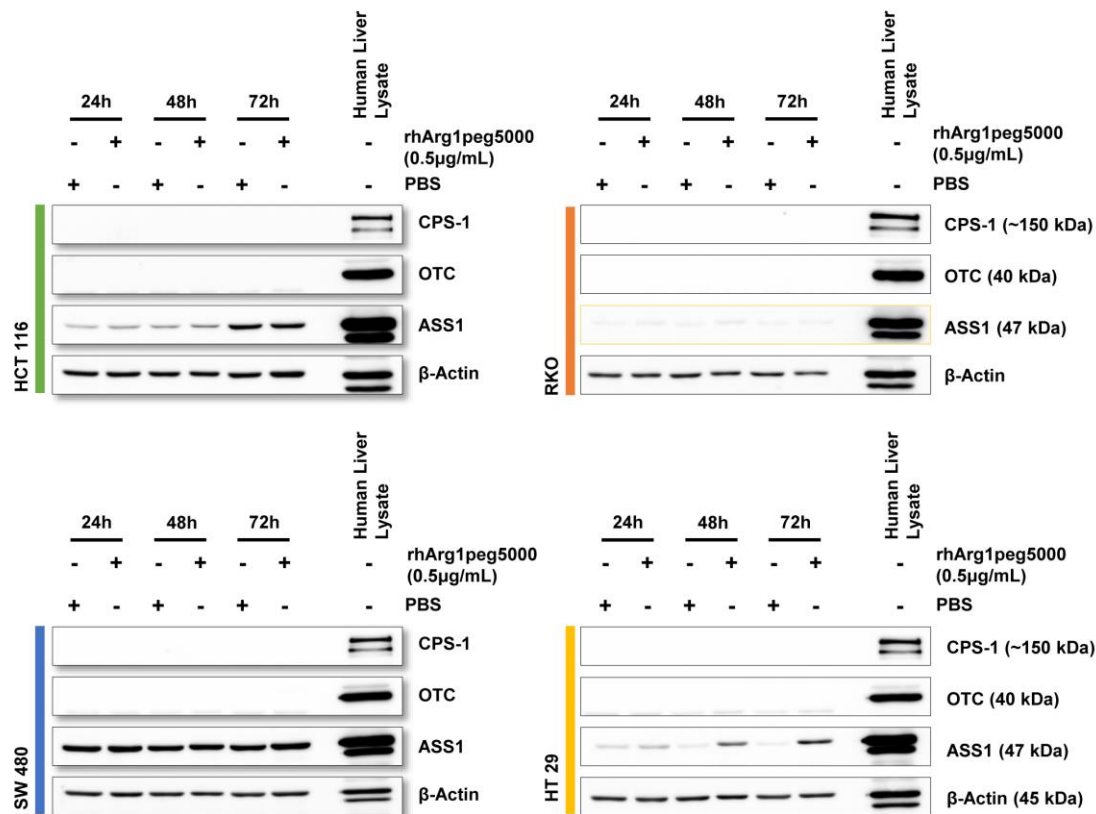
Figure 3-20: Expression profiling of OTC in CRC cell lines in response to rhArg1peg5000. *CRC cell lines exposed to rhArg1peg5000 over a time course experiment were interrogated for OTC expression at 24, 48 and 72 hr via western blotting,* ***(A)*** *HCT 116* ***(B)*** *RKO* ***(C)*** *SW 480* ***(D)*** *HT 29. Human liver lysate was used as a positive control. The results were obtained from three independent experiments (representative results).*

3.5.7   Investigating the expression levels of ASS1 in response to rhArg1peg5000

ASS1 expression profiling over a time course experiment at 24, 48 and 72 hr showed a gradual increase of ASS1 expression in HCT 116 and HT 29. In agreement with previous observations, ASS1 re-expression in HT 29 correlated with increased stabilisation of c-Myc at 48 and 72 hr (R^2=08555, *p value=0.0001*). Remarkably, in RKO, rhArg1peg5000 treatment supresses significantly the expression of ASS1 at 48 and 72 hr (Figure 3-21), suggesting that expression of ASS1 in this cell line may be controlled by alternative mechanisms influenced not just by reduced arginine availability but an also robust decrease of its substrate citrulline.
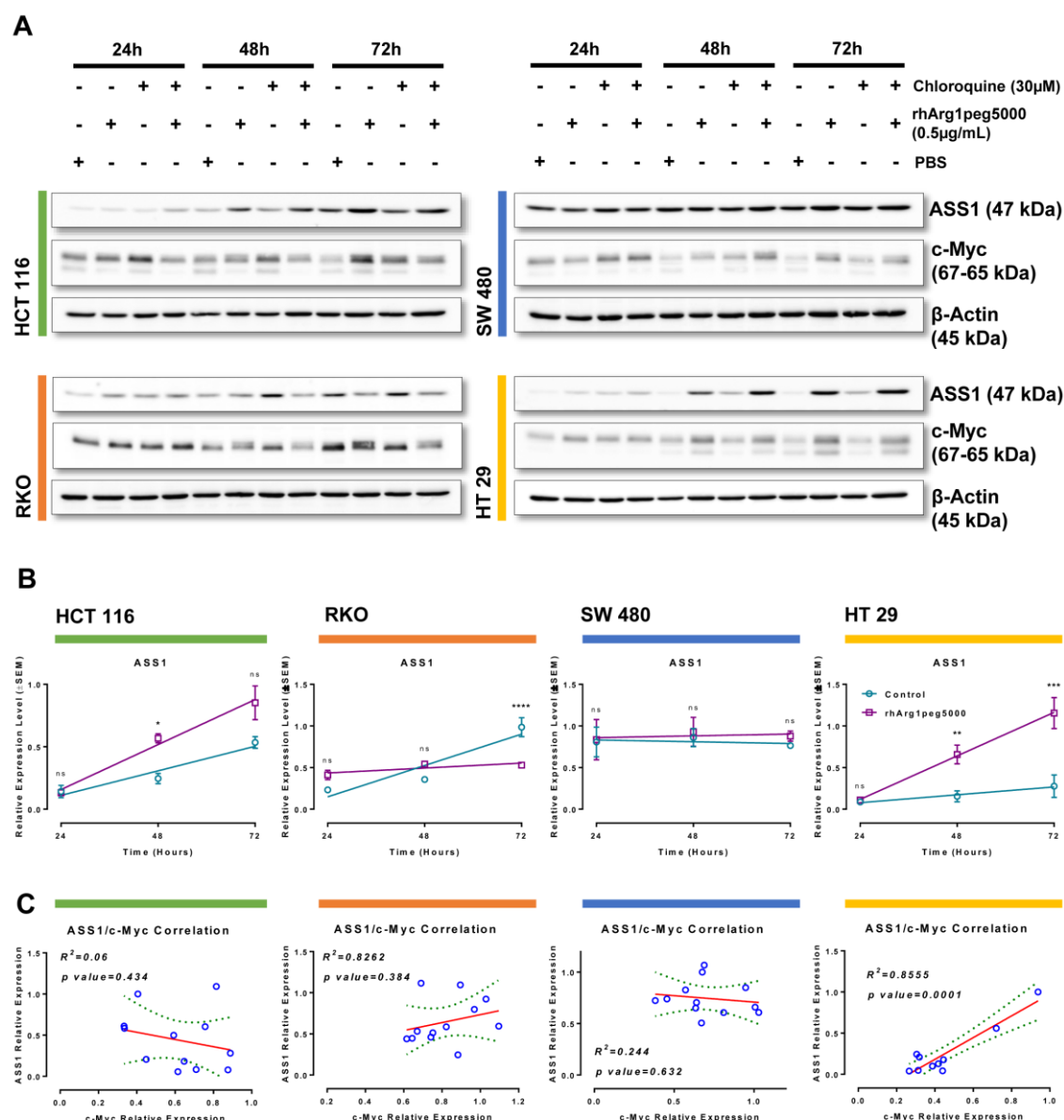
***Figure 3-21: Re expression of ASS1 is correlated with stabilisation of c-Myc in HT 29 cell lines treated with rhArg1peg5000. (A)** Time course Western blot analysis of ASS1 and c-Myc in response to rhArg1peg5000, at 24, 48 and 72 hr, **(B)** Relative Expression levels of ASS1 in response to rhArg1peg5000 (Control vs Treatment), **(C)** Linear correlation between ASS1 and c-Myc expression in CRC cell lines treated with rhArg1peg5000. The error bars represent the ± Standard Error of the Mean (±SEM, n=3) (*p<0.05, **p<0.01, ***p<0.001, ****p<0.0001, two-tailed Student's t-test).*

3.5.8 Summary

Overall, in Section 3.5 we show that CRC cell lines are sensitive in response to pharmacological depletion of arginine. Both ADI-PEG20 and rhArg1peg5000 exhibited robust anti-proliferative capabilities in corresponding cell proliferation assays, with the latter further demonstrating profound decrease in % EdU levels in FACS analysis. Despite the durable, anti-proliferative response of CRC cell lines to ADI-PEG20 treatment, EdU incorporation assay revealed significant increase in % EdU levels in HCT 116 and a less prominent but still significant decrease in RKO and HT 29. Notably, the SW 480 cell line was resistant to ADI-PEG20 treatment. Differential response to ADI-PEG20 was correlated to increased levels of ASS1 in at least 3 out of 4 cell lines. These results come to agreement with several studies that highlight re expression of ASS1 as one of the predominant mechanisms of resistance to ADI-PEG20 treatment (Shen et al., 2003, Manca et al., 2011, Tsai et al., 2012). Furthermore, Western blot analysis revealed significant accumulation of c-Myc in 2 out 4 cell lines, namely RKO and HT 29, which was also correlated with ASS1 expression. Remarkably, none of the cell lines treated with rhArg1peg5000 managed to re express OTC, thus suggesting pharmacological depletion of arginine with rhArg1peg5000 as an alternative therapeutic approach for ASS1 proficient / ADI-PEG20 refractory and OTC deficient CRCs.

3.6 Investigating the effects of arginine catabolising agents *in vivo*

3.6.1 Investigating the effect of ADI-PEG20 on the growth of RKO xenografts

Next, we investigated whether pharmacological depletion of arginine with ADI-PEG20 could negatively affect the growth of tumour xenografts *in vivo*. For the purposes of this experiment we chose to implant subcutaneously the RKO cell line, which exhibited the best *in vitro* response among the ASS1 negative lines. A week after subcutaneous injection, immunocompromised nude mice were randomised and administered 5IU of ADI-PEG20 / animal or PBS once a week. *In vivo* ADI-PEG20 dose was determined based on previous pre-clinical studies in HCC, NCSLC and AML (Kelly et al., 2012; Miraki-Moud et al., 2015; Ensor et al., 2002).

Tumour volume measurements revealed that ADI-PEG20 administration decreases significantly the volume of RKO tumour xenografts in mice (Figure 3-22A). Despite the significant difference in tumour volume, the weight of the excised tumours did not reveal any significant differences (Figure 3-22B). Body weight measurements between vehicle control and treatment groups throughout the course of the experiment indicate plausible adverse effects in regards to the welfare of the animals, however normalised body weight of the animals at the end of the experiment reveals that the initial weight of the animals did not alter significantly throughout the entire course of the experiment (Figure 3-22C), further indicating that the differences observed were due to failure of the treated mice to put on weight.

Western blot analysis of tumour lysates (Figure 3-23) shows a marginal but significant downregulation of both Cyclins D1 and D3 in comparison to the control, further supporting the differences in proliferation rates observed *in vitro*.
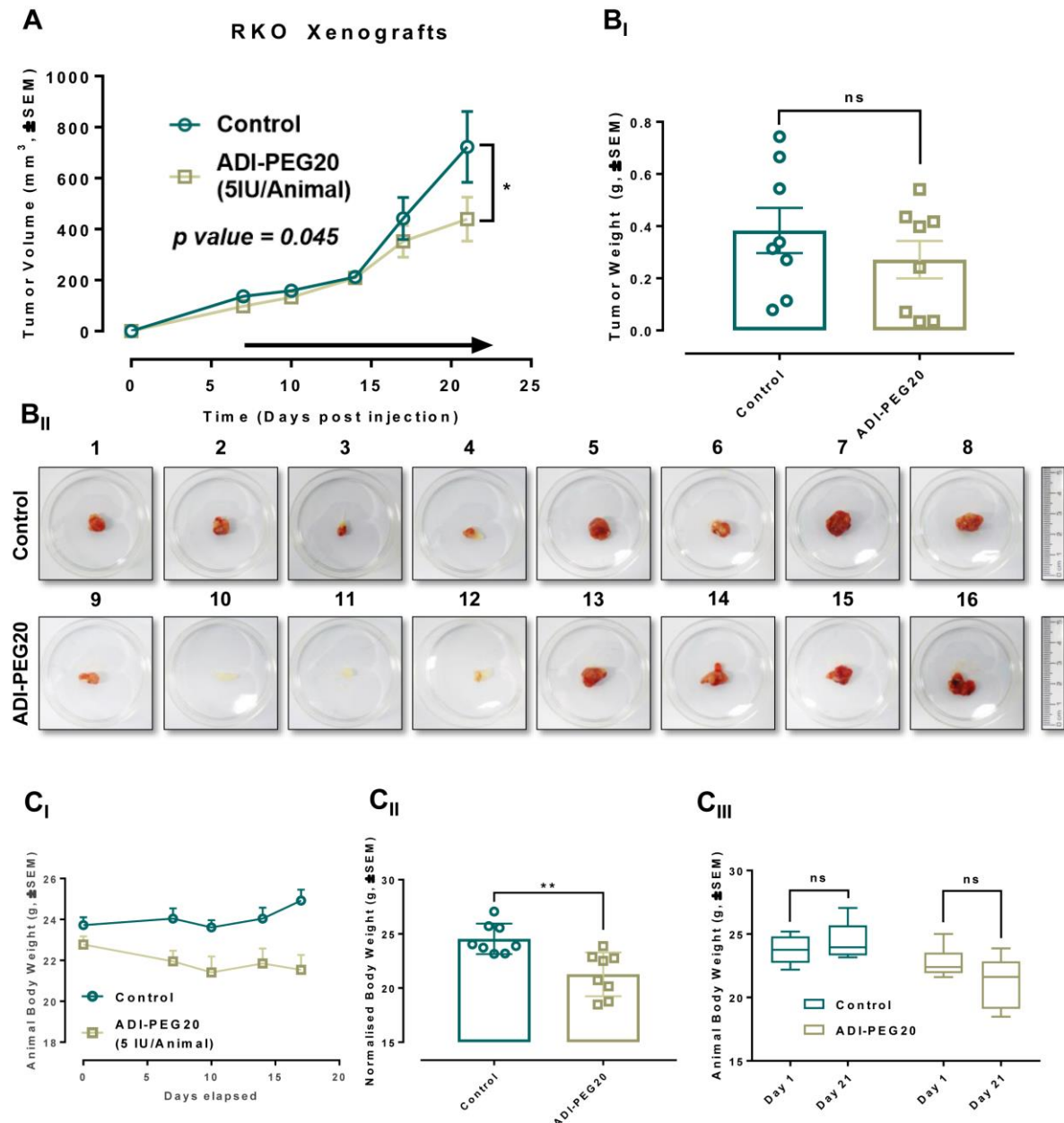
Figure 3-22: Pharmacological depletion of L-Arginine with ADI-PEG20 Decreases the Growth of RKO Xenografts in BALB/c nude mice. *Nude immunocompromised mice (n=16) were injected subcutaneously with RKO and groups of mice (n=8) were administered 5IU/animal ADI-PEG20 or PBS by I.P. once a week. Tumour size was calculated by direct calliper measurement once per week.* ***(A)*** *Growth curves of tumour xenografts in BALB/c mice with or without ADI-PEG20 (n=8 per group, p value=0.045)* ***(B$_I$)*** *Weight of excised tumour xenografts (n=8 per group)* ***(B$_{II}$)*** *Excised tumour xenografts at the of the experiment* ***(C$_I$)*** *Body weight of BALB/C mice, control vs ADI-PEG20 (n=8) and* ***(C$_{II}$, C$_{III}$)*** *normalized body (=animal weight-excised tumour weight) weight of BALB/c mice at the end of the experiment (n=8 per group, no significance). The error bars represent the ± Standard Error of the Mean (±SEM). Statistical significance of difference in tumour volume between the two groups was determined by linear regression analysis. Statistical significance of differences in tumour weight and animal weight was assessed by Student's t-test. (*p<0.05, **p<0.01, ***p<0.001, ****p<0.0001, two-tailed Student's t-test).*
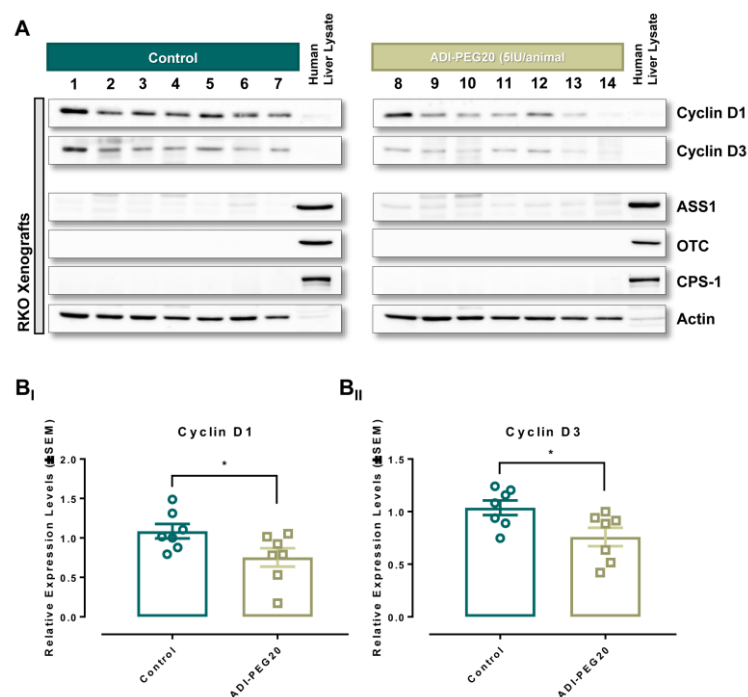
Figure 3-23: Expression Levels of Cyclin D1 and D3 in RKO xenografts treated with ADI-PEG20. *Lysates from tumour xenografts were prepared and subjected to western blotting with antibodies against Cyclin D1, Cyclin D3 Human Liver Lysate was used as a positive control for OTC, CPS-1 and ASS1. Actin was used as a loading control* ***(B$_I$, B$_{II}$)*** *Relative expression levels of Cyclin D1 and Cyclin D3 respectively). The error bars represent the ± Standard Error of the Mean (±SEM). (*p<0.05, **p<0.01, ***p<0.001, ****p<0.0001, two-tailed Student's t-test).*
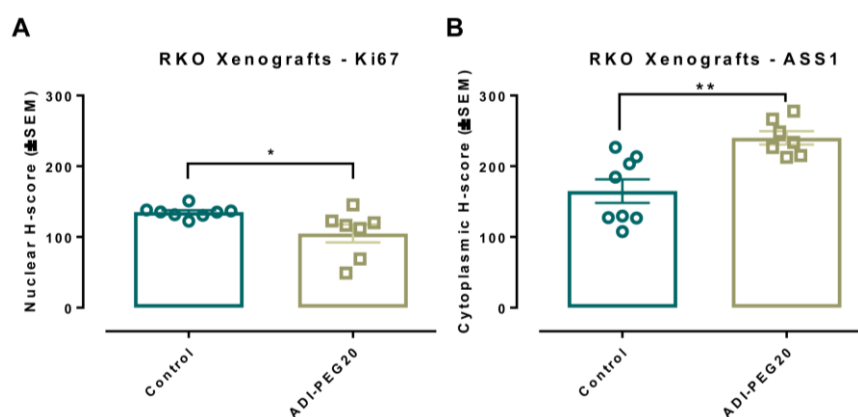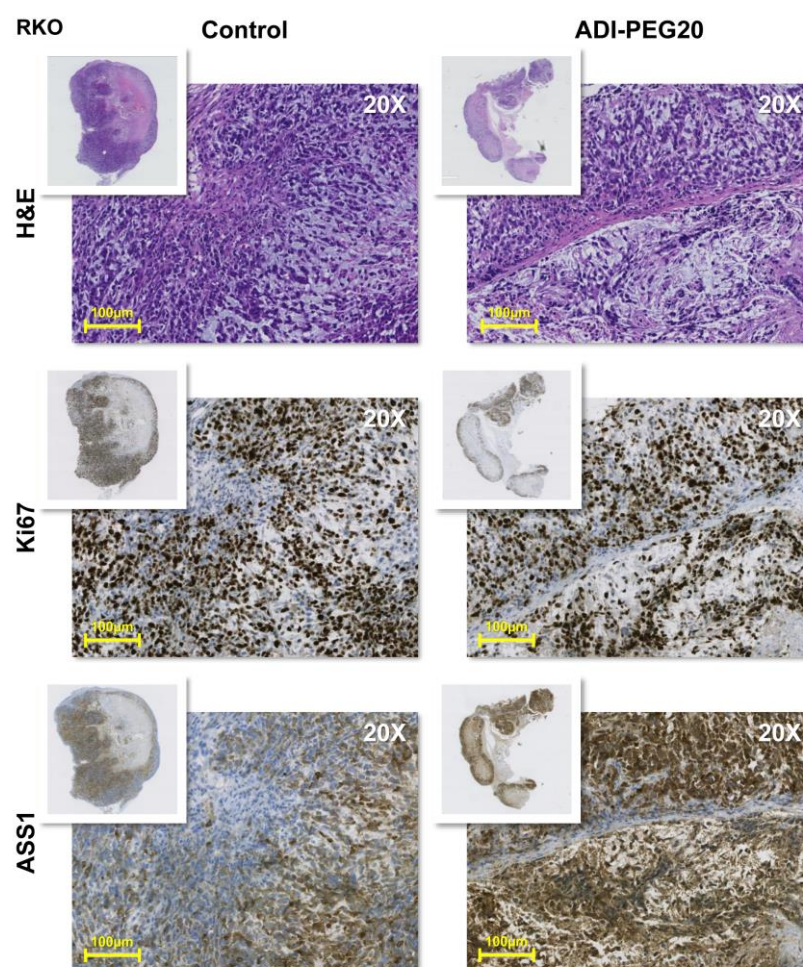
*Figure 3-24: Histology and immunohistochemical analysis of RKO xenograft tumours treated with ADI-PEG20. Immunohistochemical staining of tumour xenograft sections with H&E (Haematoxylin and Eosin), proliferation marker Ki67 and urea cycle enzyme ASS1. 10 individual fields of view where **(A)** Ki67 Immunoscoring **(B)** ASS1 Immunoscoring analysed with Aperio ImageScope®. The error bars represent the ± Standard Error of the Mean (±SEM) (*p<0.05, **p<0.01)*

Immunohistochemical staining of FFPE xenograft tissues revealed significant differences in Ki67 and ASS1 staining (Figure 3-24). The proliferation index marker Ki67 was significantly reduced in tumours treated with ADI-PEG20. In agreement with the *in vitro* data (Figure 3-15), ASS1 was significantly over-expressed in the treatment group.
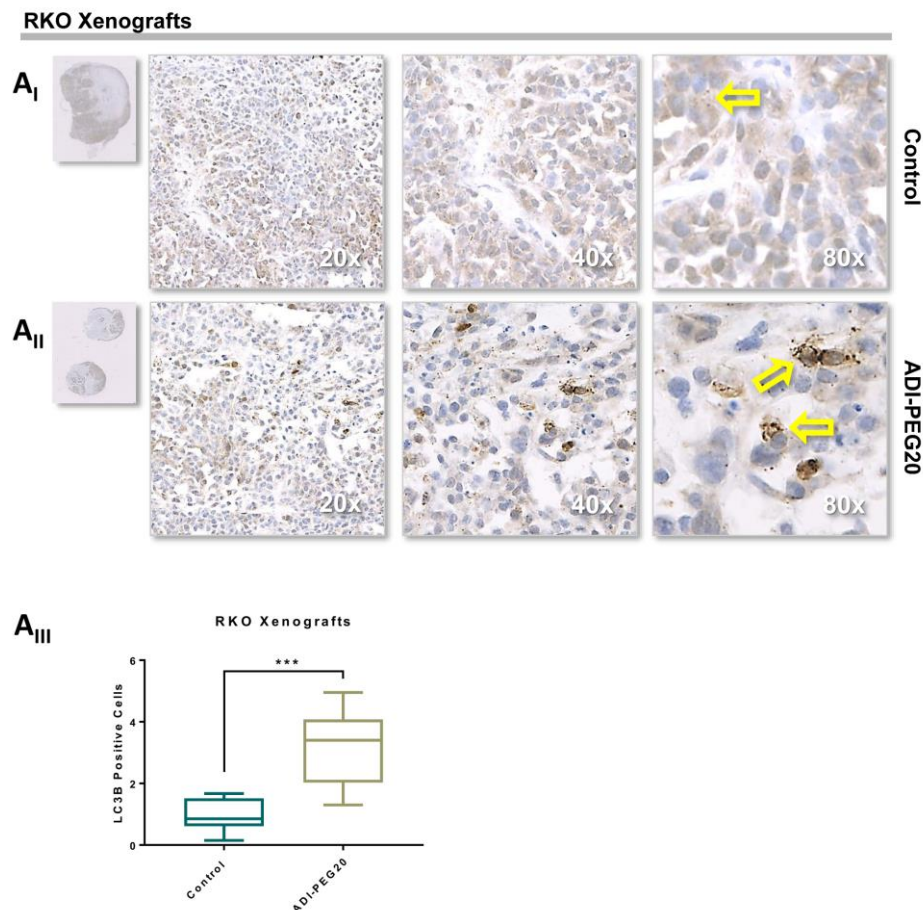
Figure 3-25: Immunohistochemical staining of LC3B in (A$_I$) *RKO control and,* ***(A$_{II}$)*** *RKO xenograft tumours treated with rhArg1peg5000. The error bars represent the ± Standard Error of the Mean (±SEM). (*p<0.05, **p<0.01, ***p<0.001, ****p<0.0001, two-tailed Student's t-test).*

Evidence from the literature suggest that induction of autophagy supports growth during arginine starvation (Delage et al., 2012), therefore we decided to investigate whether autophagic flux was present in xenograft tumours treated with ADI-PEG20. For the purposes of this experiment we probed dissected tumours via immunohistochemistry, for the autophagic marker LC3B.

Microtubule-associated protein 1A/1B-light chain 3, LC3, which has been extensively used as a marker of autophagy; is a ~17kDa soluble cytosolic protein that is expressed and distributed evenly in all cells. During the catabolic process of autophagy, LC3 is engulfed by endocytic formations called autophagosomes. During this engulfment, the cytosolic LC3A is bound to phosphatidylenolalime to form LC3B which is subsequently recruited on the membranes of autophagosomes. During lysosomal degradation, lysosomes fuse with autophagosomes to form autolysomes. This results in the rapid degradation of LC3B, hence inhibition of autophasomal degradation and subsequent accumulation of LC3B by chloroquine is considered to be an autophagic marker of lysosomal turnover (Levy et al., 2017).

Immunohistochemical staining for LC3B presented in Figure 3-25 indicates an extremely significant increase in LC3B positive cells, suggesting the induction of autophagic flux in tumours treated with ADI.

3.6.1.1   Summary

Overall, results obtained from this *in vivo* study reveal the potential anti-proliferative capabilities of ADI-PEG20 in CRC. Even after significant upregulation of ASS1 expression, ADI-PEG20 was capable of slowing down proliferation as indicated by the significant decrease in tumour volume, proliferation markers Cyclin D1, D3 and nuclear Ki67. Identifying potential alternative mechanisms of resistance in arginine depleting strategies such as regulation of ASS1 re-expression and autophagy may lead to more efficacious combination strategies in the future.

3.6.2 Investigating the effect of rhArg1peg5000 on the growth of RKO and SW 480 xenografts

Next, we sought to investigate whether pharmacological depletion of arginine via rhArg1peg5000 could effectively decrease the tumour growth in ASS1-positive and negative CRC lines *in vivo*. Toward this end, we selected ASS1-negative RKO and ASS1-positive SW 480 lines.

After a 7-day period following subcutaneous injection of cancer cells, mice were administered intraperitoneally 0.5mg of rhArg1peg5000 per animal or PBS twice a week (Dose administration was determined based on manufacturer's directions). Tumour growth was monitored weekly until tumours reached the end point limit of 17mm diameter. Results presented in Figures 3-26A and 3-27A reveal a significant decrease in tumour volume in both RKO and SW 480 in mice treated with rhArg1peg5000. The antigrowth capabilities of rhArg1peg5000 were accompanied by a significant reduction in excised tumour weight in RKO xenografts (Figure 3-26B). Despite the lower tumour growth rate observed in SW 480 xenografts, no tumour weight differences were observed (Figure 3-27B).

Comparison of normalised body weight did not reveal any differences between the control and treatment groups (Figure 3-26C and Figure 3-27C) suggesting the PEGylated arginase was well tolerated.

Additionally, tumour lysates were probed for Cyclin D1 and D3. Despite the differences in tumour growth and weight, no significant changes were observed in either Cyclins D1 or D3 in RKO (Figure 3-28) and SW 480 xenografts (Figure 3-29).

Results obtained from immunohistochemical staining against Ki67 come in line with previous observations suggesting that differences in tumour volume were not associated with alterations in proliferation rates (Figure 3-30 and 3-31).
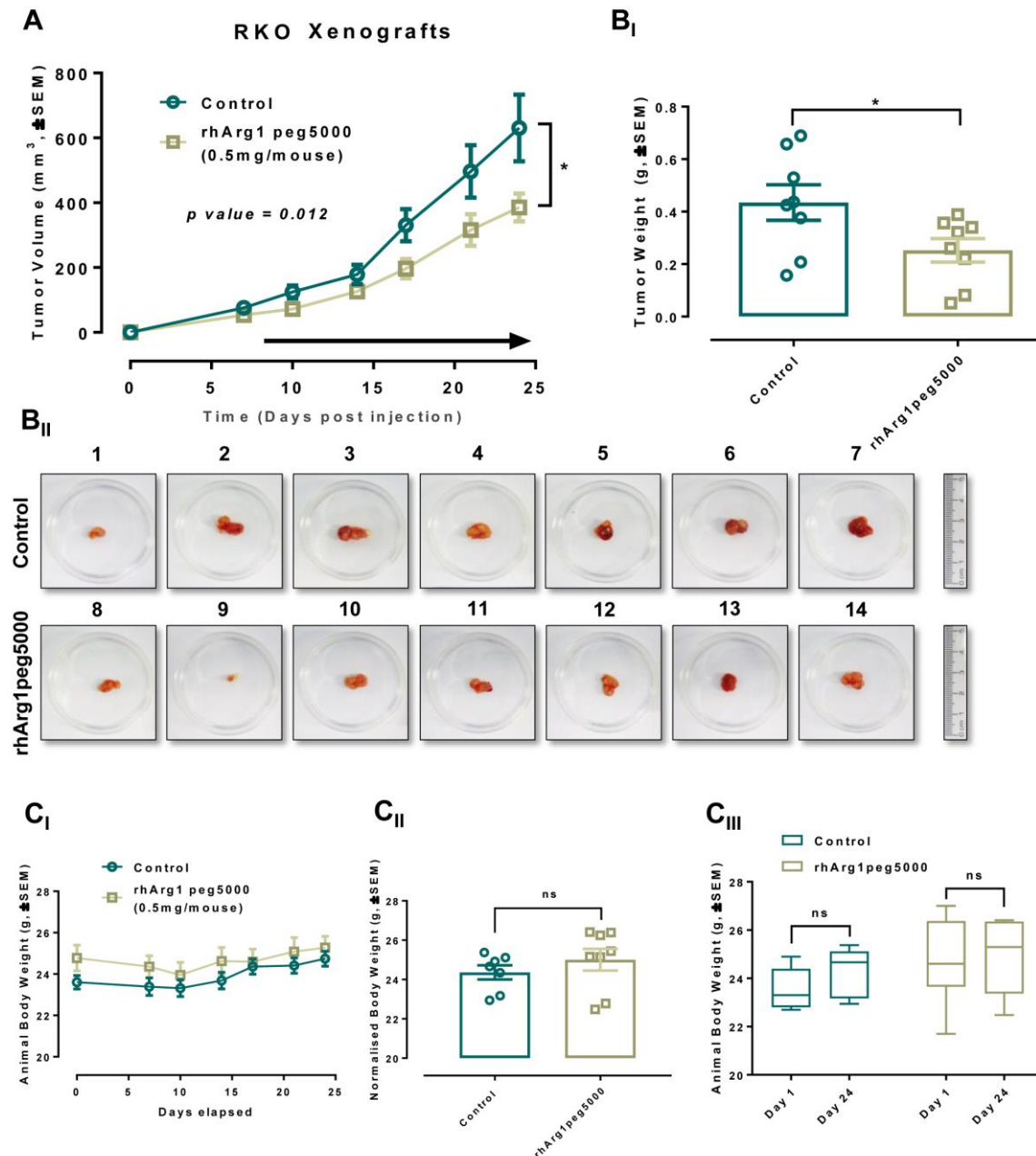
Figure 3-26: Pharmacological depletion of L-Arginine with rhArg1peg5000 Decreases the Growth of RKO Xenografts in BALB/c nude mice. *Nude immunocompromised mice (n=8) were injected subcutaneously with RKO and groups of mice (n=7) were administered 0.5mg/animal rhArg1peg5000 or PBS once a week. Tumour size was calculated by direct calliper measurement once per week. **(A)** Growth curves of tumour xenografts in BALB/c mice with or without rhArg1peg5000 (n=7 per group, p value=0.012)**(B$_I$)** Tumor weight of excised tumor xenografts (n=8 per group) **(B$_{II}$)** Excised tumour xenografts at the of the experiment **(C$_I$)** Body weight of BALB/C mice, control vs rhArg1peg5000 **(C$_{II}$, C$_{III}$)** normalized body weight of BALB/c mice at the end of the experiment (n=7 per group, no significance). The error bars represent the ± Standard Error of the Mean (±SEM). Statistical significance of difference in tumour volume between the two groups was determined by linear regression analysis. Statistical significance of differences in tumour weight and normalized final animal weight was assessed by two-tailed Student's t-test. (*p<0.05, **p<0.01, ***p<0.001, ****p<0.0001).*
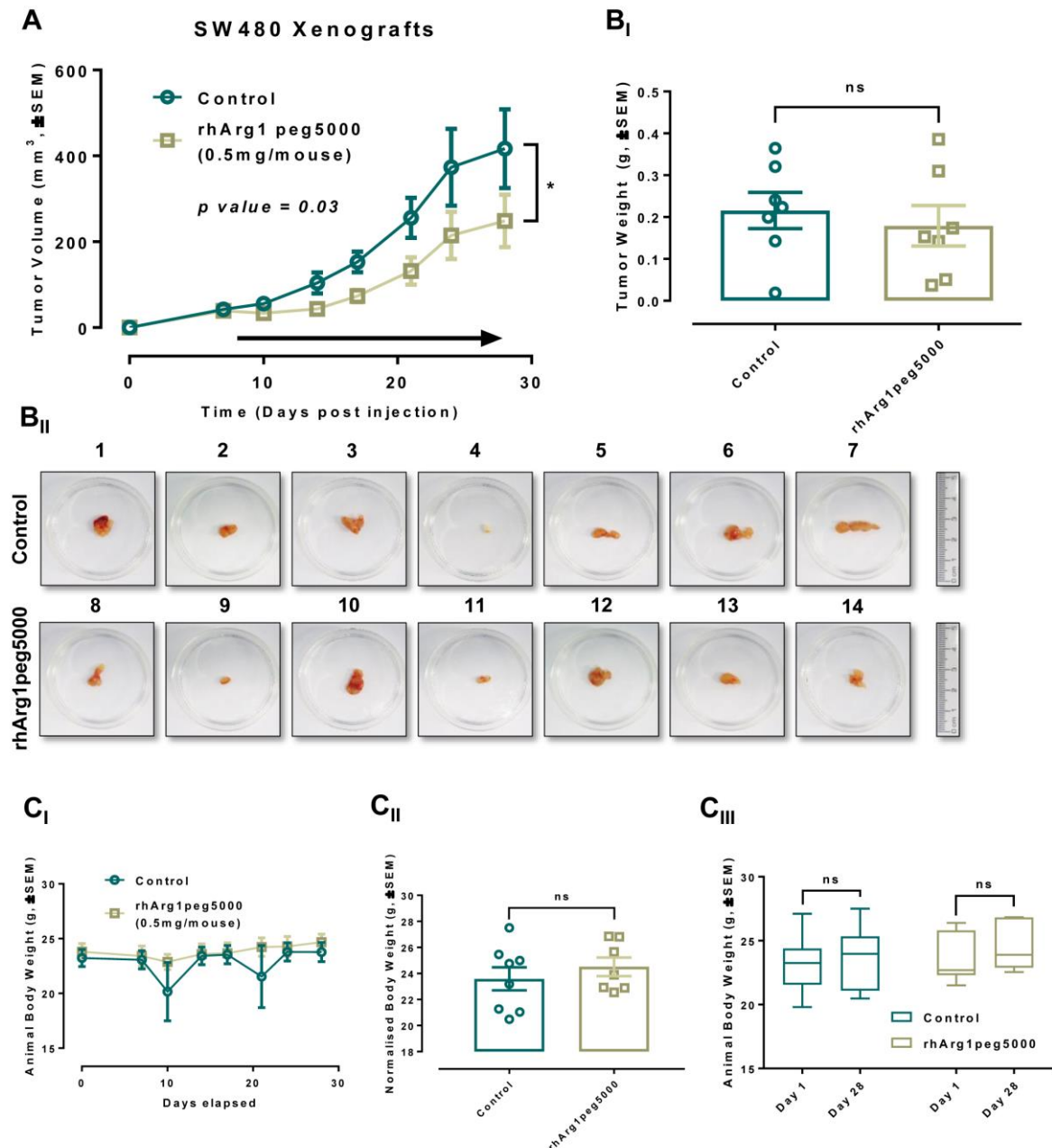
Figure 3-27: Pharmacological depletion of L-Arginine with rhArg1peg5000 Decreases the Growth of SW 480 Xenografts in BALB/c nude mice. *Nude immunocompromised mice were injected subcutaneously with RKO and administered 0.5mg/animal rhArg1peg5000 (n=7) or PBS (=7) twice a week. Tumour size was calculated by direct calliper measurement once per week. **(A)** Growth curves of tumour xenografts in BALB/c mice with or without rhArg1peg5000 (n=7 per group, p value=0.03) **(B$_I$)** Tumour weight of excised tumour xenografts (n=7 per group) **(B$_{II}$)** Excised tumour xenografts at the of the experiment **(D)** Body weight of BALB/c mice with or without rhArg1peg5000 **(C$_I$)** Final and **(C$_{II}$, C$_{III}$)** normalized body weight of BALB/c mice at the end of the experiment (n=7 per group, no significance). Statistical significance of difference in tumour volume between the two groups was determined by linear regression analysis. Statistical significance of differences in tumour weight and normalized final animal weight was assessed by Student's t-test. The error bars represent the ± Standard Error of the Mean (±SEM) (*p<0.05, **p<0.01, ***p<0.001, ****p<0.0001).*
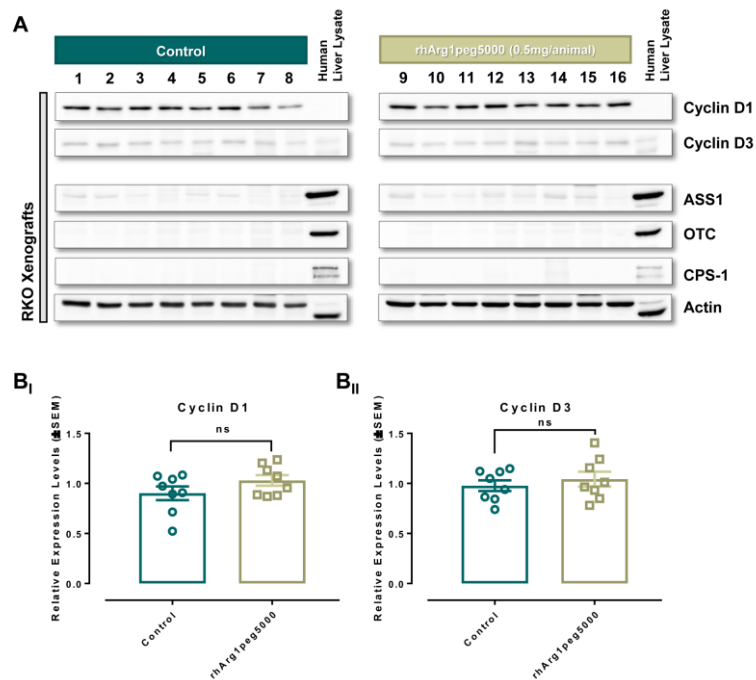
Figure 3-28: Expression Levels of Cyclin D1 and D3 in RKO xenografts treated with rhArg1peg5000. (A) *Lysates from tumor xenografts were prepared and subjected to western blotting with antibodies again Cyclin D1, Cyclin D3 Human Liver Lysate was used as a positive control for OTC, CPS-1 and ASS1. Actin was used a loading control.* **(B$_I$, B$_{II}$)** *Relative expression levels of Cyclin D1 and Cyclin D3 respectively (n=8). The error bars represent the ± Standard Error of the Mean (±SEM) (*p<0.05, **p<0.01, ***p<0.001, ****p<0.0001, two-tailed Student's t-test).*
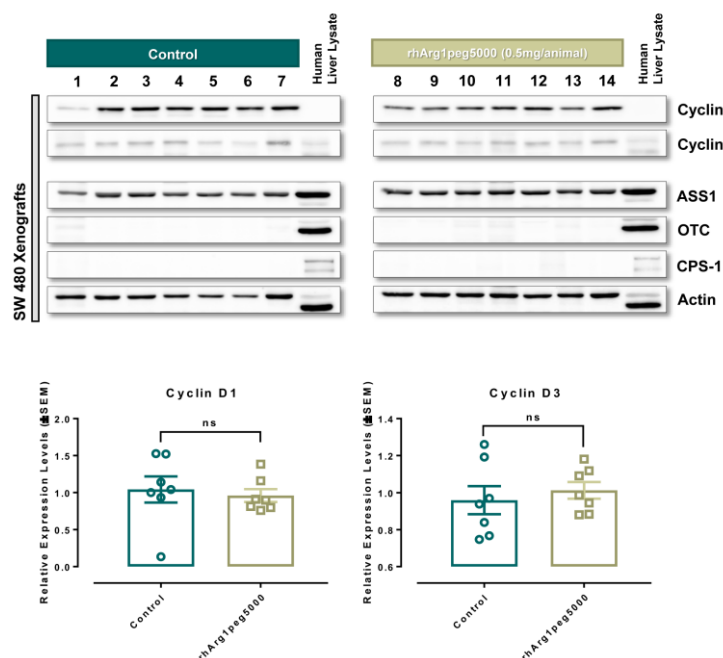
Figure 3-29: Expression Levels of Cyclin D1 and D3 in SW 480 xenografts treated with ADI-PEG20. (A) *Lysates from tumor xenografts were prepared and subjected to western blotting with antibodies again Cyclin D1, Cyclin D3 Human Liver Lysate was used as a positive control for OTC, CPS-1 and ASS1. Actin was used a loading control* **(B$_I$, B$_{II}$)** *Relative expression levels of Cyclin D1 and Cyclin D3 respectively (n=7). The error bars represent the ± Standard Error of the Mean (±SEM) (*p<0.05, **p<0.01, ***p<0.001, ****p<0.0001, two-tailed Student's t-test).*
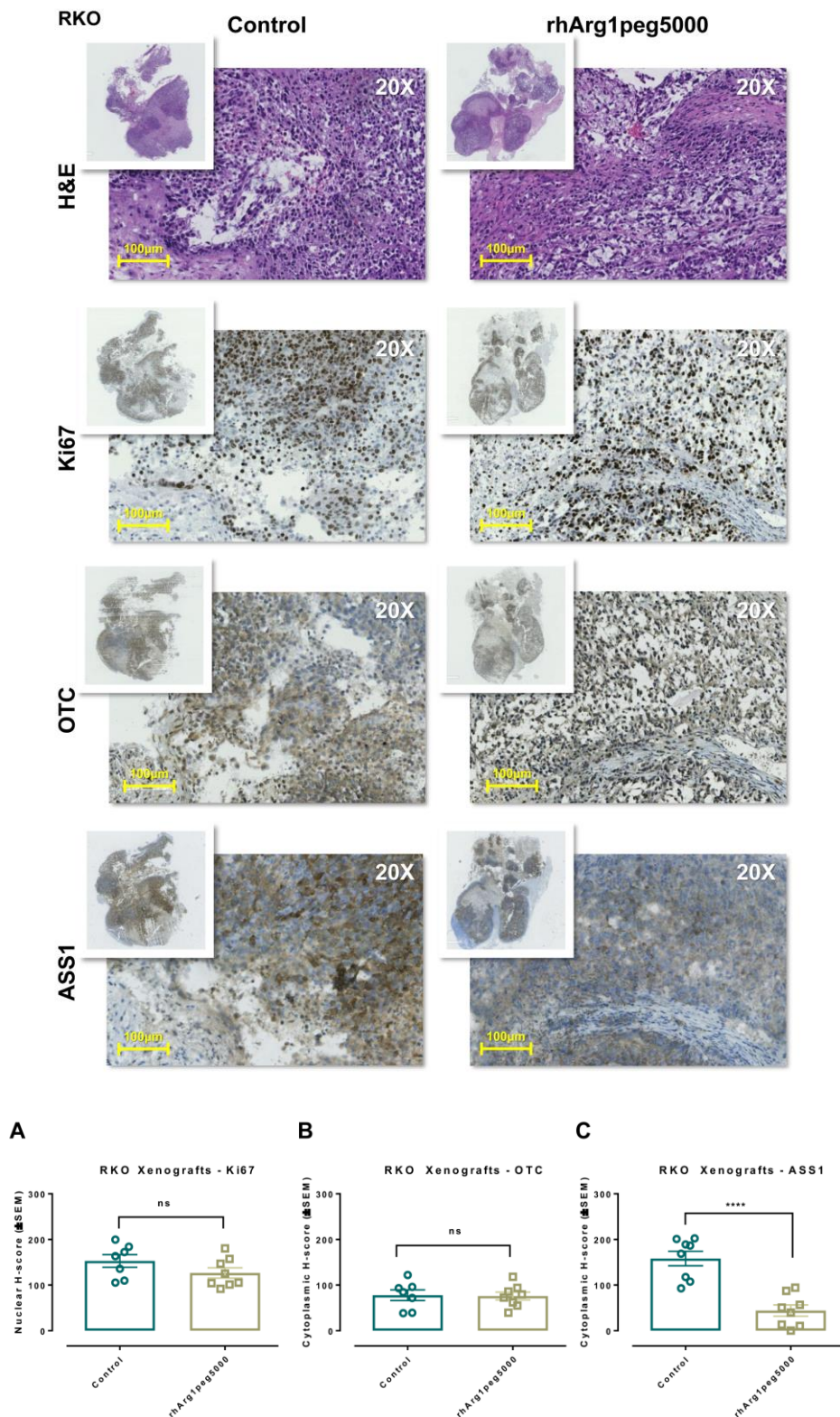
Figure 3-30: Histology and immunohistochemical analysis of RKO xenograft tumours treated with rhArg1peg5000*. Immunohistochemical staining of tumour xenograft sections with H&E (Haematoxylin and Eosin), proliferation marker Ki67 and urea cycle enzyme OTC and ASS1. 10 individual fields of view where **(A)** Ki67 Immunoscoring, **(B)** OTC Immunoscoring, **(C)** ASS1 Immunoscoring were analysed with Aperio ImageScope®. H-Scores were interrogated for statistical significance via two-tailed Student's t-test. The error bars represent the ± Standard Error of the Mean (±SEM) (*p<0.05, **p<0.01, ***p<0.001, ****p<0.0001).*
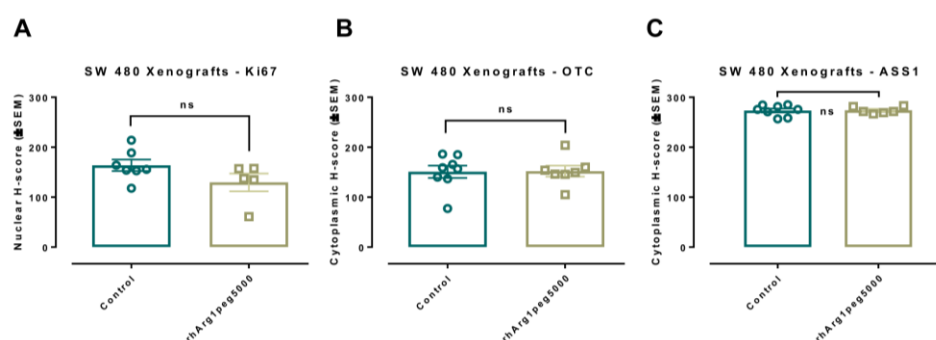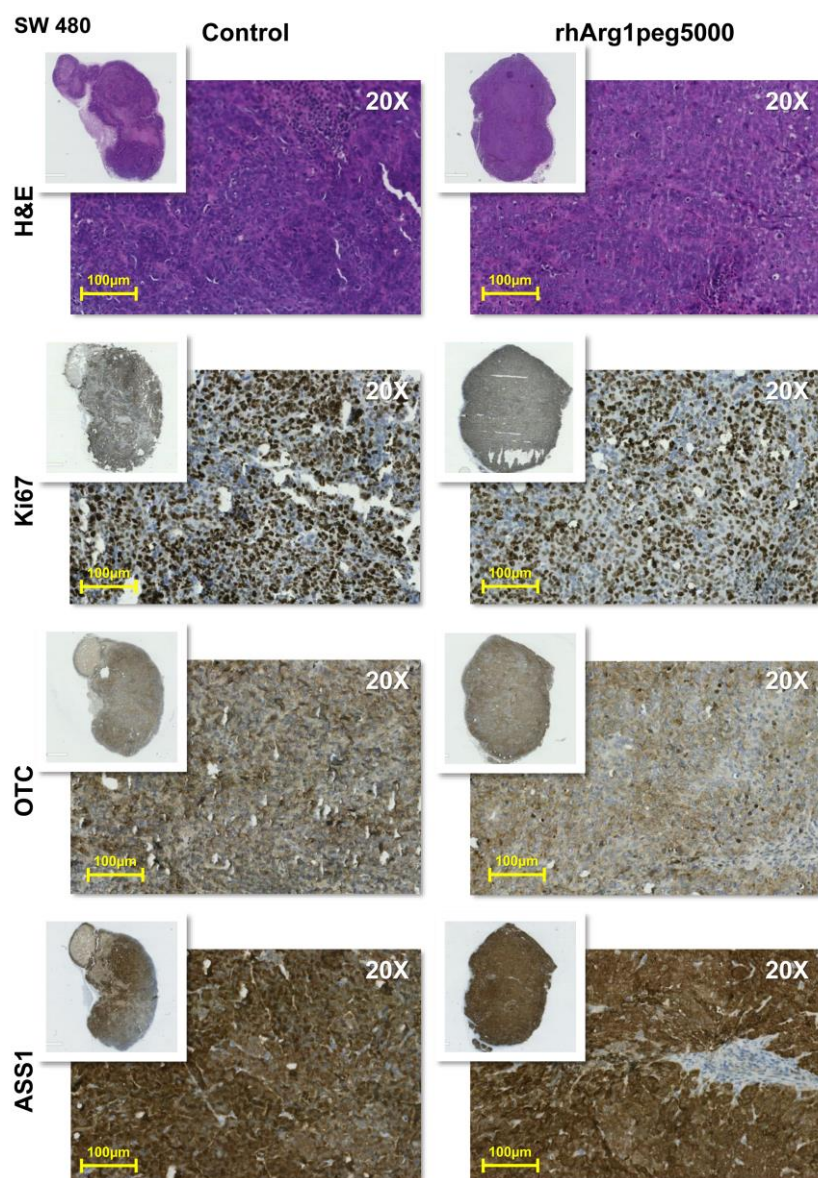
Figure 3-31: Histology and immunohistochemical analysis of SW 480 xenograft tumours treated with rhArg1peg5000. *Immunohistochemical staining of tumour xenograft sections with H&E (Haematoxylin and Eosin), proliferation marker Ki67 and urea cycle enzyme OTC and ASS1. 10 individual fields of view where (A) Ki67 Immunoscoring, (B) OTC Immunoscoring, (C) ASS1 Immunoscoring were analysed with Aperio ImageScope®. H-Scores were interrogated for statistical significance via two-tailed Student's t-test. The error bars represent the ± Standard Error of the Mean (±SEM). (*p<0.05, **p<0.01, ***p<0.001, ****p<0.0001).*

One of the primary reasons for acquired ADI resistance in tumours is the re – expression of ASS1, therefore expression profiling of urea cycle enzymes was deemed necessary to address possible adaptive mechanisms of resistance. Accordingly, tumour xenograft were also assessed for OTC and ASS1 levels by immunohistochemical analysis. Both RKO and SW 480 xenografts exhibited a mild positivity for OTC in control and treatment groups, which in both occasions was not affected by arginase treatment (Figure 3-30; 3-31).

On the other hand, ASS1 expression in RKO xenografts showed significant suppression following treatment with rhArg1peg5000. On the contrary, SW 480 xenografts remained strongly positive for ASS1 in both treatment and control groups.

As described earlier in Section 3.6.1, tumour xenografts were also assessed for the autophagic marker LC3B. Unlike ADI-PEG20 treatment, LC3B scoring in mice treated with rhArg1peg5000 demonstrated no significant accumulation of LC3B in comparison to the control (Figure 3-32).
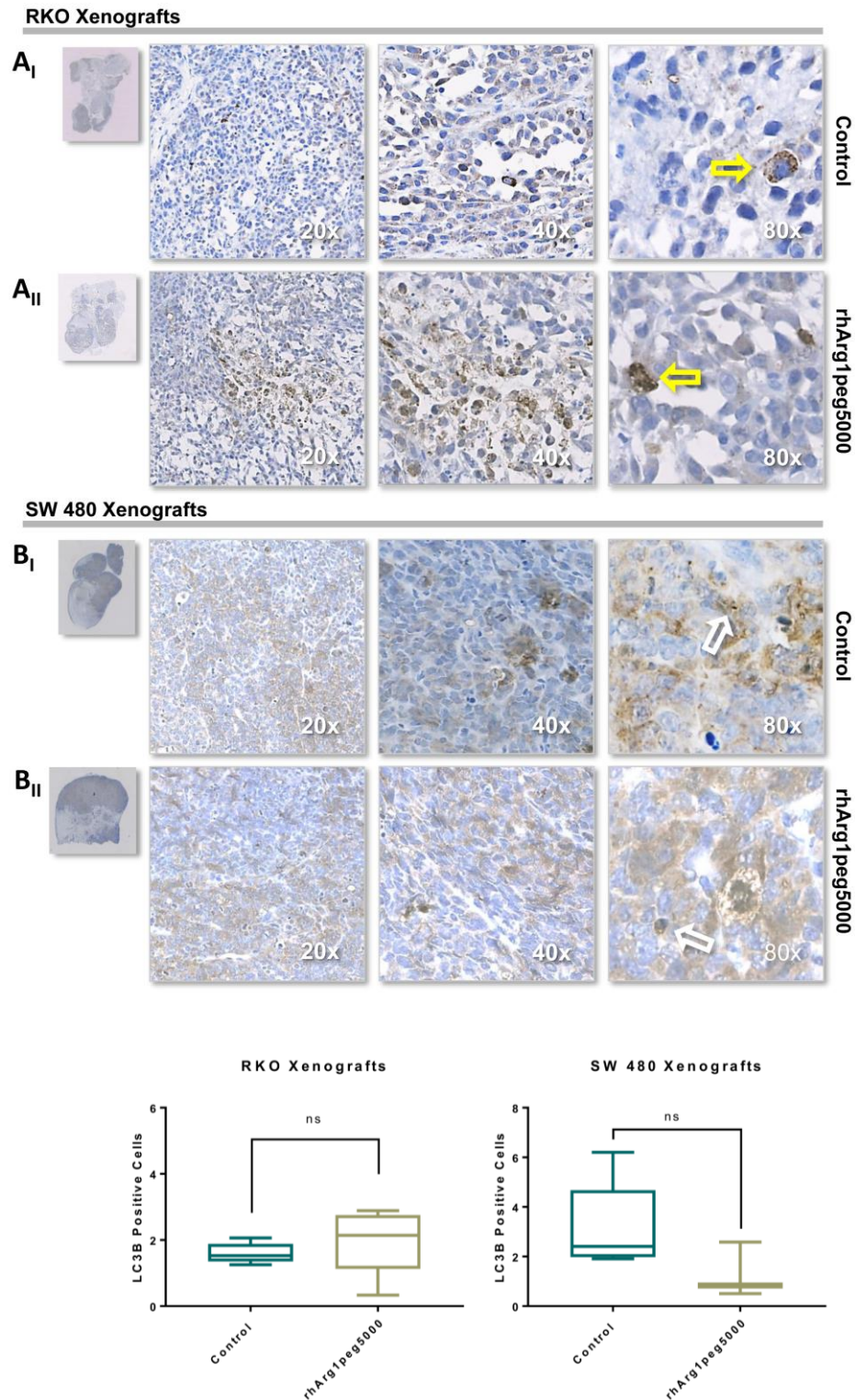
Figure 3-32: Immunohistochemical staining of LC3B in RKO and SW 480 xenograft tumours treated with rhArg1peg5000. *Neither,* ***(A)*** *RKO or* ***(B)*** *SW 480 xenografts demonstrate a significant accumulation of LC3B when mice are administered rhArg1peg50000. The error bars represent the ± Standard Error of the Mean (±SEM) (ns: so significance, two-tailed Student's t-test).*

3.6.3 Summary

The *in vivo* results presented in this section suggest a higher level of complex interactions and potential metabolic adaptations between the host, tumour and tumour microenvironment that could further affect and abolish the *in vivo* efficacy of rhArg1peg5000. Overall we showed that in both RKO and SW480, rhArg1peg5000 can significantly reduce the growth of tumour xenografts in mice as reflected by reduced tumour volume regardless of expression of ASS1 and Ki67 staining. Lack of differences in tumour weight and proliferation markers indicates plausible adaptive resistance mechanisms after prolonged exposure to rhArg1peg5000, which unlike ADI-PEG20 may not be driven by induced autophagy. Similarly to previous data (see section 3.2.3), evident lack of difference in Ki67 between control and treatment groups, despite the significant volume differences may reflect the presence of necrosis within the centre of the tumour as well as altered doubling times of cells. The Ki67 antigen is present throughout all stages of cell cycle, namely G1, S, G2 and M phase except G0 and has been used extensively used by clinicians to assess the mitotic index of tumours in patients. However, rapidly proliferating tumours, characterised by cells with short doubling times could signify only a fraction of the growing cells within the tumour. In this regards correlation of the mitotic index (Ki67 staining) and proliferation rate may not be strictly linear (Beresford et al., 2006).

Although the significance of ASS1 downregulation in rhArgpeg5000-treated RKO xenografts is not known, it may suggests that differential intracellular concentrations of arginine, citrulline, ornithine and argininosuccinate, could affect the expression patterns and localisation/channelling of urea cycle enzymes within the tumour cells.

Alternatively, limited availability of arginine and subsequent, transcriptional inactivation of c-Myc via inhibition of mTOR signalling could further result in ASS1 downregulation. Taking this into consideration further experimentation is needed to assess the levels of this metabolites in response to ADI-PEG20 and rhArg1peg5000 treatment.

Several studies over the past decade have highlighted the involvement and complex crosstalk of multiple signalling pathways in cancer cells in order to achieve a metabolic rewiring that could help tumours to overcome arginine depleting strategies. Among others, mTOR pathway (Savaraj et al., 2010; Chantranupong et al., 2016) PI3K/Ras/MAPK (Tsai et al., 2012), autophagy (Kremer et al., 2017; Savaraj et al., 2010) and ER stress induced UPS (Bobak et al.,

2016) have been reported as pathways involved in response to arginine depleting agents. In this case, lack of detection of autophagic flux suggest a more thorough investigation of these pathways and their interactions both *in vivo* and *in vitro* could help us address alternative mechanisms of resistance and identify new targets for future combinational therapeutic interventions in CRC.

3.7   Investigating the effects of arginine catabolising agents on autophagy

As previously mentioned, numerous studies have identified autophagy as an induced response in nutrient energy and amino acid starvation (Saxton and Sabatini, 2017). *In vivo* evidences from our xenograft work indicate that autophagy could potentially be involved in arginine starvation resistance as a pro-survival mechanism. Hence, in this section I will discuss our findings on autophagy in relation to pharmacological depletion of arginine in CRC cell lines.

3.7.1   Investigating the effects of ADI-PEG20 on autophagy

In a time-dependent manner, lysates from cells exposed to 0.5 µg/mL of ADI-PEG20 were investigated via Western blotting for autophagy-related markers LC3A/B and SQSTM1/p62. In an effort to estimate whether autophagic flux is occurring; results obtained were compared to cells treated with vehicle control (PBS), chloroquine only and combination of ADI-PEG20 and chloroquine.

The lysosomotropic agent chloroquine accumulates inside endosomes and lysosomes and raise the pH leading to the inhibition of lysosomal enzymes that are active in an acidic environment. Thus, this further leads to prevention of lysosome – autophagosome fusion (Klionsky et al., 2016) and subsequent inhibition of autophagy. If autophagy flux is active, chloroquine-mediated inhibition of autophagosome degradation causes autophagosome accumulation, which can be promptly detected by an increase in LC3B.

In addition to LC3B, the ubiquitin binding protein Sequestosome 1 (SQSTM1, p62) has also been used as a marker of autophagy (Klionsky et al., 2016) Studies have shown that p62 acts as a scaffold for the trafficking of polyubiquinated targets thus supports their degradation via proteasomal or lysosomal degradation. Thus, p62 expression is dependent on starvation in which case p62 synthesis is increased and simultaneously in autophagic degradation where p62 levels are reduced by autophagy (Klionsky et al., 2016).

Western blot analysis showed a significant accumulation of LC3B in 2 out of 4 cell lines treated with ADI-PEG20. HCT 116 exhibited a significant increase in LC3B when treated with a combination of ADI-PEG20 and chloroquine at 24 and 48 hr (Figure 3-33A and B) in comparison to chloroquine only. RKO demonstrated a similar accumulation of LC3B after 72 hr treatment (Figure 3-34A and B). Inhibition of autophagy with chloroquine was

accompanied by a reduction of Cyclin D1 in HCT116 cells treated with ADI-PEG20. In RKO cells despite induced autophagy at later time points no significant reduction in cyclins was observed. Neither SW 480 (Figure 3-35B) nor HT 29 (Figure 3-36B) cells showed evidences of induced autophagy in response to ADI treatment. Overall no significant changes in p62 expression were observed.

Figure 3-33: Investigation of autophagic flux in HCT 116 treated with ADI-PEG20 (A) *Western Blot analysis of Cyclin D1, D3, p62 and LC3A/B in whole cell lysates from HCT 116 untreated (DMSO) or treated with Chloroquine (30μM) and/or ADI-PEG20 (1μg/mL) as indicated for 24, 48 and 72 hr*. **(B)** *Relative expression levels of LC3B* **(C)** *Cyclin D1* **(D)** *and Cyclin D3. The error bars represent the ± Standard Error of the Mean (±SEM, n=3) (*p<0.05, **p<0.01, ***p<0.001, ****p<0.0001, two-tailed Students t-test).*
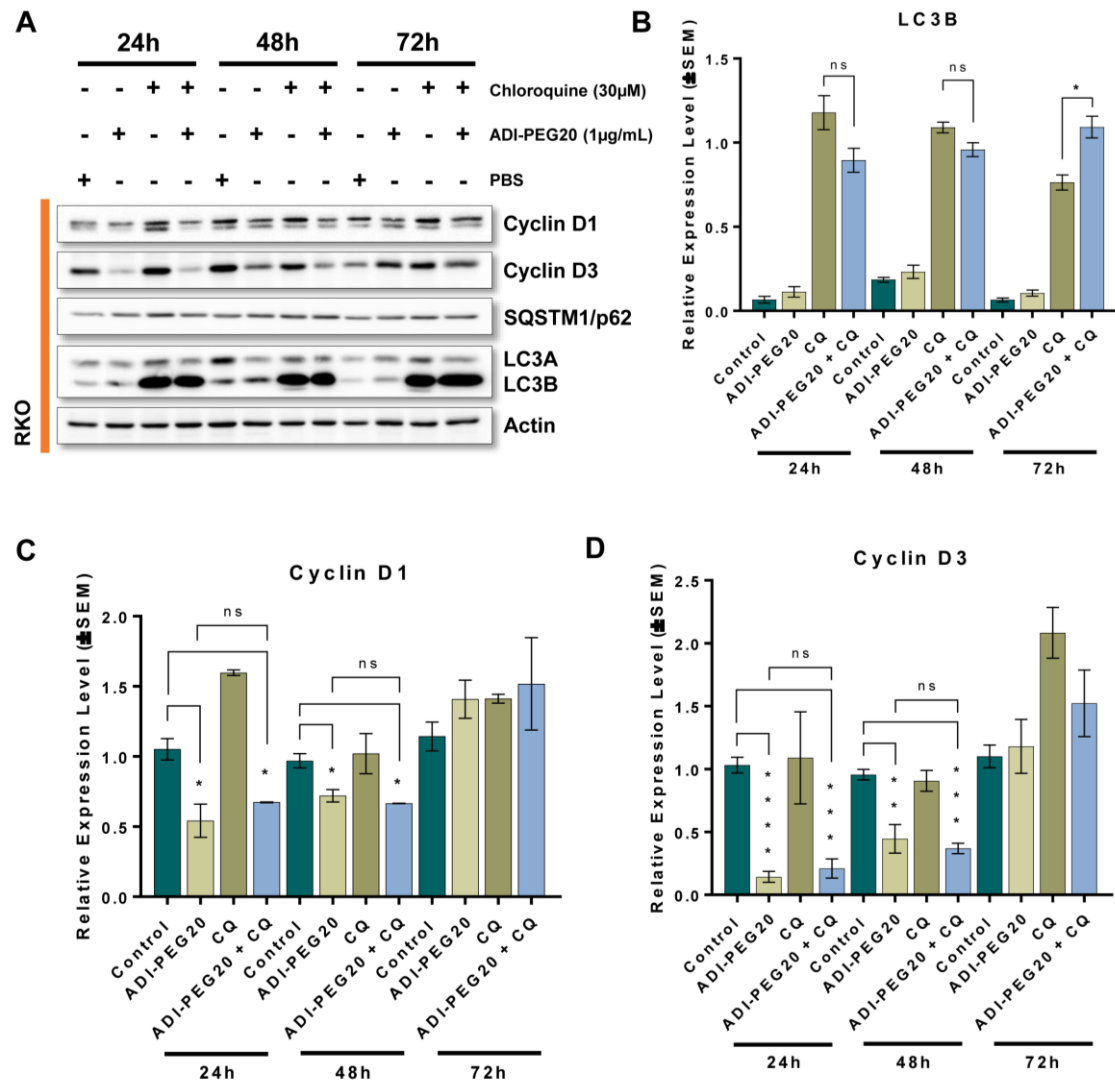
Figure 3-34: Investigation of autophagic flux in RKO treated with ADI-PEG20 (A) *Western Blot analysis of Cyclin D1, D3, p62 and LC3A/B in whole cell lysates from RKO untreated (DMSO) or treated with Chloroquine (30μm) ADI-PEG20 (1μg/mL) at 24, 48 and 72 hr.* **(B)** *Relative expression levels of LC3B* **(C)** *Cyclin D1* **(D)** *and Cyclin D3. The error bars represent the ± Standard Error of the Mean (±SEM, n=3) (*p<0.05, **p<0.01, ***p<0.001, ****p<0.0001, two-tailed Student's t-test).*
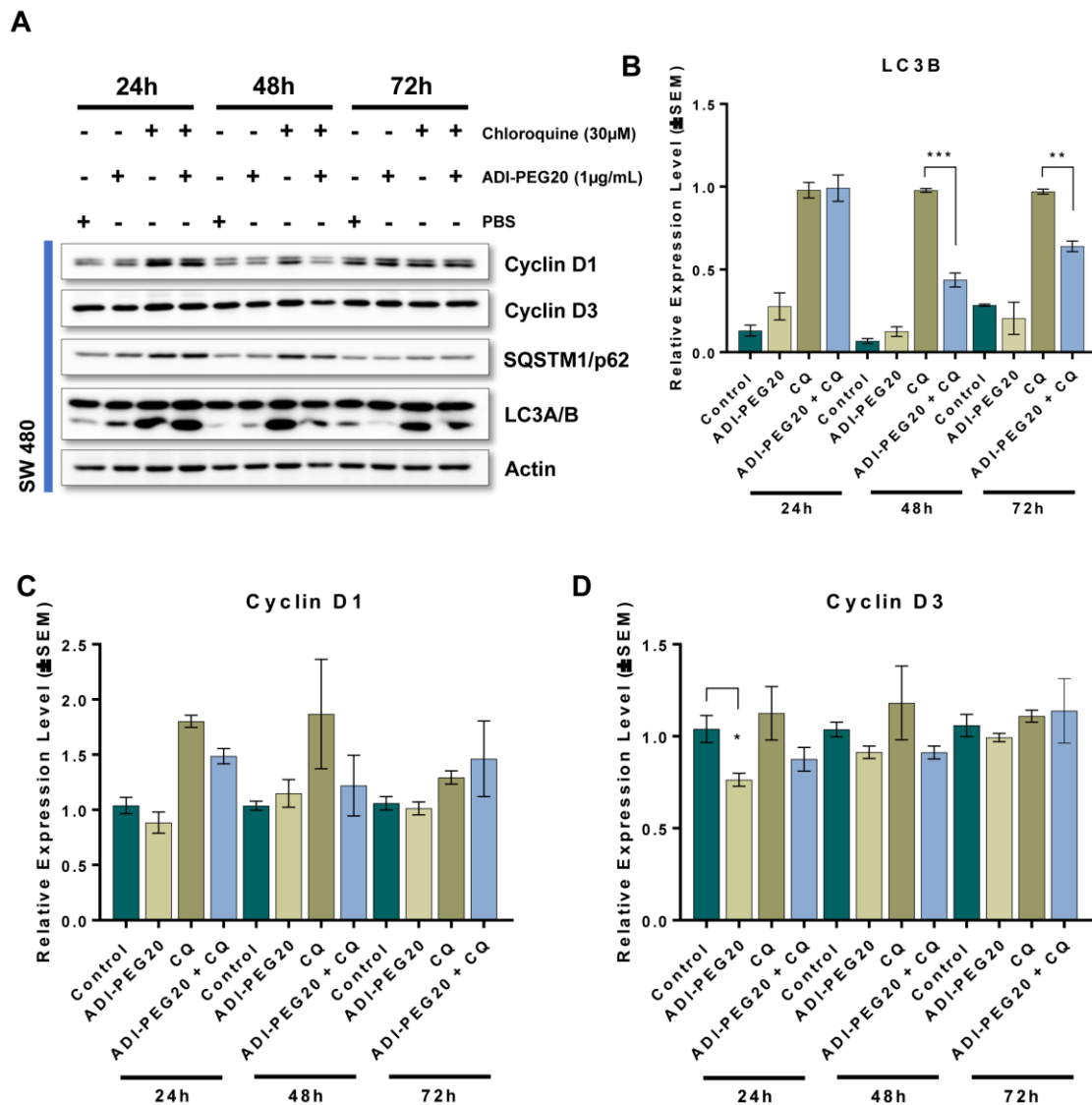
Figure 3-35: Investigation of autophagic flux in SW 480 treated with ADI-PEG20 (A) *Western Blot analysis of Cyclin D1, D3, p62 and LC3A/B in whole cell lysates from SW 480 untreated (DMSO) or treated with Chloroquine (30µm), ADI-PEG20 (1µg/mL) at 24, 48 and 72 hr.* **(B)** *Relative expression levels of LC3B* **(C)** *Cyclin D1* **(D)** *and Cyclin D3. The error bars represent the ± Standard Error of the Mean (±SEM, n=3) (*p<0.05, **p<0.01, ***p<0.001, ****p<0.0001, two-tailed Student's t-test).*
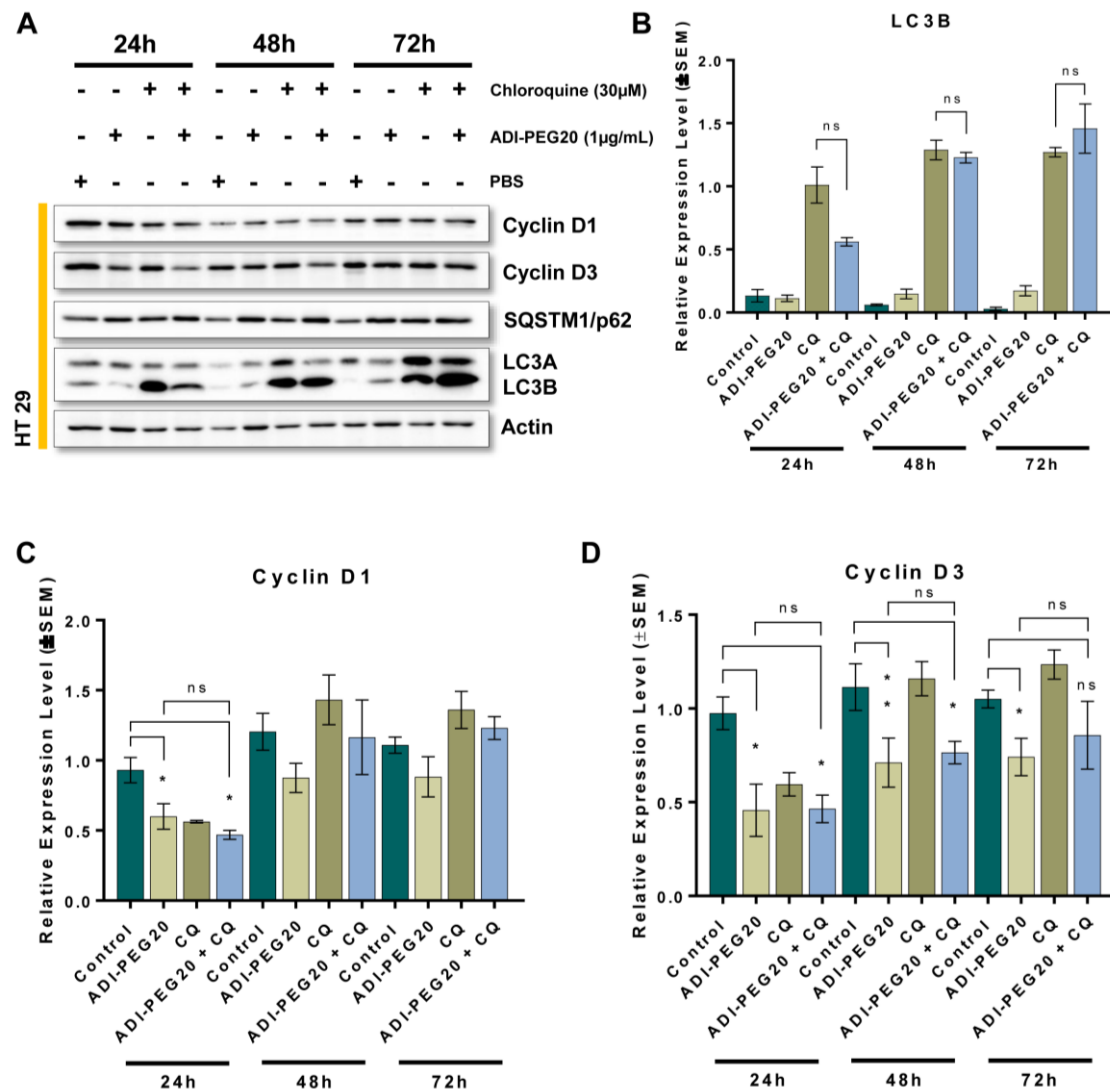
Figure 3-36: Investigation of autophagic flux in HT 29 treated with ADI-PEG20 (A) *Western Blot analysis of Cyclin D1, D3, p62 and LC3A/B in whole cell lysates from HT 29 untreated (DMSO) or treated with Chloroquine (30µm), ADI-PEG20 (1µg/mL) at 24, 48 and 72 hr.* ***(B)*** *Relative expression levels of LC3B* ***(C)*** *Cyclin D1* ***(D)*** *and Cyclin D3. The error bars represent the ± Standard Error of the Mean (±SEM, n=3) (*p<0.05, **p<0.01, ***p<0.001, ****p<0.0001, two-tailed Student's t-test).*

3.7.2   Investigating the effects of rhArg1peg5000 on autophagy

In agreement with prior observations (see Section 3.6.2) no significant increase of LC3 level was detected in RKO cells treated with rhArg1peg5000 and chloroquine (Figure 3-38). In SW480, blockage of autophagy via chloroquine in combination with rhArg1peg5000 induces a small but significant reduction in Cyclin D3 at 72 hr which was also accompanied by an also significant accumulation of LC3B and p62 (Figure 3-39).

Despite the increased accumulation of LC3B in HCT 116, no differences were observed in Cyclins D1 and D3 in response to pharmacological inhibition of autophagy (Figure 3-37). Unexpectedly, HT 29 cells exhibited a statistically significant decrease in LC3B when both chloroquine and rhArg1peg5000 were administered, whereas at the same time Cyclin D3 levels were decreased significantly at 72 hr (Figure 3-40). Regardless of the contradicting results, Western blot data showed a noteworthy accumulation of p62 in cells treated with rhArg1peg5000 and/or chloroquine at 72 hr, which suggests increased trafficking of polyubiquinated proteins for degradation.
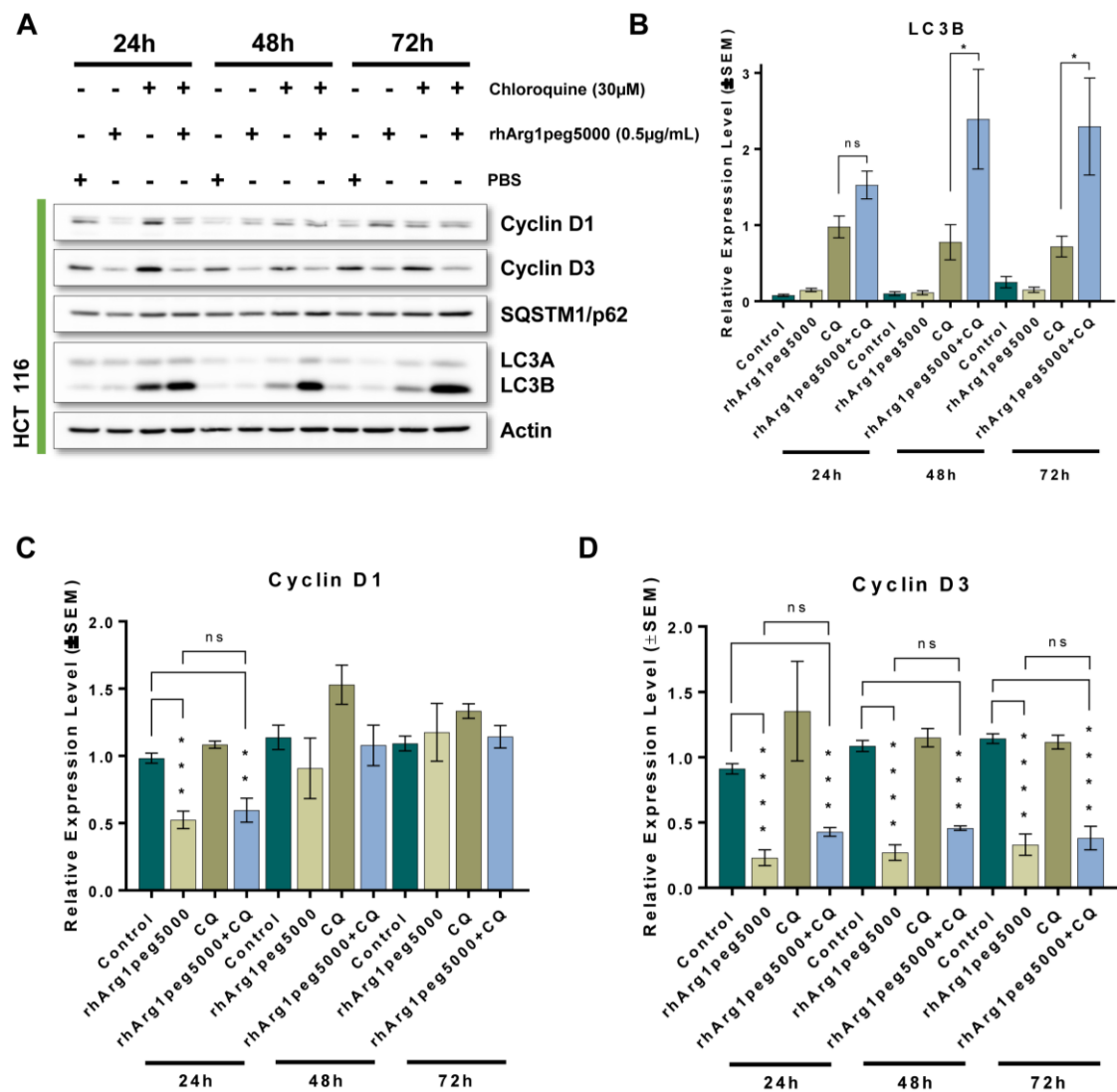
Figure 3-37: Investigation of autophagic flux in HCT 116 treated with rhArg1peg5000 (A) *Western Blot analysis of Cyclin D1, D3, p62 and LC3A/B in whole cell lysates from HCT 116 untreated (DMSO) or treated with Chloroquine (30μm), rhArg1peg5000 (0.5μg/mL) at 24, 48 and 72 hr,* **(B)** *Relative expression levels of LC3B* **(C)** *Cyclin D1* **(D)** *and Cyclin D3. The error bars represent the ± Standard Error of the Mean (±SEM, n=3) (*p<0.05, **p<0.01, ***p<0.001, ****p<0.0001, two-tailed Student's t-test).*
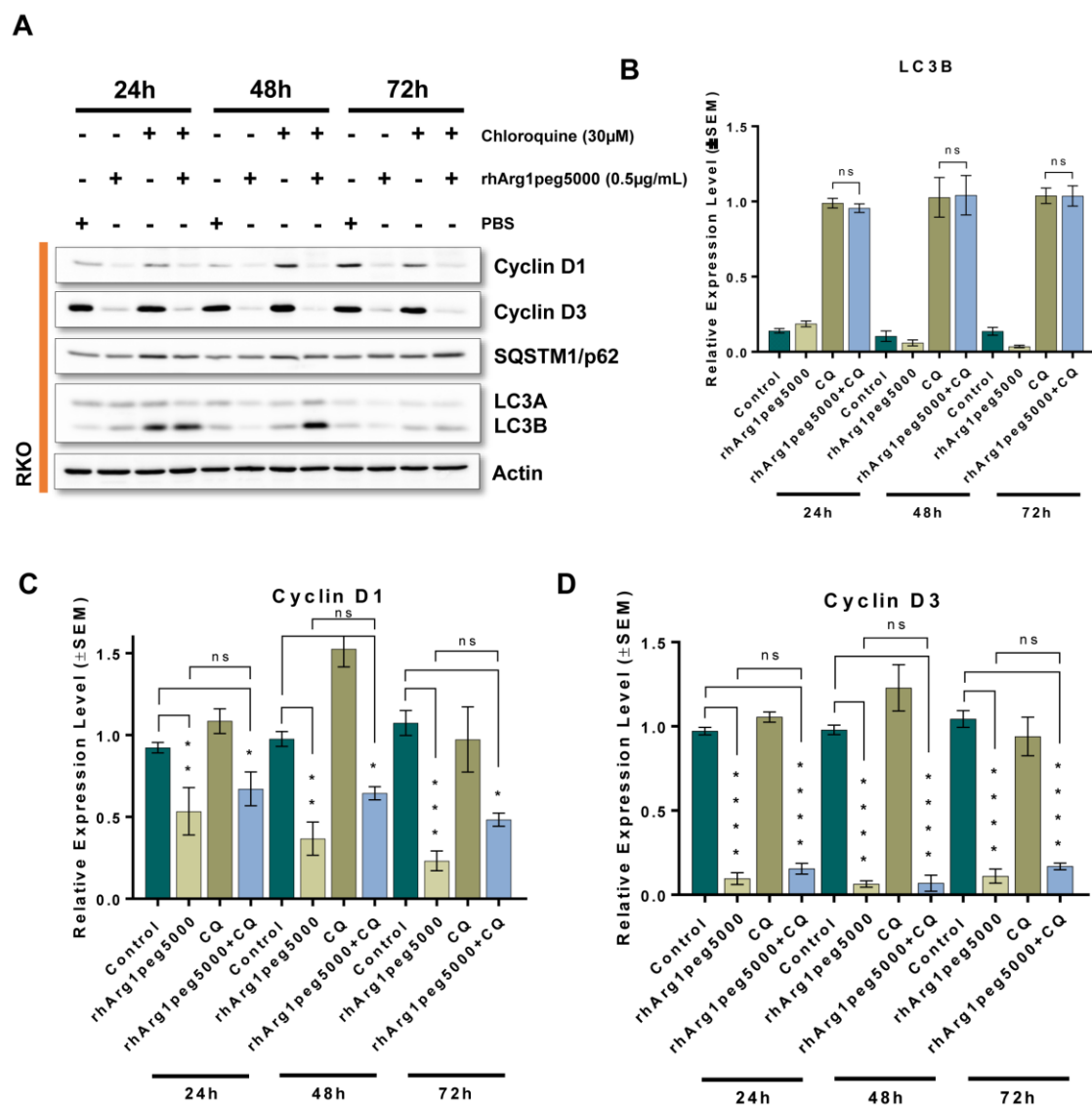
Figure 3-38: Investigation of autophagic flux in RKO treated with rhArg1peg5000 (A) *Western Blot analysis of Cyclin D1, D3, p62 and LC3A/B in whole cell lysates from RKO untreated (DMSO) or treated with Chloroquine (30µm), rhArg1peg5000 (0.5µg/mL) at 24, 48 and 72hr.* ***(B)*** *Relative expression levels of LC3B* ***(C)*** *Cyclin D1* ***(D)*** *and Cyclin D3. The error bars represent the ± Standard Error of the Mean (±SEM, n=3) (*p<0.05, **p<0.01, ***p<0.001, ****p<0.0001, two-tailed Student's t-test).*
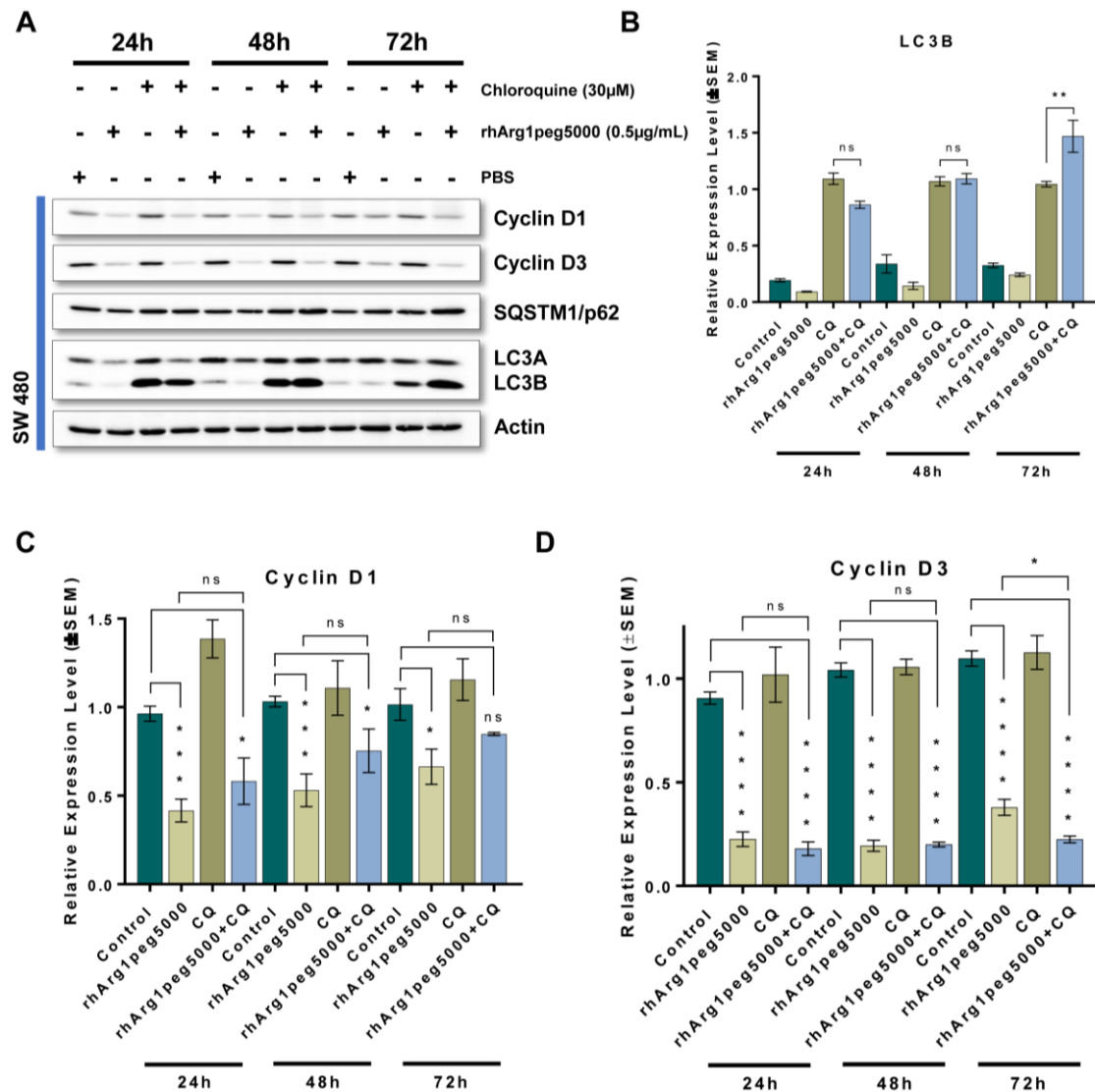
Figure 3-39: Investigation of autophagic flux in SW 480 treated with rhArg1peg5000 (A) *Western Blot analysis of Cyclin D1, D3, p62 and LC3A/B in whole cell lysates from SW 480 untreated (DMSO) or treated with Chloroquine (30µm), rhArg1peg5000 (0.5µg/mL) at 24, 48 and 72 hr.* ***(B)*** *Relative expression levels of LC3B* ***(C)*** *Cyclin D1* ***(D)*** *and Cyclin D3. The error bars represent the ± Standard Error of the Mean (±SEM, n=3) (*p<0.05, **p<0.01, ***p<0.001, ****p<0.0001, two-tailed Student's t-test).*
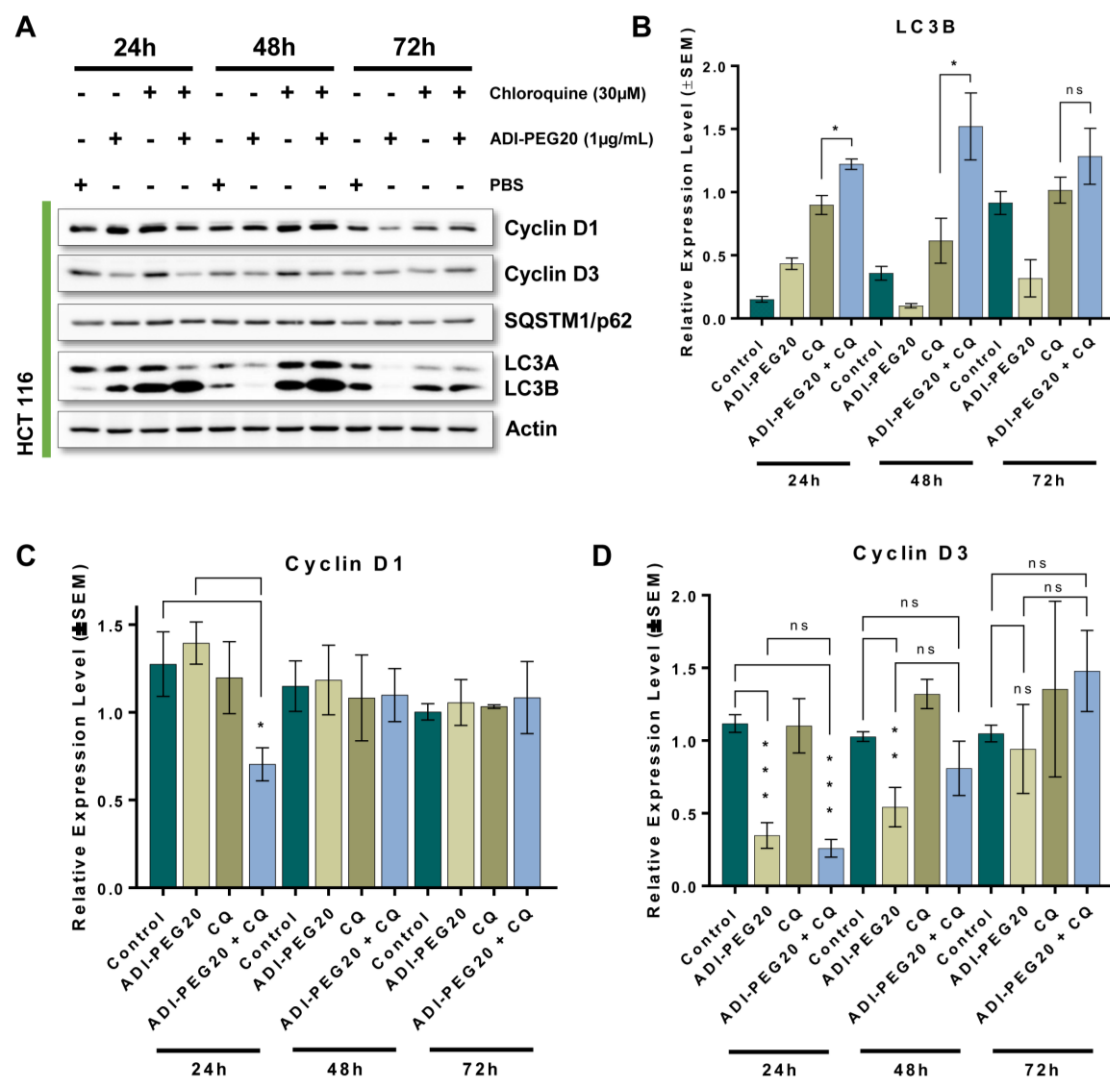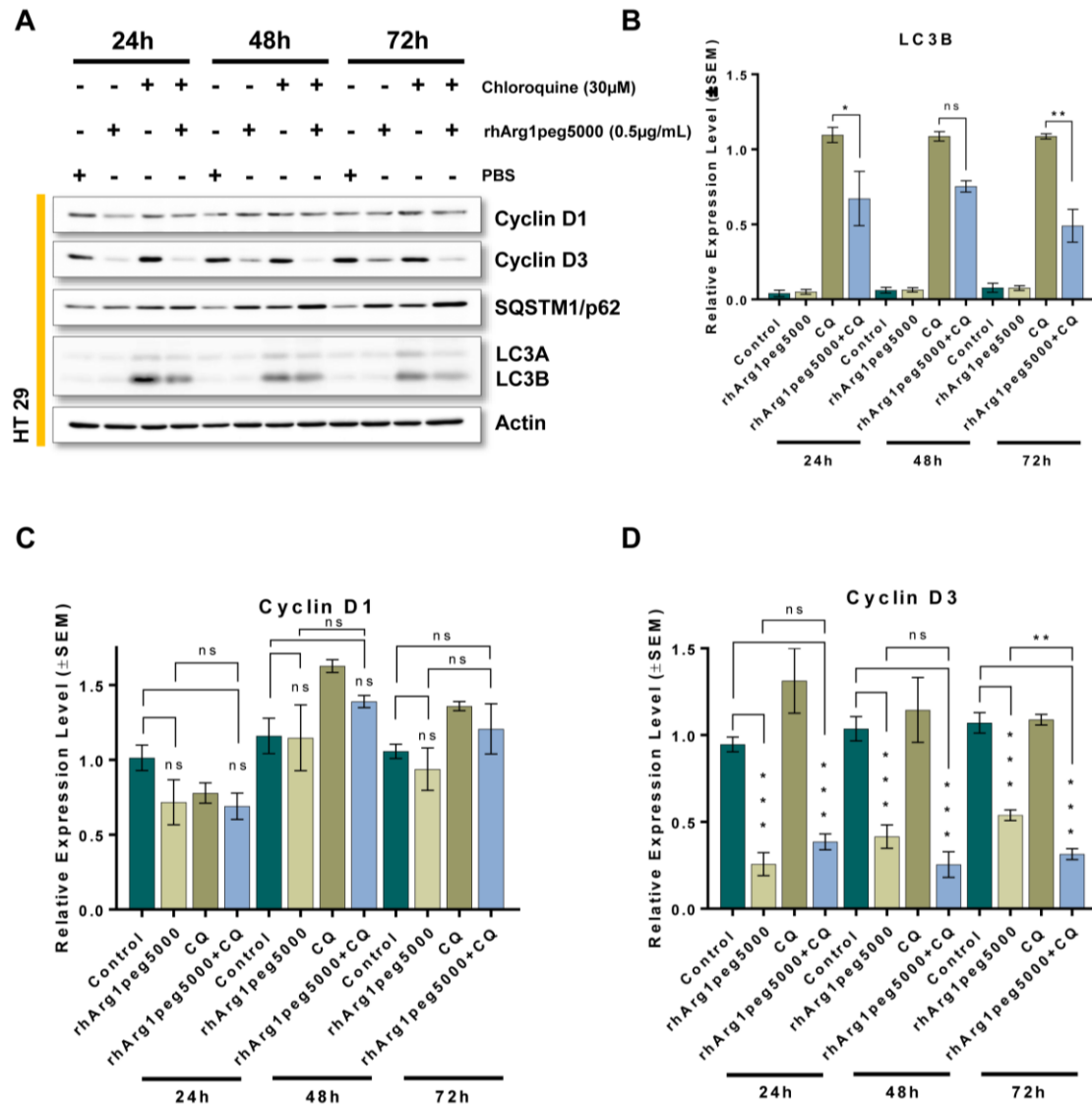
Figure 3-40: Investigation of autophagic flux in HT 29 treated with rhArg1peg5000 (A) *Western Blot analysis of Cyclin D1, D3, p62 and LC3A/B in whole cell lysates from HT 29 untreated (DMSO) or treated with Chloroquine (30μm), rhArg1peg5000 (0.5μg/mL) at 24, 48 and 72 hr.* **(B)** *Relative expression levels of LC3B* **(C)** *Cyclin D1* **(D)** *and Cyclin D3.The error bars represent the ± Standard Error of the Mean (±SEM, n=3) (*p<0.05, **p<0.01, ***p<0.001, ****p<0.0001, two-tailed Student's t-test).*

3.7.3 Investigating the effect of rhArg1peg5000 on apoptosis via inhibition of autophagy

The observation of floating cells in culture plates treated with rhArg1peg5000 led us to examine potential induction of apoptosis. Thus, in a time course experiment cells treated with rhArg1peg5000 were compared against cells treated with Etoposide, a well-known inducer of apoptosis. It is well documented that the nuclear poly ADP-ribose polymerase (PARP) is involved in DNA repair in response to environmental stress (Satoh and Lindahl, 1992). During apoptosis, this 116 kDa protein is targeted by ICE-like caspases (Lazebnik et al., 1994) and caspase-3 (Nicholson and Thornberry, 1997), generating fragments of 89kDa. Hence, cleaved PARP has been extensively used as a marker of apoptosis (Bulares et al., 1999). Western blots analysis revealed a significant accumulation of the apoptotic marker cleaved PARP in rhArg1peg5000 treated cells after 24, 48 and 72 hr in 2 out of 4 cell lines tested (Figure 3-41). Both HCT 116 and RKO exhibited a significant accumulation of cleaved PARP, further suggesting induction of apoptosis.

Our results are in line with similar studies from Xu et al., where they show that pharmacological depletion of arginine with rhArg1peg5000 in small cell lung carcinoma (SCLC) induces cell cycle arrest and apoptosis via oxidative stress (Xu et al., 2018). Adding to this, another recent study from Shen et al., in NSCLC reports that induction of autophagy in response to rhArg1peg5000 has a cytoprotective role against reactive oxygen species (ROS), while inhibition of autophagy with CQ results in induced apoptosis (Shen et al., 2017). Alternatively, Bobak et al., report that arginine withdrawal can promote endoplasmic reticulum (ER) stress and subsequent activation of the unfolded protein response (UPR) (Bobak et al., 2016). Accordingly, research has shown that prolonged ER stress, can trigger the switch from cellular survival and autophagy to cellular death and apoptosis (Garcia-Navas et al., 2012). As a proof of concept, HCT 116 cells exposed to rhArg1peg5000 were co-treated with the widely used inhibitor of autophagy, chloroquine. Western blots presented in Figure 3-41C reveal a robust increase in cleaved PARP suggesting that the induction of autophagy can potentially act as a cytoprotective response to arginine starvation.

In addition to these observations, data acquired from antibody arrays and western blotting (results presented in appendices, Figure5-4 and 5-5) suggest that mTOR inhibition during arginine starvation with rhArg1peg5000 could be primarily responsible for induced autophagy as monitored in HCT 116 in earlier and RKO in later time points. Subsequent restoration of

arginine availability via autophagy could result in extended cell survival and sustained cell proliferation which is reflected by increased phosphorylation of Akt, PRAS40 and mTOR's downstream target 4E-BP1. The proline-rich Akt substrate (PRAS) is a 40kDa protein that has been extensively characterised as an inhibitory intermediate between the Akt and mTOR. Studies have shown that phosphorylation of PRAS40 by Akt results in its dissociation from the mTOR, and further deactivation of his inhibitory activity via phosphorylation by the mTOR itself (Saxton and Sabatini, 2017).

Results shown in Figure 5-5 demonstrated a drop in phosphorylation of 4E-BP1 in HCT 116 as early as 2 hr upon treatment with rhArg1peg5000. Decreased phosphorylation remained present up to 24 hr with a recovery occurring at 48 and 72 hr respectively. On the contrary, RKO cells demonstrated a marginal reduction of phospho-4E-BP1 levels at 8h with a dramatic drop of the same phosphorylated protein taking place after 72 hr. With no surprise, this time-dependent changes in phosphorylation levels of 4E-BP1 suggest the inactivation of mTOR pathway and further support the induction of autophagy in previous experiments (Appendices, Figure 5-5).
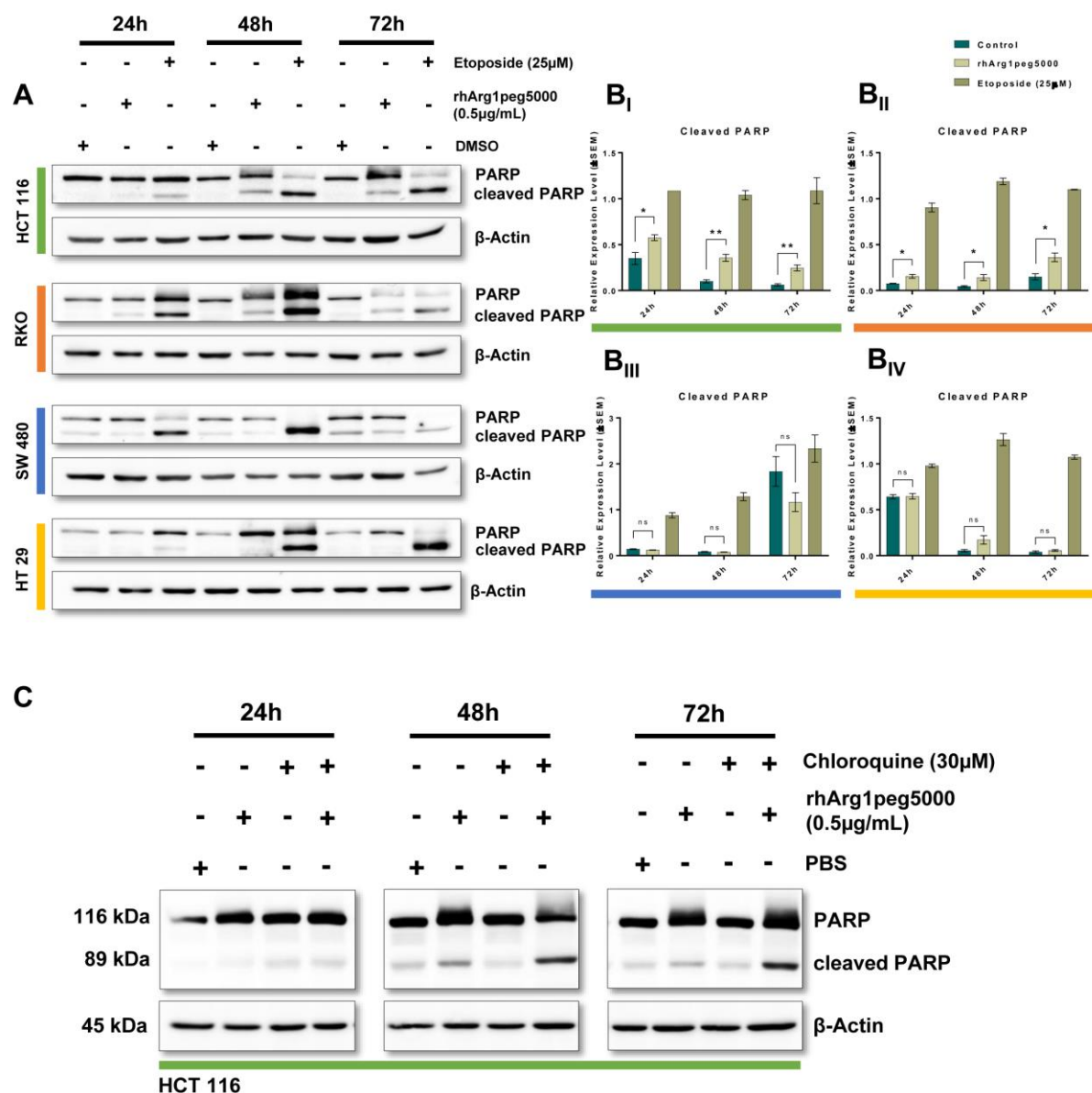
*Figure 3-41: Apoptosis as detected by cleaved PARP in CRC cell lines in response to rhArg1peg5000. Cells were incubated with rhArg1peg5000 at 0.5 µg/mL or 25µM Etoposide for 24, 48 and 72 hr. A DMSO vehicle control was also included. **(A)** Western blot analysis was utilised to detect the amount of PARP (at 116 kDa) and cleaved PARP (89 kDa) (representative results). **(B$_I$, B$_{II}$, B$_{III}$ and B$_{IV}$)** Relative expression levels of cleaved PARP (blots were compared to Etoposide and normalised against actin, Error bars represent the ±Standard Error of the Mean (±SEM, n=3), statistically significant values of *p < 0.05 were determined compared with the control (PBS treated cells) (*p<0.05, **p<0.01, ***p<0.001, ****p<0.0001, two-tailed Student's t-test).Two-tailed Student's t-test). **(C)** Western blot analysis was utilised to detect the amount of PARP (at 116 kDa) and cleaved PARP (89 kDa) (representative results) in response to combination rhArg1peg5000 + Chloroquine in HCT 116 cells.*

3.7.4 Summary

Overall, these data suggest that induction of autophagy could partially be responsible for resistance to arginine catabolising strategies in CRC. The cytoprotective role of autophagy, initiated by lack of arginine is reflected via the enhanced accumulation of LC3B in HCT 116 upon 24 hr of exposure to ADI-PEG20 and subsequent decrease in Cyclin D1 levels when cells were co-treated with chloroquine. Results come to agreement with previously described EdU incorporation experiments where we showed that HCT 116 exhibited a significant increase in DNA synthesis after 24 hr in response to ADI-PEG20. Similarly, RKO showed a significant increase in LC3B after 72 hr, which may explain the decrease in EdU incorporation levels in comparison to HCT 116.

On the contrary, HCT 116 cell line exhibited significant accumulation of LC3B in response to rhArg1peg5000 after 48 and 72 hr, which partially justifies the sharp decrease in EdU incorporation at 24 hr (Section 3.5.6). Inhibition of autophagy with chloroquine resulted in increased cleaved PARP in HCT 116 and RKO when both cell lines were exposed to rhArg1peg5000. In response to rhArg1peg5000, the ADI-PEG20 refractory cell line SW 480 demonstrated a robust increase in LC3B when this was accompanied with chloroquine. This accumulation in LC3B at 72 hr was accompanied by an also significant decrease in Cyclin D3.

Taken together, our results suggest that induction of autophagy is not only cell line dependent but also time dependent as ADI-PEG20 and rhArg1peg5000 alter differently the availability of arginine and its precursors in the media. Further experimentation is needed to elucidate the significance of autophagy in rhArg1peg5000 and ADI-PEG20 treated CRC lines.

3.8   Combination studies – *In vitro*

3.8.1   Investigating the synergistic action of arginine catabolising agents with 5-Fluororacil or Oxaliplatin

Despite the rapid developments in personalised medicine, the antimetabolite drug 5-Fluorouracil and the platinum compound Oxaliplatin remain the key drugs for treatment of CRC. Results from a recent Phase I/II clinical trial in HCC (NCT02102022) reveal favourable efficacy of ADI-PEG20 in combination with FOLFOX, while similar Phase II/III trials in pleural mesothelioma (Szlosarek et al., 2017), are currently investigating the synergistic effects of ADI-PEG20 with platinum-based therapy and antimetabolites. Hence, we investigated whether pharmacological depletion of arginine synergizes with current therapeutic approaches.

We examined the effects of combinations on cell growth utilizing the CompuSyn® software and Chou and Talalay method (Chou, 2006) In a 6x6 checkerboard layout, as previously described in materials and methods, we crossed combined a range of combinations of both ADI-PEG20 and rhArg1peg500 with 5-FU and Oxaliplatin (see Figures 3-42; 3-43). Results obtained from fixed ratio concentrations (highlighted with red squares in Figures 3-42; 3-43) were used to calculate the combination index value, CI. CI values greater than 1 (CI>1) indicate antagonism, equal to 1 (CI=1) additive effect and smaller than 1 (CI<1) synergism (for details see Table 5-2 in Appendices) (Chou, 2006).

An in depth view of the combination index values acquired from each combination/cell line is presented using classic isobolograms (Figures 3-44; 3-45). In isobolograms, lines connecting the x-axis and y-axis correspond to single doses of the two drugs required to independently reduce the growth by 50 (IC_{50}, blue), 75 (IC_{75}, red), 90 (IC_{90}, green) and 95% (IC_{95}, purple). Then, same-coloured data points displayed within the axes represent the effective combination – i.e. dose of the two combined drugs required to achieve reduction of growth at 50, 75, 90 and 95% respectively. Data falling on the lower left side of the line that connects the two single doses indicate synergism (CI<1), combination output located nearby the coloured lines additive effect (CI=1), whereas data points in the outer right-hand side of the coloured line of the chart signal antagonism (CI>1).
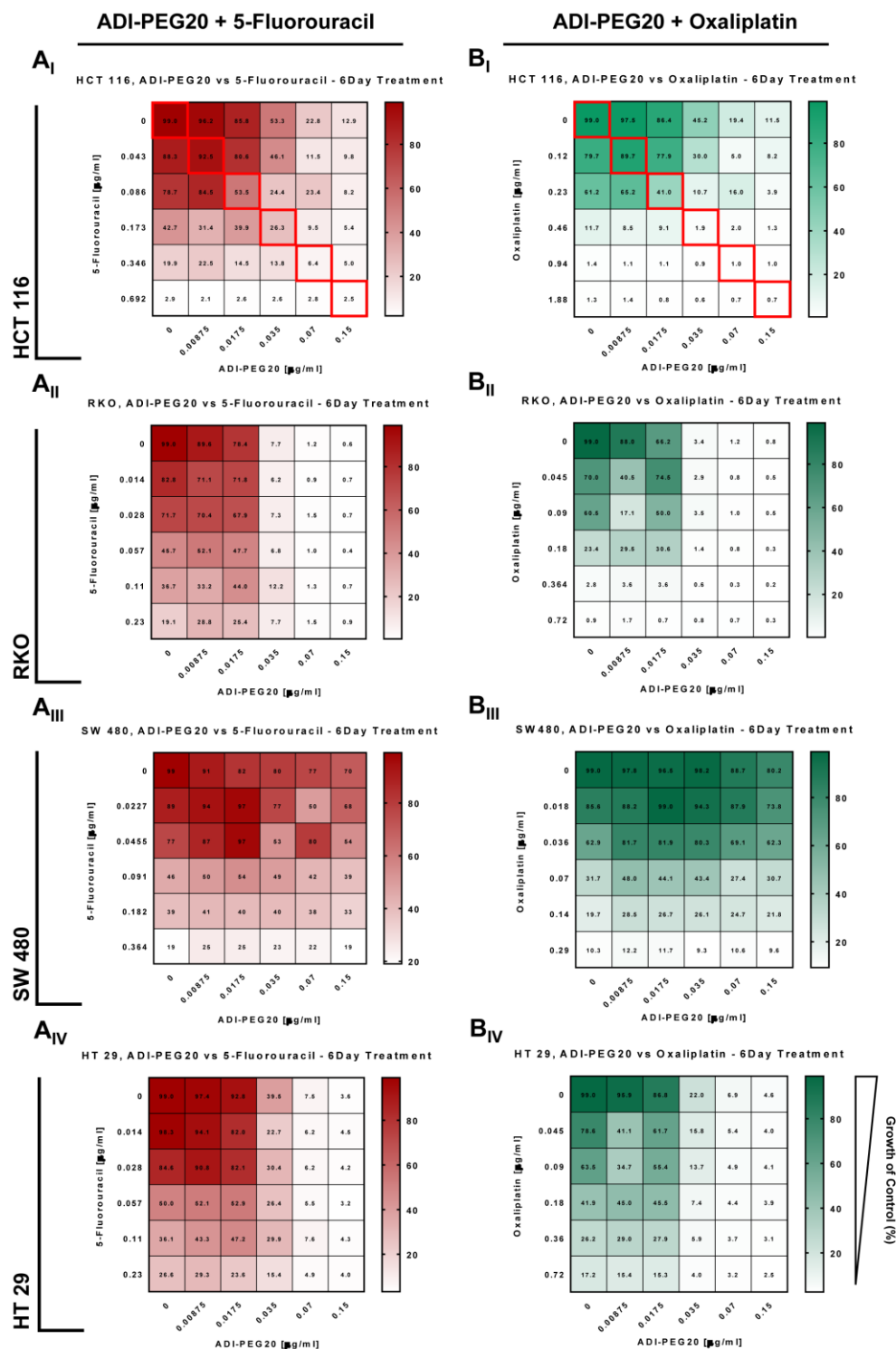
Figure 3-42: Investigating synergistic drug combinations using ADI-PEG20 + 5-Fluorouracil or Oxaliplatin - Drug combination matrix heatmaps. (A_I, B_I) *HCT 116,* ***(A_II, B_II)*** *RKO,* ***(A_III, B_III)*** *SW 480,* ***(A_IV, B_IV)*** *HT 29 drug matrixes with* ***(A_I – A_IV)*** *ADI-PEG20 + 5 Fluorouracil and* ***(B_I – B_IV)*** *ADI-PEG20 + Oxaliplatin. In a 6x6 checkerboard layout ranges of concentrations of drugs were companied and response was monitored via cell counting 6 days post treatment. Variations in maroon and green colours from light to dark depict the % of growth in comparison to the control. Results presented in this figure were obtained from three independent experiments.*
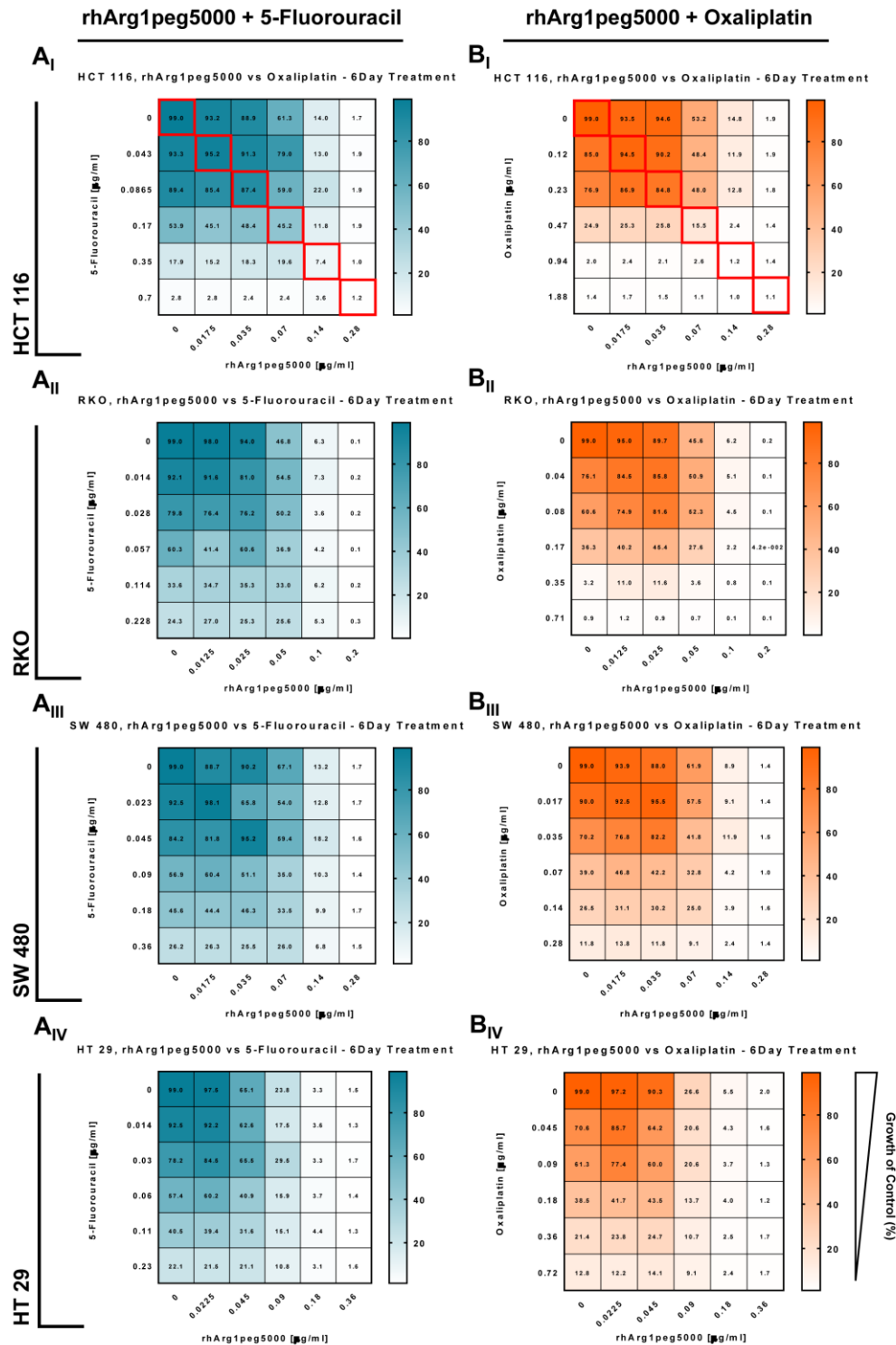
Figure 3-43: Investigating novel synergistic antiproliferative drug combinations using rhArg1peg5000 + 5-Fluorouracil or Oxaliplatin - Drug combination matrix heatmaps. (A_I, B_I) *HCT 116,* **(A_II, B_II)** *RKO,* **(A_III, B_III)** *SW 480,* **(A_IV, B_IV)** *HT 29 drug matrixes with* **(A_I – A_IV)** *rhArg1peg5000 + 5 Fluorouracil and* **(B_I – B_IV)** *rhArg1peg5000 + Oxaliplatin. In a 6x6 checkerboard layout ranges of concentrations of drugs were companied and response was monitored via cell counting 6 days post treatment. Variations in maroon and green colours from light to dark depict the % of growth in comparison to the control. Results presented in this figure were obtained from three independent experiments.*
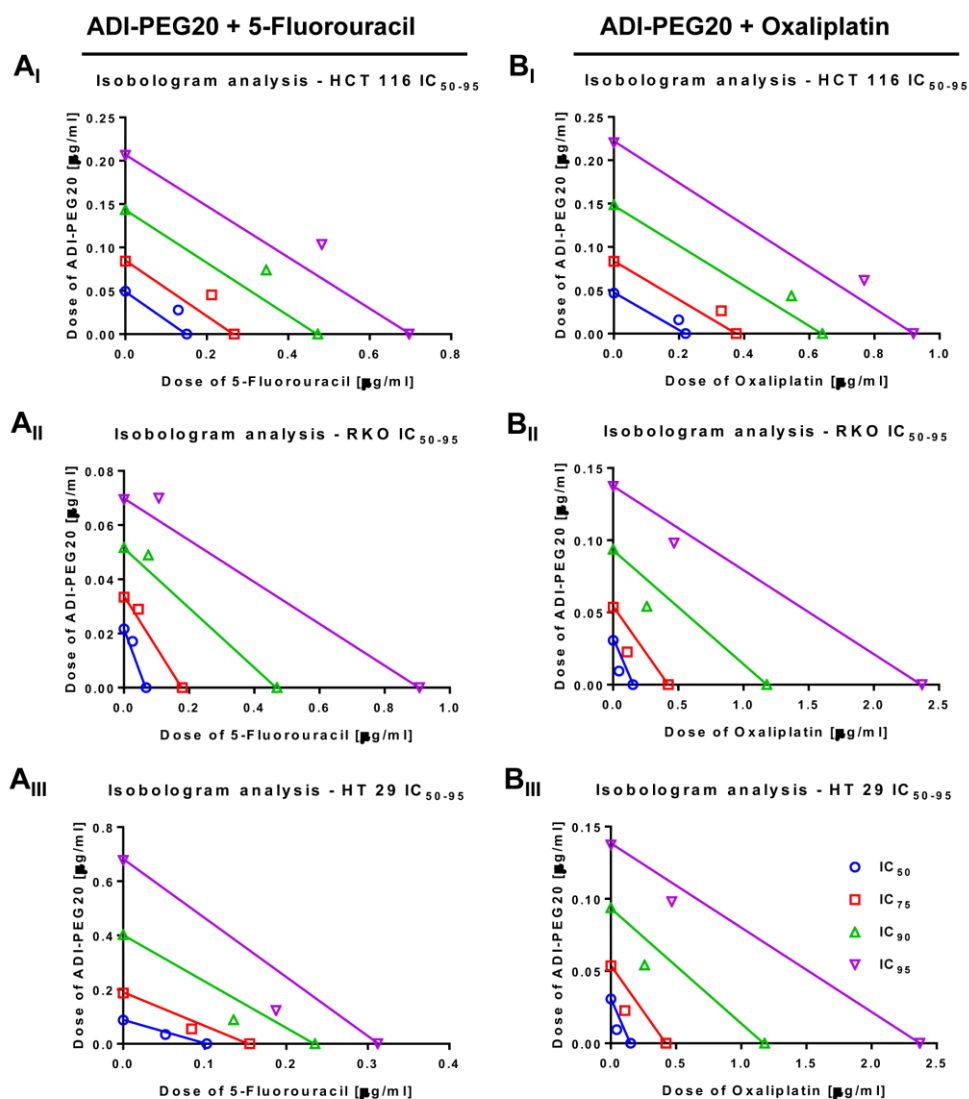
Figure 3-44: Isobologram Analysis of constant combination ratios for ADI-PEG20 + 5-Fluorouracil and ADI-PEG20 + Oxaliplatin. *Values shown on the y and x axis correspond to the dose concentrations for each single drug required to achieve a 5O% (blue), 75% (red), 90% effect (green) and 95% (purple) reduction in growth. Coloured symbols within the axes crossing lines represent the combination of the two drugs required to achieve reduction of growth at 50, 75, 90 and 95% respectively and they indicate synergism if located below the corresponding coloured line, addictive effect if in proximity of the coloured lines additive effect and antagonism if above the corresponding coloured line. **(A$_I$, A$_{II}$, A$_{III}$)** ADI-PEG20 in combination with 5-Fluorouracil; **(B$_I$, B$_{II}$, B$_{III}$)** ADI-PEG20 in combination with Oxaliplatin. Results presented in this figure were obtained from three independent experiments.*
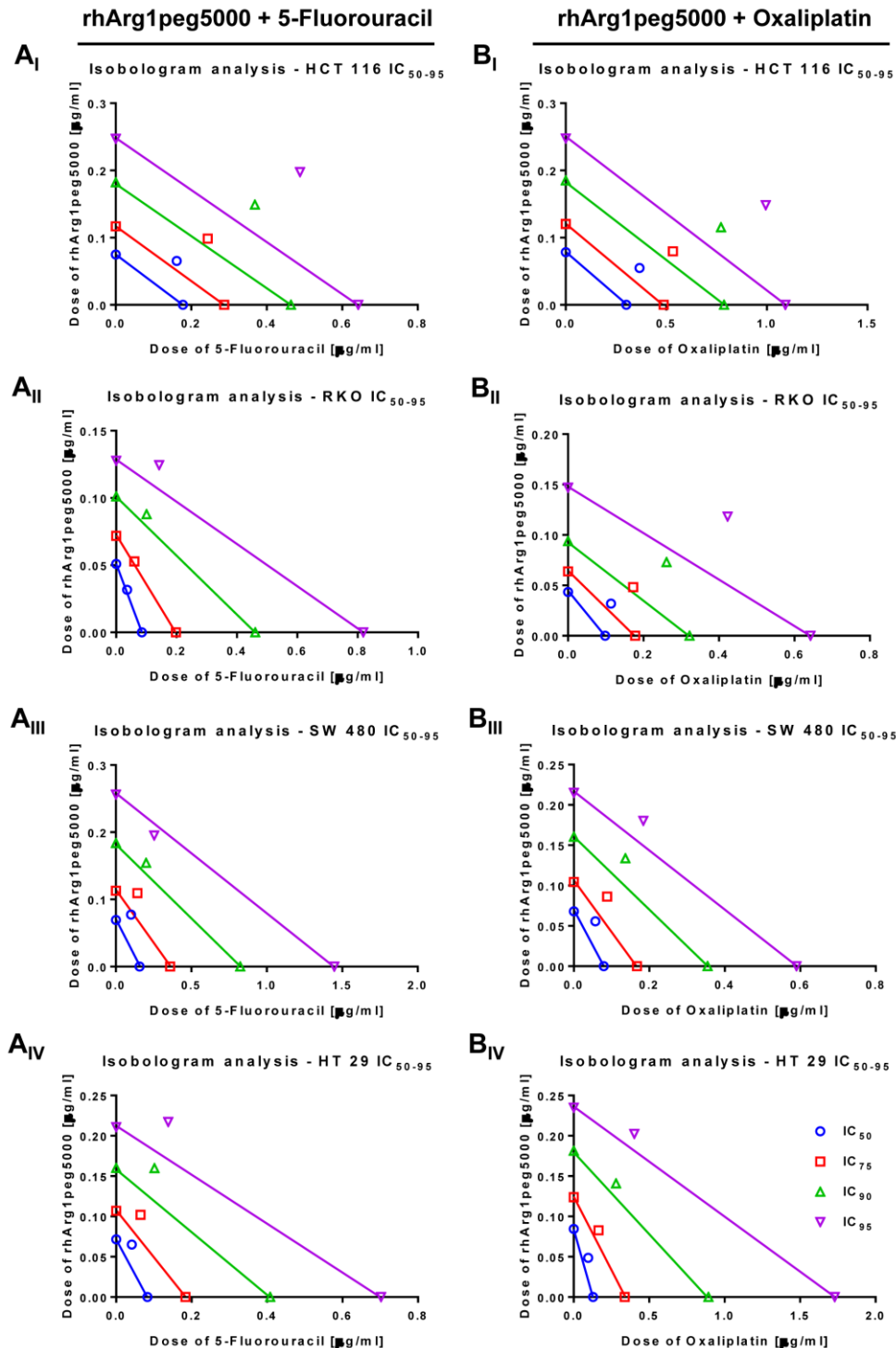
Figure 3-45: Isobologram Analysis of constant combination ratios for rhArg1peg5000 + 5-Fluorouracil and rhArg1peg5000 + Oxaliplatin. *Values shown on the y and x axis correspond to the dose concentrations for each single drug required to achieve a 5O% (blue), 75% (red), 90% effect (green) and 95% (purple) reduction in growth. Coloured symbols within the axes crossing lines represent the combination of the two drugs required to achieve reduction of growth at 50, 75, 90 and 95% respectively and they indicate synergism if located below the corresponding coloured line, addictive effect if in proximity of the coloured lines additive effect and antagonism if above the corresponding coloured line. (A$_I$, A$_{II}$, A$_{III}$, A$_{IV}$) rhArg1peg5000 in combination with 5-Fluorouracil; (B$_I$, B$_{II}$, B$_{III}$, B$_{IV}$) rhArg1peg5000 in combination with Oxaliplatin. Results presented in this figure were obtained from three independent experiments.*
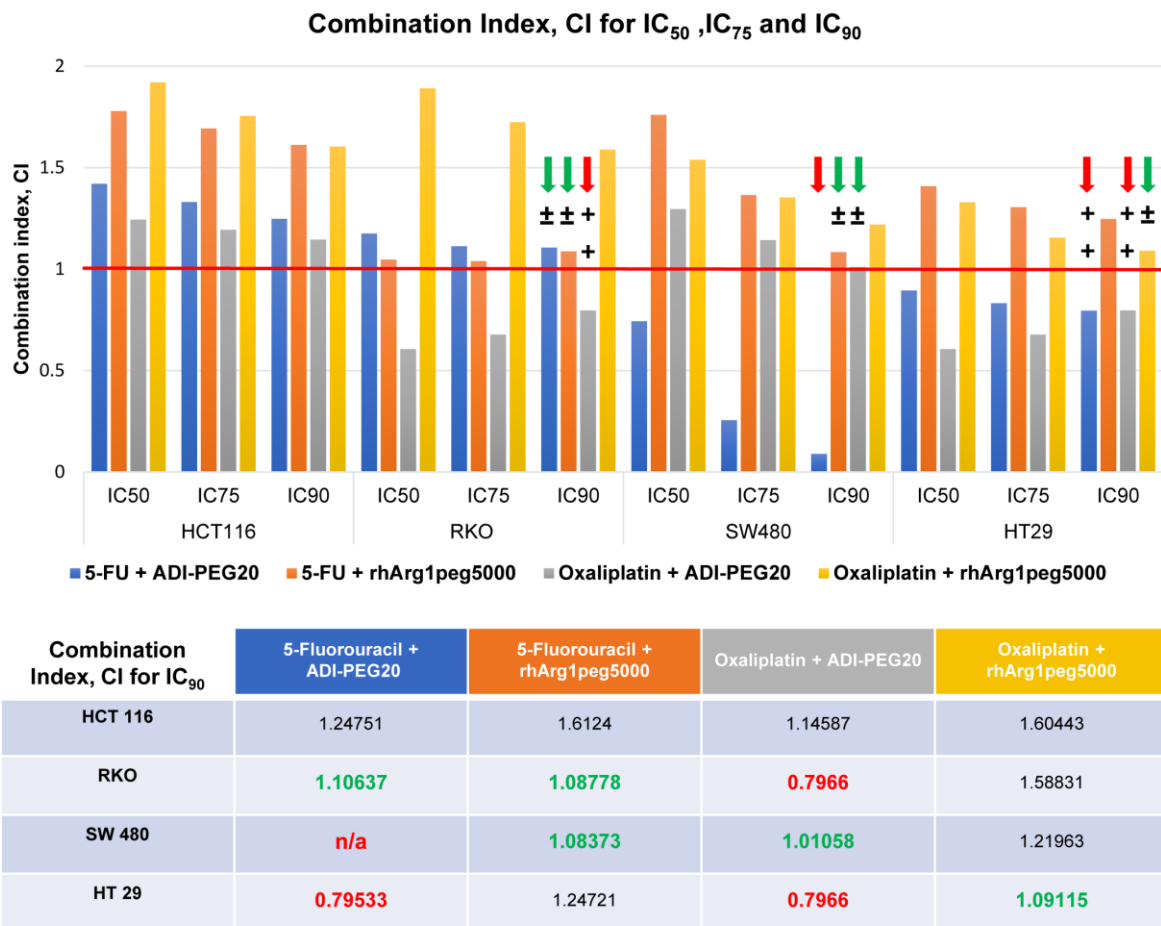
Figure 3-46: An overview of Combination index, CI values at IC$_{50}$, IC$_{75}$, and IC$_{90}$. *CI values <1 indicate synergism, equal 1 additive effect, and >1 antagonism. (For further details, refer to **Table ii**, appendices section). Results presented in this figure were obtained from three independent experiments.*

Overall at IC$_{90}$ we show that 2 out of 4 cell lines tested exhibited a nearly additive effect when treated with rhArg1peg5000 + 5-FU with CI values ranging from 1.083 to 1.087 (SW 480 and RKO respectively). Similarly, RKO, SW 480 and HT 29 showed nearly additive effects when combined with arginine catabolising agents and 5-FU or Oxaliplatin. Accordingly, the CI at IC$_{90}$ of RKO cells when administered ADI-PEG20+5-FU was 1.1. SW 480 exhibited also a nearly additive effect when treated with ADI-PEG20+Oxaliplatin (CI=1.01). Similar results were also observed with HT 29 when exposed to rhArg1peg5000+Oxaliplatin (CI=1.09) (Figure 3-46).

Pharmacological depletion of arginine exhibited synergistic effects with 5-FU and Oxaliplatin in RKO and HT 29. Moderate synergism was observed in RKO and HT 29 when cells were exposed in ADI-PEG20+Oxaliplatin with identical CI values of 0.7966. Similarly, moderate

synergism was also detected when HT 29 cells were treated with ADI-PEG20+5-FU (CI=0.795) (Figure 3-46).

Notably, in some of the combinations, we observed antagonism between rhArg1peg5000 and cytotoxic drugs, which may such potential interplay between arginine depletion and chemotherapeutic agents. Nevertheless, the ultimate goal in drug combination is to achieve a decrease in the administered dose of each single drug, while retaining the efficacy and reducing the normal tissue toxicity (Chou, 2006). Therefore, to further investigate whether drug combination is a valuable option for arginine deprivation therapy in CRC, we employed the CompuSyn® software to simulate the Fraction affected - Dose Reduction Index Plot (Fa-DRI) (Figures 3-47; 3-48). DRI can estimate the amount of –fold concentration of each agent that can be reduced in combination with a second drug to give a specific effect (Fraction affected, Fa[1]), compared against the concentrations of each agent alone. Synergism has been associated with advantageous DRI, where values greater than 1 indicate that single agents are favourable for dose reduction in combination, nevertheless even additive effects or even slight antagonism may result in a DRI>1 (Chou, 2006).

Our analysis shows that in at least 3 cells lines DRI was greater than one (DRI>1) when cells were exposed to ADI-PEG20 and 5-FU, whereas combinatorial treatment of ADI-PEG20 and Oxaliplatin did not reveal sound evidence of a favourable DRI (Figure 3-47). Interestingly, all four cell lines exhibited DRI values considerably greater than 1 when treated with rhArg1peg5000 and 5-FU or Oxaliplatin, indicating that, despite the moderate antagonism suggested by CI values (Figure 3-46), 5-FU and Oxaliplatin antiproliferative efficacy could be maintained using lower doses in combination treatments (Figure 3-48).

---

[1] *Fraction affected (Fa): opposite to the % of growth, Fa signifies the % of cells that have been affected by the treatment in comparison to the control.*
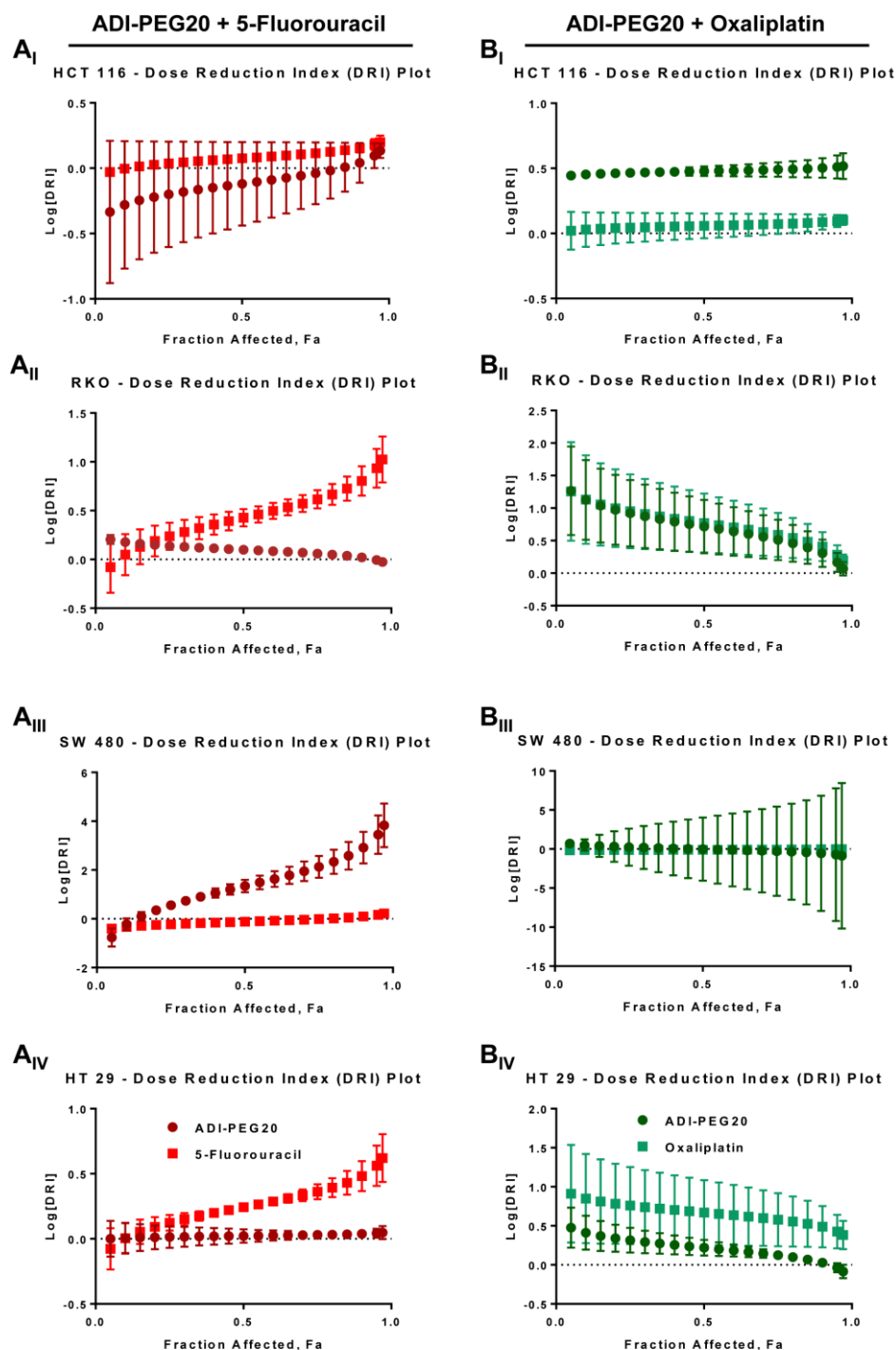
Figure 3-47: Fraction Affected (Fa) – Dose Reduction Index (DRI) plots. *Automated computer simulation of DRI values. DRI values >1 are favourable to dose reduction of the two drugs while still maintaining the same inhibitory effects. The error bars represent the ± Standard Error of the Mean (±SEM, n=3). **(A_I, A_{II}, A_{III}, A_{IV})** Fa-DRI plots of ADI-PEG20 + 5-Fluorouracil and **(B_I, B_{II}, B_{III}, B_{IV})** ADI-PEG20 + Oxaliplatin in HCT 116, RKO, SW 480 and HT 29 cell lines, respectively.*
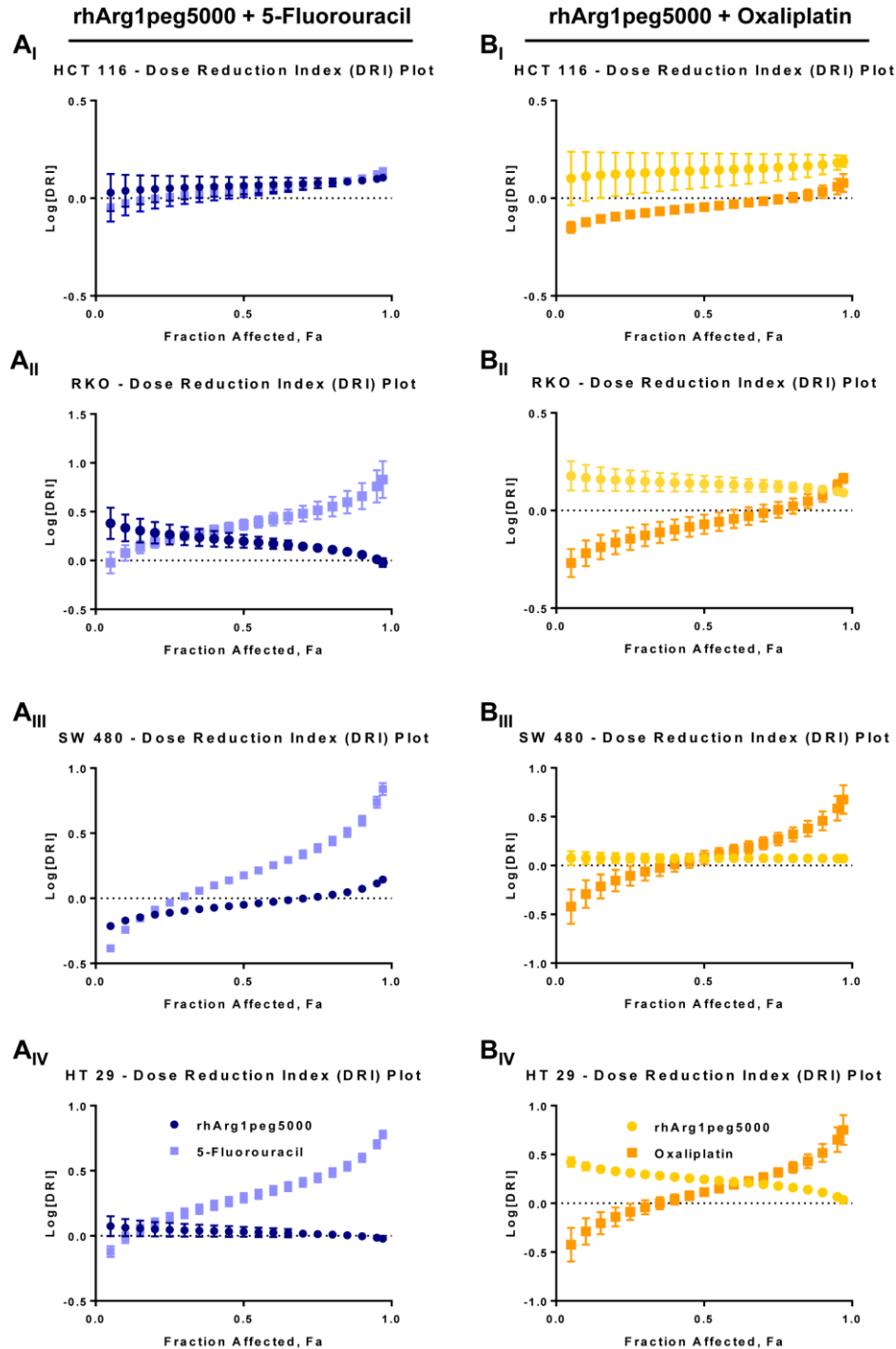
Figure 3-48: Fraction Affected (Fa) – Dose Reduction Index (DRI) plots. *Automated computer simulation of DRI values. DRI values >1 are favourable to dose reduction of the two drugs while still maintaining the same inhibitory effects. The error bars represent the ± Standard Error of the Mean (±SEM, n=3). **(A_I, A_{II}, A_{III}, A_{IV})** Fa-DRI plots of rhArg1peg5000 + 5-Fluorouracil and **(B_I, B_{II}, B_{III}, B_{IV})** rhArg1peg5000 + Oxaliplatin in HCT 116, RKO, SW 480 and HT 29 cell lines, respectively.*

Chapter 4 – Discussion

To date, CRC remains one of the leading causes of cancer associated deaths worldwide, with the UK alone recording over 16000 deaths between 2014 to 2016 (Cancer Research UK). Early detection of lesions, patient stratification strategies, as well as improved surgical procedures have contributed to a progressive decline in mortality rates over the last 50 years. The 5-year relative survival rate of CRC patients at stage I disease is estimated at approximately 90%, however this drops dramatically to almost 10% in patients who are diagnosed at stage IV. Nowadays, the first line of treatment for high risk stage II and stage III CRC patients remains the adjuvant chemotherapy with fluoropyrimidines and platinum based drugs or Irinotecan (Andre et al., 2015). Reportedly, combinations of these agents decrease the risk of relapse in stage III patients who have undergone surgical resection, extending their overall 5-year survival to approximately 60%. Conversely, almost 30% of these patients will demonstrate relapse, which sequentially leads to death within 2-3 years. In recent years, efforts to improve adjuvant therapy of advanced stage III and mCRCs with targeted immunotherapy have led to promising results (Overman et al., 2018; Douillard et al., 2010; Price et al., 2014; Helbling et al., 2013), yet a large proportion of patients still remain unresponsive to these therapies (Martini et al., 2017). Despite recent developments in first line therapy and implementation of predictive biomarkers in the clinic to tailor effective treatment strategies for individuals, there is still a need to further understand evolving mechanisms of drug resistance and identify novel biomarkers that could benefit subsets of patients susceptible to alternative, more effective and less cytotoxic regimens.

Despite first observations on altered metabolism in tumours been reported almost a century ago, recent advancements in molecular and biochemical tools have substantially reshaped and deepened our understanding of the metabolic reprogramming in cancer and how these mechanisms, and functional outcomes of cancer-related metabolic modifications contribute at different stages of the disease. Renewed research interest over the past decades made evident that metabolic rewiring involves alterations that can affect the intratumoural flux of metabolites and redirect the metabolic fate of nutrients to support and sustain the hyper proliferative status of cancer cells. In this regard, rewiring of cellular metabolism has been recognised as one of the new emerging hallmarks of cancer and several attempts have been made to exploit cancer metabolism for a positive clinical outcome. For instance, lack of asparaginase synthase in Acute Lymphoblastic Leukaemia (ALL) renders malignant cells

auxotrophic for the non-essential amino acid asparagine and therefore vulnerable to asparaginase treatment. With response rates ranging from 78-96% in younger ALL patients, asparaginase treatment represents to date one of the most successful implementations of metabolism – based strategies in the clinic (Heiden and DeBerardinis, 2017; Koprivnikar et al., 2017).

The inability of cancer cells to synthesize arginine *de novo*, mainly due to the lack of ASS1 and OTC, renders multiple malignancies auxotrophic for arginine and dependent on external arginine sources. Extended *in vitro* and *in vivo* assessment of PEGylated arginine depleting enzymes, namely, ADI-PEG20 and rhArg1peg5000, in several malignancies has highlighted the anti-tumour efficacy of arginine deprivation, which is currently being evaluated in clinical trials (Section 1.6.5.1 and 1.6.5.2). Here, in this study we made an effort to assess whether CRC is dependent on external arginine supplementation and further investigate whether CRC patients could benefit from arginine depleting strategies.

The first part of this project was focused on confirming and expanding our preliminary data, which have previously shown decreased growth of CRC lines in arginine free media. Indeed, in cell proliferation assays, we show that CRC cell lines are extremely reliant on external arginine sources as none of the 4 cell lines tested were able to grow in the absence of arginine or its precursors, ornithine and citrulline, from the media (Section 3.1.1). In agreement with results obtained from cell proliferation assays, DNA synthesis and cell cycle assessment via FACS analysis reveals an extremely significant reduction in %EdU levels, further indicating inhibition of DNA synthesis and cell cycle arrest. These observations are mirrored by a gradual and significant decrease in Cyclin D1 (Section 3.1.2). Lastly, consistent with the role of arginine as an activator of the amino acid and energy sensing mTOR pathway, removal of arginine from the medium results in reduced mTOR activity and subsequent hypo phosphorylation of its downstream targets 4E-BP1 and RS6 (Section 3.1.3).

Arguably, one of the biggest challenges in cancer research is the implementation of metabolic therapeutic approaches in clinical practice as often results obtained *in vitro* are not recapitulated *in vivo*, where both systemic metabolism and tumour microenvironment may affect tumour growth. In this study, we show that dietary restriction of the non-essential amino acid arginine was indeed able to reduce the overall volume and weight of tumour xenografts. As discussed already in the Introduction (Section 1.6.4) the anti-growth

capabilities of dietary restriction of arginine have been reported in multiple publications, however, it might be argued that the levels of circulating arginine and its precursors are still sufficient to sustain proliferation. Indeed, data acquired from Ki67 staining and imaging with IVIS®, xenograft tissues from the arginine free diet group show that HCT 116-luc2 cells are able to maintain proliferative potential, however at lower rates as depicted by the reduced tumour volume and weight. As previously discussed (Section 3.2.3), based on dietary studies in mice fed with arginine-free diet (Marini et al., 2010), we can speculate that a reduction of plasma levels of arginine by 50% is sufficient to restrict tumour growth of xenografts but, at the same time, precursors of arginine, such as dietary glutamine and proline can contribute for the *de novo* synthesis of citrulline which ultimately could be utilised for the synthesis of arginine in normal tissues as well as ASS1 positive tumours. Adding to this, HCT 116-luc2 xenografts tested positive for ASS1 during their prolonged engraftment, underling a potential metabolic adaptation for utilisation of citrulline. However, the levels of arginine and citrulline within the tumour cells remain unknown. Overall, these results suggest that CRC cell lines are arginine auxotrophic and likely to be responsive to enzymatic depletion of arginine.

To validate this hypothesis, commercially-available arginine depleting enzymes, ADI and recombinant human arginase 1 were tested *in vitro*, and compared against PEGylated formulations of the same enzymes that are currently being evaluated in clinical trials (Tables 1.2 and 1.3). Accordingly, we demonstrate that 3 out 4 cells lines are sensitive to ADI exposure, whereas all 4 cell lines exhibit a dose dependent response to recombinant human arginase 1. ASS1 expression profiling via western blotting reveals 5-fold increase higher expression in the ADI resistant SW480 cell line in comparison to sensitive cell lines. Transient knockdown of ASS1 in SW480 using siRNA results in almost 50% reduction in cell growth and expression of Cyclin D1.

The anti-proliferative efficacy of both ADI-PEG20 and rhArg1peg5000 were further investigated via FACS analysis and EdU incorporation assays. Here, we report that among the two agents, rhArg1peg5000 was the most efficacious, with all 4 cell lines tested demonstrating a dramatic decrease in EdU upon 72 hr of treatment. A less prominent, yet significant, decrease in DNA synthesis is observed in at least two cell lines when treated with ADI-PEG20. Further analysis via western blotting reveals that all cell lines manage to re express ASS1 upon 72 hr of exposure to ADI-PEG20. Results were accompanied by gradual

recovery in Cyclin D1 and D3 levels, further suggesting acquired resistance to ADI treatment. Remarkably, none of the cell lines treated with rhArg1peg5000 was tested positive for OTC and any time point. As shown by us and others, differential expression of ASS1 and OTC dictates response to ADI and recombinant arginase, respectively, and tumours deficient for ASS1 and OTC are amenable to arginine depleting strategies (Delage et al., 2010).

Scientific consensus about CRC being one of the most highly ASS1 expressing tumours, and evidence of OTC downregulation obtained through analysis of publicly available datasets, led us to further validate the levels of ASS1 and OTC in TMAs. In agreement with what was already known from the literature (Rho et al., 2008), we confirm that the vast majority of the CRC cases are positive (33.76%) or extremely positive (45%) for ASS1. Notably, a subset of patients were identified with low or undetectable ASS1 levels (15.69% and ~3% respectively), while OTC expression profiling identifies a staggering 73.65% of patients as weak positive and an additional 24.49% as negative. The ASS1 negative tumours in a subset of the cases and negative expression of OTC, together with the in vitro data, are promising evidences that CRCs may be amenable to pharmacological depletion of arginine.

Although the functional outcome of ASS1 and OTC downregulation in tumours is not fully understood, several studies have correlated ASS1 deficiency with decreased overall survival and worse prognosis (Ekmekoglou et al., 2016, Su et al., 1981; Nicholson et al., 2009). In this project, the TMA study reveals no significant correlation between ASS1 and OTC expression and accumulative survival in CRC patients, although a significant trend towards lower ASS1 levels was observed in higher grade tumours. It must be mentioned that chi-square analysis of TMAs was conducted between negative, weak positive, positive and strong positive tumours from different sites of the bowel, whereas in other studies accumulative survival is compared between 2 quartiles, namely –low and –high. Taking this into account, future comparison of CRC cases between ASS1-low vs ASS1-high and OTC-low vs OTC-high could lead to a better separation of the groups and more definitive conclusions. Furthermore, correlation with next generation sequencing data or analysis of CRC epigenome could also elucidate the driver mechanisms behind differential expression of these enzymes in CRC patients. Additionally, advances in quantitative pathology software analysis and tissue imaging could help us better understand the functional role of deregulated urea cycle enzymes in CRC. Co-profiling of CPS-1, ASL, NOS and arginine transporters along with ASS1

and OTC on the same tissues via utilisation of commercially available multiplex imaging kits, such as the Opal™ Multiplex (PerkinElmer) which can multiple fluorescently-labelled targets within the same slide could increase our ability to predictive susceptibility of CRC patients to arginine catabolising strategies and further address important questions on how deregulated urea cycle affects the progression of the disease.

Nevertheless, robust data from *in vitro* studies and TMA analysis prompt us to investigate whether the anti-proliferative effects of ADI-PEG20 and rhArg1peg5000 could be translated *in vivo*. We show that ADI-PEG20 affects the growth of ASS1-deficient cells (RKO), while rhArg1peg5000 decreases the tumour growth in mice bearing OTC-deficient cells, independently from their ASS1 status (RKO and SW 480). Despite, the significant differences in overall tumour burden, Ki67 analysis failed to show significant decrease in arginase-treated tumours. Lack of difference in proliferation rates may reflect potential adaptive mechanisms of resistance within the tumour tissues or otherwise limitations of Ki67 staining. As discussed already in Section 3.6.2.1, Ki67 may not be the most appropriate marker of cell proliferation as it is present throughout all stages of the cycle. Alternatively, for future experiments we propose the use of a BrdU pulse 2 hr prior sacrificing the mice. This could give a clearer quantification of tumour cells in S phase that actively incorporate BrdU into newly synthetized DNA.

Moreover, considering technical limitations when identifying and counting tumour cells within the xenograft tissue, we propose dual staining for tumour specific markers along with the antigen of interest. In parallel, RNA scope in situ hybridization of target genes would also increase the validity of IHC staining and, at the same time, eliminate any false positive results due to non-specific staining of the latter. Finally, an assessment of cell death through TUNEL assay or detection of cleaved caspase 3 is also warranted, as the decreased tumour volume might be partially attributed to increased cell death in treated tumours.

Although ADI-PEG20 and rhArg1peg5000 have been extensively characterised in several pre-clinical and clinical studies (Section 1.6.5.1 and 1.6.5.2), the lack of PK/PD studies in our *in vivo* experiments remains a limitation. Drug bioavailability, as well as levels of arginine and the related metabolites, ornithine and citrulline, both in plasma and within the tumours would further our understanding of the in vivo data and, perhaps, explain the lack of difference in proliferation rates and provide information on potential adaptive mechanisms

of resistance. Recent advancements in molecular analytical tools such as mass spectrometry imaging techniques would also deepen our understanding of the complex interactions between oncogenes, proteins and metabolites via giving us a thorough spatially resolved picture of the altered metabolism within the tumour xenografts from anatomical to subcellular levels (Aichler and Walch, 2015). Lastly, utilisation of patient derived xenografts (PDXs), instead of CRC cell lines in future experiments would be a more appropriate predictive pre-clinical model to evaluate the efficacy of arginine depleting strategies. Preservation of histological and cellular structure of the original tumour tissue, as well as robust maintenance of the genetic profile of the original tumour, are some of the advantages that render PDXs attractive pre-clinical models to investigate response/resistance mechanisms of targeted therapies (Pompili et al., 2016).

Nonetheless, as mentioned previously, the lack of difference in proliferation rates may not depend solely on methodological limitations, but it might stem from adaptive responses to prolonged arginine starvation. In this regard, we show that re-expression of ASS1 and induction of autophagy are evident in both *in vitro* and *in vivo* experiments. Accordingly, in 2 cell lines (RKO and HT 29), the gradual re-expression of ASS1 in response to ADI-PEG20 is correlated with significant accumulation of c-Myc, which is a well-known transcriptional regulator of the *ASS1* gene. Similar results obtained from *in vivo* testing of ADI-PEG20 confirmed the adaptive re-expression of ASS1. Furthermore, the evident increased accumulation of LC3B in xenograft tumours treated with ADI-PEG20 led us to further investigate the effect of arginine depleting strategies on induction of autophagy. Overall, significant accumulation of LC3B *in vitro* is detected at multiple time points which may differ from one cell line to another in response to both ADI-PEG20 and rhArg1peg5000, indicating that the rate and extent of autophagy induction in response to arginine starvation is cell type specific as well as drug dependent. As reported already in several studies (Delage et al., 2012; Syed et al., 2013; Manca et al., 2012; Wang et al., 2013; Kim et al., 2009), induction of autophagy appears to be a common response to arginine depleting agents, however further experimentation is needed to characterise this phenomenon and its role in arginine starvation. Despite the fact that LC3B and p62 have been used extensively over the past decades as markers of autophagy there are certainly some limitations. Different antibody affinities for LC3A and B and differential expression of LC3 and p62 among different cell lines

could perhaps be addressed with newly developed detection kits (etc. CYTO-ID® from Enzo Life Sciences, Inc.). Accordingly, these kits rely on lysosomal specific dyes which can be monitored via real time confocal microscopy, incorporating into pre-autophagosomes, autophagosomes and autophagolysosomes.

Nonetheless, inhibition of autophagy via chloroquine, in combination with rhArg1peg5000 results in significant accumulation of cleaved PARP in at least 2 cell lines. This confirms the cytoprotective role of autophagy during arginine starvation, yet further characterisation with FACS analysis / Annexin V is needed to increase the validity of these observations, together with translation of this combination approach *in vivo*. Following on from reports of atypical cellular death via impaired mitochondrial function and depolarization of mitochondrial potential and ROS production in response to arginine starvation (Changou et al., 2014; Qiu et al., 2014) further screening of cleaved caspases 3 and 9 as well as reactive oxygen species assays would further help us address the mechanisms behind arginine depletion induced apoptosis in CRC. Lastly, the generation of isogenic cell lines that exhibit different expression of OTC and ASS1 enzymes may be a more appropriate model to compare response and address mechanisms by which cells manage to overcome arginine starvation.

Arginine depleting enzymes appear to be promising alternative agents for the treatment of CRC, however substantial lack of robust efficacy in pre-clinical and clinical trials led most work focus on investigating the relevance of arginine starvation in combination with platinum based drugs and 5-FU (Nicholson et al., 2009; McAlpine et al., 2014; Long et al., 2016; Savaraj et al., 2015). In an effort to investigate potential synergistic effects of arginine depleting agents with 5-FU and oxaliplatin, we conducted a series of *in vitro* combination studies using the Chou and Talalay method (Chou, 2006). We report that ADI-PEG20 exhibits either synergistic or antagonistic effects, which are drug or cell line dependent, while combination treatment with rhArg1peg5000 reveals mostly antagonistic effects. ADI-PEG20 synergises with Oxaliplatin in all 3 ASS1 deficient lines whereas synergism with 5-FU is evident only in one of them, namely HT 29. Taken together, these data warrant caution when using arginine deprivation therapies in combination with standard chemotherapy in CRC, as responses to treatment may vary significantly. Clearly, confirmation of these data in xenograft or PDXs is also warranted.

As it stands, the effects of these combinations in signalling pathways are unknown and due to the complexity of the interactions in response to multiple chemotherapeutic drugs, thoughtful decisions in designing of future experiments need to be made. Employment of RNA sequencing (RNAseq) in combination with stable isotope labelling by amino acids in culture (SILAC)-based quantitative proteomics and subsequent enrichment analysis will be able to identify target genes and changes in protein phosphorylation affected in response to the treatment. This could further provide a detailed mechanistic insight that could potentially be used to predict response to combination therapies that could be tested in patient derived xenograft avatars and 3-dimensional organoid cultures derived from primary tumours.

Overall, we show that CRC cell lines are unable to grow in arginine-free medium, while *in vivo* dietary withdrawal of arginine decreases the growth of xenograft tumours in mice subcutaneously implanted with ASS1-deficient CRC cells. Additionally, CRC cell lines with low or undetectable expression of ASS1 are sensitive to pharmacological arginine depletion mediated by ADI treatment. Remarkably, ASS1-expressing, ADI-resistant cell lines remain auxotrophic for arginine and are susceptible to arginase activity *in vitro* and *in vivo*. All CRC cell lines analysed show lack of expression of OTC and analysis of tissue microarrays unveils a common lack of OTC expression in CRC patients, suggesting that defective expression of OTC could contribute the observed arginine auxotrophy. Finally, in drug combination studies, we demonstrate that ADI and arginase synergise with the chemotherapeutic agents 5-FU and Oxaliplatin in at least 2 of the cell lines tested. Taken all together, we propose that reduced expression of ASS1 and OTC enzymes results in arginine auxotrophy in CRC, a metabolic vulnerability that is amenable to arginine depleting strategies (Alexandrou et al., 2018).

Chapter 5 - Appendices
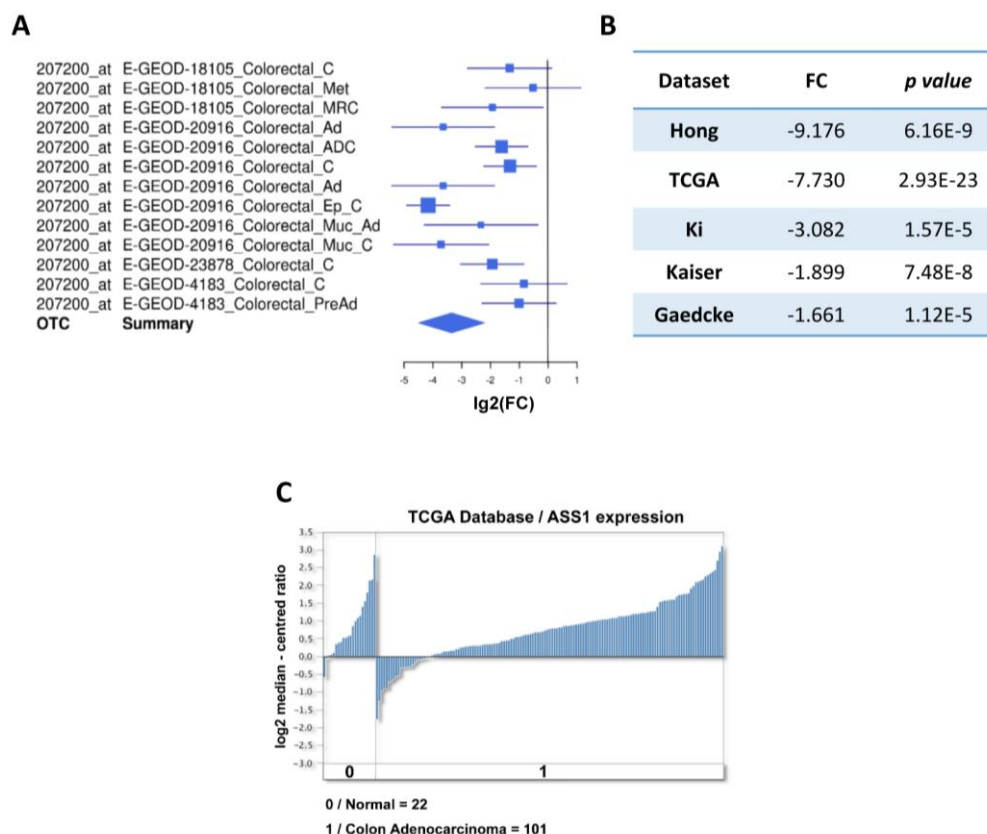
Figure 5-1: Online Dataset Analysis for OTC and ASS1 expression in CRC (A) *meta-analysis of OTC expression in CRC datasets performed using the online tool cancerMA (p<0.001). The forest plot showing the expression levels of OTC gene in CRC. Each dataset is illustrated by a square; the position on the x-axis representing the measure estimate of OTC gene expression (expressed as logarithm of ''fold over control tissue'', lg2FC ratio), the size of the square being proportional to the weight of the study, and the horizontal line through it reflecting the confidence interval of the estimate. The diamond sign indicated the calculated average OTC lg2FC ratio and its confidence interval.* ***(B)*** *FC= fold over normal tissue control values and associated p values* ***(C)*** *log2 median expression of ASS1 in normal vs colon adenocarcinoma as indicated by online dataset analysis of TCGA performed using the online tool Oncomine (https://www.oncomine.org.)*

Table 5-1: Clinicopathological information of CRC patient samples (Tissue Microarray)

Characteristic	Number patients	Percentage (%)	Relationship with survival
Sex			
Male	340	52.3	$\chi2= 0.027, p=0.870$
Female	310	47.7	
Age			
<70	305	46.9	$\chi2=29.213, p<0.001$
≥70	345	53.1	
Screen detected			
Yes	52	8	$\chi2=16.381, p<0.001$
No	598	92	
Tumour site			
Proximal colon	261	40.2	Proximal v distal, $\chi2= 8.418, p=0.004$
Distal colon	245	37.7	Distal v rectal, $\chi2= 0.906, p=0.341$
Rectum	144	22.2	Colon v rectum, $\chi2=0.098, p=0.754$
Tumour differentiation			
Well/moderate	600	92.3	$\chi2=0.976, p=0.323$
Poor	50	7.7	
Extra-mural venous invasion			
Present	140	21.5	$\chi2=100.946, p<0.001$
Absent	510	78.5	
Mismatch repair protein status			
Deficient	96	15.2	$\chi2=2.848, p=0.091$
Proficient	536	84.8	
pT stage			
T1	30	4.6	T1 v T2, $\chi2=0.382, p=0.536$
T2	114	17.5	T2 v T3, $\chi2=24.739, p<0.001$
T3	411	63.2	T3 v T4, $\chi2=30.159, p<0.001$
T4	95	14.6	
pN stage			
N0	364	56	N0 v N1, $\chi2=54.071, p<0.001$
N1	177	27.2	N1 v N2, $\chi2=17.636, p<0.001$
N2	109	16.8	
Dukes stage			
A	120	18.5	A v B, $\chi2=5.059, p=0.025$
B	244	37.5	B v C, $\chi2=65.510, p<0.001$
C	286	44	
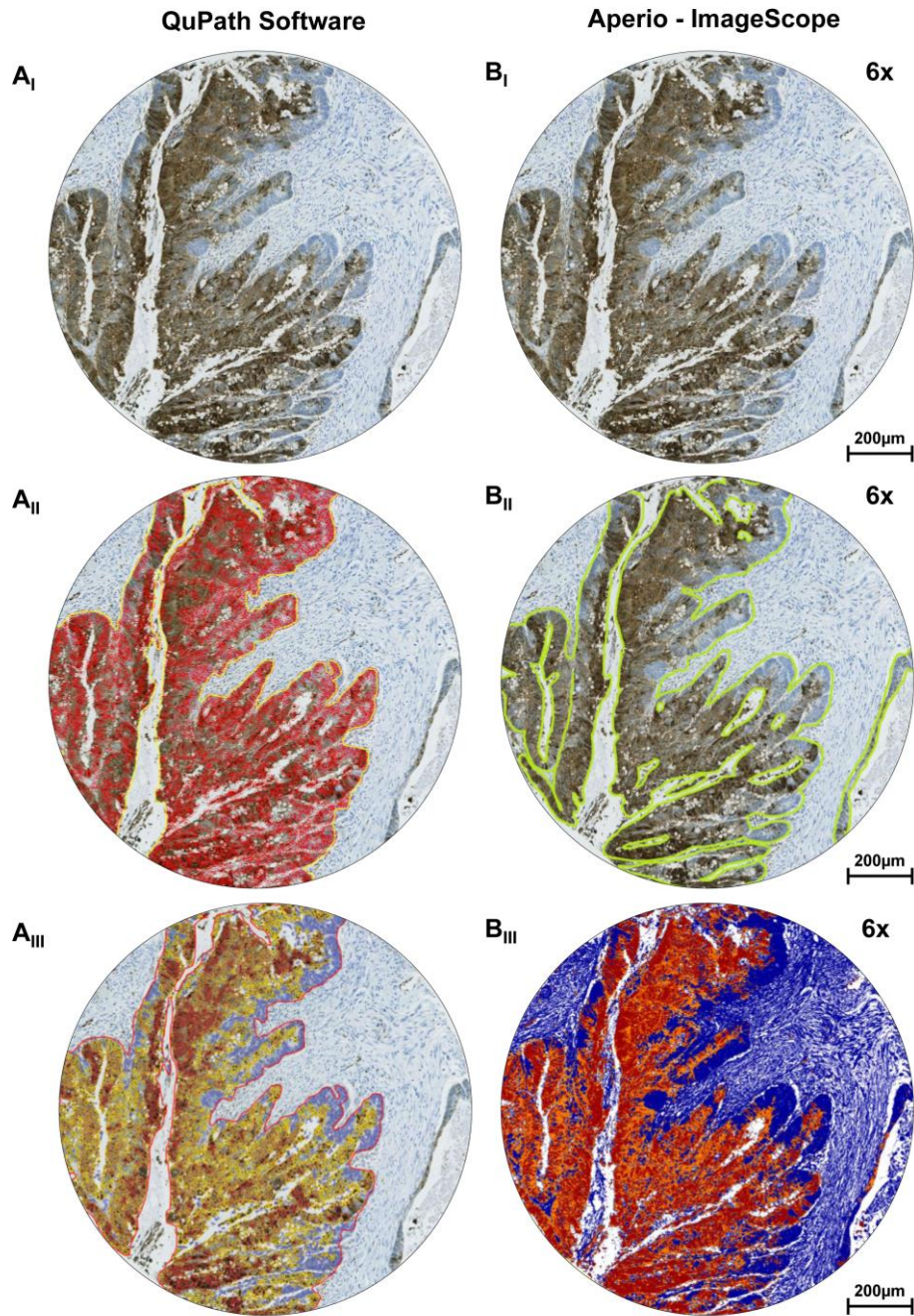
Figure 5-2: Software image analysis – Tissue Microarray scoring assessment of ASS1 in CRC patients. (A_I, A_II, A_III) QuPath Software analysis, (B_I, B_II, B_III) Aperio - ImageScope. *Prior to staining scoring, tissue microarray cores were de arrayed and tumoural areas were identified utilizing sophisticated software algorithms. Individual tumour cells were then identified and distinguished from stromal and immune cells before final scoring of the DAP intensity.*
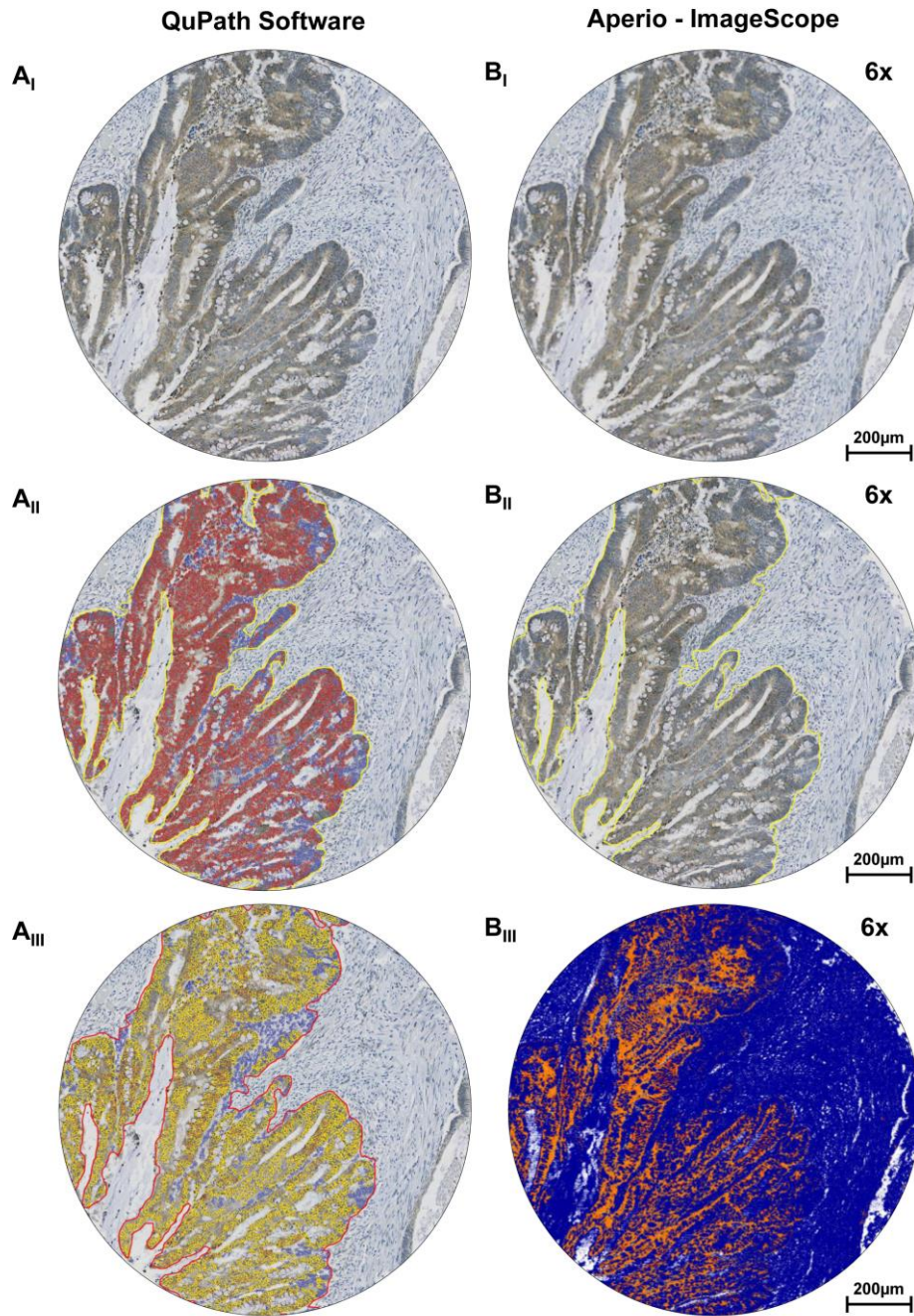
Figure 5-3: Software image analysis – IHC scoring assessment of OTC in CRC patients. *(A_I, A_{II}, A_{III}) QuPath Software analysis, (B_I, B_{II}, B_{III}) Aperio - ImageScope. Prior to staining scoring, tissue microarray cores were de arrayed and tumoural areas were identified utilizing sophisticated software algorithms. Individual tumour cells were then identified and distinguished from stromal and immune cells before final scoring of the DAP intensity.*
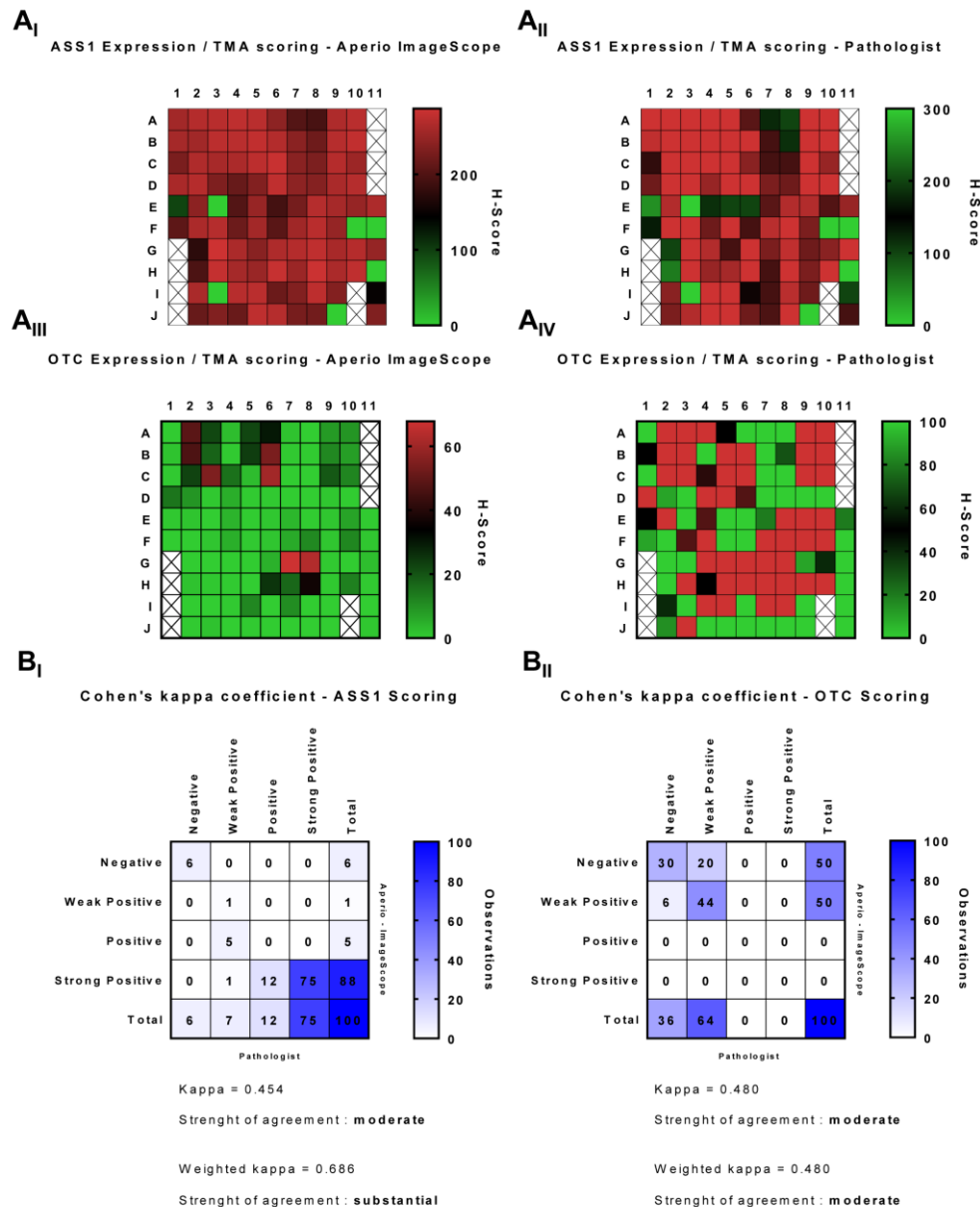
Figure 5-4: Human (manual) vs Software Scoring of TMAs, Interrater reliability – Cohen's kappa coefficient. Cohen's Kappa values ≤ 0 indicate no agreement, 0.01-0.20 none to slight, 0.21-0.4 fair, 0.41-0.6 moderate, 0.6-0.8 substantial and 0.81-1 almost perfect agreement.
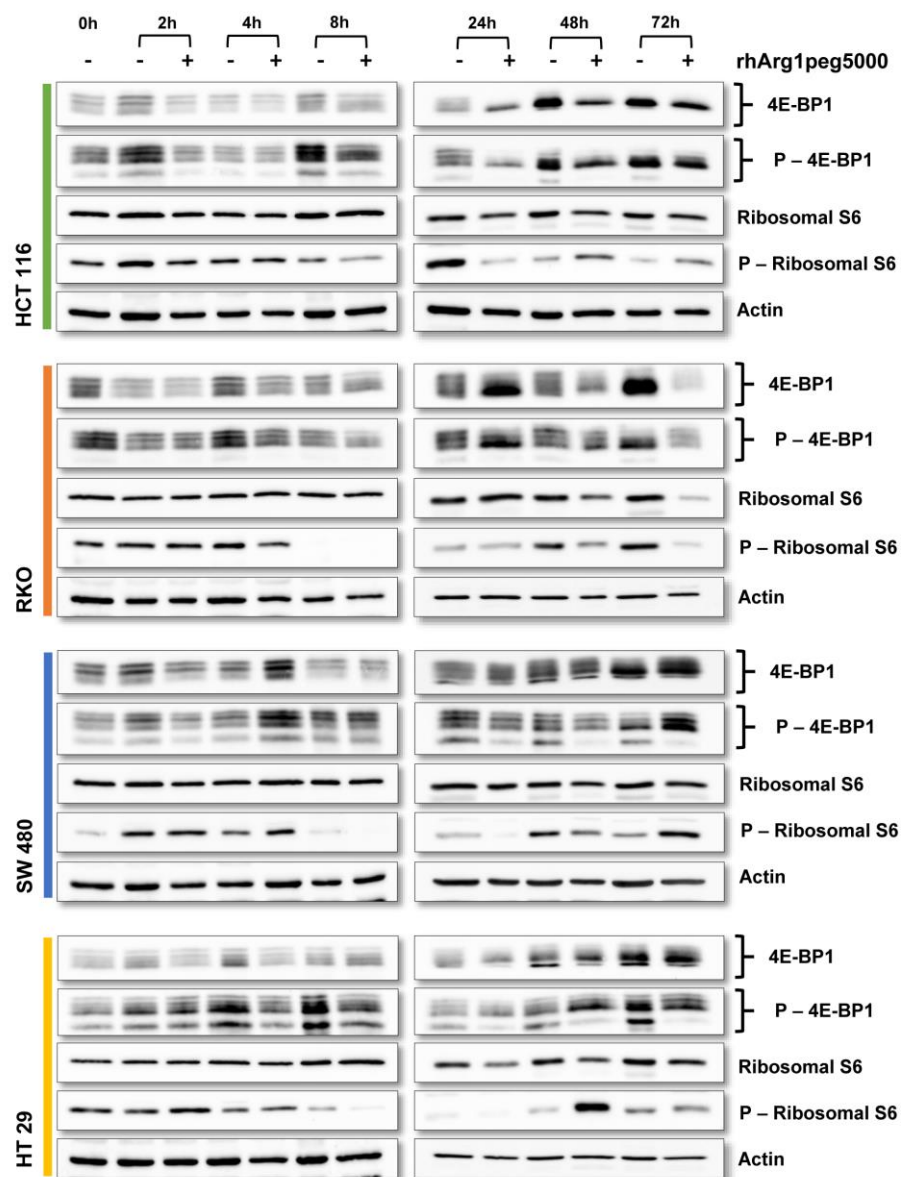
Figure 5-5: Investigating the effects of rhArg1peg5000 on mTOR pathway. *Representative images from western blots of Total / Phospho 4E-BP1 (Thr37/46) and Total / Phospho S6 Ribosomal Protein (S240/244).*
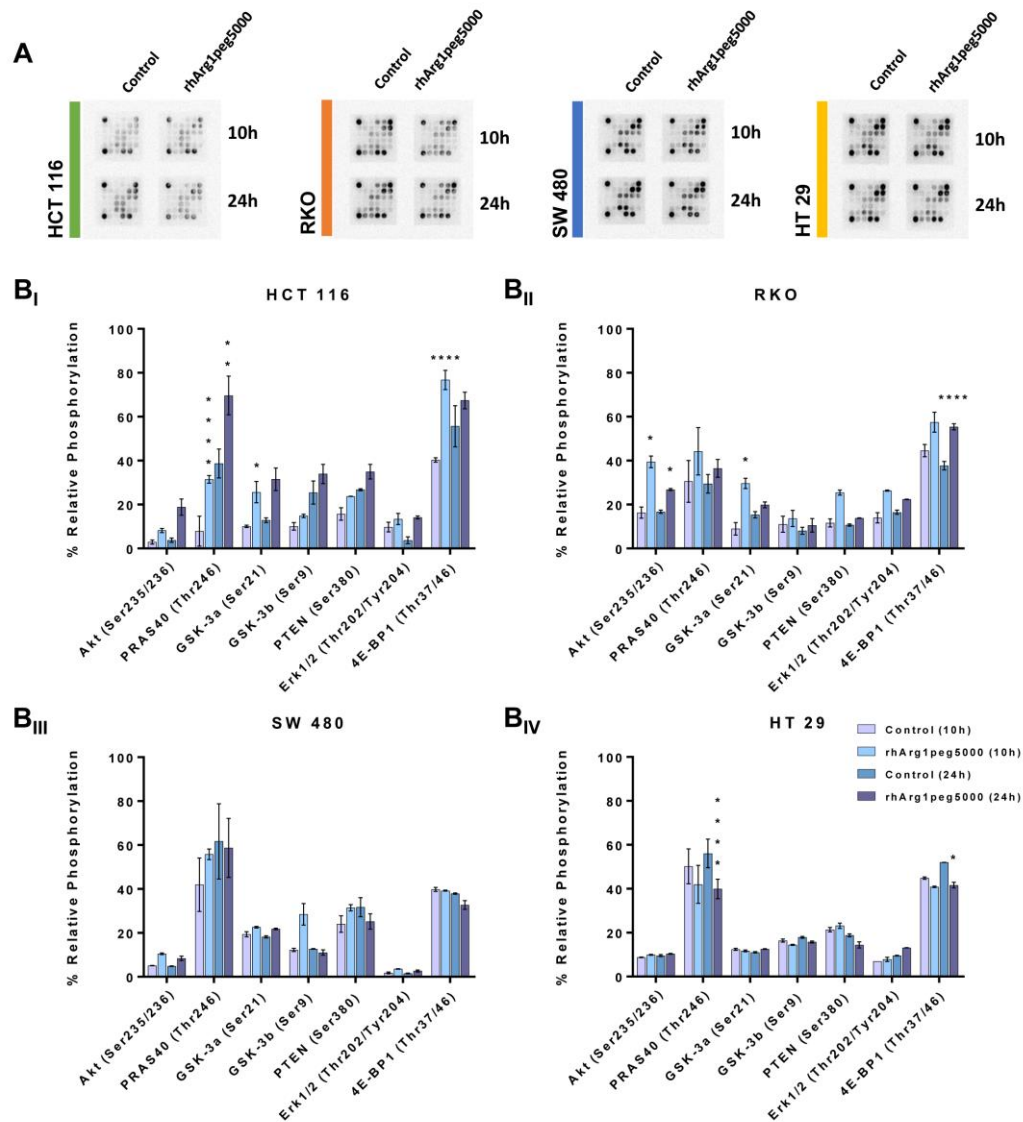
Figure 5-6: PathScan® Akt Signalling Antibody Array analysis of HCT116, RKO, SW 480 and HT 29 after 10 and 24 hours treatment with 0.5 µM rhArg1peg5000. (B_I, B_II, B_III, B_IV) Relative intensity of multiple phosphorylated proteins is shown. The error bars represent the ± Standard Error of the Mean (±SEM) (*p<0.05, **p<0.01, ***p<0.001, ****p<0.0001, two-tailed Student's t-test).
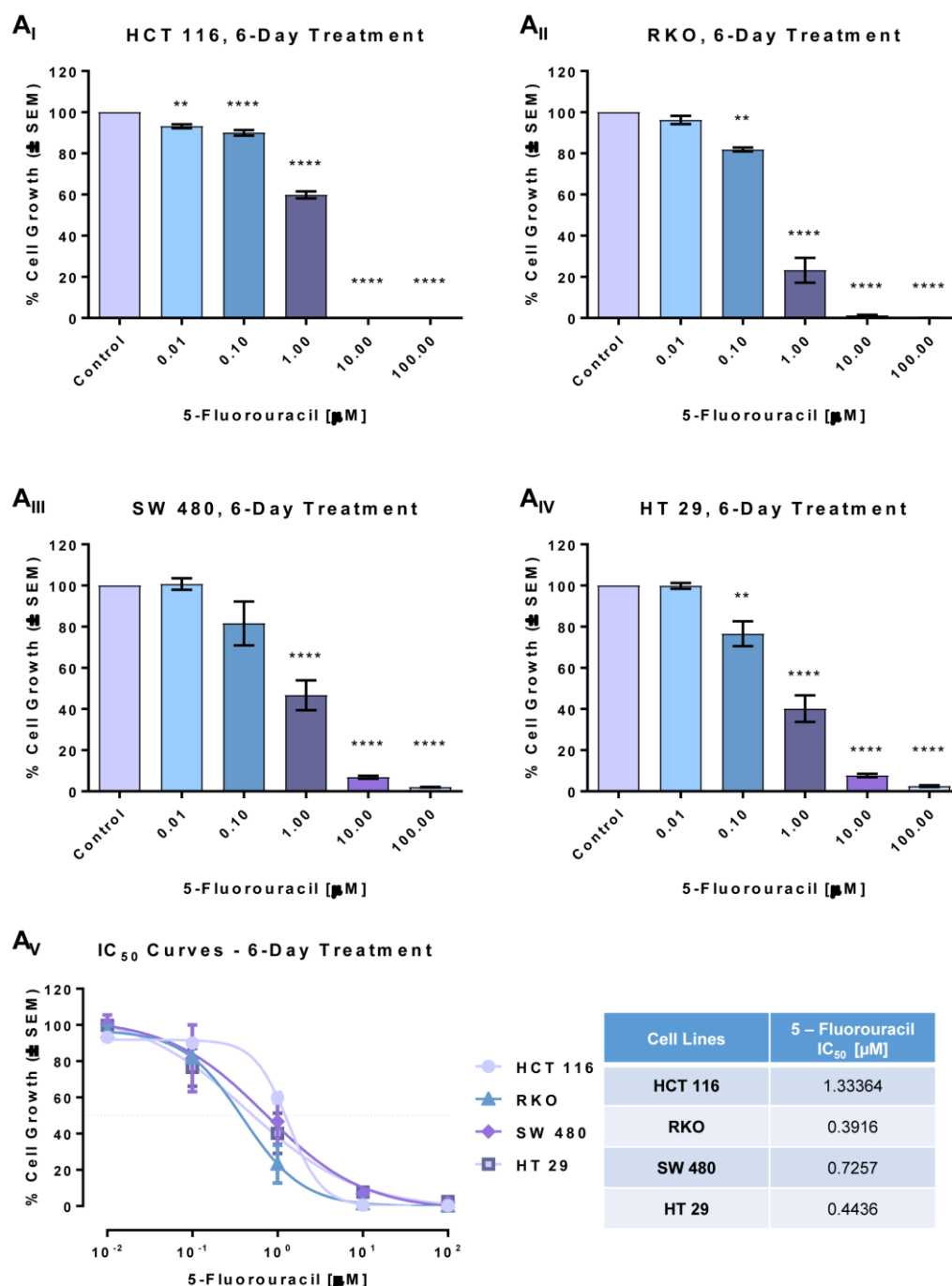
Figure 5-7: The effect of 5-Fluorouracil on cell growth after treating colorectal cancer cell lines for 6 days. (A_I) *HCT 116, **(A_{II})** RKO, **(A_{III})** SW 480, **(A_{IV})** HT 29, were cultured in DMEM/F12 medium containing the indicated concentrations of 5-Fluorouracil. Quadruplicate samples were assessed for cell growth after a 6-Day Period of treatment by cell counting. The percentage (%) of Cell Growth from 5-Fluorouracil treated cells was calculated relative to the cell numbers in corresponding PBS-treated (Control) cells, which was chosen as 100 **(A_V) Dose – Response Nonlinear Regression Curves.** IC₅₀ values were obtained from a nonlinear regression analysis of concentration of the drug vs. response curves utilizing GraphPad Prism. The results were obtained from three independent experiments. The error bars represent the ± Standard Error of the Mean (±SEM). (*p<0.05, **p<0.01, ***p<0.001, ****p<0.0001, two-tailed Student's t-test).*
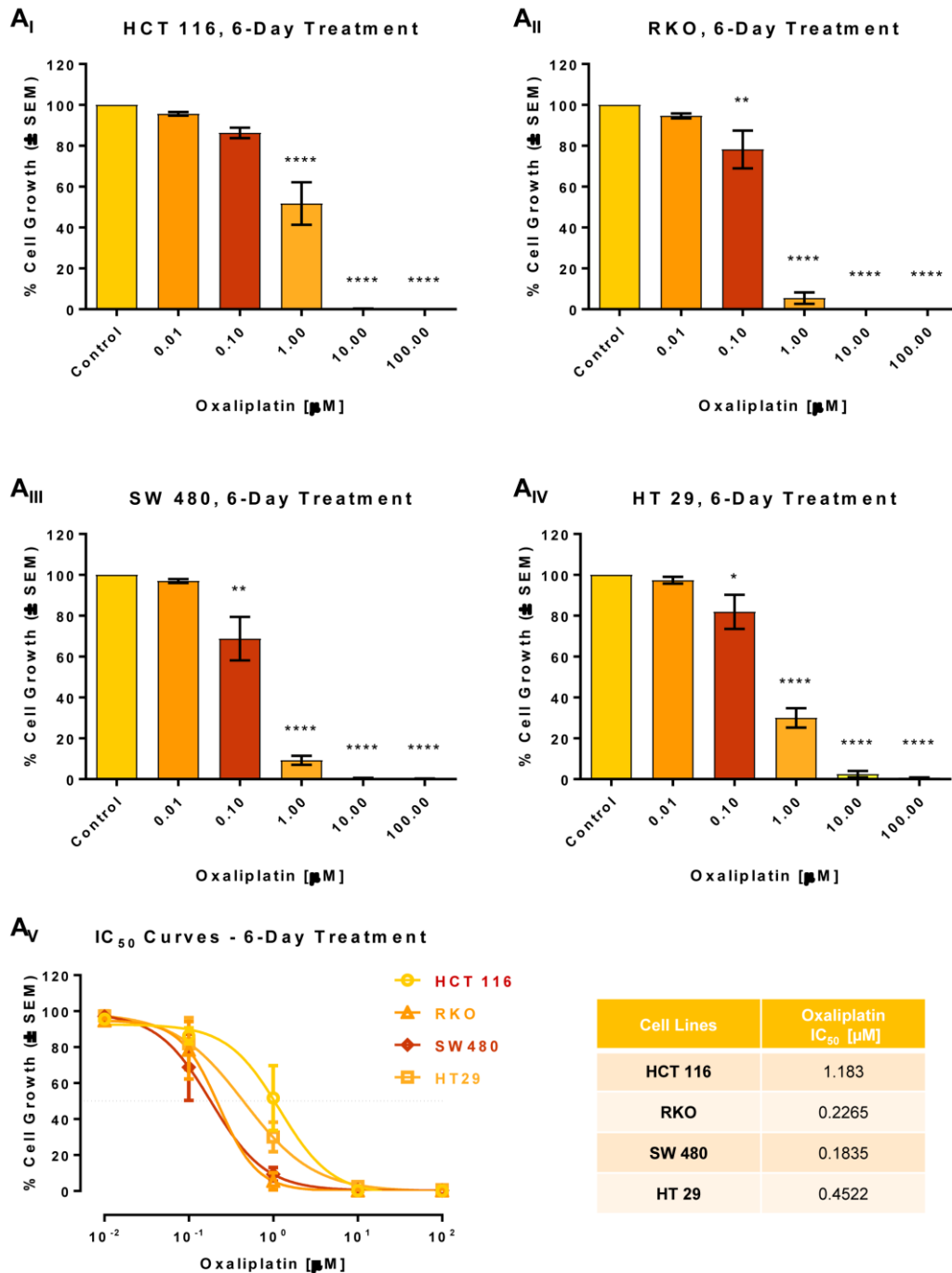
Figure 5-8: The effect of Oxaliplatin on cell growth after treating colorectal cancer cell lines for 6 days. (A_I) *HCT 116, **(A_II)** RKO, **(A_III)** SW 480, **(A_IV)** HT 29, were cultured in DMEM/F12 medium containing the indicated concentrations of Oxaliplatin. Quadruplicate samples were assessed for cell growth after a 6-Day Period of treatment by cell counting. The percentage (%) of Cell Growth from Oxaliplatin treated cells was calculated relative to the cell numbers in corresponding PBS-treated (Control) cells, which was chosen as 100 **(A_v) Dose – Response Nonlinear Regression Curves.** IC_50 values were obtained from a nonlinear regression analysis of concentration of the drug vs. response curves utilizing GraphPad Prism. The results were obtained from three independent experiments. The error bars represent the ± Standard Error of the Mean (±SEM). (*p<0.05, **p<0.01, ***p<0.001, ****p<0.0001, two-tailed Student's t-test).*

Table 5-2: Description and symbols of synergism or antagonism in drug combination studies analysed with the combination index method (Table adapted from Chou, 2006).

Range of Combination Index	Description	Graded Symbols
<0.1	Very strong synergism	+++++
0.1-0.3	Strong synergism	++++
0.3-0.7	Synergism	+++
0.7-0.85	Moderate synergism	++
0.85-0.9	Slight synergism	+
0.9-1.1	Nearly additive	±
1.1-1.2	Slight antagonism	-
1.2-1.45	Moderate antagonism	--
1.45-3.3	Antagonism	---
3.3-10	Strong antagonism	----
>10	Very strong antagonism	-----

Chapter 6 – References

"Colon Cancer." Edited by Roberto Biasini, 123RF Stock Photos, 2018, www.123rf.com/photo_24194463_colon-cancer.html. ; 31(7):e111-3.

Aaltonen, L. A., Peltomaki, P., Leach, F. S., Sistonen, P., Pylkkanen, L., Mecklin, J. P., … et al. (1993). Clues to the pathogenesis of familial colorectal cancer. Science, 260(5109), 812–816.

Aberle, H., Bauer, A., Stappert, J., Kispert, A., & Kemler, R. (1997). beta-catenin is a target for the ubiquitin-proteasome pathway. The EMBO Journal, 16(13), 3797–3804.

Abou-Alfa, G. K., Qin, S., Ryoo, B.-Y., Lu, S.-N., Yen, C.-J., Feng, Y.-H., … Chen, L.-T. (2018). Phase III randomized study of second line ADI-PEG 20 plus best supportive care versus placebo plus best supportive care in patients with advanced hepatocellular carcinoma. Annals of Oncology, 29(6), 1402–1408.

Abubaker, J., Bavi, P., Al-Harbi, S., Ibrahim, M., Siraj, A. K., Al-Sanea, N., … Al-Kuraya, K. S. (2008). Clinicopathological analysis of colorectal cancers with PIK3CA mutations in Middle Eastern population. Oncogene, 27(25), 3539–3545.

Abumrad NN, Barbul A; (2004). The use of arginine in clinical practice. In: Cynober LA, editor. Metabolic and Therapeutic Aspects of Amino Acids in Clinical Nutrition. Boca Raton: CRC Press; p. 595–611.

Agrawal Vaidehi, Sarah Ej Alpini, Everett M Stone, Eugene P Frenkel, Arthur E Frankel (2012). Targeting methionine auxotrophy in cancer : Discovery & exploration.

Ahmad, I., Patel, R., Liu, Y., Singh, L. B., Taketo, M. M., Wu, X. R., Sansom, O. J. (2011). Ras mutation cooperates with β-catenin activation to drive bladder tumourigenesis. Cell Death and Disease, 2(3), 1–9.

Ahmed, D., Eide, P. W., Eilertsen, I. A., Danielsen, S. A., Eknæs, M., Hektoen, M., … Lothe, R. A. (2013). Epigenetic and genetic features of 24 colon cancer cell lines. Oncogenesis, 2(9), e71–.

Aichler, Michaela, and Axel Walch. (2015). MALDI Imaging Mass Spectrometry: Current Frontiers and Perspectives in Pathology Research and Practice. Laboratory Investigation, vol. 95, no. 4, pp. 422–431.

Alberici, P., & Fodde, R. (2006). The Role of the APC Tumor Suppressor in Chromosomal Instability. Genome and Disease Genome Dynamics,149-170.

Alberola-Ila, J., & Hernandez-Hoyos, G. (2003). The Ras/MAPK cascade and the control of positive selection. Immunological Reviews,191(1), 79-96.

Alexandrou, C., Al-Aqbi, S. S., Higgins, J. A., Boyle, W., Karmokar, A., Andreadi, C., … Rufini, A. (2018). Sensitivity of Colorectal Cancer to Arginine Deprivation Therapy is shaped by Differential Expression of Urea Cycle Enzymes. Scientific Reports, 8, 12096.

Allen, M. D., Luong, P., Hudson, C., Leyton, J., Delage, B., Ghazaly, E., . . . Szlosarek, P. W. (2013). Prognostic and Therapeutic Impact of Argininosuccinate Synthetase 1 Control in Bladder Cancer as Monitored Longitudinally by PET Imaging. Cancer Research,74(3), 896-907.

Allen, M. D., Luong, P., Hudson, C., Leyton, J., Delage, B., Ghazaly, E., . . . Szlosarek, P. W. (2013). Prognostic and Therapeutic Impact of Argininosuccinate Synthetase 1 Control in Bladder Cancer as Monitored Longitudinally by PET Imaging. Cancer Research,74(3), 896-907.

Anastasi, S., Fiorentino, L., Fiorini, M., Fraioli, R., Sala, G., Castellani, L., . . . Segatto, O. (2003). Feedback inhibition by RALT controls signal output by the ErbB network. Oncogene,22(27), 4221-4234.

André T, de Gramont A, Vernerey D, Chibaudel B, Bonnetain F, Tijeras-Raballand A, Scriva A, Hickish T, Tabernero J, Van Laethem JL, Banzi M, Maartense E, Shmueli E, Carlsson GU, Scheithauer W, Papamichael D, Möehler M, Landolfi S, Demetter P, Colote S, Tournigand C, Louvet C, Duval A, Fléjou JF, de Gramont A, (2015). Adjuvant Fluorouracil, Leucovorin, and Oxaliplatin in Stage II to III Colon Cancer: Updated 10-Year Survival and Outcomes According to BRAF Mutation and Mismatch Repair Status of the MOSAIC Study. Journal of Clinical Oncology; 33: 4176-4187.

Aoki, K., & Taketo, M. M. (2007). Adenomatous polyposis coli (APC): a multi-functional tumor suppressor gene. Journal of Cell Science, 120(19), 3327–3335.

Arriba, M., García, J. L., Rueda, D., Pérez, J., Brandariz, L., Nutu, O. A., … Perea, J. (2017). Unsupervised Analysis of Array Comparative Genomic Hybridization Data from Early-Onset Colorectal Cancer Reveals Equivalence with Molecular Classification and Phenotypes. Neoplasia (New York, N.Y.), 19(1), 28–34.

Ascierto, S. Scala, G. Castello, A. Daponte, E. Simeone, A. Ottaiano, (2005). PEGylated arginine deiminase treatment of patients with metastatic melanoma: results from phase I and II studies, Journal of Clinical Oncology; 23:7660–7668.

Astler, V. B., & Coller, F. A. (1954). The Prognostic Significance Of Direct Extension Of Carcinoma Of The Colon And Rectum. Annals of Surgery,139(6), 846-852.

Bach, S. J., & Swaine, D. (1965). The Effect of Arginase on the Retardation of Tumour Growth. British Journal of Cancer, 19(2), 379–386.

Barber, T. D., Mcmanus, K., Yuen, K. W., Reis, M., Parmigiani, G., Shen, D., . . . Hieter, P. (2008). Chromatid cohesion defects may underlie chromosome instability in human colorectal cancers. Proceedings of the National Academy of Sciences,105(9), 3443-3448.

Barbul, A. (1986). Arginine: Biochemistry, Physiology, and Therapeutic Implications. Journal of Parenteral and Enteral Nutrition,10(2), 227-238.

Bar-Peled, L., Chantranupong, L., Cherniack, A.D., Chen, W.W., Ottina, K.A., Grabiner, B.C., Spear, E.D., Carter, S.L., Meyerson, M., and Sabatini, D.M. (2013). A Tumor suppressor complex with GAP activity for the Rag GTPases that signal amino acid sufficiency to mTORC1. Science 340, 1100–1106.

Bar-Peled, L., Schweitzer, L.D., Zoncu, R., and Sabatini, D.M. (2012). Ragulator is a GEF for the rag GTPases that signal amino acid levels to mTORC1. Cell 150, 1196–1208.

Barthel, A., Okino, S. T., Liao, J., Nakatani, K., Li, J., Whitlock, J. P., & Roth, R. A. (1999). Regulation ofGLUT1Gene Transcription by the Serine/Threonine Kinase Akt1. Journal of Biological Chemistry,274(29), 20281-20286.

Basuroy, U. K., & Gerner, E. W. (2006). Emerging Concepts in Targeting the Polyamine Metabolic Pathway in Epithelial Cancer Chemoprevention and Chemotherapy. The Journal of Biochemistry,139(1), 27-33.

Batzer, A. G., Rotin, D., Ureña, J. M., Skolnik, E. Y., & Schlessinger, J. (1994). Hierarchy of binding sites for Grb2 and Shc on the epidermal growth factor receptor. Molecular and Cellular Biology,14(8), 5192-5201.

Bazan, V., Migliavacca M, Zanna I, Tubiolo C, Grassi N, Latteri MA, La Farina M, Albanese I, Dardanoni G, Salerno S (2002). Specific codon 13 K-ras mutations are predictive of clinical outcome in colorectal cancer patients, whereas codon 12 K-ras mutations are associated with mucinous histotype. Annals of Oncology,13(9), 1438-1446.

Beahrs OH (1982). Colorectal cancer staging as a prognostic feature. Cancer; 50:2615-2617.

Beddowes, E., Spicer, J., Chan, P. Y., Khadeir, R., Corbacho, J. G., Repana, D., . . . Szlosarek, P. W. (2017). Phase 1 Dose-Escalation Study of Pegylated Arginine Deiminase, Cisplatin, and Pemetrexed in Patients With Argininosuccinate Synthetase 1–Deficient Thoracic Cancers. Journal of Clinical Oncology,35(16), 1778-1785.

Bello-Fernandez, C., Packham, G., & Cleveland, J. L. (1993). The ornithine decarboxylase gene is a transcriptional target of c-Myc. Proceedings of the National Academy of Sciences,90(16), 7804-7808.

Beloussow, K., Wang, L., Wu, J., Ann, D., & Shen, W. (2002). Recombinant arginine deiminase as a potential anti-angiogenic agent. Cancer Letters, 183(2), 155-162.

Ben-Sahra, I., Howell, J.J., Asara, J.M., and Manning, B.D. (2013). Stimulation of de novo pyrimidine synthesis by growth signalling through mTOR and S6K1. Science 339, 1323–1328.

Bernards, A., & Settleman, J. (2004). GAP control: Regulating the regulators of small GTPases. Trends in Cell Biology, 14(7), 377-385.

Bettington, M. L., Walker, N. I., Rosty, C., Brown, I. S., Clouston, A. D., Mckeone, D. M., . . . Whitehall, V. L. (2014). A clinicopathological and molecular analysis of 200 traditional serrated adenomas. Modern Pathology, 28(3), 414-427.

Bettington, M., Walker, N., Clouston, A., Brown, I., Leggett, B., & Whitehall, V. (2013). The serrated pathway to colorectal carcinoma: Current concepts and challenges. Histopathology,62(3), 367-386.

Bezencon C, le Coutre J, Damak S. (2007). Taste-signalling proteins are co-expressed in solitary intestinal epithelial cells. Chemical Senses; 32:41–49.

Bokemeyer, C., Bondarenko, I., Hartmann, J. T., Braud, F. D., Schuch, G., Zubel, A., . . . Koralewski, P. (2011). Efficacy according to biomarker status of cetuximab plus FOLFOX-4 as

first-line treatment for metastatic colorectal cancer: The OPUS study. Annals of Oncology, 22(7), 1535-1546.

Bokemeyer, C., Bondarenko, I., Makhson, A., Hartmann, J. T., Aparicio, J., Braud, F. D., . . . Koralewski, P. (2009). Fluorouracil, Leucovorin, and Oxaliplatin With and Without Cetuximab in the First-Line Treatment of Metastatic Colorectal Cancer. Journal of Clinical Oncology, 27(5), 663-671.

Boulares, a H., Yakovlev, A. G., Ivanova, V., Stoica, B. a, Wang, G., Iyer, S., … Chem, M. J. B. (1999). Role of Poly (ADP-ribose) Polymerase (PARP) Cleavage in Apoptosis. The Journal of Biological Chemistry, 274(33), 22932–22940.

Bowel cancer screening; Available from: http://www.nhs.uk/Conditions/bowel-cancer-screening/Pages/Introduction.aspx.

Brenner, H., Hoffmeister, M., Stegmaier, C., Brenner, G., Altenhofen, L., & Haug, U. (2007). Risk of progression of advanced adenomas to colorectal cancer by age and sex: estimates based on 840 149 screening colonoscopies. Gut, 56(11), 1585–1589.

Brocardo, M., & Henderson, B. R. (2008). APC shuttling to the membrane, nucleus and beyond. Trends in Cell Biology,18(12), 587-596.

Brunn, G.J., Hudson, C.C., Sekulic, A., Williams, J.M., Hosoi, H., Houghton, P.J., Lawrence, J.C., Jr., and Abraham, R.T. (1997). Phosphorylation of the translational repressor PHAS-I by the mammalian target of rapamycin. Science 277, 99–101.

Burke, J. E., & Williams, R. L. (2015). Synergy in activating class I PI3Ks. Trends in Biochemical Sciences, 40(2), 88-100.

Burke, J. E., Perisic, O., Masson, G. R., Vadas, O., & Williams, R. L. (2012). Oncogenic mutations mimic and enhance dynamic events in the natural activation of phosphoinositide 3-kinase p110 (PIK3CA). Proceedings of the National Academy of Sciences, 109(38), 15259-15264.

Cairns, R. a, Harris, I. S., & Mak, T. W. (2011). Regulation of cancer cell metabolism. Nature Reviews. Cancer, 11(2), 85–95.

Campbell PJ, Yachida S, Mudie LJ, Stephens PJ, Pleasance ED, Stebbings LA, (2010). The patterns and dynamics of genomic instability in metastatic pancreatic cancer. Nature; 467: 1109–1113.

Cancer Research UK. (n.d.). Retrieved from https://www.cancerresearchuk.org/

Carracedo, A., & Pandolfi, P. P. (2008). The PTEN-PI3K pathway: Of feedbacks and cross-talks. Oncogene, 27(41), 5527–5541.

Carracedo, A., Ma, L., Teruya-Feldstein, J., Rojo, F., Salmena, L., Alimonti, A., Egia, A., Sasaki, A.T., Thomas, G., Kozma, S.C., et al. (2008). Inhibition of mTORC1 leads to MAPK pathway activation through a PI3K-dependent feedback loop in human cancer. Journal of Clinical Investigations; 118: 3065–3074.

Carson, J., Van Aller, G., Lehr, R., Sinnamon, R., Kirkpatrick, R., Auger, K., . . . Luo, L. (2008). Effects of oncogenic p110α subunit mutations on the lipid kinase activity of phosphoinositide 3-kinase. Biochemical Journal, 409(2), 519-524.

Chalhoub, N., & Baker, S. J. (2009). PTEN and the PI3-Kinase Pathway in Cancer. Annual Review of Pathology: Mechanisms of Disease; 4(1), 127-150.

Chan TL, ZhaoW, Leung SY, Yuen ST, Cancer Genome Project. (2003). BRAF and KRAS mutations in colorectal hyperplastic polyps and serrated adenomas. Cancer Research. 63:4878–81.

Changou, C. A., Chen, Y., Xing, L., Yen, Y., Chuang, F. Y., Cheng, R. H., . . . Kung, H. (2014). Arginine starvation-associated atypical cellular death involves mitochondrial dysfunction, nuclear DNA leakage, and chromatin autophagy. Proceedings of the National Academy of Sciences, 111(39), 14147-14152.

Chantranupong, L., Scaria, S.M., Saxton, R.A., Gygi, M.P., Shen, K., Wyant, G.A.,Wang, T.,Harper, J.W., Gygi, S.P.,andSabatini, D.M. (2016).The CASTOR Proteins Are Arginine Sensors for the mTORC1 Pathway. Cell 165, 153–164.

Cheng, P. N., Lam, T., Lam, W., Tsui, S., Cheng, A. W., Lo, W., & Leung, Y. (2007). PEGylated Recombinant Human Arginase (rhArg-peg5,000mw) Inhibits the In vitro and In vivo

Proliferation of Human Hepatocellular Carcinoma through Arginine Depletion. Cancer Research, 67(1), 309-317.

Childs, A. C., Mehta, D. J., & Gerner, E. W. (2003). Cellular and Molecular Life Sciences Polyamine-dependent gene expression, 60, 1394–1406.

Cho, K. R., & Vogelstein, B. (1990). Genetic Alterations in Colorectal Tumors. Hereditary Colorectal Cancer, 477-482.

Chou, T. (2006). Theoretical Basis, Experimental Design, and Computerized Simulation of Synergism and Antagonism in Drug Combination Studies. Pharmacological Reviews,58(3), 621-681.

Christl, S. U., & Scheppach, W. (1997). Metabolic Consequences of Total Colectomy. Scandinavian Journal of Gastroenterology, 32(Sup222), 20-24.

Clevers, H. and R. Nusse. (2012). Wnt/beta-catenin Signaling and disease. Cell, 149(6): p. 1192-205.

Clevers, H. C., & Bevins, C. L. (2013). Paneth Cells: Maestros of the Small Intestinal Crypts. Annual Review of Physiology, 75(1), 289–311.

Cohade M.; Leal, J.; Wahl, R. L., C. . O. (2003). Direct comparison of (18)F-FDG PET and PET/CT in patients with colorectal carcinoma. J Nucl Med, 44(11), 1797–1803.

Colussi, D., Brandi, G., Bazzoli, F., & Ricciardiello, L. (2013). Molecular Pathways Involved in Colorectal Cancer: Implications for Disease Behavior and Prevention. International Journal of Molecular Sciences, 14(8), 16365–16385.

Comprehensive molecular characterization of human colon and rectal cancer. (2012). Nature; 487(7407), 330-337.

Cossa, G., Gatti, L., Cassinelli, G., Lanzi, C., Zaffaroni, N., & Perego, P. (2012). Modulation of Sensitivity to Antitumor Agents by Targeting the MAPK Survival Pathway. Current Pharmaceutical Design,19(5), 883-894.

Cunningham JM, Christensen ER, Tester DJ, Kim CY, Roche PC, Burgart LJ, (1998). Hypermethylation of the hMLH1 promoter in colon cancer with microsatellite instability. Cancer Research; 58(15):3455–60.

Currie, G. A., & Basham, C. (1978). Differential arginine dependence and the selective cytotoxic effects of activated macrophages for malignant cells in vitro. British Journal of Cancer,38(6), 653-659.

Cutsem, E. V., Cervantes, A., Nordlinger, B., & Arnold, D. (2014). Metastatic colorectal cancer: ESMO Clinical Practice Guidelines for diagnosis, treatment and follow-up. Annals of Oncology,25, Iii1-Iii9.

Cutsem, E. V., Köhne, C., Hitre, E., Zaluski, J., Chien, C. C., Makhson, A., . . . Rougier, P. (2009). Cetuximab and Chemotherapy as Initial Treatment for Metastatic Colorectal Cancer. New England Journal of Medicine,360(14), 1408-1417.

Cutsem, E. V., Köhne, C., Láng, I., Folprecht, G., Nowacki, M. P., Cascinu, S., . . . Ciardiello, F. (2011). Cetuximab Plus Irinotecan, Fluorouracil, and Leucovorin As First-Line Treatment for Metastatic Colorectal Cancer: Updated Analysis of Overall Survival According to Tumor KRAS and BRAF Mutation Status. Journal of Clinical Oncology,29(15), 2011-2019.

Dang, C. V., Le, A., & Gao, P. (2009). MYC-Induced Cancer Cell Energy Metabolism and Therapeutic Opportunities. Clinical Cancer Research,15(21), 6479-6483. doi:10.1158/1078-0432.ccr-09-0889

De Gramont A, Tournigand C, Louvet C, (1997). Oxaliplatin, folinic acid and 5-fluorouracil (FOLFOX) in pre-treated patients with metastatic advanced cancer. The GERCOD. Revue de Medecine Interne; 18(10):769-775.

Delage, B., Fennell, D. a, Nicholson, L., McNeish, I., Lemoine, N. R., Crook, T., & Szlosarek, P. W. (2010). Arginine deprivation and argininosuccinate synthetase expression in the treatment of cancer. International Journal of Cancer. 126(12), 2762–72.

Delage, B., Luong, P., Maharaj, L., O'Riain, C., Syed, N., Crook, T., Szlosarek, P. W. (2012). Promoter methylation of argininosuccinate synthetase-1 sensitises lymphomas to arginine deiminase treatment, autophagy and caspase-dependent apoptosis. Cell Death and Disease, 3(7), 1–9.

Denoix PF. (1954). French Ministry of Public Health National Institute of Hygiene, Monograph no. 4. Paris.

DeVita VT Jr, Hellman S, Rosenburg SA. (2001). Cancer: Principles and Practice of Oncology. Philadelphia: Lippincott Williams & Wilkins.

Dhanasekaran, N., & Reddy, E. P. (1998). Signaling by dual specificity kinases. Oncogene,17(11), 1447-1455.

Dhillon, A. S., Hagan, S., Rath, O., & Kolch, W. (2007). MAP kinase signalling pathways in cancer. Oncogene; 26(22), 3279-3290.

Dienstmann, R., Vermeulen, L., Guinney, J., Kopetz, S., Tejpar, S., & Tabernero, J. (2017). Consensus molecular subtypes and the evolution of precision medicine in colorectal cancer. Nature Reviews Cancer, 17(2), 79–92.

Dillon, B. J., Prieto, V. G., Curley, S. A., Ensor, C. M., Holtsberg, F. W., Bomalaski, J. S., & Clark, M. A. (2004). Incidence and distribution of argininosuccinate synthetase deficiency in human cancers. Cancer,100(4), 826-833.

DiPiro, J. T. (2008). Pharmacotherapy: A pathophysiologic approach. New York: McGraw-Hill Medical.

Douillard JY, Group VS. (2000). Irinotecan and high-dose fluorouracil/Leucovorin for metastatic colorectal cancer. Oncology; 14: 51–55.

Douillard JY, Siena S, Cassidy J, Tabernero J, Burkes R, Barugel M, Humblet Y, Bodoky G, Cunningham D, Jassem J, Rivera F, Kocáková I, Ruff P, Błasińska-Morawiec M, Šmakal M, Canon JL, Rother M, Oliner KS, Wolf M, Gansert J, (2010). Randomized, phase III trial of panitumumab with infusional fluorouracil, leucovorin, and oxaliplatin (FOLFOX4) versus FOLFOX4 alone as first-line treatment in patients with previously untreated metastatic colorectal cancer: the PRIME study. Journal of Clinical Oncology; 28: 4697-4705.

Downward, J. (1998). Ras signalling and apoptosis. Current Opinion in Genetics and Development, 8(1), 49–54.

Downward, J. (2003). Targeting RAS signalling pathways in cancer therapy. Nature Reviews Cancer,3(1), 11-22.

Dranitsaris, G., Shah, A., Spirovski, B., & Vincent, M. (2007). Severe Diarrhea in Patients with Advanced- Stage Colorectal Cancer Receiving FOLFOX or FOLFIRI Chemotherapy: The Development of a Risk Prediction Tool. Clinical Colorectal Cancer,6(5), 367-373.

Dufner, A., & Thomas, G. (1999). Ribosomal S6 kinase signalling and the control of translation. Experimental Cell Research, 253(1), 100–109.

Dukes CE. (1932). The classification of cancer of the rectum. Journal of Pathology; 35:323.

Dunlop, E., & Tee, A. (2013). The kinase triad, AMPK, mTORC1 and ULK1, maintains energy and nutrient homoeostasis. Biochemical Society Transactions,41(4), 939-943.

Duvel, K., Yecies, J.L., Menon, S., Raman, P., Lipovsky, A.I., Souza, A.L., Triantafellow, E., Ma, Q., Gorski, R., Cleaver, S., (2010). Activation of a metabolic gene regulatory network downstream of mTOR complex 1. Molecular Cell; 39: 171–183.

Eagle H. (1959). Amino acid metabolism in mammalian cell cultures. Science.;130:432–7.

East, J. E., Atkin, W. S., Bateman, A. C., Clark, S. K., Dolwani, S., Ket, S. N., … Rees, C. J. (2017). British Society of Gastroenterology position statement on serrated polyps in the colon and rectum. Gut, 66(7), 1181–1196.

Ekmekcioglu, S., Ellerhorst, J. A., Prieto, V. G., Johnson, M. M., Broemeling, L. D., & Grimm, E. A. (2006). Tumor iNOS predicts poor survival for stage III melanoma patients. International Journal of Cancer,119(4), 861-866.

Ensor, C. M., Holtsberg, F. W., Bomalaski, J. S. & Clark, M. A. (2002) PEGylated arginine deiminase (ADI-SS PEG20,000 mw) inhibits human melanomas and hepatocellular carcinomas in vitro and in vivo. Cancer Research. 62: 5443– 5450.

Erdman SH, Ignatenko NA, Powell MB. (1999). APC-dependent changes in expression of genes influencing polyamine metabolism, and consequences for gastrointestinal carcinogenesis, in the Min mouse. Carcinogenesis; 20(9):1709–1713.

Fang, J. Y., & Richardson, B. C. (2005). The MAPK signalling pathways and colorectal cancer. The Lancet Oncology,6(5), 322-327.

Fearon ER, Vogelstein B. (1990). A genetic model for colorectal tumorigenesis. Cell 61:759–67

Ferlay, J., Steliarova-Foucher, E., Lortet-Tieulent, J., Rosso, S., Coebergh, J., Comber, H., . . . Bray, F. (2015). Cancer incidence and mortality patterns in Europe: Estimates for 40 countries in 2012. European Journal of Cancer,51(9), 1201-1202.

Fernandez, J., Lopez, A. B., Wang, C., Mishra, R., Zhou, L., Yaman, I., . . . Hatzolgou, M. (2003). Transcriptional Control of the Arginine/Lysine Transporter, Cat-1, by Physiological Stress. Journal of Biological Chemistry,278(50), 50000-50009.

Fink D, Zheng H, Nebel S, Norris PS, Aebi S, Lin TP, Nehme A, Christen RD, Haas M, MacLeod CL, Howell SB (1997). In vitro and in vivo resistance to cisplatin in cells that have lost DNA mismatch repair. Cancer Research 57: 1841–1845.

Fishel, R., & Kolodner, R. D. (1995). Identification of mismatch repair genes and their role in the development of cancer. Current Opinion in Genetics & Development,5(3), 382-395.

Flynn, N., Meininger, C., Haynes, T., & Wu, G. (2002). The metabolic basis of arginine nutrition and pharmacotherapy. Biomedicine & Pharmacotherapy,56(9), 427-438.

Fontenelle, L. J., & Henderson, J. (1969). Sources of nitrogen as rate-limiting factors for purine biosynthesis de novo in Ehrlich ascites tumor cells. Biochimica Et Biophysica Acta (BBA) - General Subjects,177(1), 88-93.

Frias, M.A., Thoreen, C.C., Jaffe, J.D., Schroder, W., Sculley, T., Carr, S.A., and Sabatini, D.M. (2006). mSin1 is necessary for Akt/PKB phosphorylation, and its isoforms define three distinct mTORC2s. Curr. Biol. 16, 1865–1870.

Frisch, S., & Francis, H. (1994). Disruption of epithelial cell matrix interactions induces apoptosis. J. Cell Biol., 124(4), 619–626.

Fruman, D. A., & Rommel, C. (2014). PI3K and cancer: Lessons, challenges and opportunities. Nature Reviews Drug Discovery,13(2), 140-156.

Fultz, K. E., & Gerner, E. W. (2002). APC-dependent regulation of ornithine decarboxylase in human colon tumor cells. Molecular Carcinogenesis,34(1), 10-18.

Galizia, G., Lieto, E., Ferraraccio, F., Vita, F. D., Castellano, P., Orditura, M., . . . Ciardiello, F. (2006). Prognostic Significance of Epidermal Growth Factor Receptor Expression in Colon Cancer Patients Undergoing Curative Surgery. Annals of Surgical Oncology,13(6), 823-835.

Gao, P., Tchernyshyov, I., Chang, T.-C., Lee, Y.-S., Kita, K., Ochi, T., ... Dang, C. V. (2009). c-Myc suppression of miR-23 enhances mitochondrial glutaminase and glutamine metabolism. Nature, 458(7239), 762–765.

Garnett, M.J. and R. Marais, (2004). Guilty as charged: B-RAF is a human oncogene. Cancer Cell; p. 313-319.

Gerbe, F., Sidot, E., Smyth, D. J., Ohmoto, M., Matsumoto, I., Dardalhon, V., ... Jay, P. (2016). Intestinal epithelial tuft cells initiate type 2 mucosal immunity to helminth parasites. Nature, 529(7585), 226–230.

Gerner EW, Meyskens FL Jr. (2004). Polyamines and cancer: old molecules, new understanding. Nature Cancer Reviews; 4:781–92.

Ghoshal, K. & Jacob, S. T. (1994). Specific inhibition of preribosomal RNA processing in extracts from the lymphosarcoma cells treated with 5-fluorouracil. Cancer Research. 54, 632–636.

Giehl K. (2005). Oncogenic Ras in tumour progression and metastasis. Biological Chemistry; 386:193e205.

Gilroy, E. (1930). The influence of arginine upon the growth rate of a transplantable tumour in the mouse. Biochemical Journal,24(3), 589-595.

Gingras, A., Gygi, S. P., Raught, B., Polakiewicz, R. D., Abraham, R. T., Hoekstra, M. F., . . . Sonenberg, N. (1999). Regulation of 4E-BP1 phosphorylation: A novel two-step mechanism. Genes & Development,13(11), 1422-1437.

Glazer, E. S., Piccirillo, M., Albino, V., Giacomo, R. D., Palaia, R., Mastro, A. A., . . . Izzo, F. (2010). Phase II Study of Pegylated Arginine Deiminase for Nonresectable and Metastatic Hepatocellular Carcinoma. Journal of Clinical Oncology,28(13), 2220-2226.

Goldstein NS, Armin M. (2001). Epidermal growth factor receptor immunohistochemical reactivity in patients with American Joint Committee on Cancer Stage IV colon adenocarcinoma: implications for a standardized scoring system. Cancer; 92:1331–1346.

Gottlob, K. , Majewski N, Kennedy S, Kandel E, Robey RB, Hay N. (2001). Inhibition of early apoptotic events by Akt/PKB is dependent on the first committed step of glycolysis and mitochondrial hexokinase. Genes & Development,15(11), 1406-1418.

Grady, W. M. (2004). Genomic instability and colon cancer. Cancer and Metastasis Reviews,23(1/2), 11-27.

Gramont, A. D., Figer, A., Seymour, M., Homerin, M., Hmissi, A., Cassidy, J., . . . Bonetti, A. (2000). Leucovorin and Fluorouracil With or Without Oxaliplatin as First-Line Treatment in Advanced Colorectal Cancer. Journal of Clinical Oncology,18(16), 2938-2947.

Gribble, F. M., & Reimann, F. (2016). Enteroendocrine Cells: Chemosensors in the Intestinal Epithelium. Annual Review of Physiology,78(1), 277-299.

Gur, G., Rubin, C., Katz, M., Amit, I., Citri, A., Nilsson, J., . . . Yarden, Y. (2004). LRIG1 restricts growth factor signalling by enhancing receptor ubiquitination and degradation. The EMBO Journal,23(16), 3270-3281.

H. Li, H.-C. Hung, S.-C. Yu, J. Lan, Y.-L. Shiue, C.-H. Hsing, L.-T. Chen, and C.-F. Li. (2013). ASS1 as a Novel Tumor Suppressor Gene in Myxofibrosarcomas: Aberrant Loss via Epigenetic DNA Methylation Confers Aggressive Phenotypes, Negative Prognostic Impact, and Therapeutic Relevance. Clinical Cancer Research 19.11 2861-872.

Hamer, H. M., Jonkers, D., Venema, K., Vanhoutvin, S., Troost, F. J., & Brummer, R. J. (2008). Review article: The role of butyrate on colonic function. Alimentary Pharmacology and Therapeutics, 27(2), 104–119.

Hanada, N., Lo, H., Day, C., Pan, Y., Nakajima, Y., & Hung, M. (2005). Co-regulation of B-Myb expression by E2F1 and EGF receptor. Molecular Carcinogenesis,45(1), 10-17.

Hanahan, D., & Weinberg, R. A. (2000). The Hallmarks of Cancer Review, 100, 57–70.

Hanahan, D., & Weinberg, R. A. (2011). Hallmarks of cancer: the next generation. Cell, 144(5), 646–74.

Hann, S. R., & Eisenman, R. N. (1984). Proteins encoded by the human c-myc oncogene: Differential expression in neoplastic cells. Molecular and Cellular Biology, 4(11), 2486-2497.

Hara, K., Maruki, Y., Long, X., Yoshino, K., Oshiro, N., Hidayat, S., Tokunaga, C., Avruch, J., and Yonezawa, K. (2002). Raptor, a binding partner of target of rapamycin (TOR), mediates TOR action. Cell 110, 177–189.

He, T. (1998). Identification of c-MYC as a Target of the APC Pathway. Science,281(5382), 1509-1512.

Heiden, M. G. V., & DeBerardinis, R. J. (2017). Understanding the intersections between metabolism and cancer biology. Cell, 168(4), 657–669.

Heiden, M. G., & Deberardinis, R. J. (2017). Understanding the Intersections between Metabolism and Cancer Biology. Cell,168(4), 657-669.

Helbling, D., Bodoky, G., Gautschi, O., Sun, H., Bosman, F., Gloor, B., . . . Koeberle, D. (2012). Neoadjuvant chemoradiotherapy with or without panitumumab in patients with wild-type KRAS, locally advanced rectal cancer (LARC): A randomized, multicenter, phase II trial SAKK 41/07. Annals of Oncology,24(3), 718-725.

Hernandez, C. P., Morrow, K., Lopez-Barcons, L. A., Zabaleta, J., Sierra, R., Velasco, C., . . . Rodriguez, P. C. (2010). Pegylated arginase I: A potential therapeutic approach in T-ALL. Blood, 115(25), 5214-5221.

Höfer, D., Püschel, B., & Drenckhahn, D. (1996). Taste receptor-like cells in the rat gut identified by expression of alpha-gustducin. Proceedings of the National Academy of Sciences of the United States of America, 93(13), 6631–6634.

Holley R.W., (1967). Evidence that a rat liver "inhibitor" of the synthesis of DNA in cultured mammalian cells is arginase, Biochimica et Biophysica Acta; 145:525–527.

Holtsberg, F. W., Ensor, C. M., Steiner, M. R., Bomalaski, J. S., & Clark, M. A. (2002). Poly(ethylene glycol) (PEG) conjugated arginine deiminase: Effects of PEG formulations on its pharmacological properties. Journal of Controlled Release,80(1-3), 259-271.

Horn, F. (1933). The breakdown of arginine to citrulline by Bacillus pyocyaneus. Hoppe-Seyler's Z. Physiological Chemistry 216:244-247.

Horn, Y., Schechter, P. J., & Marton, L. J. (1987). Phase I–II clinical trial with alpha-difluoromethylornithine — An inhibitor of polyamine biosynthesis. European Journal of Cancer and Clinical Oncology,23(8), 1103-1107.

Horton, J. K., & Tepper, J. E. (2005). Staging of Colorectal Cancer: Past, Present, and Future. Clinical Colorectal Cancer,4(5), 302-312.

Hsieh, A.C., Costa, M., Zollo, O., Davis, C., Feldman, M.E., Testa, J.R., Meyu-has, O., Shokat, K.M., and Ruggero, D. (2010). Genetic dissection of the onco-genic mTOR pathway reveals druggable addiction to translational control via 4EBP-eIF4E. Cancer Cell 17, 249–261.

Hsueh, E. C., Knebel, S. M., Lo, W. H., Leung, Y. C., Cheng, P. N. M., & Hsueh, C. T. (2012). Deprivation of arginine by recombinant human arginase in prostate cancer cells. Journal of Hematology and Oncology, 5, 2–7.

Hu, M. C., Lee, D., Xia, W., Golfman, L. S., Ou-yang, F., Yang, J., … Hung, M. (2007).I k B Kinase Promotes Tumorigenesis through Inhibition of Forkhead FOXO3a, 117, 1427–1428.

Hu, X., Chao, M., & Wu, H. (2017). Central role of lactate and proton in cancer cell resistance to glucose deprivation and its clinical translation. Signal Transduction and Targeted Therapy,2, 16047.

Huang, H., Wu, W., Wang, Y., Wang, J., Fang, F., Tsai, J., . . . Li, C. (2013). ASS1 as a Novel Tumor Suppressor Gene in Myxofibrosarcomas: Aberrant Loss via Epigenetic DNA Methylation Confers Aggressive Phenotypes, Negative Prognostic Impact, and Therapeutic Relevance. Clinical Cancer Research,19(11), 2861-2872.

Hubbard, S. R., & Miller, W. T. (2007). Receptor tyrosine kinases: Mechanisms of activation and signaling. Current Opinion in Cell Biology,19(2), 117-123.

Hughes LA, Khalid-de Bakker CA, Smits KM, van den Brandt PA, Jonkers D, Ahuja N, (2012). The CpG island methylator phenotype in colorectal cancer: progress and problems. Biochimica et Biophysica Acta; 1825:77-85.

Humphries, A., & Wright, N. a. (2008). Colonic crypt organization and tumorigenesis. Nature Reviews. Cancer, 8(6), 415–424.

Hurwitz H, Fehrenbacher L, Novotny W (2004). Bevacizumab plus Irinotecan, fluorouracil, and leucovorin for metastatic colorectal cancer. New England Journal of Medicine; 350: 2335–2342.

Husson, A., Brasse-Lagnel, C., Fairand, A., Renouf, S., & Lavoinne, A. (2003). Argininosuccinate synthetase from the urea cycle to the citrulline-NO cycle. European Journal of Biochemistry,270(9),

Huxley RR, Ansary-Moghaddam A, Clifton P, Czernichow S, Parr CL, Woodward M. (2009). The impact of dietary and lifestyle risk factors on risk of colorectal cancer: a quantitative overview of the epidemiological evidence. International Journal of Cancer 125:171–80.

Ignatenko NA, Gerner EW, Besselsen DG. (2011). Defining the role of polyamines in colon carcinogenesis using mouse models. Journal of Carcinogenesis; 10:10.

Inoki, K., Li, Y., Zhu, T., Wu, J., and Guan, K.L. (2002). TSC2 is phosphorylated and inhibited by Akt and suppresses mTOR signalling. Nature Cell Biology; 4, 648–657.

Izzo, F., Marra, P., Beneduce, G., Castello, G., Vallone, P., De Rosa, V., Cremona, F., Ensor, C. M., Holtsberg, F. W., Bomalaski, J. S., Clark, M. A., Ng, C. & Curley, S. A. (2004). PEGylated arginine deiminase treatment of patients with unresectable hepatocellular carcinoma: results from phase I/II studies. Journal of Clinical Oncology 22: 1815–1822.

Jackson, M. J., Beaudet, A. L., & Obrien, W. E. (1986). Mammalian Urea Cycle Enzymes. Annual Review of Genetics,20(1), 431-464.

Jass JR. (2007). Classification of colorectal cancer based on correlation of clinical, morphological and molecular features. Hisopathology 50:113–30

Jefferies, H. B., Fumagalli, S., Dennis, P. B., Reinhard, C., Pearson, R. B., & Thomas, G. (1997). Rapamycin suppresses 5'TOP mRNA translation through inhibition of p70s6k. The EMBO Journal, 16(12), 3693–3704.

Jenkins MA, Hayashi S, O'Shea AM, Burgart LJ, Smyrk TC, (2007). Pathology features in Bethesda guidelines predict colorectal cancer microsatellite instability: a population-based study. Gastroenterology 133:48–56.

Jessup JM, Compton C, Greene F, (2002). Colon and rectum. In: American Joint Committee on Cancer: AJCC Cancer Staging Manual, 6th edition:113-123.

Johnson, L., Greenbaum, D., Cichowski, K., Mercer, K., Murphy, E., Schmitt, E., . . . Jacks, T. (1997). K-ras is an essential gene in the mouse with partial functional overlap with N-ras. Genes & Development, 11(19), 2468-2481.

Jung, J., Genau, H.M., and Behrends, C. (2015). Amino Acid-Dependent mTORC1 Regulation by the Lysosomal Membrane Protein SLC38A9. Molecular and Cellular Biology; 35, 2479–2494.

Kanamaru, R., Kakuta, H., Sato, T., Ishioka, C., & Wakui, A. (1986). The inhibitory effects of 5-fluorouracil on the metabolism of preribosomal and ribosomal RNA in L-1210 cells in vitro. Cancer Chemotherapy and Pharmacology,17(1), 43-46.

Kario E, Marmor MD, Adamsky K, (2005). Suppressors of cytokine Signaling 4 and 5 regulate epidermal growth factor receptor signalling. Journal of Biological Chemistry; 280:7038–7048.

Karnoub AE, Weinberg RA, (2008). Ras oncogenes: split personalities. Nature Reviews Molecular Cell Biology; 9:517e53.

Kastenhuber, E. R., & Lowe, S. W. (2017). Putting p53 in Context. Cell, 170(6), 1062–1078.

Kim R.H., J.M. Coates, T.L. Bowles, G.P. McNerney, J. Sutcliffe, J.U. Jung, (2009). Arginine deiminase as a novel therapy for prostate cancer induces autophagy and caspase-independent apoptosis, Cancer Research; 69:700–708.

Kim RH, Bold RJ, Kung HJ. ADI, (2009). Autophagy and apoptosis: metabolic stress as a therapeutic option for prostate cancer. Autophagy. 5(4):567-8.

Kim, D.H., Sarbassov, D.D., Ali, S.M., Latek, R.R., Guntur, K.V., Erdjument- Bromage, H., Tempst, P., and Sabatini, D.M. (2003). GbetaL, a positive regu- lator of the rapamycin-sensitive pathway required for the nutrient-sensitive interaction between raptor and mTOR. Mol. Cell 11, 895–904.

Kim, Y., Kobayashi, E., Kubota, D., Suehara, Y., Mukaihara, K., Akaike, K. Kitano, S. (2016). Reduced argininosuccinate synthetase expression in refractory sarcomas: Impacts on therapeutic potential and drug resistance. Oncotarget, 7(43), 70832–70844.

Kitagawa, M., Hatakeyama, S., Shirane, M., Matsumoto, M., Ishida, N., Hattori, K. Nakayama, K. (1999). An F-box protein, FWD1, mediates ubiquitin-dependent proteolysis of β-catenin. The EMBO Journal, 18(9), 2401–2410.

Ko Hler, M., Ro Ring, M., Schorch, B., Heilmann, K., Stickel, N., Fiala, G. J., . . . Brummer, T. (2015). Activation loop phosphorylation regulates B-Raf in vivo and transformation by B-Raf mutants. The EMBO Journal, 35(2), 143-161.

Kobayashi, E., Masuda, M., Nakayama, R., Ichikawa, H., Satow, R., Shitashige, M., . . . Yamada, T. (2010). Reduced Argininosuccinate Synthetase Is a Predictive Biomarker for the Development of Pulmonary Metastasis in Patients with Osteosarcoma. Molecular Cancer Therapeutics,9(3), 535-544.

Koprivnikar, J., McCloskey, J., & Faderl, S. (2017). Safety, efficacy, and clinical utility of asparaginase in the treatment of adult patients with acute lymphoblastic leukemia. OncoTargets and Therapy, 10, 1413–1422.

Korde Choudhari, S., Chaudhary, M., Bagde, S., Gadbail, A. R., & Joshi, V. (2013). Nitric oxide and cancer: a review. World Journal of Surgical Oncology, 11, 118.

Kraemer, P. M., Defend, V., Hayflick, L., & Manson, L. A. (1963). Mycoplasma (PPLO) Strains with Lytic Activity for Murine Lymphoma Cells in vitro. Experimental Biology and Medicine,112(2), 381-387.

Kraemer, P. M., Defend, V., Hayflick, L., & Manson, L. A. (1963). Mycoplasma (PPLO) Strains with Lytic Activity for Murine Lymphoma Cells in vitro. Experimental Biology and Medicine,112(2), 381-387.

Krycer, J. R., Sharpe, L. J., Luu, W., & Brown, A. J. (2010). The Akt–SREBP nexus: Cell signalling meets lipid metabolism. Trends in Endocrinology & Metabolism,21(5), 268-276.

Laederich MB, Funes-Duran M, Yen L, (2004). The leucine-rich repeat protein LRIG1 is a negative regulator of ErbB family receptor tyrosine kinases. Journal of Biological Chemistry; 279:47050–47056.

Lagarde, S. M., P. E. Ver Loren Van Themaat, Moerland, P. D., Gilhuijs-Pederson, L. A., Kate, F. J., Reitsma, P. H., . . . Lanschot, J. J. (2008). Analysis of Gene Expression Identifies Differentially Expressed Genes and Pathways Associated with Lymphatic Dissemination in Patients with Adenocarcinoma of the Esophagus. Annals of Surgical Oncology,15(12), 3459-3470.

Lan, J., Tai, H., Lee, S., Chen, T., Huang, H., & Li, C. (2014). Deficiency in expression and epigenetic DNA Methylation of ASS1 gene in nasopharyngeal carcinoma: Negative prognostic impact and therapeutic relevance. Tumor Biology, 35(1), 161-169.

Landau, Z. Bercovich, M.H. Park, C. Kahana, (2010). The role of polyamines in supporting growth of mammalian cells is mediated through their requirement for translation initiation and elongation, Journal of Biological Chemistry; 285: 12474–12481.

Lao, V. V., & Grady, W. M. (2011). Epigenetics and colorectal cancer. Nature Reviews Gastroenterology & Hepatology,8(12), 686-700. doi:10.1038/nrgastro.2011.173.

Lazebnik, Y. A., Kaufmann, S. H., Desnoyers, S., Poirier, G. G., & Earnshaw, W. C. (1994). Cleavage of poly(ADP-ribose) polymerase by a proteinase with properties like ICE. Nature,371(6495), 346-347.

Lee, J., Liu, R., Li, J., Zhang, C., Wang, Y., Cai, Q., Lu, Z. (n.d.). Stabilization of phosphofructokinase 1 platelet isoform by AKT promotes tumorigenesis, 1–14.

Leslie A. Bateman, Wan-Min Ku, Martin J. Heslin, Carlo M. Contreras, Christine F. Skibola, and Daniel K. Nomura (2017) Argininosuccinate Synthase 1 is a Metabolic Regulator of Colorectal Cancer Pathogenicity ACS Chemical Biology 12 (4), 905-911.

Levy, J. M. M., Towers, C. G., & Thorburn, A. (2017). Targeting autophagy in cancer. Nature Reviews Cancer, 17(9), 528–542.

Lien, E.C., Lyssiotis, C.A., and Cantley, L.C. (2016). Metabolic Reprogramming by the PI3K-Akt-mTOR Pathway in Cancer. Recent Results Cancer Research. 207, 39–72.

Lin SY, Makino K, XiaW, (2001). Nuclear localization of EGF receptor and its potential new role as a transcription factor. Nature Cellular Biology; 3:802-8.

Linblom A, Tannergard P, Werelius B, Nordenskjold M. (1993). Genetic mapping of a second locus predisposing to hereditary non-polyposis colon cancer. Nature Genetics; 5:279–82

Ljuslinder I, Melin B, Henriksson ML, Öberg Å, Palmqvist R. (2011). Increased epidermal growth factor receptor expression at the invasive margin is a negative prognostic factor in colorectal cancer. International Journal of Cancer; 128:2031–2037.

Lo HW, Hsu SC, Ali-SeyedM, (2005). Nuclear interaction of EGFR and STAT3 in the activation of the iNOS/ NO pathway. Cancer Cell; 7:575-89.

Logan, R. F., Patnick, J., Coleman, L., & Nickerson, C. (2010). 927 Outcomes of the Bowel Cancer Screening Programme (BCSP) in England after the First 1 Million Tests. Gastroenterology, 138(5).

Long Y, Tsai WB, Wangpaichitr M, (2013). L -Arginine deiminase resistance in melanoma cells is associated with metabolic reprogramming, glucose dependence and glutamine addiction. Molecular Cancer Therapeutics; 12: 2581–90.

Lopez, A., Wang, C., Huang, C., Yaman, I., Li, Y., Chakravarty, K., . . . Hatzoglou, M. (2007). A feedback transcriptional mechanism controls the level of the arginine/lysine transporter cat-1 during amino acid starvation. Biochemical Journal,402(1), 163-173.

Lowenstein EJ, Daly RJ, Batzer AG, (1992). The SH2 and SH3 domain-containing protein GRB2 links receptor tyrosine kinases to Ras signalling. Cell; 70: 431-42.

Lowy, D. R., & Willumsen, B. M. (1993). Function and Regulation of Ras. Annual Review of Biochemistry,62(1), 851-891.

Lu, Y., Wang, W., Wang, J., Yang, C., Mao, H., Fu, X., … Chen, B. (2013). Overexpression of Arginine Transporter CAT-1 Is Associated with Accumulation of L-Arginine and Cell Growth in Human Colorectal Cancer Tissue. PLoS ONE, 8(9), e73866.

Lu, Z. and S. Xu, (2006). ERK1/2 MAP kinases in cell survival and apoptosis. IUBMB Life; 58(11): p. 621-31.

Lynch, H. T. (1966). Hereditary factors in cancer. Study of two large Midwestern kindred's. Archives of Internal Medicine, 117(2), 206-212.

Ma XT, Wang S, Ye YJ, Du RY, Cui ZR, and Somsouk M. (2004). Constitutive activation of Stat3 Signaling pathway in human colorectal carcinoma. World Journal of Gastroenterology; 10: 1569-73.

Mace, O. J., Affleck, J., Patel, N., & Kellett, G. L. (2007). Sweet taste receptors in rat small intestine stimulate glucose absorption through apical GLUT2. The Journal of Physiology, 582(Pt 1), 379–392.

Malumbres M, Barbacid M. 2003. RAS oncogenes: the first 30 years. Nature Reviews Cancer; 3:459–65.

Manca A, Sini MC, Izzo F, Ascierto PA, Tatangelo F, Botti G, (2011). Induction of argininosuccinate synthetase (ASS) expression affects the antiproliferative activity of arginine deiminase (ADI) in melanoma cells. Oncology Reports; 25(6):1495 502.

Manning, B.D., Tee, A.R., Logsdon, M.N., Blenis, J., and Cantley, L.C. (2002). Identification of the tuberous sclerosis complex-2 tumor suppressor gene product tuberin as a target of the phosphoinositide 3-kinase/akt pathway. Molecular Cell 10, 151–162.

Margolis, B. and E.Y. Skolnik, (1994). Activation of Ras by receptor tyrosine kinases. Journal of the American Society of Nephrology; 5(6): p. 1288-99.

Markowitz, S. D., & Bertagnolli, M. M. (2010). Molecular Basis of Colorectal Cancer, 2449–2460.

Marmor MD, Yarden Y. (2004). Role of protein ubiquitination in regulating endocytosis of receptor tyrosine kinases. Oncogene. 23:2057–2070.

Martina, J.A., Chen, Y., Gucek, M., and Puertollano, R. (2012). MTORC1 functions as a transcriptional regulator of autophagy by preventing nuclear trans- port of TFEB. Autophagy 8, 903–914.

Martinez, M. E., Obrien, T. G., Fultz, K. E., Babbar, N., Yerushalmi, H., Qu, N., . . . Gerner, E. W. (2003). Pronounced reduction in adenoma recurrence associated with aspirin use and a polymorphism in the ornithine decarboxylase gene. Proceedings of the National Academy of Sciences, 100(13), 7859-7864.

Mauldin, J. P., Zeinali, I., Kleypas, K., Woo, J. H., Blackwood, R. S., Jo, C.-H., Frankel, A. E. (2012). Recombinant Human Arginase Toxicity in Mice Is Reduced by Citrulline Supplementation. Translational Oncology, 5(1), 26–31.

McAlpine, J. A., Lu, H.-T., Wu, K. C., Knowles, S. K., & Thomson, J. A. (2014). Down-regulation of argininosuccinate synthetase is associated with cisplatin resistance in hepatocellular carcinoma cell lines: implications for PEGylated arginine deiminase combination therapy. BMC Cancer, 14, 621.

McCormick, F., & Tetsu, O. (1999). Beta-Catenin regulates expression of cyclin D1 in colon carcinoma cells. Nature, 398(6726), 422–426.

Meek, D. W. (2004). The p53 response to DNA damage. DNA Repair,3(8-9), 1049-1056.

Mercer, K., Giblett, S., Green, S., Lloyd, D., Dias, S. D., Plumb, M., . . . Pritchard, C. (2005). Expression of Endogenous OncogenicV600EB-rafInduces Proliferation and Developmental Defects in Mice and Transformation of Primary Fibroblasts. Cancer Research,65(24), 11493-11500.

Messerini L, Mori S, Zampi G. 1996. Pathologic features of hereditary non-polyposis colorectal cancer. Tumorigenesis; 82:114–16.

Meyskens FL Jr., McLaren CE, Pelot D, Fujikawa - Brooks' S, Carpenter PM, Hawk E, Kelloff G, Lawson MJ, Kidao J, McCracken J, (2008). Difluoromethylornithine plus sulindac for the prevention of sporadic colorectal adenomas: a randomized placebo-controlled, double-blind trial. Cancer Prevention Research; 1:32–8.

Minamoto T, Sawaguchi K, Mai M, Yamashita N, Sugimura T, Esumi H, (1994). Infrequent K-Ras activation in superficial-type (flat) colorectal adenomas and adenocarcinomas. Cancer Research; 54:2841–4.

Miraki-moud, F., Ghazaly, E., Ariza-mcnaughton, L., Hodby, K. A., Clear, A., Anjos-afonso, F., … Taussig, D. C. (2015). Arginine deprivation using PEGylated arginine deiminase has activity against primary acute myeloid leukemia cells in vivo, 125(26), 4060–4069.

Miyazaki, H. Takaku, M. Umeda, T. Fujita,W.D. Huang, T. Kimura, (1990). Potent growth inhibition of human tumor cells in culture by arginine deiminase purified from a culture medium of a Mycoplasma-infected cell line, Cancer Research; 50: 4522–4527.

Mizushima, N. (2007). Autophagy: Process and function. Genes & Development,21(22), 2861-2873.

Mizushima, N., Yoshimori, T. & Ohsumi, Y. (2011). The role of Atg proteins in autophagosome formation. Annual Review of Cell and Developmental Biology; 27, 107–132.

Montagut C, Settleman J. (2009). Targeting the RAF–MEK–ERK pathway in cancer therapy. Cancer Letters; 283:125–34.

Morris Jr., (2004). Enzymes of arginine metabolism, Journal of Nutrition; 134: 2743S– 2747S.

Morris SM Jr. (1999). Arginine synthesis, metabolism, and transport: Regulators of nitric oxide synthesis. In: Laskin JD, Laskin DL, editors. Cellular and Molecular Biology of Nitric Oxide. New York: Marcel Dekker, p. 57–85.

Muleris M, Salmon RJ, Dutrillaux B. (1990). Cytogenetics of colorectal adenocarcinomas. Cancer Genetics and Cytogenetics. 46:143–56.

Muleris M, Salmon RJ, Zafrani B, Girodet J, Dutrillaux B. (1985). Consistent deficiencies of chromosome 18 and of the short arm of chromosome 17 in eleven cases of human large bowel cancer: a possible recessive determinism. Annual review of Genetics; 28:206–13.

Muñoz-Pinedo, C., El Mjiyad, N., & Ricci, J.-E. (2012). Cancer metabolism: current perspectives and future directions. Cell Death & Disease, 3, e248.

Nagasaka T, Rhees J, Kloor M, Gebert J, Naomoto Y, Boland CR, (2010). Somatic hypermethylation of MSH2 is a frequent event in Lynch syndrome colorectal cancers. Cancer Research; 70(8):3098–108.

Neuzillet C, Hammel P, Tijeras-Raballand A, Couvelard A, Raymond E. (2013). Targeting the Ras–ERK pathway in pancreatic adenocarcinoma. Cancer Metastasis Reviews; 32:147–62.

Newsholme, E. A., Crabtree, B. & Ardawi, M. S. (1985). The role of high rates of glycolysis and glutamine utilization in rapidly dividing cells. Bioscience Reports; 5: 393–400.

Nicholson, D. W., & Thornberry, N. A. (1997). Caspases: Killer proteases. Trends in Biochemical Sciences,22(8), 299-306.

Nojima, H., Tokunaga, C., Eguchi, S., Oshiro, N., Hidayat, S., Yoshino, K., Hara, K., Tanaka, N., Avruch, J., and Yonezawa, K. (2003). The mammalian target of rapamycin (mTOR) partner, raptor, binds the mTOR substrates p70 S6 kinase and 4E-BP1 through their TOR signaling (TOS) motif. J. Biol. Chem. 278, 15461–15464.

Nordgaard, I., Hansen, B. S., & Mortensen, P. B. (1998). Importance of colonic support for energy absorption as small-bowel failure proceeds. The American Journal of Clinical Nutrition,64(2), 222-231.

Ocvirk J, Brodowicz T, Wrba F, (2010). Cetuximab plus FOLFOX6 or FOLFIRI in metastatic colorectal cancer: CECOG trial. World Journal of Gastroenterology; 16(25):3133-3143.

Ott, R.D. Carvajal, N. Pandit-Taskar, A.A. Jungbluth, E.W. Hoffman, B.W.Wu, (2013). Phase I/II study of PEGylated arginine deiminase (ADI-PEG 20) in patients with advanced melanoma, Investigational New Drugs; 31:425–434.

Overman J, Sara Lonardi, Ka Yeung Mark Wong, Heinz-Josef Lenz, Fabio Gelsomino, Massimo Aglietta, Michael A. Morse, Eric Van Cutsem, Ray McDermott, Andrew Hill, Michael B. Sawyer, Alain Hendlisz, Bart Neyns, Magali Svrcek, Rebecca A. Moss, Jean-Marie Ledeine, Z. Alexander Cao, Shital Kamble, Scott Kopetz, and Thierry André, (2018). Durable Clinical Benefit with Nivolumab Plus Ipilimumab in DNA Mismatch Repair Deficient/Microsatellite Instability–High Metastatic Colorectal Cancer Journal of Clinical Oncology 36:8, 773-779.

Pancione M, Remo A, Colantuoni V. (2012). Genetic and epigenetic events generate multiple pathways in colorectal cancer progression. Pathology Research International; 2012:509348.

Parsons, R., Li, G., Longley, M. J., Fang, W., Papadopoulos, N., Jen, J., . . . Modrich, P. (1993). Hypermutability and mismatch repair deficiency in RER tumor cells. Cell,75(6), 1227-1236.

Patai, Á. V., Molnár, B., Tulassay, Z., & Sipos, F. (2013). Serrated pathway: Alternative route to colorectal cancer. World Journal of Gastroenterology, 19(5), 607–615.

Pearce, L.R., Huang, X., Boudeau, J., Paw1owski, R., Wullschleger, S., Deak, M., Ibrahim, A.F., Gourlay, R., Magnuson, M.A., and Alessi, D.R. (2007). Iden- tification of Protor as a novel Rictor-binding component of mTOR complex-2. Biochem. J. 405, 513–522.

Peltomaki P, Aaltonen LA, Sistonen P, Pylkkanen L, Mecklin JP, (1993). Genetic mapping of a locus predisposing to human colorectal cancer. Science 260:810–12.

Peterson, R. T., & Schreiber, S. L. (1998). Translation control: connecting mitogens and the ribosome. Current Biology : CB, 8(7), R248–R250.

Peterson, T.R., Laplante, M., Thoreen, C.C., Sancak, Y., Kang, S.A., Kuehl, W.M., Gray, N.S., and Sabatini, D.M. (2009). DEPTOR is an mTOR inhibitor frequently overexpressed in multiple myeloma cells and required for their sur- vival. Cell 137, 873–886.

Phillips, M. M., Sheaff, M. T., & Szlosarek, P. W. (2013). Targeting Arginine-Dependent Cancers with Arginine-Degrading Enzymes: Opportunities and Challenges. Cancer Research and Treatment,45(4), 251-262.

Pino, M. S., & Chung, D. C. (2010). The chromosomal instability pathway in colorectal cancer. Gastroenterology, 138(6), 2059–2072.

Polakis, P. (2007). The many ways of Wnt in cancer. Current Opinion in Genetics & Development,17(1), 45-51.

Polakis, P. (2010). An Introduction to Wnt Signaling. Targeting the Wnt Pathway in Cancer,1-18.

Polter, A., Beurel, E., Yang, S., Garner, R., Song, L., Miller, C.A., Sweatt, J.D., McMahon, L., Bartolucci, A.A., Li, X., and Jope, R.S. (2010). Deficiency in the inhibitory serine-phosphorylation of glycogen synthase kinase-3 increases sensitivity to mood disturbances. Neuropsychopharmacology 35, 1761–1774.

Pompili, L., Porru, M., Caruso, C., Biroccio, A., & Leonetti, C. (2016). Patient-derived xenografts: a relevant preclinical model for drug development. Journal of Experimental & Clinical Cancer Research : CR, 35, 189.

Potter, J. D. (1999). Colorectal Cancer: Molecules and Populations. JNCI Journal of the National Cancer Institute, 91(11), 916-932.

Powell SM, Zilz N, Beazer-Barclay Y, Bryan TM, Hamilton SR, Thibodeau SN,…(1992). APC mutations occur early during colorectal tumorigenesis. Nature.; 359:235–7.

Pretlow, T. P., & Pretlow, T. G. (2005). Mutant KRAS in aberrant crypt foci (ACF): Initiation of colorectal cancer? Biochimica Et Biophysica Acta (BBA) - Reviews on Cancer, 1756(2), 83-96.

Price, T. J., Peeters, M., Kim, T. W., Li, J., Cascinu, S., Ruff, P., . . . Sidhu, R. (2014). Panitumumab versus cetuximab in patients with chemotherapy-refractory wild-type KRAS exon 2 metastatic colorectal cancer (ASPECCT): A randomised, multicentre, open-label, non-inferiority phase 3 study. The Lancet Oncology,15(6), 569-579.

Pylayeva-Gupta Y, Grabocka E, Bar-Sagi D. (2011). RAS oncogenes: weaving a tumorigenic web. Nature Cancer Reviews; 11:761e774.

Qiu, F., Chen, Y., Liu, X., Chu, C., Shen, L., Xu, J., . . . Ann, D. K. (2014). Arginine Starvation Impairs Mitochondrial Respiratory Function in ASS1-Deficient Breast Cancer Cells. Science Signaling, 7(319).

Quesnelle, K. M., Boehm, A. L. and Grandis, J. R. (2007), STAT-mediated EGFR signalling in cancer. Journal of Cellular Biochemistry. 102: 311-319.

Rabinovich, S., Adler, L., Yizhak, K., Sarver, A., Silberman, A., Agron, S., Erez, A. (2015). Diversion of aspartate in ASS1-deficient tumours fosters de novo pyrimidine synthesis. Nature, 527(7578).

Ramjaun AR, Downward J. (2007). Ras and phosphoinositide 3-kinase: partners in development and Tumorigenesis. Cell Cycle; 6: 2902–2905.

Randerath, K., Tseng, W. C., Harris, J. S. & Lu, L. J. (1983) Specific effects of 5-fluoropyrimidines and 5-azapyrimidines on modification of the 5 position of pyrimidines, in particular the synthesis of 5-methyluracil and 5-methylcytosine in nucleic acids. Recent Results Cancer Research. 84, 283–297.

Raponi, M., Winkler, H., & Dracopoli, N. C. (2008). KRAS mutations predict response to EGFR inhibitors. Current Opinion in Pharmacology, 8(4), 413–418.

Rathmell JC, Fox CJ, Plas DR, Hammerman PS, Cinalli RM, Thompson CB, (2003). Akt-Directed Glucose Metabolism Can Prevent Bax Conformation Change and Promote Growth Factor-Independent Survival. Molecular and Cellular Biology; 23: 7315–7328.

Rebsamen, M., Pochini, L., Stasyk, T., de Araujo, M.E., Galluccio, M., Kandas- amy, R.K., Snijder, B., Fauster, A., Rudashevskaya, E.L., Bruckner, M., (2015). SLC38A9 is a component of the lysosomal amino acid sensing machin- ery that controls mTORC1. Nature 519, 477–481.

Rego RL, Foster NR, Smyrk TC, (2010). Prognostic effect of activated EGFR expression in human colon carcinomas: comparison with EGFR status. British Journal of Cancer; 102:165–172.

Resnick MB, Routhier J, Konkin T, Sabo E, Pricolo VE (2004). Epidermal growth factor receptor, c-MET, beta-catenin, and p53 expression as prognostic indicators in stage II colon cancer: a tissue microarray study. Clinical Cancer Research; 10:3069–3075.

Rho, J., Qin, S., Wang, J. Y., & Roehrl, M. H. (2008). Proteomic Expression Analysis of Surgical Human Colorectal Cancer Tissues: Up-Regulation of PSB7, PRDX1, and SRP9 and Hypoxic Adaptation in Cancer. Journal of Proteome Research; 7(7), 2959-2972.

Robey RB, Hay N. (2006). Mitochondrial hexokinases, novel mediators of the antiapoptotic effects of growth factors and Akt. Oncogene; 25: 4683– 4696.

Robitaille, A.M., Christen, S., Shimobayashi, M., Cornu, M., Fava, L.L., Moes, S., Prescianotto-Baschong, C., Sauer, U., Jenoe, P., and Hall, M.N. (2013). Quantitative phosphoproteomics reveal mTORC1 activates de novo pyrimi- dine synthesis. Science 339, 1320–1323.

Roczniak-Ferguson, A., Petit, C.S., Froehlich, F., Qian, S., Ky, J., Angarola, B., Walther, T.C., and Ferguson, S.M. (2012). The transcription factor TFEB links mTORC1 signalling to transcriptional control of lysosome homeostasis. Science. Signalling. 5, ra42.

Rombeau JL. (2003). Re-thinking the human colon: a dynamic metabolic organ. Contemporary Surgery; 59:450–452.

Rombeau JL., (2003). Re-thinking the human colon: a dynamic metabolic organ. Contemporary Surgery; 59:450–2.

Rustgi, A. K. (2007). The genetics of hereditary colon cancer. Genes & Development,21(20), 2525-2538.

Saltz LB, Clarke S, Diaz-Rubio E, (2008). Bevacizumab in combination with Oxaliplatin-based chemotherapy as first-line therapy in metastatic colorectal cancer: a randomized phase III study. Journal of Clinical Oncology; 26: 2013–2019.

Samuels Y, Wang Z, Bardelli A, Silliman N, Ptak J, (2004). High frequency of mutations of the PIK3CA gene in human cancers. Science 304:554.

Sancak, Y., Bar-Peled, L., Zoncu, R., Markhard, A.L., Nada, S., and Sabatini, D.M. (2010). Ragulator-Rag complex targets mTORC1 to the lysosomal surface and is necessary for its activation by amino acids. Cell 141, 290–303.

Santi, D. V. & Hardy, L. W. (1987). Catalytic mechanism and inhibition of tRNA (uracil-5) methyltransferase: evidence for covalent catalysis. Biochemistry 26, 8599–8606.

Santi, D. V., McHenry, C. S. & Sommer, H. (1974). Mechanism of interaction of thymidylate synthetase with 5-fluorodeoxyuridylate. Biochemistry 13, 471–481.

Satoh, Masahiko S., and Tomas Lindahl. (1992) "Role of Poly(ADP-Ribose) Formation in DNA Repair." Nature, vol. 356, no. 6367, p. 356.,

Saxton, R. A., & Sabatini, D. M. (2017). mTOR signalling in Growth, Metabolism, and Disease. Cell, 168(6), 960–976.

Saxton, R.A., Chantranupong, L., Knockenhauer, K.E., Schwartz, T.U., and Sabatini, D.M. (2016b). Mechanism of arginine sensing by CASTOR1 upstream of mTORC1. Nature 536, 229–233.

Scaltriti, M., & Baselga, J. (2006). The Epidermal Growth Factor Receptor Pathway: A Model for Targeted Therapy. Clinical Cancer Research,12(18), 5268-5272.

Schepers, A., & Clevers, H. (2012). Wnt Signaling, Stem Cells, and Cancer of the Gastrointestinal Tract. Cold Spring Harbor Perspectives in Biology,4(4).

Schlessinger J. (2000). Cell signalling by receptor tyrosine kinases. Cell; 103:211–25.

Sears, R., Nuckolls, F., Haura, E., Taya, Y., Tamai, K., and Nevins, J.R. (2000). Multiple Ras-dependent phosphorylation pathways regulate Myc protein stability. Genes and Development. 14, 2501–2514.

Secreto., L.H., H., & J.J., W. (2009). Wnt signaling during fracture repair. Current Osteoporosis Reports, 7(2), 64–69.

Semrin, M.G., et al., 2010. Anatomy, Histology, Embryology, and Developmental Anomalies of the Stomach and Duodenum, in Sleisenger and Fordtran's Gastrointestinal and Liver Disease (9th edition), Saunders, Philadelphia, U.S.A. . p. 773-785.

Seshagiri, S., Stawiski, E. W., Durinck, S., Modrusan, Z., Storm, E. E., Conboy, C. B., … de Sauvage, F. J. (2012). Recurrent R-spondin fusions in colon cancer. Nature, 488(7413), 660–664.

Settembre, C., Zoncu, R., Medina, D.L., Vetrini, F., Erdin, S., Erdin, S., Huynh, T., Ferron, M., Karsenty, G., Vellard, M.C., et al. (2012). A lysosome-to-nucleus signalling mechanism senses and regulates the lysosome via mTOR and TFEB. EMBO J. 31, 1095–1108.

Shen, L., (2009). Functional morphology of the gastrointestinal tract. Current Topics in Microbiology and Immunology; 337: p. 1-35.

Shen, W., Zhang, X., Fu, X., Fan, J., Luan, J., Cao, Z., . . . Ju, D. (2017). A novel and promising therapeutic approach for NSCLC: Recombinant human arginase alone or combined with autophagy inhibitor. Cell Death & Disease, 8(3).

Shinya, H., & Wolff, W. I. (1979). Morphology, anatomic distribution and cancer potential of colonic polyps. Annals of Surgery, 190(6), 679–683.

Shtutman, M., Zhurinsky, J., Simcha, I., Albanese, C., D'Amico, M., Pestell, R., & Ben-Ze'ev, A. (1999). The cyclin D1 gene is a target of the beta-catenin/LEF-1 pathway. Proceedings of the National Academy of Sciences, 96(10), 5522–5527.

Siani, L. M., & Pulica, C. (2014). Laparoscopic Complete Mesocolic Excision with Central Vascular Ligation in right colon cancer: Long-term oncologic outcome between mesocolic and non-mesocolic planes of surgery. Scandinavian Journal of Surgery,104(4), 219-226.

Siegel, R. L., Miller, K. D., Fedewa, S. A., Ahnen, D. J., Meester, R. G., Barzi, A., & Jemal, A. (2017). Colorectal cancer statistics, 2017. CA: A Cancer Journal for Clinicians,67(3), 177-193.

Sjoblom, T. (2006).The consensus coding sequences of human breast and colorectal cancers. Science; 314, 268–274.

Slattery JL. (2000). Diet, lifestyle, and colon cancer. Seminars in Gastrointestinal Disease. 11:1142–46.

Sommer, H., & Santi, D. V. (1974). Purification and amino acid analysis of an active site peptide from thymidylate synthetase containing covalently bound 5-fluoro-2'-deoxyuridylate and methylenetetrahydrofolate. Biochemical and Biophysical Research Communications,57(3), 689-695.

Sood R, Porter AC, Olsen DA, (2000). A mammalian homologue of GCN2 protein kinase important for translational control by phosphorylation of eukaryotic initiation factor-2a. Genetics; 154: 787–801.

Souglakos, J., Philips, J., Wang, R., et al., (2009). Prognostic and predictive value of common mutations for treatment response and survival in patients with metastatic colorectal cancer. British Journal of Cancer 101, 465–472.

Spring, K. J., Zhao, Z. Z., Karamatic, R., Walsh, M. D., Whitehall, V. L., Pike, T., . . . Leggett, B. A. (2006). High Prevalence of Sessile Serrated Adenomas With BRAF Mutations: A Prospective Study of Patients Undergoing Colonoscopy. Gastroenterology,131(5), 1400-1407.

Stelter L, Fuchs S, Jungbluth AA, (2013). Evaluation of Arginine Deiminase Treatment in Melanoma Xenografts Using 18F-FLT PET. Molecular imaging and biology.;15(6):768-775.

Stephen AG, Esposito D, Bagni RK, (2014). Dragging Ras Back in the Ring. Cancer Cell.;25:272–81.

Stryker SJ, WolffBG, Culp CE,Libbe SD, Ilstrup DM,MacCartyRL. (1987). Natural history of untreated colonic polyps. Gastroenterology 93:1009–13

Su TS, Bock HG, O'Brien WE, Beaudet AL. (1981). Cloning of cDNA for argininosuccinate synthetase mRNA and study of enzyme overproduction in a human cell line. Journal of Biological Chemistry; 256:11826 31.

Syed, N., Langer, J., Janczar, K., Singh, P., Nigro, C. L., Lattanzio, L., . . . Crook, T. (2013). Epigenetic status of argininosuccinate synthetase and argininosuccinate lyase modulates autophagy and cell death in glioblastoma. Cell Death & Disease, 4: e458.

Sylvia Packham, Yingbo Lin, Zhiwei Zhao, Dudi Warsito, Dorothea Rutishauser, and Olle Larsson (2015) The Nucleus-Localized Epidermal Growth Factor Receptor Is SUMOylated Biochemistry 54 (33), 5157-5166

Szlosarek, P. W., Luong, P., Phillips, M. M., Baccarini, M., Ellis, S., Szyszko, T., . . . Avril, N. (2013). Metabolic Response to Pegylated Arginine Deiminase in Mesothelioma With Promoter Methylation of Argininosuccinate Synthetase. Journal of Clinical Oncology,31(7).

Szmulowicz, U. M., & Hull, T. L. (2016). The ASCRS Textbook of Colon and Rectal Surgery.

T.L. Lam, G.K. Wong, H.Y. Chow, H.C. Chong, T.L. Chow, S.Y. Kwok, (2011). Recombinant human arginase inhibits the in vitro and in vivo proliferation of human melanoma by inducing cell cycle arrest and apoptosis, Pigment Cell Melanoma Research. 24 366–376.

Takaku, H., Takase, M., Abe, S., Hayashi, H., & Miyazaki, K. (1992). In vivo anti-tumor activity of arginine deiminase purified from Mycoplasma arginini. International Journal of Cancer,51(2), 244-249.

Takayama T, Miyanishi K, Hayashi T, Sato Y, Niitsu Y. (2006). Colorectal cancer: genetics of development and metastasis. Journal of Gastroenteroly; 41: 185-192.

Tarcic, G., Boguslavsky, S. K., Wakim, J., Kiuchi, T., Liu, A., Reinitz, F., . . . Yarden, Y. (2009). An Unbiased Screen Identifies DEP-1 Tumor Suppressor as a Phosphatase Controlling EGFR Endocytosis. Current Biology,19(21), 1788-1798. doi:10.1016/j.cub.2009.09.048

Tatum, J. L. (2006). Hypoxia: Importance in tumor biology, non-invasive measurement by imaging, and value of its measurement in the management of cancer therapy. International Journal of Radiation Biology, 82(10), 699-757.

Thibodeau SN, BrenG, Schaid D. (1993). Microsatellite instability in cancer of the proximal colon. Science 260:816–19

Thirlwell, C., Will, O. C. C., Domingo, E., Graham, T. A., McDonald, S. A. C., Oukrif, D., … Leedham, S. J. (2010). Clonality Assessment and Clonal Ordering of Individual Neoplastic Crypts Shows Polyclonality of Colorectal Adenomas. Gastroenterology, 138(4), 1441–1454.

Thomas, D. C., Umar, A., & Kunkel, T. A. (1996). Microsatellite instability and mismatch repair defects in cancer cells. Mutation Research/Fundamental and Molecular Mechanisms of Mutagenesis, 350(1), 201–205.

Thomas, L. R., & Tansey, W. P. (2011). Proteolytic Control of the Oncoprotein Transcription Factor Myc. Advances in Cancer Research,77-106.

Thoreen, C.C., Chantranupong, L., Keys, H.R., Wang, T., Gray, N.S., and Sa-batini, D.M. (2012). A unifying model for mTORC1-mediated regulation of mRNA translation. Nature 485, 109–113.

Todd RC, Lippard SJ. (2009). Inhibition of transcription by platinum antitumor compounds. Metallomics; 1(4):280-291.

Torlakovic, E. E., Gomez, J. D., Driman, D. K., Parfitt, J. R., Wang, C., Benerjee, T., & Snover, D. C. (2008). Sessile Serrated Adenoma (SSA) vs. Traditional Serrated Adenoma (TSA). The American Journal of Surgical Pathology, 32(1), 21-29.

Toyota M, Ahuja N, Ohe-Toyota M, Herman JG, Baylin SB, Issa JP. (1999). CpG island methylator phenotype in colorectal cancer. PNAS; 96: 8681–8686.

Tsai WB, Aiba I, Long Y, Lin HK, Feun L, Savaraj N. (2012). Activation of Ras/PI3K/ERK pathway induces c-Myc stabilization to upregulate argininosuccinate synthetase, leading to arginine deiminase resistance in melanoma cells. Cancer Research; 72(10):2622-33.

Tsai, W., Aiba, I., Lee, S., Feun, L., Savaraj, N., & Kuo, M. T. (2009). Resistance to arginine deiminase treatment in melanoma cells is associated with induced argininosuccinate synthetase expression involving c-Myc/HIF-1 /Sp4. Molecular Cancer Therapeutics,8(12), 3223-3233.

Tsui, S., Lam, W., Lam, T., Chong, H., So, P., Kwok, S., Leung, Y. (2009). PEGylated derivatives of recombinant human arginase (rhArg1) for sustained in vivo activity in cancer therapy: Preparation, characterization and analysis of their pharmacodynamics in vivo and in vitro and action upon hepatocellular carcinoma cell (HCC). Cancer Cell International,9(1), 9.

Turnbull RB Jr. (1975). The "no touch" isolation technic of resection. JAMA; 231:1181-1182.

Umetani, N., Sasaki, S., Masaki, T., Watanabe, T., Matsuda, K., & Muto, T. (2000). Involvement of APC and K-ras mutation in non-polypoid colorectal tumorigenesis. British Journal of Cancer, 82(1), 9-15.

Vander Heiden, M. G. (2011). Targeting cancer metabolism: a therapeutic window opens. Nature Reviews. Drug Discovery, 10(9), 671–684.

Vander Heiden, M. G., Cantley, L. C. & Thompson, C. B. (2009). Understanding the Warburg effect: the metabolic requirements of cell proliferation. Science 324, 1029–1033

Vargas AJ, Wertheim BC, Gerner EW, Thomson CA, Rock CL, Thompson PA. (2012). Dietary polyamine intake and risk of colorectal adenomatous polyps. American Journal of Clinical Nutrition; 96:133–41.

Vilar E, Gruber SB. (2010). Microsatellite instability in colorectal cancer—the stable evidence. Nature Reviews Clinical Oncology; 7:153–62.

Vogelstein B, Fearon ER, Hamilton SR, Kern SE, Preisinger AC, Leppert M, Nakamura Y, White R, Smits AM, Bos JL. (1988). Genetic alterations during colorectal-tumor development. The New England Journal of Medicine; 319:525–532.

Vogelstein, B., Papadopoulos, N., Velculescu, V. E., Zhou, S., Diaz, L. A., & Kinzler, K. W. (2013). Cancer Genome Landscapes. Science (New York, N.Y.), 339(6127), 1546–1558.

Wang, S., Tsun, Z.Y., Wolfson, R.L., Shen, K., Wyant, G.A., Plovanich, M.E., Yuan, E.D., Jones, T.D., Chantranupong, L., Comb, W., et al. (2015). Metabolism. Lysosomal amino acid transporter SLC38A9 signals arginine sufficiency to mTORC1. Science 347, 188–194.

Wang, Z., Shi, X., Li, Y., Zeng, X., Fan, J., Sun, Y., . . . Ju, D. (2013). Involvement of autophagy in recombinant human arginase-induced cell apoptosis and growth inhibition of malignant melanoma cells. Applied Microbiology and Biotechnology, 98(6), 2485-2494.

Warburg O. (1930). Notiz uber den Stoffwechsel der Tumoren. Biochemish Zeitschr; 228(1/3):257

Warburg O. (1956). On the origin of cancer cells. Science; 123:309–14.

Weisenberger, D. J., Siegmund, K. D., Campan, M., Young, J., Long, T. I., Faasse, M. A., . . . Laird, P. W. (2006). CpG island methylator phenotype underlies sporadic microsatellite instability and is tightly associated with BRAF mutation in colorectal cancer. Nature Genetics, 38(7), 787-793.

Welch, H. G., & Robertson, D. J. (2016). Colorectal Cancer on the Decline — Why Screening Can't Explain It All. New England Journal of Medicine; 374(17), 1605-1607.

Welcker, M., Orian, A., Jin, J., Grim, J.E., Harper, J.W., Eisenman, R.N., and Clurman, B.E. (2004). The Fbw7 tumor suppressor regulates glycogen synthase kinase 3 phosphorylation-dependent c-Myc protein degradation. PNAS; 101, 9085–9090.

Whibley C, Pharoah PDP, Hollstein M. (2009). p53 polymorphisms: cancer implications. Nature Reviews Cancer; 9: 95–107.

White BD, Chien AJ, Dawson DW. (2012). Dysregulation of Wnt/β-catenin signalling in gastrointestinal cancers. Gastroenterology; 142:219–32.

White RL. (1998). Tumor suppressing pathways. Cell; 92:591–2.

Williams, C., Hoppe, H., Rezgui, D., Strickland, M., Forbes, B. E., Grutzner, F., . . . Hassan, A. B. (2012). An Exon Splice Enhancer Primes IGF2:IGF2R Binding Site Structure and Function Evolution. Science; 338(6111), 1209-1213.

Wolfson, R. L., Chantranupong, L., Wyant, G. A., Gu, X., Orozco, J. M., Shen, K., . . . Sabatini, D. M. (2017). KICSTOR recruits GATOR1 to the lysosome and is necessary for nutrients to regulate mTORC1. Nature; 543(7645), 438-442.

Woo, S.Y., Kim, D.H., Jun, C.B., Kim, Y.M., Haar, E.V., Lee, S.I., Hegg, J.W., Bandhakavi, S., Griffin, T.J., and Kim, D.H. (2007). PRR5, a novel component of mTOR complex 2, regulates platelet-derived growth factor receptor beta expression and signaling. J. Biol. Chem. 282, 25604–25612.

Wood LD, Parsons DW, Jones S, Lin J, Sjoblom T,… (2007). The genomic landscapes of human breast and colorectal cancers. Science; 318:1108–13

Xu, S., Lam, S., Cheng, P. N., & Ho, J. C. (2018). Recombinant human arginase induces apoptosis via oxidative stress and cell cycle arrest in small cell lung cancer. Cancer Science.

Y. Ni, U. Schwaneberg, Z.H. Sun, (2008). Arginine deiminase, a potential anti-tumor drug, Cancer Letters. 261 1–11.

Yada M, Hatakeyama S, Kamura T, (2004). Phosphorylation-dependent degradation of c-Myc is mediated by the F-box protein Fbw7. EMBO Journal; 23:2116–25.

Yamagishi, H., Kuroda, H., Imai, Y., & Hiraishi, H. (2016). Molecular pathogenesis of sporadic colorectal cancers. Chinese Journal of Cancer; 35(1).

Yang, H., Rudge, D.G., Koos, J.D., Vaidialingam, B., Yang, H.J., and Pavletich, N.P. (2013). mTOR kinase structure, mechanism and regulation. Nature 497, 217–223.

Yang, J. (2008). Effect of ERK on tumorigenesis and on inhibition of FOXO3a via MDM2-mediated degradation. Journal of Clinical Oncology; 26 11101-11101.

Yang, Q., Inoki, K., Ikenoue, T., and Guan, K.L. (2006). Identification of Sin1 as an essential TORC2 component required for complex formation and kinase activity. Genes Dev. 20, 2820–2832.

Yang, T., Lu, S., Chao, Y., Sheen, I., Lin, C., Wang, T., . . . Chen, L. (2010). A randomised phase II study of PEGylated arginine deiminase (ADI-PEG 20) in Asian advanced hepatocellular carcinoma patients. British Journal of Cancer; 103(7), 954-960.

Yang, Y. (2002). Activation of Fatty Acid Synthesis during Neoplastic Transformation: Role of Mitogen-Activated Protein Kinase and Phosphatidylinositol 3-Kinase. Experimental Cell Research; 279(1), 80-90.

Yau, T., Cheng, P. N., Chan, P., Chen, L., Yuen, J., Pang, R., Poon, R. T. (2015). Preliminary efficacy, safety, pharmacokinetics, pharmacodynamics and quality of life study of PEGylated recombinant human arginase 1 in patients with advanced hepatocellular carcinoma. Investigational New Drugs; 33(2), 496–504.

Yeatman, T. J. (1991). Depletion of Dietary Arginine Inhibits Growth of Metastatic Tumor. Archives of Surgery; 126(11), 1376.

Yerushalmi, H. F., Besselsen, D. G., Ignatenko, N. A., Blohm-Mangone, K. A., Padilla-Torres, J. L., Stringer, D. E., . . . Gerner, E. W. (2006). Role of polyamines in arginine-dependent colon carcinogenesis inApcMin/ mice. Molecular Carcinogenesis; 45(10), 764-773.

You, M., Savaraj, N., Kuo, M. T., Wangpaichitr, M., Varona-Santos, J., Wu, C., . . . Feun, L. (2012). TRAIL induces autophagic protein cleavage through caspase activation in melanoma cell lines under arginine deprivation. Molecular and Cellular Biochemistry; 374(1-2), 181-190.

Zafirellis, K., Zachaki, A., Agrogiannis, G., & Gravani, K. (2010). Inducible nitric oxide synthase expression and its prognostic significance in colorectal cancer. Apmis,118(2), 115-124.

Zhang, D. L., Gu, L. J., Liu, L., Wang, C. Y., Sun, B. S., Li, Z., & Sung, C. K. (2009). Effect of Wnt Signaling pathway on wound healing. Biochemical and Biophysical Research Communications; 378(2), 149–151.

Zhao, Y., Ando, K., Oki, E., Ikawa-Yoshida, A., Ida, S., Kimura, Y., … Maehara, Y. (2014). Aberrations of BUBR1 and TP53 gene mutually associated with chromosomal instability in human colorectal cancer. Anticancer Research, 34(10), 5421–5427.

Zinkin, L. D. (1983). A critical review of the classifications and staging of colorectal cancer. Diseases of the Colon & Rectum,26(1), 37-43.

Zoncu, R., Bar-Peled, L., Efeyan, A., Wang, S., Sancak, Y., and Sabatini, D.M. (2011). mTORC1 senses lysosomal amino acids through an inside-out mechanism that requires the vacuolar H(+)-ATPase. Science; 334, 678–683.

SCIENTIFIC REPORTS

Sensitivity of Colorectal Cancer to Arginine Deprivation Therapy is Shaped by Differential Expression of Urea Cycle Enzymes

Constantinos Alexandrou[1], Saif Sattar Al-Aqbi[1,2], Jennifer A. Higgins[1], William Boyle[3], Ankur Karmokar[1], Catherine Andreadi[1], Jin-Li Luo[1], David A. Moore[4], Maria Viskaduraki[5], Matthew Blades[5], Graeme I. Murray[6], Lynne M. Howells[1], Anne Thomas[1], Karen Brown[1], Paul N. Cheng[7] & Alessandro Rufini[1]

Tumors deficient in the urea cycle enzymes argininosuccinate synthase-1 (ASS1) and ornithine transcarbamylase (OTC) are unable to synthesize arginine and can be targeted using arginine-deprivation therapy. Here, we show that colorectal cancers (CRCs) display negligible expression of OTC and, in subset of cases, ASS1 proteins. CRC cells fail to grow in arginine-free medium and dietary arginine deprivation slows growth of cancer cells implanted into immunocompromised mice. Moreover, we report that clinically-formulated arginine-degrading enzymes are effective anticancer drugs in CRC. Pegylated arginine deiminase (ADI-PEG20), which degrades arginine to citrulline and ammonia, affects growth of ASS1-negative cells, whereas recombinant human arginase-1 (rhArg1peg5000), which degrades arginine into urea and ornithine, is effective against a broad spectrum of OTC-negative CRC cell lines. This reflects the inability of CRC cells to recycle citrulline and ornithine into the urea cycle. Finally, we show that arginase antagonizes chemotherapeutic drugs oxaliplatin and 5-fluorouracil (5-FU), whereas ADI-PEG20 synergizes with oxaliplatin in ASS1-negative cell lines and appears to interact with 5-fluorouracil independently of ASS1 status. Overall, we conclude that CRC is amenable to arginine-deprivation therapy, but we warrant caution when combining arginine deprivation with standard chemotherapy.

Arginine is a semi-essential amino acid in adult mammals that is required for protein synthesis, and is the main substrate for the biosynthesis of nitric oxide, polyamines, proline, creatine, and agmantine[1]. Moreover, arginine, together with leucine, is chiefly responsible for the activation of the mTOR pathway, which in turn stimulates protein translation and other metabolic pathways, such as lipid metabolism and nucleotide biosynthesis[2]. Under physiological conditions, cells satisfy their arginine requirements through direct uptake from the bloodstream and/or through biosynthesis mediated by urea cycle enzymes. Two main enzymes are necessary to produce arginine; ASS1 condensates citrulline and aspartate to form argininosuccinate, which is then converted to arginine and fumarate by argininosuccinate lyase (ASL) (Supplementary Fig. S1)[1].

A variety of cancers display reduced expression of ASS1 and, to a lesser extent, ASL[3,4]. These tumors are unable to synthesize arginine and are therefore auxotrophic, i.e. depending on external supplementation of arginine for their growth and survival. Resolute efforts to harness this metabolic vulnerability have led to the development of arginine deprivation therapies enabled by the availability of arginine degrading enzymes[5]. Two compounds are currently under clinical evaluation in several malignancies: mycoplasma-derived arginine deiminase

[1]Department of Genetics and Genome Biology, Leicester Cancer Research Centre, University of Leicester, Leicester, LE2 7LX, UK. [2]Department of Pathology and Poultry Diseases, Faculty of Veterinary Medicine, University of Kufa, Kufa, Iraq. [3]Birmingham Women's Hospital, Birmingham, B15 2TG, UK. [4]Department of Pathology, UCL Cancer Centre, UCL, London, UK. [5]Bioinformatics and Biostatistics Support Hub, University of Leicester, Leicester, LE1 7RH, UK. [6]Department of Pathology, School of Medicine, Medical Sciences and Nutrition, University of Aberdeen, Foresterhill, Aberdeen, AB25, 2ZD, UK. [7]Bio-Cancer Treatment International Limited, Hong Kong, Hong Kong. Correspondence and requests for materials should be addressed to A.R. (email: ar230@le.ac.uk)

(ADI-PEG20) and human arginase-1 (rhArg1peg5000, BCT-100)[6,7]. ADI-PEG20 degrades arginine into citrulline and ammonia, whereas arginase hydrolyses arginine into urea and ornithine. Cells lacking ASS1 or ASL are incapable of recycling citrulline and ornithine and are therefore susceptible to arginine deprivation.

ASS1 expression is transcriptionally regulated. In some tumors, such as glioblastoma, bladder cancer and hepatocellular carcinoma, methylation of the promoter region of the *ASS1* gene mediates its silencing; alternatively, hypoxia-inducible factor 1α (HIF1α)-mediated repression of the *ASS1* promoter has also been reported in cancers such as melanoma[4,8–15]. Traditionally, ASS1 has been adopted as the predictive biomarker for sensitivity to arginine deprivation therapy[5]. Hence, tumors with low expression of ASS1 have been extensively tested for their response to arginine degrading enzymes, whereas tumors with higher expression of ASS1, including CRC[16], have been deemed ineligible to arginine deprivation therapy. Nonetheless, mounting evidence indicates that modulation of other urea cycle enzymes, such as OTC, can cause arginine auxotrophy and sensitivity to arginine deprivation therapies[4,17–19].

Here, we unmask a striking arginine auxotrophy in CRC. We show that CRC cell lines are unable to proliferate in arginine-free media and their growth *in vivo* is diminished by administration of an arginine-free diet. Mechanistically, we identify a methylation-independent downregulation of the OTC enzyme in CRC. Reduced OTC expression correlates with sensitivity of CRC cell lines to rhArg1peg5000 treatment *in vitro* and *in vivo*, independently of ASS1 expression. Indeed, resistance to arginase treatment necessitates recycling of ornithine into the urea cycle. This event is mediated by the mitochondrial enzyme OTC, which conjugates ornithine and carbaoylphosphate, a compound synthesized by mitochondrial carmaboylphosphate synthase 1 (CPS1), to form citrulline (Supplementary Fig. S1A). Intriguingly, we also describe a subset of CRC specimens and cell lines expressing low levels of ASS1 and responsive to ADI-PEG20 treatment. Finally, using the Chou-Talalay method for drug combination, we report the feasibility of using arginine deprivation therapy in combination with current chemotherapeutic regimens for CRC. Overall, our results reveal that CRC is amenable to treatment with arginine-deprivation therapy.

Results

CRC cell lines display arginine auxotrophy.
To assess whether external arginine supplementation is necessary to sustain CRC growth, we cultured CRC cell lines in arginine-free medium or in a control medium containing all amino acids. Notably, all cell lines tested failed to grow in the absence of arginine (Fig. 1A), indicating auxotrophy. The halted growth was accompanied by an arrest of DNA replication (Fig. 1B and C) and decreased expression of the cell cycle marker Cyclin D1 (Fig. 1D), and was reverted upon arginine repletion (Supplementary Fig. S1B). Consistent with the role of arginine in regulating mTOR signaling, we observed decreased mTOR activity, as indicated by the loss of the higher molecular weights rapamycin-sensitive phosphosites of the 4E-BP1 protein[20] (Supplementary Fig. S2).

To investigate whether the identified arginine addiction prevails *in vivo*, HCT116 cells where subcutaneously injected in immunocompromised athymic nude mice. After injection, mice were randomized to an arginine-free diet or a control diet (0.83% arginine) and tumor growth measured by calipers. Nutritional deprivation of arginine was effective in slowing tumor growth, as demonstrated by diminished tumor volume and weight (Fig. 1E and F and Supplementary Fig. S3). Notably, dietary arginine deprivation did not affect animal body weight during the 35-day duration of the experiment (Fig. 1G). Overall, these findings identify arginine auxotrophy as a metabolic vulnerability in CRC.

Downregulation of OTC and ASS1 expression in CRC.
To investigate the mechanism responsible for the arginine dependence of CRC, we scored a TMA cohort, consisting of over 600 cases of CRC (Supplementary Table S1), for expression of OTC and ASS1 proteins. OTC expression was low or absent in virtually all cases. Interestingly, we also identified a subset of CRC patients (~18%) that expressed low or undetectable ASS1 levels (Fig. 2A and B, Supplementary Fig. S4).

Low expression of OTC and ASS1 was then confirmed by assessment of protein levels in a panel of CRC cells lines (Fig. 2C). No cell line showed evidence of OTC expression, which was promptly detected in control human liver. With regard to ASS1, its expression pattern in cell lines mirrored the heterogeneity observed in TMA; SW480 cells showed sustained expression of the enzyme, HCT116 cells expressed ASS1 moderately, whereas the expression of the enzyme was absent in HT29 and RKO cell lines. Finally, we analyzed gene expression datasets using the online platforms CancerMA and Oncomine[21,22] and we confirmed downregulation of the *OTC* gene expression in colorectal tumors (Supplementary Fig. S5).

CpG island methylator phenotype (CIMP), which causes epigenetic gene silencing through methylation of cytosine residues at CpG-rich DNA sequences, contributes to the progression of CRC[23]. Both RKO and HT29 cells are CIMP positive[24]. Hence, in the light of the reported role of promoter methylation in mediating silencing of the genes coding for the urea cycle enzymes, we investigated whether reversion of DNA methylation with the DNA methylase inhibitor 5-azacytidine (5-AZA) could rescue expression of ASS1 and OTC. Our results indicate that ASS1 suppression in RKO is indeed methylation-dependent, whereas CIMP is unlikely to mediate the loss of ASS1 in HT29. On the other hand, 5-AZA treatment did not rescue OTC expression in any of the cell line analyzed, suggesting that the regulation of *OTC* gene is not regulated through promoter methylation (Fig. 2C).

CRC cell lines are sensitive to arginine deprivation by rhArg1peg5000.
Prompted by the marked arginine addiction of CRC cell lines and the impaired expression of urea cycle enzymes in cancer patients, we tested the feasibility of targeting CRC using pharmacological arginine deprivation. Because of the prevalent loss of OTC expression, we investigated whether depletion of arginine using rhArg1peg5000 could affect CRC cell growth. We found that all cell lines tested, independently of ASS1 expression, showed a robust, dose-dependent decrease in cell number upon rhArg1peg5000 treatment, with IC50 concentrations lower than 0.1 μg/ml (Fig. 3A).
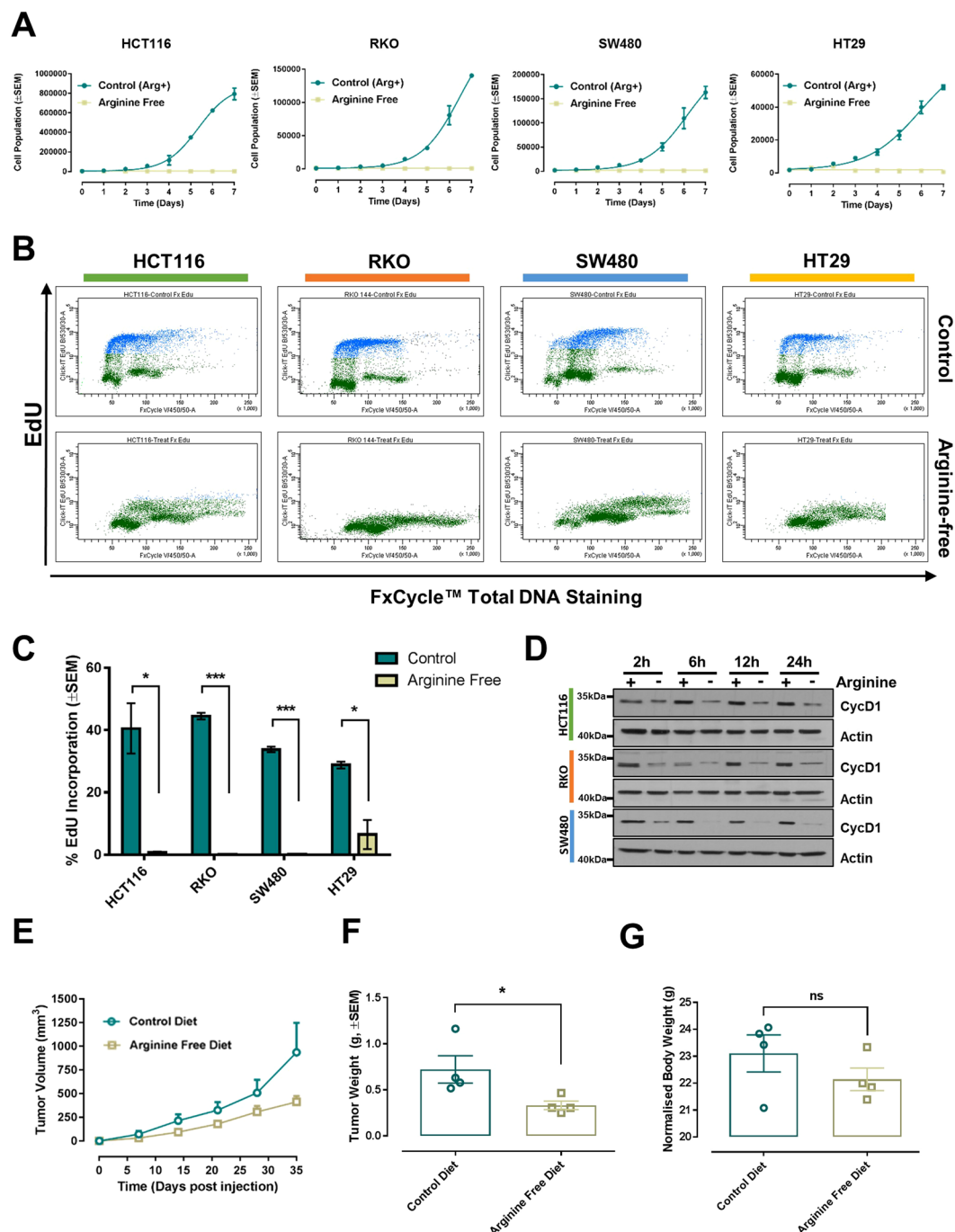
Figure 1. Arginine auxotrophy in CRC. (**A**) Growth curves of the indicated cell lines with or without arginine supplementation. Data are presented as mean ± SEM of three independent experiments. (**B**) Representative flow cytometry scatterplots of EdU incorporation in HCT116, RKO, HT29 and SW480 CRC cell lines grown in control medium or arginine-free medium for 24 h. EdU was measured using the Click-iT® EdU Alexa Fluor® kit and total DNA stained using FxCycle™ Violet Stain. (**C**) Quantification of EdU incorporation from three independent experiments. Data are presented as mean ± SEM, two-tailed t-test. *P < 0.05, ***P < 0.001. (**D**) Western blot analysis of Cyclin D1 (CycD1) protein expression in HCT116, RKO and SW480 CRC cell lines following arginine deprivation for the indicated times. Actin was used as endogenous loading control. Original western blots are reported in Supplementary Fig. S15. (**E**) Graph showing the growth of xenografted HCT116 cells in immunocompromised mice fed a control diet or an arginine-free diet. Data are plotted as mean ± SEM and were analyzed using mixed linear regression analysis (P = 0.03; P < 0.05 indicates a statistically significant difference in tumor growth rate between control and treated animals over time). (**F**) Weight of excised tumor measured at endpoint. Data are plotted as mean ± SEM. *P < 0.05, two-tailed t-test (n = 4 animal per group). (**G**) Animal body weights at endpoint plotted as mean ± SEM. No statistical differences were detected between the two diet groups, two-tailed t-test (n = 4 animals per group).
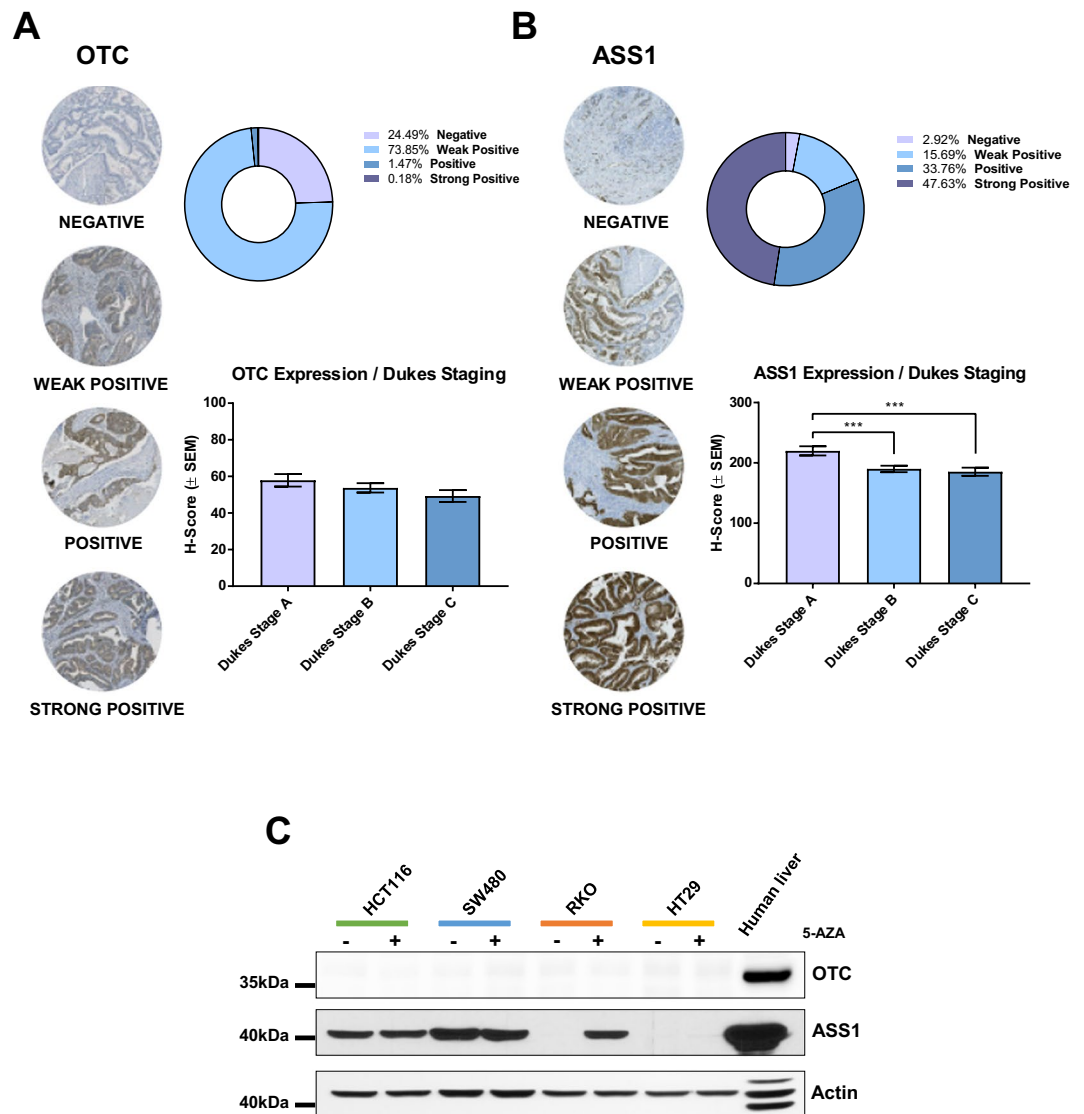
Figure 2. Reduced expression of OTC and ASS1 in CRC. (**A**) OTC and (**B**) ASS1 H-score were assessed on CRC TMA. Representative histo-spots are shown on the left. The bar graphs indicate H-score distribution according to Duke's stage, whereas the distribution of protein expression within the whole TMA cohort is reported in the pie chart. *P < 0.05 (**C**) Western blot analysis of OTC and ASS1 after 72 h treatment with 5 μM 5-Azacytidine (5-AZA). Human liver extract was used as positive control for urea cycle enzymes, actin was used as endogenous loading control. Original western blots are reported in Supplementary Fig. S15.

To explore the mechanism responsible for the observed growth reduction, we measured cellular proliferation using the EdU incorporation assay and found that arginine depletion led to a sharp decrease in DNA synthesis (Fig. 3B and C), indicative of proliferative arrest. In agreement with this result, arginine-deprived cells displayed reduced expression of the cell cycle markers Cyclin D3 and Cyclin D1 (Fig. 3D and E). Notably, rhArg1peg5000 treatment elicited expression of ASS1 in HCT116, RKO and HT29 (Supplementary Fig. S6). ASS1 expression also correlated with enhanced c-Myc expression in RKO and HT29 cells, in line with data showing c-Myc-mediated ASS1 re-expression in cells treated with arginine deprivation therapy[25]. Intriguingly, no compensatory expression of OTC was observed during the 72 h treatment (Supplementary Fig. S7).

Few floating cells were observed in the plates treated with rhArg1peg5000, possibly signifying a marginal induction of cell death. Indeed, the apoptotic marker cleaved-PARP was induced in arginine-deprived HCT116 and RKO cells (Supplementary Fig. S8).

Next, we investigated whether rhArg1peg5000 treatment affects the mTOR pathway in a way similar to that observed in arginine-free medium. To this end, the phosphorylation status of two main mTOR downstream targets, the ribosomal S6 protein and 4E-BP1, was investigated by western blotting over a short (up to 8 h) and long (up to 72 h) time course. However, we did not observe durable and consistent changes in phosphorylation levels of mTOR targets (Supplementary Fig. S9).
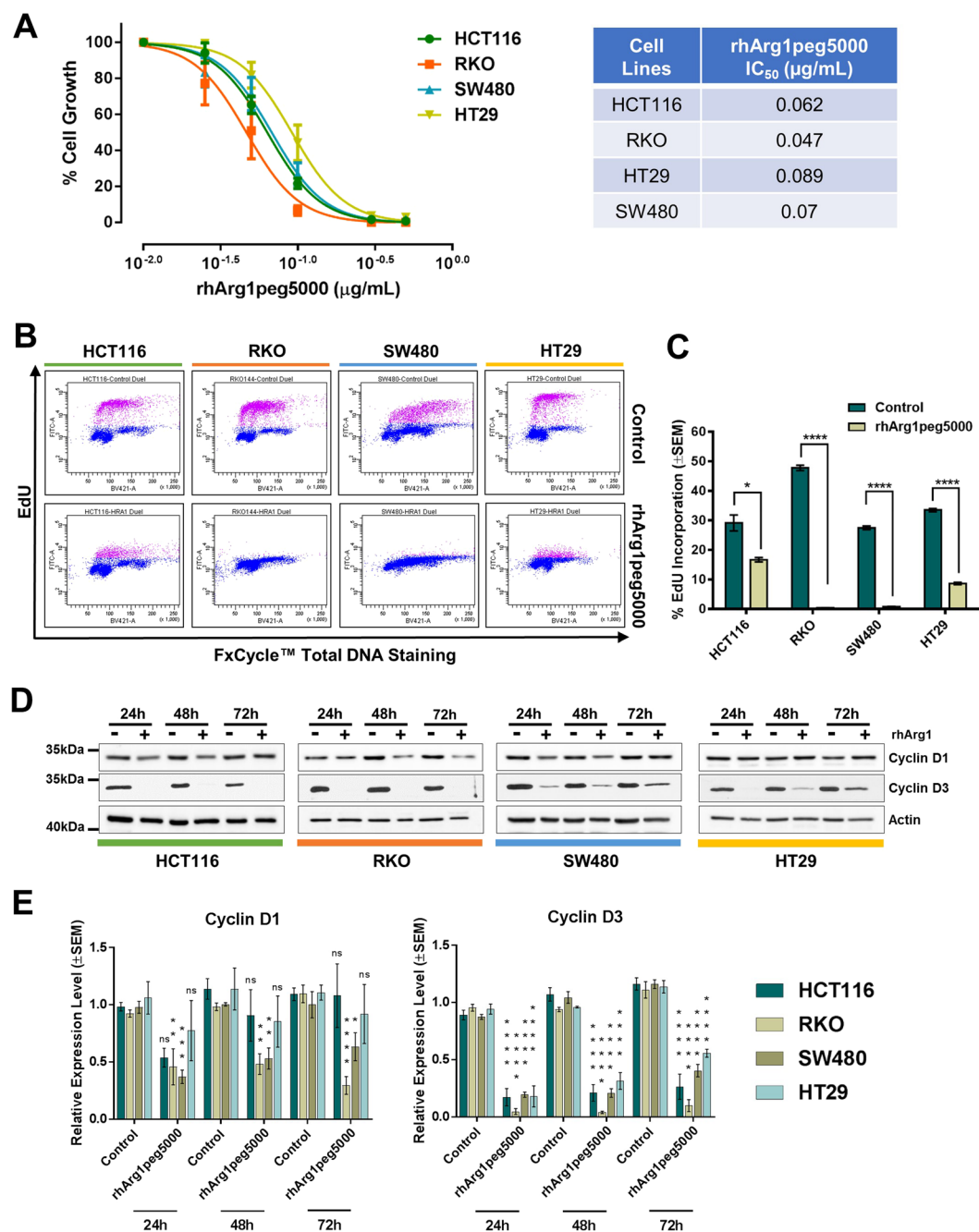
Figure 3. CRC cells are sensitive to arginase treatment. (**A**) Dose-Response Non-Linear Regression Curves and IC$_{50}$ values of the indicated CRC cell lines treated with the rhArg1peg5000. The percentage (%) of cell growth was calculated relative to the cell numbers in corresponding PBS-treated control samples, which was selected as 100%. IC$_{50}$ values were obtained from non-linear regression analysis of concentration of the drug vs response curves. The results were obtained from three independent experiments. Quadruplicate samples were assessed for cell growth after a 6-day period of treatment by cell counting for each individual experiment. The error bars represent ± SEM. (**B**) Representative flow cytometry scatterplots of EdU incorporation in HCT116, RKO, HT29 and SW480 CRC cell lines after 72 h treatment with rhArg1peg5000 (0.5 μg/mL) or PBS-vehicle control. EdU was measured using the Click-iT® EdU Alexa Fluor® kit and total DNA stained using FxCycle™ Violet Stain. (**C**) Quantification of EdU incorporation from three independent experiments. Data are presented as mean ± SEM. *P < 0.05, ****P < 0.0001, two-tailed t-test. (**D**) Western blot analysis of the cell cycle markers Cyclin D1 and D3 in cells treated for the indicated time with rhArg1peg5000 (0.5 μg/mL). Actin was used as endogenous loading control. (**E**) Quantification of Cyclin D1 and D3 protein expression from triplicate experiments. Original western blots are reported in Supplementary Fig. S15. Data are presented as mean ± SEM. *P < 0.05, **P < 0.01, ***P < 0.001, ****P < 0.0001, two-way ANOVA.
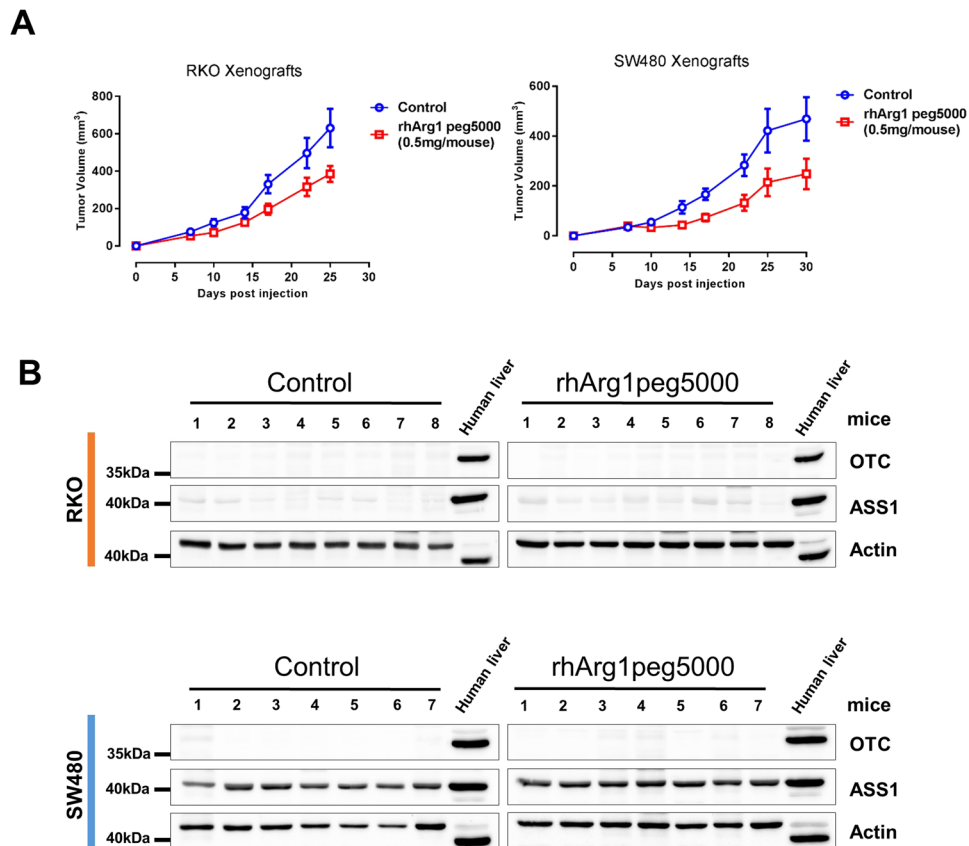
Figure 4. Pharmacological depletion of arginine using rhArg1peg5000 reduces tumor growth *in vivo*. (**A**) Tumor growth in athymic nude mice subcutaneously injected with 10^6 RKO or SW480 CRC cells. Mice were randomized into Control (n = 8) and Treatment (n = 8) groups. Treated mice were administered intraperitoneally with 0.5 mg of rhArg1peg5000/animal twice a week, while control mice were injected with an equal volume of PBS. Data are plotted as mean ± SEM and were analyzed using mixed linear regression analysis (P = 0.012 for RKO and P = 0.03 for SW480, P < 0.05 indicates a statistically significant difference in tumor growth rate between control and treated animals over time). (**B**) Western blotting of lysates from tumor xenografts for assessment of urea cycle enzymes OTC and ASS1. Human liver lysate was used as a positive control and actin as endogenous loading control. Original western blots are reported in Supplementary Fig. S15.

rhArg1peg5000 reduces tumor growth *in vivo*.   To test whether arginine deprivation mediated by rhArg1peg5000 could impair tumor growth *in vivo*, we subcutaneously implanted ASS1-negative RKO cells and ASS1-positive SW480 cells into the hind flanks of immunocompromised athymic nude mice, which were then randomized to twice a week treatment schedule (0.5 mg of rhArg1peg5000 per animal) or vehicle control. Arginase administration significantly slowed tumor growth in animals into which either cell line had been implanted (Fig. 4A). Pegylated arginine was well tolerated and there was no difference in body weight recorded between control and treated animals (Supplementary Fig. S10).

Western blotting analysis with antibodies selective for the human protein confirmed robust expression of ASS1 in SW480-derived tumors, as well as ASS1 negativity in RKO xenograft samples (Fig. 4B). Notably, no expression of OTC was detected in tumor isolated from rhArg1peg5000 treated animals (Fig. 4B). These findings suggest that tumors did not acquire resistance against arginase through re-expression of urea cycle enzymes, at least in the time frame of these experiments.

Overall, these data indicate that CRC cells are sensitive to pharmacological depletion of arginine via pegylated-arginase in an ASS1-independent fashion.

CRC cell lines are sensitive to arginine deprivation by ADI-PEG20.   As described above, RKO and HT29 cell lines do not express detectable ASS1 protein, and around 20% of CRC patients present with no or low expression of this biomarker (Fig. 2B and C). Hence, we investigate whether the mycoplasma-derived enzyme arginine deiminase could represent an alternative treatment opportunity for those patients. As expected, ASS1-positive SW480 cell lines were resistant to treatment with ADI-PEG20 *in vitro*, whereas ASS1-negative HT29 and RKO showed an exquisite sensitivity to ADI-PEG20-mediated arginine deprivation, with an identical IC50 of 0.034 μg/mL (Fig. 5A). In agreement with recently reported findings[26,27], HCT116 growth was greatly reduced by ADI-PEG20, despite detectable levels of ASS1 (Fig. 5A). The reason for the HCT116 sensitivity to ADI-PEG20 is unclear, as HCT116 cells also express ASL enzyme[26]. Others have attributed the effect of ADI-PEG20 treatment to downregulation of the mTOR pathway and induction of the unfolded protein
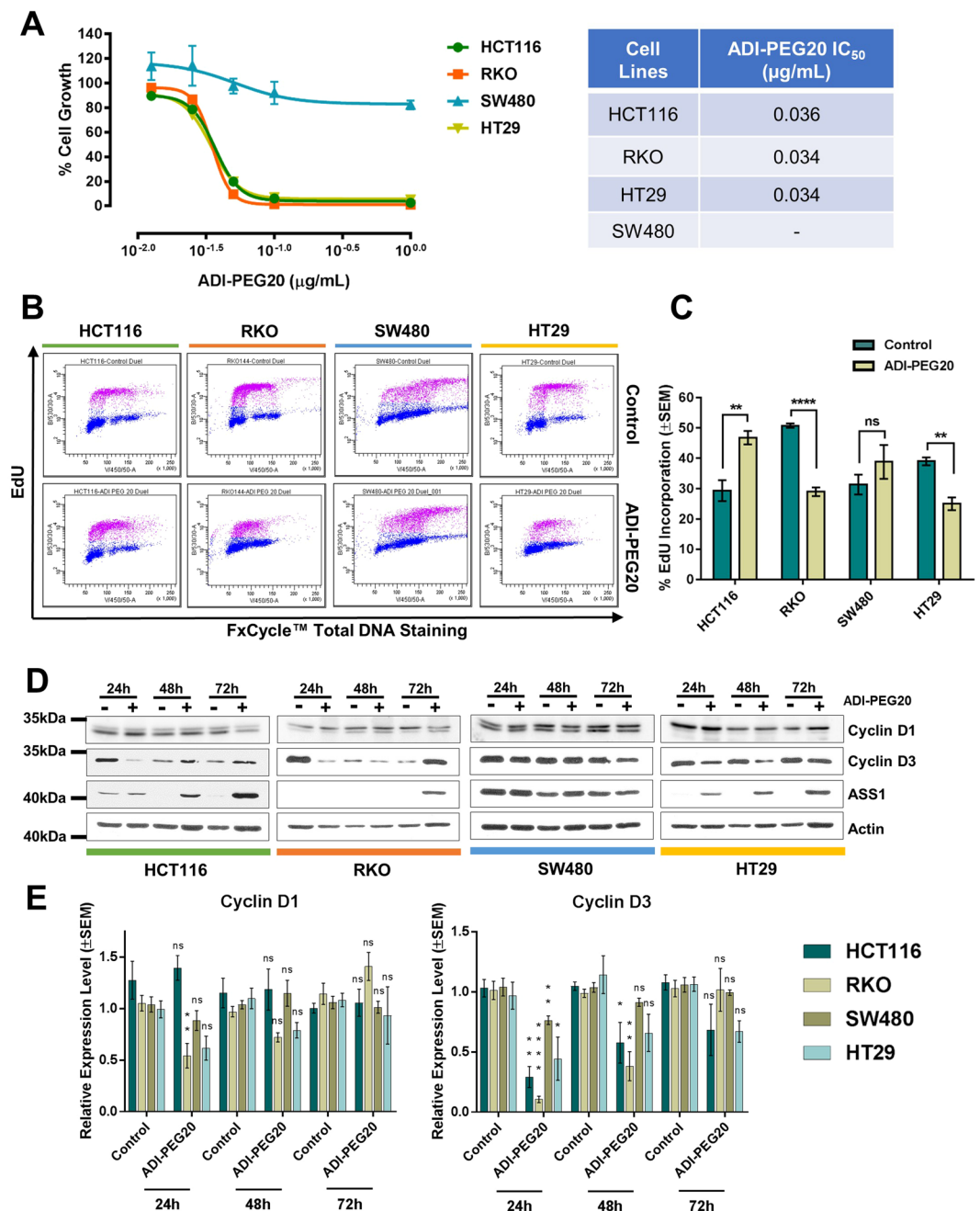
Figure 5. CRC cells are sensitive to arginine deiminase treatment. (**A**) Dose-Response Non-Linear Regression Curves and IC$_{50}$ values of the indicated CRC cell lines treated with the ADI-PEG20. The percentage (%) of cell growth was calculated relative to the cell numbers in corresponding PBS-treated control samples, which was selected as 100%. IC$_{50}$ values were obtained from non-linear regression analysis of concentration of the drug vs response curves. The results were obtained from three independent experiments. Quadruplicate samples were assessed for cell growth after a 6-day period of treatment by cell counting for each individual experiment. The error bars represent ±SEM. (**B**) Representative flow cytometry scatterplots of EdU incorporation in HCT116, RKO, HT29 and SW480 CRC cell lines after 72 h treatment with ADI-PEG (1 μg/mL) or PBS-vehicle control. EdU was measured using the using Click-iT® EdU Alexa Fluor® kit and total DNA stained using FxCycle™ Violet Stain. (**C**) Quantification of EdU incorporation from three independent experiments. Data are presented as mean ± SEM. *P < 0.05, ****P < 0.0001, two-tailed t-test. (**D**) Western blot analysis of the cell cycle markers Cyclin D1 and D3 and the urea cycle enzyme ASS1 in cells treated for the indicated time with ADI-PEG20 (1 μg/mL). Actin was used as endogenous loading control. Original western blots are reported in Supplementary Fig. S15. (**E**) Quantification of Cyclin D1 and D3 protein expression from triplicate experiments. Data are presented as mean ± SEM. *P < 0.05, **P < 0.01, ***P < 0.001, ****P < 0.0001, two-way ANOVA.

response[26], a possibility corroborated by the reduced phosphorylation of the mTOR targets 4E-BP1 and S6 after 72 h of arginine deiminase treatment (Supplementary Fig. S11).

When proliferation was assessed after 72 h exposure to ADI-PEG20, we noticed a significant reduction of EdU incorporation only in ASS1-negative cells, but not in ASS1-positive SW480 and HCT116 (Fig. 5B and C). Further analysis indicated that, in all ADI-PEG20 sensitive cell lines, expression of the cell cycle markers Cyclin D1 and D3 was reduced 24 h to 48 h after drug treatment, but had returned to normal levels at the time point of the cell cycle analysis (72 h) (Fig. 5D and E). Similarly, the expression of ASS1 was boosted by ADI-PEG20 treatment (Fig. 5D). These findings could explain why DNA synthesis was still substantial at the 72 h time point of arginine deprivation, and they indicate the possibility of rapidly ensuing resistance.

ADI-PEG20 reduces tumor growth *in vivo*. To determine whether ADI-PEG20 could slow tumor growth *in vivo*, ASS1-negative RKO cells were subcutaneously implanted into nude mice, which were then randomly allocated to either treatment (5IU of ADI-PEG20/animal/week) or vehicle control groups. ADI-PEG20 administration reduced tumor volume (Fig. 6A), although treated mice failed to gain body weight (Supplementary Fig. S12). The reduced tumor volume, was accompanied by a moderate but significant decrease in the Ki67 proliferation index (Fig. 6B), as well as Cyclin D1 and D3 expression in ADI-PEG20 treated xenografts and (Fig. 6C and D). Finally, as observed *in vitro*, ASS1 protein levels were increased in tissue isolated from arginine-deprived animals (Fig. 6E).

Overall, these data indicate that ADI-PEG20 treatment reduces *in vivo* tumorigenicity of ASS1-deficient CRC cells.

Combination of arginine deprivation with traditional chemotherapy. Chemotherapy based on the platinum compound Oxaliplatin and the antimetabolite 5-FU remains a key combination for first line treatment of metastatic CRC or in adjuvant settings[28,29]. Several publications suggest that ADI-PEG20 has a synergistic effect when combined with platinum-based compounds[9,15,30–32]. Hence, we endeavored to assess whether combining arginine deprivation therapy with chemotherapy might improve the treatment of CRC. To this end, we investigated effects of combinations on cell growth employing the Chou-Talalay method and the CompuSyn software[33] (Table 1, Supplementary Figs S13 and S14). Arginase treatment mostly resulted in antagonism (Combinatorial Index, CI > 1) when tested with either Oxaliplatin or 5-FU. Additive effects (CI = 1) were observed under a minority of conditions. Conversely, ADI-PEG20 in combination with Oxaliplatin elicited synergistic growth inhibition in the ASS1-negative cell lines RKO and HT29 (CI < 1). Of note, with the exception of ADI-PEG20-treated HT29, we never observed synergism between 5-FU and arginine deprivation therapy, rather, antagonism was the most common outcome of co-treatments.

Overall, these combinatorial studies outline a complex interaction between arginine deprivation and chemotherapy. Whereas arginase treatment often appears to be antagonistic with chemotherapeutic drugs, ADI-PEG20, in some circumstances, displays synergism in ASS1-deficient cells.

Discussion

ADI-PEG20 and rhArg1peg5000 (BCT-100) are under intense clinical testing in numerous malignancies. ADI-PEG20 degrades arginine into citrulline and ammonia, whereas rhArg1peg5000 generates ornithine and urea. Resistance of cells against these drugs depends on the expression of the urea cycle enzymes which are capable of resynthesizing arginine from the catabolic products. Expression of ASS1 and ASL is necessary for resistance to ADI-PEG20 monotherapy[34], whereas resistance to arginase requires the additional expression of the enzyme OTC[19]. When investigating biomarkers of arginine auxotrophy in CRC, we recorded a consistently poor expression of the urea cycle enzyme OTC in CRC specimens. In mammals OTC protein is expressed only in the liver and intestine[35] and catalyzes the reaction between carbamoyl-phosphate and ornithine to generate citrulline[1]. This reaction is enabled by the Carbamoyl-Phosphate Synthase 1 (CPS1)-mediated biosynthesis of carbamoyl-phosphate, which channels nitrogen from glutamine into the urea cycle. The reason for OTC downregulation in CRC remains unclear. Loss of ASS1 expression has been associated with poor prognosis in bladder cancer and glioblastoma[4,8] and recent data indicate that ASS1 downregulation supports cancer growth allowing aspartate channeling into pyrimidine biosynthesis[36]. With regard to regulation of urea cycle enzymes, CRC is anomalous as OTC downregulation is often accompanied by high expression of ASS1[16]. In CRC, ASS1 has been proposed to support proliferation of cancer cells, possibly through the enhancement of the glycolytic flux[37]. Interestingly, preliminary evidence suggests that CPS1 is also downregulated in advanced CRC[38], intimating that the entire pathway leading to citrulline production is compromised. The reason for this phenomenon is not clear, but it is tempting to speculate that lack of OTC and CPS1 expression enable recycling of nitrogen for reactions such as nucleotide, amino acid, or polyamine biosynthesis. Whatever the benefit, OTC downregulation renders cancer cells sensitive to treatment with human arginase, independently of ASS1 expression. Indeed, our *in vivo* studies show that pegylated arginase diminish the growth of both ASS1-positive and negative CRC cells. This finding is particularly interesting, as the potential therapeutic benefit of arginase in the treatment of solid tumors has hitherto been rarely investigated[19,39,40], even though it has been well-established in blood malignancies[17,41–44].

Intriguingly, our TMA analysis indicates that in a fraction of CRC patients ASS1 is poorly expressed or undetectable, an occurrence mirrored by RKO and HT29 cell lines, which both demonstrated significant sensitivity to arginine deprivation via ADI-PEG20 treatment *in vitro* and *in vivo*. These data intimate that a subset of CRC patients may be eligible to treatment with arginine deiminase, although the rapid reappearance of ASS1 in cells treated with ADI-PEG20 monotherapy is suggestive of a rapid adaptation and fast ensuing resistance. Indeed, restored expression of ASS1 has been reported in patients treated with single agent ADI-PEG20[45] and it is a common mechanism of acquired resistance against arginine deprivation[25,34,46]. Our data indicate that a similar
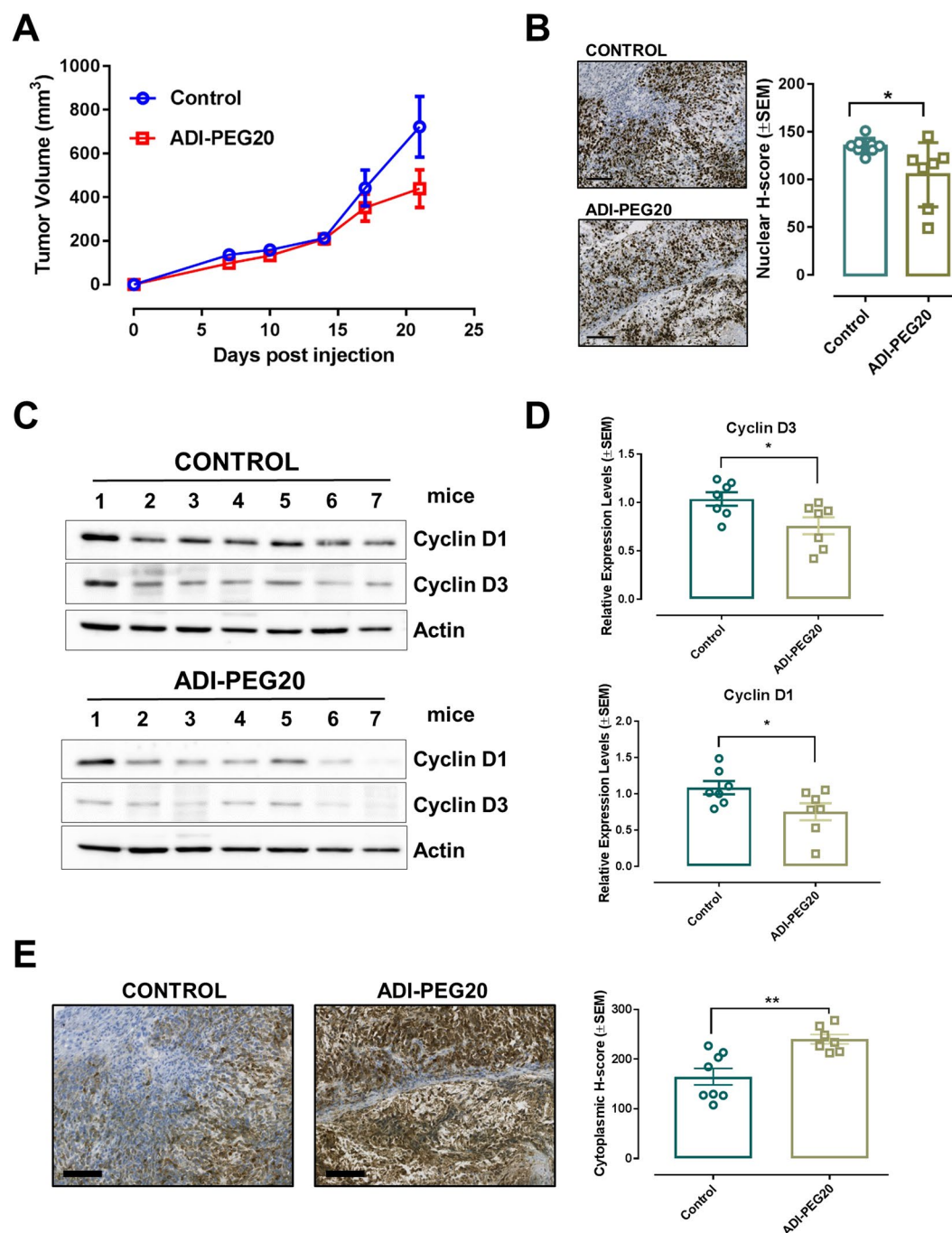
Figure 6. Pharmacological depletion of arginine using ADI-PEG20 reduces tumor growth *in vivo*. (**A**) Tumor xenografts growth in athymic nude mice subcutaneously injected with 10^6 RKO CRC cells. Mice were randomized into Control (n = 8) and Treatment (n = 8) groups. Treated mice were administered intraperitoneally (IP) with 5IU of ADI-PEG20 per animal per week, while control mice were injected with equal volume of PBS. Data are plotted as mean ± SEM and were analyzed using mixed linear regression analysis (P = 0.045, P < 0.05 indicates a statistically significant difference in tumor growth rate between control and treated animals over time). (**B**) Representative images of ki67-stained xenograft tumors and ki67 proliferation index of tumors from vehicle-treated and ADI-PEG20-injected animals. Data are presented as mean ± SEM (n = 7 animals per group). *P < 0.05, two-tailed t-test. Size bars = 100 μm. (**C**) Western blot analysis of the cell cycle markers Cyclin D1 and D3 and urea cycle enzyme ASS1 in xenograft tumors isolated from PBS-injected controls and ADI-PEG20-treated animals. Actin was used as endogenous loading control. Original western blots are reported in Supplementary Fig. S15. (**D**) Graph bars show quantification of Cyclins levels using Image J software. Data are presented as mean ± SEM (n = 7 animals per group). *P < 0.05, two-tailed t-test. (**E**) Representative images of ASS1-stained xenograft tumors and ASS1 H-score index of tumors from vehicle-treated and ADI-PEG20-injected animals. Data are presented as mean ± SEM (n = 7 animals per group). **P < 0.01, two-tailed t-test. Size bars = 100 μm.

	ADI-PEG20		rhArg1peg5000	
	IC50	IC90	IC50	IC90
5-FU				
HCT116	1.42	1.25	1.73	1.63
SW480	—	—	1.76	1.08
RKO	1.18	1.1	1.05	1.09
HT29	0.89	**0.80**	1.41	1.25
Oxaliplatin				
HCT116	1.24	1.46	1.92	1.60
SW480	—	—	1.54	1.22
RKO	**0.61**	**0.80**	1.89	1.59
HT29	**0.61**	**0.80**	1.33	1.09

Table 1. Combination studies between ADI-PEG20 or rhArg1peg5000 and chemotherapy. CI values are reported for both IC_{50} and IC_{90} combinations in the indicated cell lines. $CI < 1$ indicates synergism, $CI = 1$ indicates addictive effect, $CI > 1$ indicates antagonism. Cells were counted after 6 days of treatment and data obtained from diagonal constant ratio combinations were analyzed for synergism, additivity or antagonism using the CompuSyn Software (CompuSyn Inc.) according to the Chou and Talalay method. Bold highlights significant synergisms ($P < 0.05$).

re-expression of ASS1 activity is likely to occur in CRC, but, surprisingly, we did not observe re-expression of OTC, at least under the experimental conditions used. Currently, the mechanism mediating this persistent loss of OTC expression remains elusive, although experiments with the DNA methylase inhibitor suggest that it is likely to be independent of promoter methylation.

In several malignancies, ADI-PEG20 synergizes with platinum based chemotherapy[9,15,30,31], and a recent clinical trial reinforces the relevance of this interaction in combination with the folate antagonist pemetrexed in thoracic malignancies[32]. Chemotherapy of CRC relies on oxaliplatin and 5-FU (FOLFOX), and an ongoing clinical trial (NCT02102022) aims at treating patients with advanced gastrointestinal malignancies, including CRC, with a combinations of ADI-PEG20 and FOLFOX therapy. This projected trial inspired us to search for synergistic interactions between arginine degrading enzymes and the chemotherapeutic drugs oxaliplatin and 5-FU. Unexpectedly, arginase and arginine deiminase behaved dissimilarly in the combination studies. We failed to identify synergistic effects of rhArg1peg5000, which mostly antagonized both oxaliplatin and 5-FU, whereas ADI-PEG20 showed either synergistic or antagonistic effects, depending on drug used in the combination and cell line. We observed synergism between ADI-PEG20 and oxaliplatin in ASS1-deficient CRC cell lines, but we only observed synergism with 5-FU in ASS-1-negative HT29 cells. Therefore, our data warrant caution when using arginine deprivation therapy in combination with traditional chemotherapy in CRC, as patients' responses might differ substantially, perhaps consistent with the well-established molecular heterogeneity of colon malignancies[47]. On the other hand, the evidence of synergistic interactions intimates interesting therapeutic opportunities, at least for a subset of patients. Indeed, in a clinical study combining ADI-PEG20 with nab-paclitaxel and gemcitabine in pancreatic cancer, objective results were observed in both ASS1-proficient and -deficient patients[48]. This suggests that ASS1-deficiency may be less relevant if ADI-PEG20 is combined with other anticancer agents. Also, some malignant cell lines downregulate ASS1 expression when exposed to ADI-PEG20[34], suggesting that they may be more sensitive to ADI-PEG20 monotherapy, as well as ADI-PEG20 combination therapy. Furthermore, ADI-PEG20 inhibits migration of endothelial cells, even when co-cultured with ASS1 proficient tumors, at least in part by altering the composition and distribution of filamentous actin and attenuating tumor-produced vascular endothelial growth factor[49]. This demonstrates that, in some cases, ADI-PEG20 can alter tumor growth in an ASS1-proficient environment, similarly to what we observed with ASS1-positive HCT116 cells. Thus, in the absence of rigorous predictive biomarkers that identify synergistic outcomes, it is intriguing to envisage that patient derived xenograft avatars, 3-dimensional organoid cultures or tumor tissue explants[50–52] could be implemented to predict individual patient's response and to identify those subjects likely to benefit from ADI-PEG20 and FOLFOX co-treatment. Similarly, the use of arginine deprivation therapy as single treatment remains a promising therapeutic strategy that warrant further investigation in the preclinical and clinical settings.

Materials and Methods

TMA Patient cohort. The patient cohort was retrospectively acquired from the Grampian Biorepository (www.biorepository.nhsgrampian.org) and contains tissue samples from 650 patients who had undergone surgery for primary CRC between 1994 and 2009 at Aberdeen Royal Infirmary (Aberdeen, UK). Exclusion criteria included patients who had received neoadjuvant chemotherapy or radiotherapy. The median survival was 103 months (95% CI = 86–120 months), the mean survival was 115 months (95% CI = 108–123 months) and the median follow-up time ("reverse Kaplan-Meier" method) was 88 months (95% CI = 79–97 months). Clinical-pathological characteristics of the patients are summarized in Supplementary Table S1.

TMA also contains 50 normal colon mucosal samples acquired from at least 10 cm distant from the primary cancer TMA and was constructed as previously described[53–55]. All the cases were reviewed and areas of tissue to be sampled were first identified and marked on the appropriate haematoxylin and eosin stained slide by an expert

consultant gastro-intestinal pathologist. Two cores each measuring 1 mm in diameter were taken from areas of the corresponding FFPE block and placed in a recipient paraffin block.

The use of human colorectal tissue samples in this study was approved by the Grampian Biorepository scientific access group committee (TR000054). No written consent was required for the use of FFPE tissue samples in the CRC TMA. All animal work was carried out under the PPL# 60/4370 in accordance with the Animals Scientific Procedures Act of 1986. Animal research was approved by the local ethical committee at the University of Leicester.

TMA slides were processed according to standard immunohistochemical protocol described below. Expression levels of ASS1 and OTC were assessed blindfolded using PathXL (Clinical Pathology platform) and the semi quantitative approach of H-Score. Results were validated against automated classification of expression levels using Aperio ImageScope (Leica) and analyzed for agreement using the Cohen's Kappa coefficient.

Cell Culture and drugs. All cell lines were maintained in a humidified incubator (37 °C, 5% CO_2). HCT116 cells were cultured in McCoy's 5A + GlutaMAX™ + 10% FCS, SW480 and HT29 in Dulbecco's Modified Eagle's Medium (DMEM) (4500 mg glucose/L) + GlutaMAX™ + 10% FCS, RKO in Minimum Essential Medium Eagle (MEM) + GlutaMAX™ + 10% FCS. All treatments were in DMEM/F12 (1:1) + GlutaMAX™ and 10% FCS. Cells were exposed to 1 μg/mL ADI-PEG20 (Polaris Pharmaceuticals, San Diego, CA, USA), or 0.5 μg/mL rhArg-1peg5000 (Bio-Cancer Treatment International, Hong Kong) or 5 μM of 5-Aza-2′-deoxycytidine (Sigma, UK) or vehicle phosphate-buffered saline (PBS, Thermo-Scientific, UK) control, unless stated otherwise. Oxaliplatin and 5-FU were purchased from Sigma and formulated according to manufacturer's instructions.

Cell Proliferation Assays. 4000/well cells were seeded in 24-well plates 24 h before treatment. After 24 h cells were counted (day 0) and changed to DMEM/F12 (1:1) (Gibco®, UK) + 10% Dialyzed Fetal Bovine Serum (FBS) (GE Healthcare Life Sciences) containing various concentrations of drugs or arginine. Quadruplicate samples of each concentration were assessed for cell growth by cell counting with the Beckman Z™ Series Coulter Counter. Prior to cell counting, the treatment media was discarded, cells were washed with PBS and trypsinised with 2x Trypsin-EDTA. Trypsin was neutralized with medium and 1 mL of cell suspension was transferred into a Coulter cup with 9 mL of Coulter® Isoton® II diluent (Beckman Coulter, UK). Cells were counted between 8–20 μm.

Drug Combination studies and evaluation of synergy. Single drug IC_{50} values obtained from corresponding dose-response curves were used for the design of the combination experiments. In a checkerboard 6×6 layout; drug concentrations were crossed combined at an equipotency ratio $[(IC_{50})_1/(IC_{50})_2]$ to ensure that the observed effects were achieved by equal contribution of both drugs. Cells were counted after 6 days of treatment and data obtained from diagonal constant ratio combinations were analyzed for synergism, additivity or antagonism using the CompuSyn Software (CompuSyn Inc.) according to the Chou and Talalay method[33].

EdU Incorporation. 10^6 cells were seeded 24 h before treatment and then changed to medium containing arginine catabolizing agents for 72 h. Prior to FACS analysis cells were pulsed with 10 μM 5-ethyl-2′-deoxyuridine (EdU) for 1 h, harvested according to routine tissue culture protocols and washed with 1% BSA in PBS. After fixation and permeabilization, cells were incubated 15 minutes at room temperature protected from light. Click-iT® Reaction Cocktail was added to cells according to manufacturer's instructions. Samples were incubated at room temperature for 30 minutes protected from light. Total DNA was stained with 1 μL FxCycle™ Violet stain (Life Technologies, UK) in samples containing 1 mL cell suspension. Samples were incubated for additional 30 minutes on ice in the dark. Samples were analyzed on BD FACSARIA™ II, using 405 nm excitation and 450/50 band-pass emission for total DNA content, whereas a 488 nm excitation with a green emission filter (530/30 nm) was used for detection of EdU with Alexa Fluor® 488 azide. Samples of untreated cells, stained and unstained with EdU or FxCycle™, were also included.

Antibodies. The antibody against ASS1 was kindly provided by Polaris Pharmaceuticals Inc. Antibodies targeting Cyclin D1 (DCS6 and 92G2) and Cyclin D3 (DCS22), total (53H11) total and phospho (Thr37/46) (236B4) 4E-BP1, total (5G10) and phospho (Ser235/236) (D57.2.2E) ribosomal protein S6, and total/cleaved-PARP (46D11) were from Cell Signalling Technology (Leiden, The Netherlands). Actin (C-11) primary antibody and secondary mouse (sc-2005), rabbit (sc-2030) and goat (sc-2020) antibodies were purchased from Santa Cruz. OTC (ab91418) and Ki67 (ab833) antibodies were from Abcam (Cambridge, MA, USA). All primary antibodies for western blotting were diluted at in 3% BSA at a working concentration 1:1,000 overnight. All secondary antibodies were diluted at 1:10,000 in 3% milk.

Western-blot. Whole-cell lysates of CRC cell lines and xenograft tissues were prepared in Complete Lysis-M buffer (Roche, Germany). Protein quantification was performed using the Pierce™ BCA protein assay (Thermo Fisher Scientific, UK). 30 μg of total protein per lane was loaded on acrylamide gel. Following the SDS-PAGE electrophoresis, proteins were transferred to a nitrocellulose membrane (Geneflow, UK), blocked for 1 h in 5% milk and incubated overnight with primary antibodies at 4 °C. Membranes were then washed with PBS-0,01%Tween (SIGMA, UK) and incubated with appropriate secondary antibodies at room temperature for 1 h. Proteins were visualized using the Enhanced Chemiluminescence Luminol (ECL) reagent (Geneflow Ltd., UK). Images were captured using the GeneGnome XRQ system (Syngene, UK) or Kodak X-Ray films. The protein band intensity was measured using ImageJ software and the relative expression levels of the proteins were normalized against actin. The protein band intensity was measured using densitometry performed with ImageJ software. Proteins

presented as double bands were selected and quantified as a whole. The relative expression levels of the proteins were normalized against actin.

Immunohistochemistry (IHC). The immunostaining was performed using Novolink™ Polymer Detection System (Leica Biosystems, UK). Following deparaffinization, rehydrated sections were boiled for 20 minutes in antigen retrieval buffer (1X Tris-EDTA, pH 9). Endogenous peroxidase activity was neutralized using peroxidase block for 5 minutes. Sections were then blocked in protein block buffer for 30 minutes and incubated with primary antibodies for 2 h at room temperature. Peroxidase chromogenic reaction was developed with DAB working solution according to manufacturer's instructions. Slides were counterstained with haematoxylin and mounted with DPX mounting media and scanned with Hamamatsu NanoZoomer-XR Digital scanner. Staining was evaluated with Aperio ImageScope software (Leica) and the semi-quantitative H-score calculated using the following formula:

$$[1x\ (\%\ \text{weak positive cells}) + 2x\ (\%\ \text{positive cells}) + 3x\ (\%\ \text{strong positive cells})].$$

***In vivo* xenograft studies.** 8-week-old, female Foxn1^{nu} mice were purchased from Charles River, UK. Mice were kept in ventilated cages exposed to 12 h light/dark cycles under pathogen free conditions. Prior to xenografting, HCT116-luc2 (Perkin Elmer), RKO and SW480 cells were harvested at 70–80% confluency and resuspended to a final concentration of 10^7 cells per 1 ml Matrigel (BD Biosciences):Serum Free medium [1:1]. 10^6 cells were then injected subcutaneously unto the flank of each animal. A week after, mice with established tumors were randomized and treated with ADI-PEG20 5IU/animal once a week or rhArg1peg5000 5 mg/animal twice a week or vehicle control (PBS). Mice bearing HCT116 tumors were randomized to arginine-free diet (57M7) or control diet (5CC7) (TestDiet®) right after the initial cell injections. Body weight and tumor size were measured weekly. Further to the manual measurements, mice bearing HCT-116 luc2 tumors were monitored via the IVIS Spectrum Preclinical Imaging System (PerkinElmer®) once a week. Prior to *in vivo* imaging mice were administered subcutaneously with 150 mg/kg Xenolight RediJect D-Luciferin (PerkinElmer®), anesthetised and imaged with IVIS 10 minutes post injection. When tumors reached 17 mm diameter animals were sacrificed under terminal anesthesia (3–5% Isoflurane). Blood was collected by cardiac puncture. Tumors were excised, weighted, and fixed in formalin or snap-frozen. Study groups were not based on power calculations and experimenters were not blinded to the randomly allocated treatment groups.

Statistical analysis. The error bars represent the ±Standard Error of the Mean (±SEM). Statistical significance between two groups was determined by two-tailed unpaired Student's t-test, whereas multiple One-Way Anova analysis was conducted to compare controls against multiple drug concentrations (Prism version 7.0, GraphPad Software, Inc.). The animal xenograft studies were assessed for statistical significance using the mixed linear regression model in Stata software (StataCorp LP, College Station, TX, USA). Statistical analysis of TMA cohort patient data including the Mann-Whitney U test, Wilcoxon signed rank test, chi-squared test, and Cox multi-variate analysis (variables entered as categorical variables) was performed using IBM SPSS version 24 for Windows 7™ (IBM, UK).

References
1. Wu, G. & Morris, S. M. Jr. Arginine metabolism: nitric oxide and beyond. *Biochem J* **336**(Pt 1), 1–17 (1998).
2. Saxton, R. A. & Sabatini, D. M. mTOR Signaling in Growth, Metabolism, and Disease. *Cell* **168**, 960–976, https://doi.org/10.1016/j.cell.2017.02.004 (2017).
3. Delage, B. *et al*. Arginine deprivation and argininosuccinate synthetase expression in the treatment of cancer. *International journal of cancer* **126**, 2762–2772, https://doi.org/10.1002/ijc.25202 (2010).
4. Syed, N. *et al*. Epigenetic status of argininosuccinate synthetase and argininosuccinate lyase modulates autophagy and cell death in glioblastoma. *Cell death & disease* **4**, e458, https://doi.org/10.1038/cddis.2012.197 (2013).
5. Phillips, M. M., Sheaff, M. T. & Szlosarek, P. W. Targeting arginine-dependent cancers with arginine-degrading enzymes: opportunities and challenges. *Cancer Res Treat* **45**, 251–262, https://doi.org/10.4143/crt.2013.45.4.251 (2013).
6. Holtsberg, F. W., Ensor, C. M., Steiner, M. R., Bomalaski, J. S. & Clark, M. A. Poly(ethylene glycol) (PEG) conjugated arginine deiminase: effects of PEG formulations on its pharmacological properties. *J Control Release* **80**, 259–271 (2002).
7. Yau, T. *et al*. Preliminary efficacy, safety, pharmacokinetics, pharmacodynamics and quality of life study of pegylated recombinant human arginase 1 in patients with advanced hepatocellular carcinoma. *Investigational new drugs* **33**, 496–504, https://doi.org/10.1007/s10637-014-0200-8 (2015).
8. Allen, M. D. *et al*. Prognostic and therapeutic impact of argininosuccinate synthetase 1 control in bladder cancer as monitored longitudinally by PET imaging. *Cancer research* **74**, 896–907, https://doi.org/10.1158/0008-5472.CAN-13-1702 (2014).
9. Nicholson, L. J. *et al*. Epigenetic silencing of argininosuccinate synthetase confers resistance to platinum-induced cell death but collateral sensitivity to arginine auxotrophy in ovarian cancer. *International journal of cancer* **125**, 1454–1463, https://doi.org/10.1002/ijc.24546 (2009).
10. Szlosarek, P. W. *et al*. *In vivo* loss of expression of argininosuccinate synthetase in malignant pleural mesothelioma is a biomarker for susceptibility to arginine depletion. *Clinical cancer research: an official journal of the American Association for Cancer Research* **12**, 7126–7131, https://doi.org/10.1158/1078-0432.CCR-06-1101 (2006).
11. Szlosarek, P. W. *et al*. Metabolic response to pegylated arginine deiminase in mesothelioma with promoter methylation of argininosuccinate synthetase. *Journal of clinical oncology: official journal of the American Society of Clinical Oncology* **31**, e111–113, https://doi.org/10.1200/JCO.2012.42.1784 (2013).
12. Tsai, W. B. *et al*. Resistance to arginine deiminase treatment in melanoma cells is associated with induced argininosuccinate synthetase expression involving c-Myc/HIF-1alpha/Sp4. *Molecular cancer therapeutics* **8**, 3223–3233, https://doi.org/10.1158/1535-7163.MCT-09-0794 (2009).
13. Huang, H. Y. *et al*. ASS1 as a novel tumor suppressor gene in myxofibrosarcomas: aberrant loss via epigenetic DNA methylation confers aggressive phenotypes, negative prognostic impact, and therapeutic relevance. *Clinical cancer research: an official journal of the American Association for Cancer Research* **19**, 2861–2872, https://doi.org/10.1158/1078-0432.CCR-12-2641 (2013).

14. Miraki-Moud, F. *et al.* Arginine deprivation using pegylated arginine deiminase has activity against primary acute myeloid leukemia cells *in vivo*. *Blood* **125**, 4060–4068, https://doi.org/10.1182/blood-2014-10-608133 (2015).

15. McAlpine, J. A., Lu, H. T., Wu, K. C., Knowles, S. K. & Thomson, J. A. Down-regulation of argininosuccinate synthetase is associated with cisplatin resistance in hepatocellular carcinoma cell lines: implications for PEGylated arginine deiminase combination therapy. *BMC cancer* **14**, 621, https://doi.org/10.1186/1471-2407-14-621 (2014).

16. Rho, J. H., Qin, S., Wang, J. Y. & Roehrl, M. H. Proteomic expression analysis of surgical human colorectal cancer tissues: up-regulation of PSB7, PRDX1, and SRP9 and hypoxic adaptation in cancer. *J Proteome Res* **7**, 2959–2972, https://doi.org/10.1021/pr8000892 (2008).

17. Mussai, F. *et al.* Arginine dependence of acute myeloid leukemia blast proliferation: a novel therapeutic target. *Blood* **125**, 2386–2396, https://doi.org/10.1182/blood-2014-09-600643 (2015).

18. Bobak, Y. P., Vynnytska, B. O., Kurlishchuk, Y. V., Sibirny, A. A. & Stasyk, O. V. Cancer cell sensitivity to arginine deprivation *in vitro* is not determined by endogenous levels of arginine metabolic enzymes. *Cell Biol Int* **34**, 1085–1089, https://doi.org/10.1042/CBI20100451 (2010).

19. Cheng, P. N. *et al.* Pegylated recombinant human arginase (rhArg-peg5,000mw) inhibits the *in vitro* and *in vivo* proliferation of human hepatocellular carcinoma through arginine depletion. *Cancer research* **67**, 309–317, https://doi.org/10.1158/0008-5472.CAN-06-1945 (2007).

20. Gingras, A. C. *et al.* Hierarchical phosphorylation of the translation inhibitor 4E-BP1. *Genes Dev* **15**, 2852–2864, https://doi.org/10.1101/gad.912401 (2001).

21. Feichtinger, J., McFarlane, R. J. & Larcombe, L. D. CancerMA: a web-based tool for automatic meta-analysis of public cancer microarray data. *Database (Oxford)* **2012**, bas055, https://doi.org/10.1093/database/bas055 (2012).

22. Rhodes, D. R. *et al.* ONCOMINE: a cancer microarray database and integrated data-mining platform. *Neoplasia* **6**, 1–6 (2004).

23. Walther, A. *et al.* Genetic prognostic and predictive markers in colorectal cancer. *Nat Rev Cancer* **9**, 489–499, https://doi.org/10.1038/nrc2645 (2009).

24. Ahmed, D. *et al.* Epigenetic and genetic features of 24 colon cancer cell lines. *Oncogenesis* **2**, e71, https://doi.org/10.1038/oncsis.2013.35 (2013).

25. Tsai, W. B. *et al.* Activation of Ras/PI3K/ERK pathway induces c-Myc stabilization to upregulate argininosuccinate synthetase, leading to arginine deiminase resistance in melanoma cells. *Cancer research* **72**, 2622–2633, https://doi.org/10.1158/0008-5472.CAN-11-3605 (2012).

26. Burrows, N. *et al.* Hypoxia-induced nitric oxide production and tumour perfusion is inhibited by pegylated arginine deiminase (ADI-PEG20). *Sci Rep* **6**, 22950, https://doi.org/10.1038/srep22950 (2016).

27. Vynnytska-Myronovska, B. O. *et al.* Arginine starvation in colorectal cancer cells: Sensing, impact on translation control and cell cycle distribution. *Exp Cell Res* **341**, 67–74, https://doi.org/10.1016/j.yexcr.2016.01.002 (2016).

28. Van Cutsem, E., Cervantes, A., Nordlinger, B., Arnold, D. & Group, E. G. W. Metastatic colorectal cancer: ESMO Clinical Practice Guidelines for diagnosis, treatment and follow-up. *Ann Oncol* **25**(Suppl 3), iii1–9, https://doi.org/10.1093/annonc/mdu260 (2014).

29. Kohne, C. H. Current stages of adjuvant treatment of colon cancer. *Ann Oncol* **23**(Suppl 10), x71–76, https://doi.org/10.1093/annonc/mds354 (2012).

30. Long, Y. *et al.* Cisplatin-induced synthetic lethality to arginine-starvation therapy by transcriptional suppression of ASS1 is regulated by DEC1, HIF-1alpha, and c-Myc transcription network and is independent of ASS1 promoter DNA methylation. *Oncotarget* **7**, 82658–82670, https://doi.org/10.18632/oncotarget.12308 (2016).

31. Savaraj, N. *et al.* Targeting argininosuccinate synthetase negative melanomas using combination of arginine degrading enzyme and cisplatin. *Oncotarget* **6**, 6295–6309, https://doi.org/10.18632/oncotarget.3370 (2015).

32. Beddowes, E. *et al.* Phase 1 Dose-Escalation Study of Pegylated Arginine Deiminase, Cisplatin, and Pemetrexed in Patients With Argininosuccinate Synthetase 1-Deficient Thoracic Cancers. *Journal of clinical oncology: official journal of the American Society of Clinical Oncology* **35**, 1778–1785, https://doi.org/10.1200/JCO.2016.71.3230 (2017).

33. Chou, T. C. Theoretical basis, experimental design, and computerized simulation of synergism and antagonism in drug combination studies. *Pharmacol Rev* **58**, 621–681, https://doi.org/10.1124/pr.58.3.10 (2006).

34. Shen, L. J., Lin, W. C., Beloussow, K. & Shen, W. C. Resistance to the anti-proliferative activity of recombinant arginine deiminase in cell culture correlates with the endogenous enzyme, argininosuccinate synthetase. *Cancer letters* **191**, 165–170 (2003).

35. Ryall, J. C., Quantz, M. A. & Shore, G. C. Rat liver and intestinal mucosa differ in the developmental pattern and hormonal regulation of carbamoyl-phosphate synthetase I and ornithine carbamoyl transferase gene expression. *Eur J Biochem* **156**, 453–458 (1986).

36. Rabinovich, S. *et al.* Diversion of aspartate in ASS1-deficient tumours fosters *de novo* pyrimidine synthesis. *Nature* **527**, 379–383, https://doi.org/10.1038/nature15529 (2015).

37. Bateman, L. A. *et al.* Argininosuccinate Synthase 1 is a Metabolic Regulator of Colorectal Cancer Pathogenicity. *ACS Chem Biol* **12**, 905–911, https://doi.org/10.1021/acschembio.6b01158 (2017).

38. Cardona, D. M., Zhang, X. & Liu, C. Loss of carbamoyl phosphate synthetase I in small-intestinal adenocarcinoma. *Am J Clin Pathol* **132**, 877–882, https://doi.org/10.1309/AJCP74XGRFWTFLJU (2009).

39. Wang, Z. *et al.* Involvement of autophagy in recombinant human arginase-induced cell apoptosis and growth inhibition of malignant melanoma cells. *Appl Microbiol Biotechnol* **98**, 2485–2494, https://doi.org/10.1007/s00253-013-5118-0 (2014).

40. Hsueh, E. C. *et al.* Deprivation of arginine by recombinant human arginase in prostate cancer cells. *J Hematol Oncol* **5**, 17, https://doi.org/10.1186/1756-8722-5-17 (2012).

41. Hernandez, C. P. *et al.* Pegylated arginase I: a potential therapeutic approach in T-ALL. *Blood* **115**, 5214–5221, https://doi.org/10.1182/blood-2009-12-258822 (2010).

42. Morrow, K. *et al.* Anti-leukemic mechanisms of pegylated arginase I in acute lymphoblastic T-cell leukemia. *Leukemia* **27**, 569–577, https://doi.org/10.1038/leu.2012.247 (2013).

43. Zeng, X. *et al.* Recombinant human arginase induced caspase-dependent apoptosis and autophagy in non-Hodgkin's lymphoma cells. *Cell death & disease* **4**, e840, https://doi.org/10.1038/cddis.2013.359 (2013).

44. Tanios, R. *et al.* Human recombinant arginase I(Co)-PEG5000 [HuArgI(Co)-PEG5000]-induced arginine depletion is selectively cytotoxic to human acute myeloid leukemia cells. *Leuk Res* **37**, 1565–1571, https://doi.org/10.1016/j.leukres.2013.08.007 (2013).

45. Feun, L. & Savaraj, N. Pegylated arginine deiminase: a novel anticancer enzyme agent. *Expert Opin Investig Drugs* **15**, 815–822, https://doi.org/10.1517/13543784.15.7.815 (2006).

46. Manca, A. *et al.* Induction of arginosuccinate synthetase (ASS) expression affects the antiproliferative activity of arginine deiminase (ADI) in melanoma cells. *Oncol Rep* **25**, 1495–1502, https://doi.org/10.3892/or.2011.1220 (2011).

47. Guinney, J. *et al.* The consensus molecular subtypes of colorectal cancer. *Nat Med* **21**, 1350–1356, https://doi.org/10.1038/nm.3967 (2015).

48. Lowery, M. A. *et al.* A phase 1/1B trial of ADI-PEG 20 plus nab-paclitaxel and gemcitabine in patients with advanced pancreatic adenocarcinoma. *Cancer.* https://doi.org/10.1002/cncr.30897 (2017).

49. Zhuo, W., Song, X., Zhou, H. & Luo, Y. Arginine deiminase modulates endothelial tip cells via excessive synthesis of reactive oxygen species. *Biochem Soc Trans* **39**, 1376–1381, suppl 1372 p following1382, https://doi.org/10.1042/BST0391376 (2011).

50. Nunes, M. *et al.* Evaluating patient-derived colorectal cancer xenografts as preclinical models by comparison with patient clinical data. *Cancer research* **75**, 1560–1566, https://doi.org/10.1158/0008-5472.CAN-14-1590 (2015).

51. Karekla, E. *et al. Ex Vivo* Explant Cultures of Non-Small Cell Lung Carcinoma Enable Evaluation of Primary Tumor Responses to Anticancer Therapy. *Cancer research* **77**, 2029–2039, https://doi.org/10.1158/0008-5472.CAN-16-1121 (2017).
52. Vlachogiannis, G. *et al.* Patient-derived organoids model treatment response of metastatic gastrointestinal cancers. *Science* **359**, 920–926, https://doi.org/10.1126/science.aao2774 (2018).
53. O'Dwyer, D., Ralton, L. D., O'Shea, A. & Murray, G. I. The proteomics of colorectal cancer: identification of a protein signature associated with prognosis. *PLoS One* **6**, e27718, https://doi.org/10.1371/journal.pone.0027718 (2011).
54. Brown, G. T. *et al.* The expression and prognostic significance of retinoic acid metabolising enzymes in colorectal cancer. *PLoS One* **9**, e90776, https://doi.org/10.1371/journal.pone.0090776 (2014).
55. Swan, R., Alnabulsi, A., Cash, B., Alnabulsi, A. & Murray, G. I. Characterisation of the oxysterol metabolising enzyme pathway in mismatch repair proficient and deficient colorectal cancer. *Oncotarget* **7**, 46509–46527, https://doi.org/10.18632/oncotarget.10224 (2016).

Acknowledgements

Author Contributions

A.R. and C.A. designed the study; C.A., S.S.A., J.A.H., A.K., C.A. and L.M.H. performed the experiments; W.B., D.A.M. and G.I.M. helped with TMA analysis; J.L. and B.M. helped with bioinformatics; M.V. supported statistical analysis; P.N.C. provided reagents; A.R., G.I.M., C.A., C.A., K.B. and A.T. analyzed the data; A.R. wrote the paper. All authors have reviewed the manuscript.

Additional Information

Supplementary information accompanies this paper at https://doi.org/10.1038/s41598-018-30591-7.

Competing Interests: Paul N. Cheng is founder and CEO of Bio-Cancer Treatment and has a financial interest in rhArg1peg5000. All other authors declare no conflict of interest.

Publisher's note: Springer Nature remains neutral with regard to jurisdictional claims in published maps and institutional affiliations.